*Supporting Information*

*for*

# *N^N* vs *N^E* (E = S or Se) Coordination Behavior of Imino-Phosphanamidinate Chalcogenide Ligands towards Aluminum Alkyls. Efficient Hydroboration Catalysis of Nitriles, Alkynes, and Alkenes

Himadri Karmakar,[a] Ravi Kumar,[a] Jyoti Sharma,[a] Jayanta Bag,[b] Kuntal Pal,[b] Vadapalli Chandrasekhar*,[c,d] and Tarun K. Panda*[a]

**Table of Contents**

1. **X-ray crystallographic analyses**: Single crystals of complexes **2a-H**, **2b-H**, **3a-H**, **3b-H**, **4a-H** and **4b-H** were obtained from a concentrated solution of toluene in an argon-filled atmosphere at -35 °C. However, single crystals of **5a**, **5b**, **7a**, and **7b** were obtained from a toluene/hexane mixture (1:1) solution at -35 °C, whereas **6a**, **6b** was crystallized from THF/hexane mixture (1:1) solution at room temperature. In each case, a crystal of suitable dimensions was mounted on a CryoLoop (Hampton Research Corp) with a layer of light mineral oil. All measurements were made on a Bruker SCXRD D8 VENTURE or an Rigaku Supernova X-calibur Eos CCD detector with graphite monochromatic Mo-Kα (0.71073 Å) radiation. Crystal data and structure refinement parameters are summarized in Table TS1 and TS2. The structures were solved by direct methods (SIR2004) and refined on $F^2$ by full-matrix least-squares methods, using SHELXL-97.[1] Non-hydrogen atoms were anisotropically refined. H-atoms were included in the refinement on calculated positions riding on their carrier atoms. The ORTEP-3[2] program was used to draw the molecule with 30% probability displacement ellipsoids and H atoms omitted for clarity. Crystallographic data (excluding structure factors) for the structures reported in this paper have been deposited with the Cambridge Crystallographic Data Centre as supplementary publication no. CCDC 2221974 – 2221983 and 2221985. Copies of the data can be obtained free of charge on application to CCDC, 12 Union Road, Cambridge CB21EZ, UK (fax: + (44)1223-336-033; email: deposit@ccdc.cam.ac.uk).

**(i) T1. Crystallographic data and refinement parameters of 2a-H, 2b-H and 3a-H.**

| Crystal parameters | **2a-H** | **2b-H** | **3a-H** |
|---|---|---|---|
| CCDC NO. | 2221974 | 2221975 | 2221976 |
| Empirical formula | $C_{45}H_{59}N_4PS$ | $C_{45}H_{59}N_4Pse$ | $C_{39}H_{47}N_4PS$ |
| Formula weight | 719.03 | 765.89 | 634.83 |
| *T* (K) | 250(10) | 293(2) | 273.15 |
| *λ* (Å) | 0.71073 | 0.71073 | 0.71073 |
| Crystal system | Orthorhombic | Monoclinic | Triclinic |
| Space group | *P*bca | $P2_1/c$ | *P*-1 |
| *a* (Å) | 16.2250(6) | 14.0131(6) | 8.446(6) |
| *b* (Å) | 24.0393(10) | 16.1376(7) | 12.251(9) |
| *c* (Å) | 25.4474(10) | 22.0541(10) | 18.836(15) |

| | | | |
|---|---|---|---|
| $\alpha$ (°) | 90 | 90 | 94.52(3) |
| $\beta$ (°) | 90 | 101.734(4) | 100.34(2) |
| $\gamma$ (°) | 90 | 90 | 105.00(3) |
| $V$ (Å$^3$) | 9925.4(7) | 4883.0(4) | 1836(2) |
| $Z$ | 8 | 4 | 2 |
| $D_{calc}$ (g cm$^{-3}$) | 0.962 | 1.042 | 1.148 |
| $\mu$ (mm$^{-1}$) | 0.127 | 0.832 | 0.163 |
| $F$(000) | 3104.0 | 1624 | 680 |
| Theta range for data collection | 2.648 to 29.057 deg. | 2.524 to 28.966 deg. | 2.18 to 27.102 deg. |
| Limiting indices | $-21 \le h \le 22$,<br>$-24 \le k \le 32$,<br>$-31 \le l \le 34$ | $-18 \le h \le 18$,<br>$-21 \le k \le 21$,<br>$-25 \le l \le 29$ | $-10 \le h \le 10$,<br>$-15 \le k \le 15$,<br>$-22 \le l \le 24$ |
| Reflections collected / unique | 138337 / 12256 [R(int) = 0.0652] | 47830 / 11293 [R(int) = 0.0677] | 27080 / 7717 [R(int) = 0.0633] |
| Completeness of theta | 99.76 % | 99.51 % | 95 % |
| Absorption correction | Multi-scan | Multi-scan | Multi-scan |
| Max. and min. transmission | 1.00000 and 0.06282 | 1.00000 and 0.78383 | 1.00000 and 0.82770 |
| Refinement method | Full-matrix least-squares on $F^2$ | Full-matrix least-squares on $F^2$ | Full-matrix least-squares on $F^2$ |
| Data / restraints / parameters | 12256 / 31 / 585 | 11293 / 1 / 468 | 7717 / 0 / 422 |
| Goodness-of-fit on $F^2$ | 1.043 | 1.073 | 1.023 |
| Final R indices [I>2Sigma(I)] | $R_1 = 0.0687$, $wR_2 = 0.1866$ | $R_1 = 0.0458$, $wR_2 = 0.1216$ | $R_1 = 0.0667$, $wR_2 = 0.1540$ |
| R indices (all data) | $R_1 = 0.1071$, $wR_2 = 0.2028$ | $R_1 = 0.0790$, $wR_2 = 0.1337$ | $R_1 = 0.1298$, $wR_2 = 0.1821$ |

**(i) T1. (contd). Crystallographic data and refinement parameters of 3b-H, 4a-H and 4b-H.**

| Crystal parameters | **3b-H** | **4a-H** | **4b-H** |
|---|---|---|---|
| CCDC NO. | 2221977 | 2221978 | 2221979 |
| Empirical formula | $C_{39}H_{47}N_4PSe$ | $C_{29}H_{43}N_4PS$ | $C_{29}H_{43}N_4PSe$ |
| Formula weight | 681.77 | 510.72 | 557.60 |
| $T$ (K) | 293(2) | 273.15 | 249.99(10) |
| $\lambda$ (Å) | 0.71073 | 0.71073 | 0.71073 |
| Crystal system | Triclinic | Monoclinic | Monoclinic |
| Space group | $P$-1 | $P2_1/n$ | $P2_1/n$ |
| $a$ (Å) | 8.5632(2) | 13.8855(6) | 13.9301(5) |
| $b$ (Å) | 12.1933(3) | 15.1007(6) | 15.0618(6) |
| $c$ (Å) | 18.6985(4) | 14.1929(7) | 14.1789(6) |
| $\alpha$ (°) | 94.188(2) | 90 | 90 |
| $\beta$ (°) | 101.343(2) | 92.918(2) | 93.560(4) |
| $\gamma$ (°) | 104.459(2) | 90 | 90 |
| $V$ (Å$^3$) | 1838.21(8) | 2972.1(2) | 2969.2(2) |
| $Z$ | 2 | 4 | 4 |
| $D_{calc}$ (g cm$^{-3}$) | 1.232 | 1.137 | 1.247 |
| $\mu$ (mm$^{-1}$) | 1.096 | 0.186 | 1.342 |
| $F$(000) | 716 | 1096 | 1176 |
| Theta range for data collection | 2.519 to 28.89 deg. | 1.971 to 27.13 deg. | 2.705 to 28.881 deg. |
| Limiting indices | $-10 \le h \le 11$,<br>$-15 \le k \le 15$,<br>$-24 \le l \le 23$ | $-17 \le h \le 17$,<br>$-19 \le k \le 17$,<br>$-18 \le l \le 18$ | $-18 \le h \le 18$,<br>$-19 \le k \le 19$,<br>$-19 \le l \le 15$ |
| Reflections collected / unique | 34496 / 8478 [R(int) = 0.0702] | 43812 / 6564 [R(int) = 0.0551] | 35067 / 7018 [R(int) = 0.0757] |
| Completeness of theta | 99.51 % | 99.13 % | 99.62 % |
| Absorption correction | Multi-scan | Multi-scan | Multi-scan |
| Max. and min. transmission | 1.00000 and 0.69716 | 1.00000 and 0.82770 | 1.00000 and 0.28231 |
| Refinement method | Full-matrix least-squares on $F^2$ | Full-matrix least-squares on $F^2$ | Full-matrix least-squares on $F^2$ |
| Data / restraints / parameters | 8478 / 1 / 426 | 6564 / 13 / 336 | 7018 / 39 / 343 |

| | | | |
|---|---|---|---|
| Goodness-of-fit on $F^2$ | 1.037 | 1.039 | 1.093 |
| Final R indices [I>2Sigma(I)] | $R_1$ = 0.0502, $wR_2$ = 0.1069 | $R_1$ = 0.0598, $wR_2$ = 0.1493 | $R_1$ = 0.0609, $wR_2$ = 0.1103 |
| R indices (all data) | $R_1$ = 0.0820, $wR_2$ = 0.1150 | $R_1$ = 0.0906, $wR_2$ = 0.1666 | $R_1$ = 0.1092, $wR_2$ = 0.1207 |

**(ii) T2. Crystallographic data and refinement parameters of 5a, 5b and 6a.**

| Crystal parameters | **5a** | **5b** | **6a.THF** |
|---|---|---|---|
| CCDC NO. | 2221980 | 2221981 | 2221982 |
| Empirical formula | $C_{47}H_{64}AlN_4PS$ | $C_{47}H_{64}AlN_4PSe$ | $C_{45}H_{60}AlN_4OPS$ |
| Formula weight | 775.03 | 821.93 | 762.98 |
| $T$ (K) | 250(10) | 249.99(10) | 273.15 |
| $\lambda$ (Å) | 0.71073 | 0.71073 | 0.71073 |
| Crystal system | Orthorhombic | Orthorhombic | Monoclinic |
| Space group | $P2_12_12_1$ | $P2_12_12_1$ | $P2_1/c$ |
| $a$ (Å) | 10.6056(4) | 10.5605(5) | 13.8759(6) |
| $b$ (Å) | 20.2557(7) | 20.3370(10) | 11.9000(5) |
| $c$ (Å) | 21.7565(7) | 21.8728(9) | 27.3412(10) |
| $\alpha$ (°) | 90 | 90 | 90 |
| $\beta$ (°) | 90 | 90 | 94.2650(10) |
| $\gamma$ (°) | 90 | 90 | 90 |
| $V$ (Å$^3$) | 4673.8(3) | 4697.6(4) | 4502.2(3) |
| $Z$ | 4 | 4 | 4 |
| $D_{calc}$ (g cm$^{-3}$) | 1.101 | 1.162 | 1.019 |
| $\mu$ (mm$^{-1}$) | 0.157 | 0.886 | 0.156 |
| $F$(000) | 1672 | 1744 | 1480 |
| Theta range for data collection | 2.682 to 28.952 deg. | 2.681 to 28.923 deg. | 2.018 to 25.169 deg. |
| Limiting indices | $-14 \le h \le 10$,<br>$-27 \le k \le 26$,<br>$-28 \le l \le 23$ | $-13 \le h \le 13$,<br>$-26 \le k \le 24$,<br>$-29 \le l \le 29$ | $-15 \le h \le 16$,<br>$-14 \le k \le 12$,<br>$-32 \le l \le 32$ |
| Reflections collected / unique | 44544 / 10900 [R(int) = 0.0400] | 60932 / 11137 [R(int) = 0.0570] | 39617 / 7971 [R(int) = 0.0974] |

| | | | |
|---|---|---|---|
| Completeness of theta | 99.68 % | 99.76 % | 99.13 % |
| Absorption correction | Multi-scan | Multi-scan | Multi-scan |
| Max. and min. transmission | 1.00000 and 0.70905 | 1.00000 and 0.52605 | 0.7455 and 0.6896 |
| Refinement method | Full-matrix least-squares on $F^2$ | Full-matrix least-squares on $F^2$ | Full-matrix least-squares on $F^2$ |
| Data / restraints / parameters | 10900 / 0 / 502 | 11140 / 0 / 502 | 7971 / 0 / 446 |
| Goodness-of-fit on $F^2$ | 1.023 | 1.012 | 1.014 |
| Final R indices [I>2Sigma(I)] | $R_1$ = 0.0395, $wR_2$ = 0.0899 | $R_1$ = 0.0466, $wR_2$ = 0.0772 | $R_1$ = 0.0599, $wR_2$ = 0.1526 |
| R indices (all data) | $R_1$ = 0.0562, $wR_2$ = 0.0952 | $R_1$ = 0.0817, $wR_2$ = 0.0835 | $R_1$ = 0.1091, $wR_2$ = 0.1739 |

**(ii) T2. (contd). Crystallographic data and refinement parameters of 6b and 7b.**

| Crystal parameters | **6b** | **7b** |
|---|---|---|
| CCDC NO. | 2221983 | 2221985 |
| Empirical formula | $C_{41}H_{52}AlN_4PSe$ | $C_{31}H_{48}AlN_4PSe$ |
| Formula weight | 737.81 | 613.64 |
| $T$ (K) | 273(2) | 270.67(10) |
| $\lambda$ (Å) | 0.71073 | 0.71073 |
| Crystal system | Monoclinic | Monoclinic |
| Space group | $P2_1/n$ | $P2_1/c$ |
| $a$ (Å) | 10.1884(10) | 16.5351(4) |
| $b$ (Å) | 17.2889(19) | 11.7260(3) |
| $c$ (Å) | 22.976(3) | 17.1772(5) |
| $\alpha$ (°) | 90 | 90 |
| $\beta$ (°) | 91.623(3) | 102.702(2) |
| $\gamma$ (°) | 90 | 90 |
| $V$ (Å$^3$) | 4045.5(8) | 3248.99(15) |
| $Z$ | 4 | 4 |
| $D_{calc}$ (g cm$^{-3}$) | 1.215 | 1.255 |

| | | |
|---|---|---|
| $\mu$ ($mm^{-1}$) | 1.022 | 1.257 |
| $F$(000) | 1556 | 1296 |
| Theta range for data collection | 2.129 to 25.036 deg. | 2.987 to 29.116 deg. |
| Limiting indices | $-12 \leq h \leq 12$,<br>$-20 \leq k \leq 20$,<br>$-27 \leq l \leq 27$ | $-22 \leq h \leq 22$,<br>$-15 \leq k \leq 15$,<br>$-23 \leq l \leq 21$ |
| Reflections collected / unique | 53392 / 7114 [R(int) = 0.0544] | 36691 / 7689 [R(int) = 0.0545] |
| Completeness of theta | 99.71 % | 99.70 % |
| Absorption correction | Multi-scan | Multi-scan |
| Max. and min. transmission | 1.00000 and 0.95218 | 1.00000 and 0.46369 |
| Refinement method | Full-matrix least-squares on $F^2$ | Full-matrix least-squares on $F^2$ |
| Data / restraints / parameters | 7114 / 0 / 445 | 7689/0/355 |
| Goodness-of-fit on $F^2$ | 1.033 | 1.100 |
| Final R indices [I>2Sigma(I)] | $R_1 = 0.0352$, $wR_2 = 0.0848$ | $R_1 = 0.0351$, wR2 = 0.0884 |
| R indices (all data) | $R_1 = 0.0507$, $wR_2 = 0.0937$ | $R_1 = 0.0451$, wR2 = 0.0916 |

## 2. Solid state structure of 2b-H, 3a-H, 3b-H, 4a-H, 4b-H, 5a, 6a, 6b, 7a and 7b

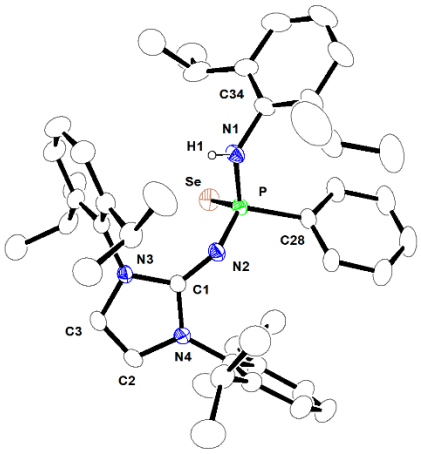


**Figure S1**. The molecular structure of **2b-H** with thermal displacement parameters was drawn at 30% probability. Hydrogen atoms, except H1, are omitted for clarity. Selected bond lengths (Å) and angles (°) are given: P1-N1 1.6754(16), P1-N2 1.5909(16), P1-Se1 2.1094(5), P1-C28 1.819(2), N2-C1 1.305(2), N3-C1 1.371(2), N4-C1 1.359(2), N1-P1-N2 102.78(9), N1-P1-Se1 116.28(6), N2-P1-Se1 116.09(6), C28-P1-Se1 108.55(7), C28-P1-N1 105.41(9), C28-P1-N2 106.87(9), N3-C1-N4 105.69(15).

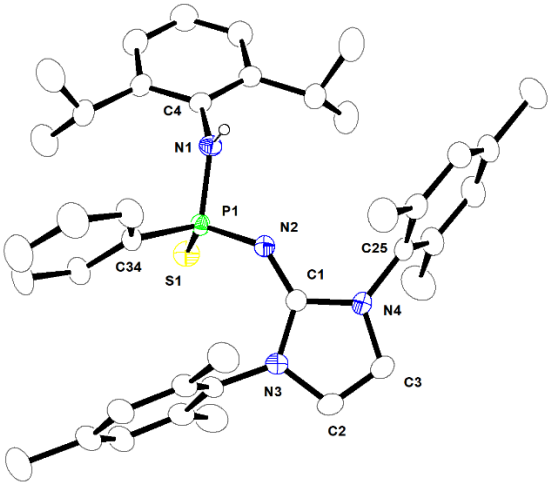


**Figure S2**. The molecular structure of **3a-H** with thermal displacement parameters was drawn at 30% probability. Hydrogen atoms, except H1, are omitted for clarity. Selected bond lengths (Å) and angles (°) are given: P1-N1 1.691(3), P1-N2 1.621(3), P1-S1 2.0970(7) 1.9411(14), P1-C34 1.803(3), N2-C1 1.311(4), N3-C1 1.377(3), N4-C1 1.362(4), N1-P1-N2 98.34(11), N1-P1-S1

113.10(9), N2-P1-S1 119.59(10), C34-P1-S1 112.11(10), C34-P1-N1 103.75(13), C34-P1-N2 108.09(12), N3-C1-N4 104.6(2).

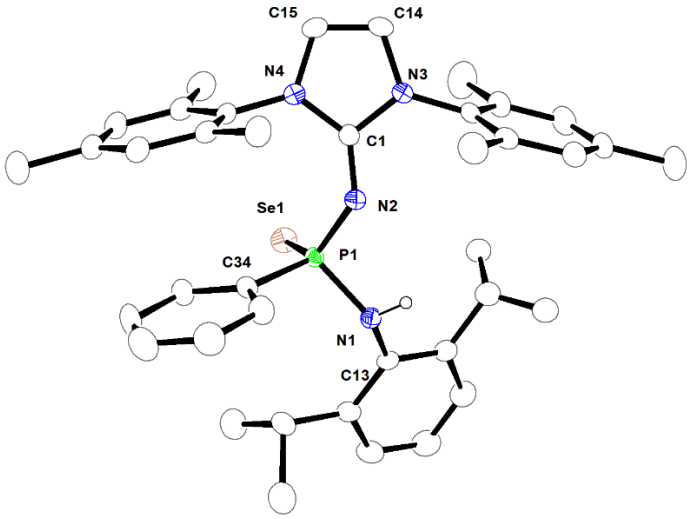


**Figure S3**. The molecular structure of **3b-H** with thermal displacement parameters was drawn at 30% probability. Hydrogen atoms, except H1, are omitted for clarity. Selected bond lengths (Å) and angles (°) are given: P1-N1 1.7019(18), P1-N2 1.6229(18), P1-Se1 2.0972(6), P1-C34 1.824(2), N2-C1 1.304(3), N3-C1 1.369(3), N4-C1 1.373(3), N1-P1-N2 98.25(9), N1-P1-Se1 113.15(7), N2-P1-Se1 118.91(7), C34-P1-Se1 112.82(8), C34-P1-N1 102.90(10), C34-P1-N2 108.81(10), N3-C1-N4 105.22(18).

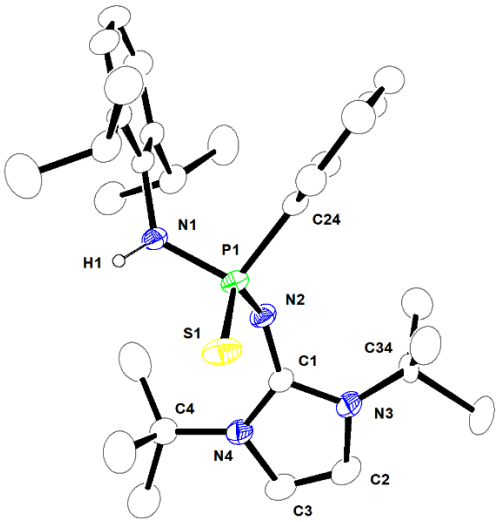


**Figure S4**. The molecular structure of **4a-H** with thermal displacement parameters was drawn at 30% probability. Hydrogen atoms, except H1, are omitted for clarity. Selected bond lengths (Å)

and angles (°) are given: P1-N1 1.693(2), P1-N2 1.596(2), P1-S1 1.9639(9), P1-C24 1.827(2), N2-C1 1.324(3), N3-C1 1.377(3), N4-C1 1.369(3), N1-P1-N2 109.42(11), N1-P1-S1 108.56(8), N2-P1-S1 117.02(8), C24-P1-S1 112.16(8), C24-P1-N1 101.31(10), C24-P1-N2 107.20(11), N3-C1-N4 105.8(2).

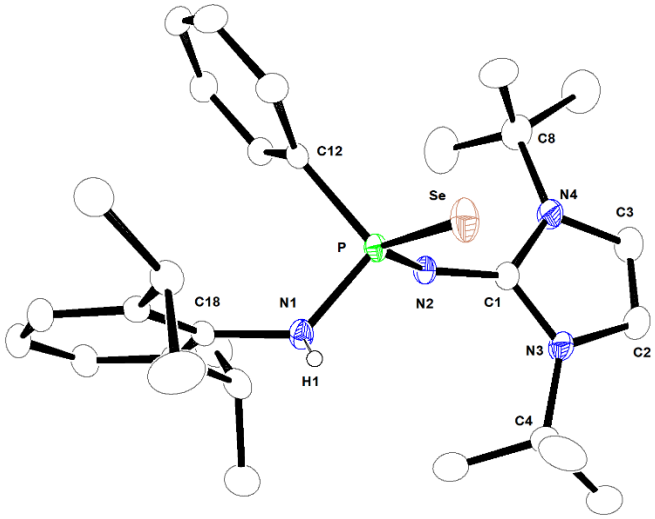


**Figure S5**. The molecular structure of **4b-H** with thermal displacement parameters was drawn at 30% probability. Hydrogen atoms, except H1, are omitted for clarity. Selected bond lengths (Å) and angles (°) are given: P1-N1 1.695(3), P1-N2 1.601(2), P1-Se1 2.1244(8), P1-C12 1.828(3), N2-C1 1.325(4), N3-C1 1.372(4), N4-C1 1.371(4), N1-P1-N2 110.07(13), N1-P1-Se1 107.92(10), N2-P1-Se1 116.79(10), C12-P1-Se1 112.48(10), C12-P1-N1 101.03(13), C12-P1-N2 107.41(14), N3-C1-N4 105.9(3).

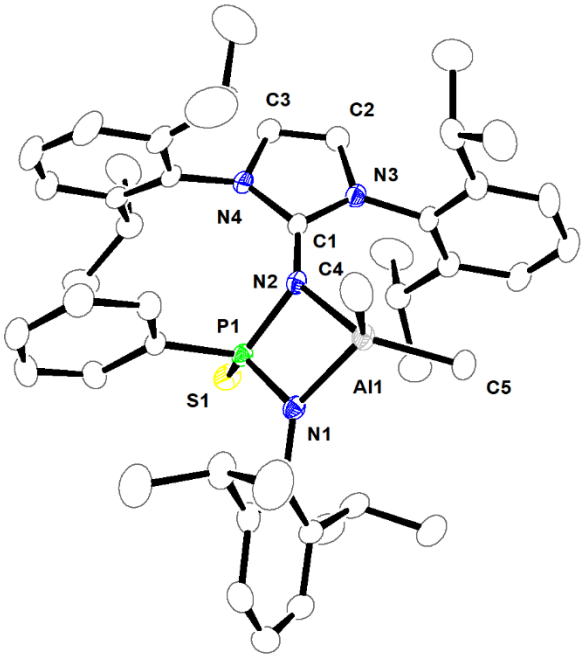


**Figure S6**. The molecular structure of **5a** with thermal displacement parameters was drawn at 30% probability. Hydrogen atoms are omitted for clarity. Selected bond lengths (Å) and angles (°) are given: Al1-N1 1.8824(19), Al1-N2 1.9918(18), Al1-C4 1.971(3), Al1-C5 1.959(3), N2-C1 1.337(3), N3-C1 1.357(3), N4-C1 1.365(3), N1-P1 1.6474(18), N2-P1 1.7050(18), P1-S1 1.9400(8), N1-P1-N2 91.32(9), N1-Al1-N2 76.43(8), N1-Al1-C4 118.95(12), N1-Al1-C5 112.47(11), C4-Al1-C5 112.30(13), N2-Al1-C4 108.30(12), N2-Al1-C5 124.55(10), P1-N1-Al1 99.08(9), P1-N2-Al1 93.05(9), N3-C1-N4 105.14(19).

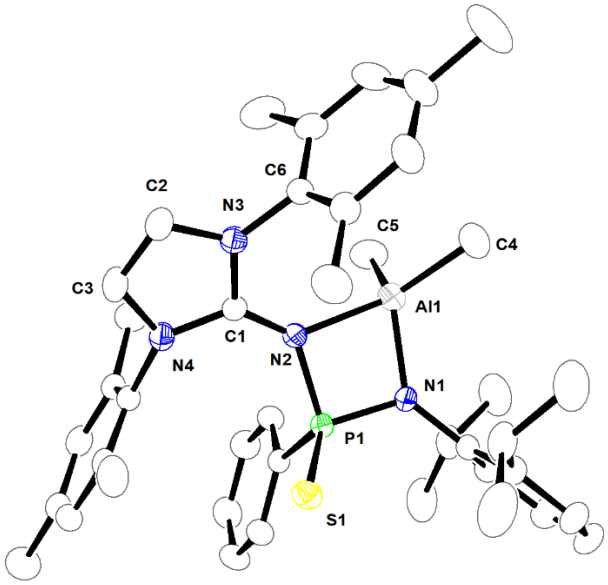

**Figure S7**. The molecular structure of **6a** with thermal displacement parameters was drawn at 30% probability. Hydrogen atoms are omitted for clarity. Selected bond lengths (Å) and angles (°) are given: Al1-N1 1.876(2), Al1-N2 2.024(3), Al1-C4 1.945(4), Al1-C5 1.971(4), N2-C1 1.335(4), N3-C1 1.358(4), N4-C1 1.368(4), N1-P1 1.642(2), N2-P1 1.689(2), P1-S1 1.9364(11), N1-P1-N2 91.21(12), N1-Al1-N2 75.12(10), N1-Al1-C4 111.22(16), N1-Al1-C5 121.09(15), C4-Al1-C5 108.56(19), N2-Al1-C4 131.24(15), N2-Al1-C5 107.57(15), P1-N1-Al1 100.04(12), P1-N2-Al1 92.89(11), N3-C1-N4 105.3(3).

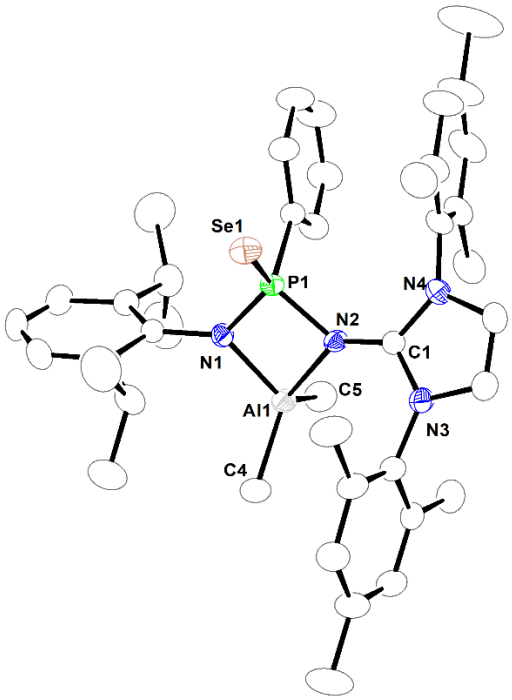


**Figure S8**. The molecular structure of **6b** with thermal displacement parameters was drawn at 30% probability. Hydrogen atoms are omitted for clarity. Selected bond lengths (Å) and angles (°) are given: Al1-N1 1.8900(19), Al1-N2 1.9861(18), Al1-C4 1.945(3), Al1-C5 1.973(3), N2-C1 1.973(3), N3-C1 1.357(3), N4-C1 1.362(3), N1-P2 1.6440(18), N2-P2 1.7005(18), P2-Se1 2.0871(6), N1-P2-N2 91.04(9), N1-Al1-N2 75.97(8), N1-Al1-C4 113.46(11), N1-Al1-C5 118.45(11), C4-Al1-C5 111.22(13), N2-Al1-C4 124.80(11), N2-Al1-C5 109.35(11), P2-N1-Al1 98.97(9), P2-N2-Al1 93.46(8), N3-C1-N4 105.10(19).

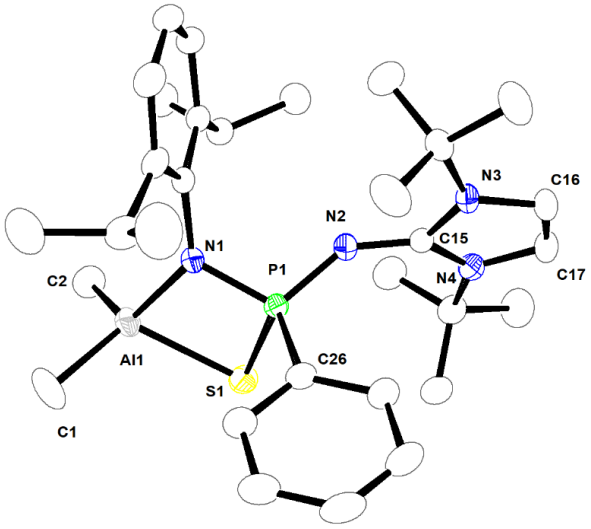


**Figure S9**. The molecular structure of **7a** with thermal displacement parameters was drawn at 30% probability. Hydrogen atoms are omitted for clarity.

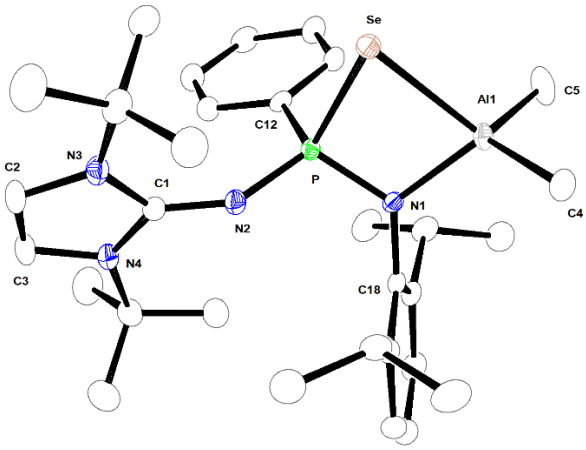


**Figure S10**. The molecular structure of **7b** with thermal displacement parameters was drawn at 30% probability. Hydrogen atoms are omitted for clarity. Selected bond lengths (Å) and angles (°) are given: Al1-N1 1.8989(15), Al1-Se1 2.4767(5), Al1-C4 1.9581(19), Al1-C5 1.964(2), N2-C1 1.318(2), N3-C1 1.382(2), N4-C1 1.375(2), N1-P1 1.6337(14), N2-P1 1.5780(16), P1-Se1 2.2270(5), N1-P1-Se1 95.75(6), N1-Al1-Se1 81.55(5), N1-Al1-C4 116.02(8), N1-Al1-C5 117.35(8), C4-Al1-C5 111.20(9), Se1-Al1-C4 113.69(6), Se1-Al1-C5 114.10(7), P1-N1-Al1 106.99(8), P1-Se1-Al1 74.190(18), N3-C1-N4 105.92(15).

## 3. NMR spectra of ligands 2a-H, 2b-H, 3a-H, 3b-H, 4a-H and 4b-H

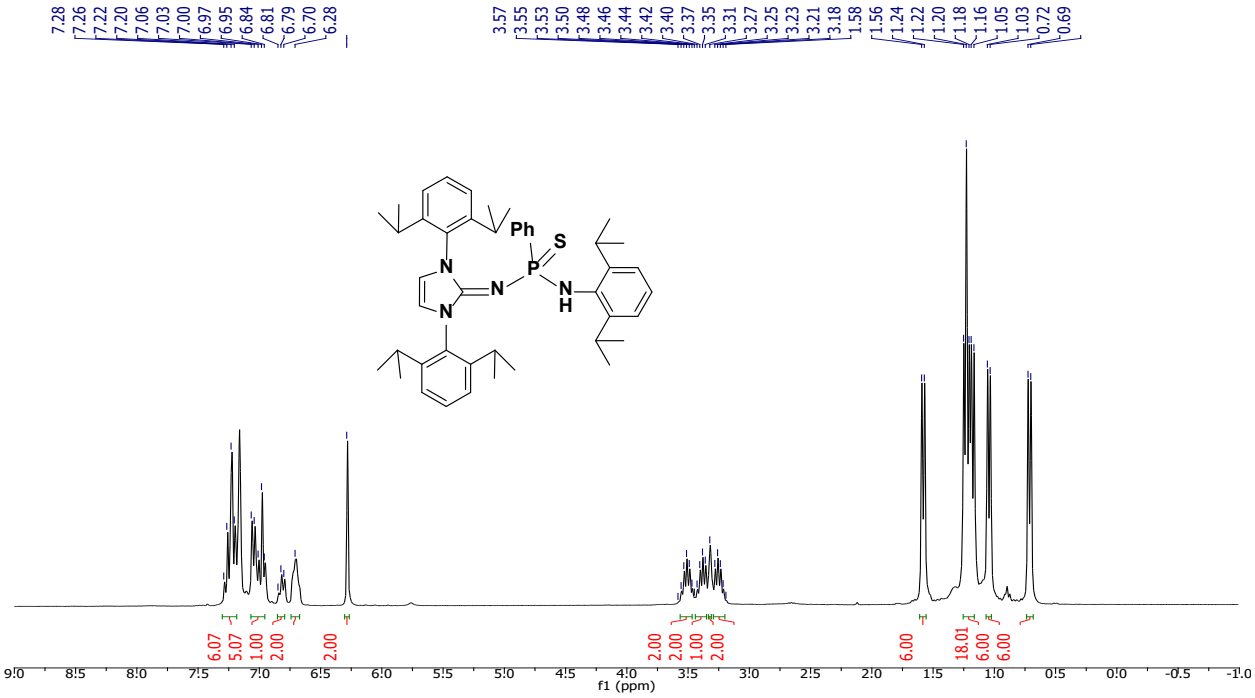


**Figure S11**. $^{1}H$ NMR (300 MHz, $C_6D_6$, 298 K) spectrum of **2a-H**.

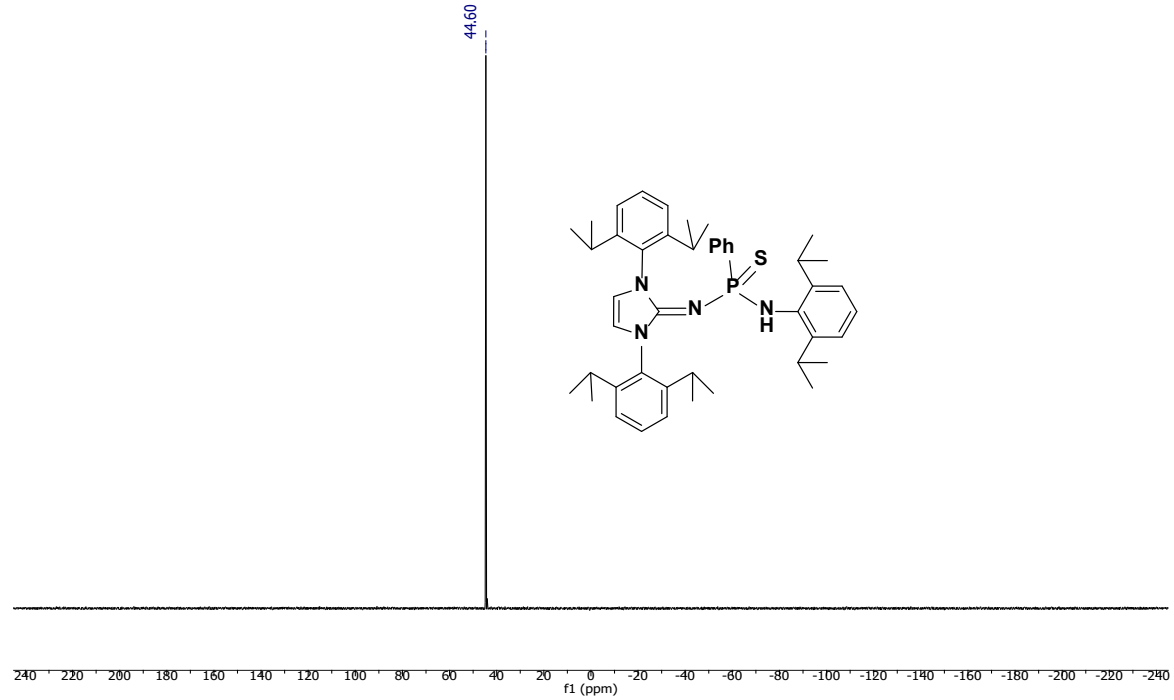


**Figure S12**. $^{31}P\{^{1}H\}$ NMR (121.5 MHz, $C_6D_6$, 298 K) spectrum of **2a-H**.

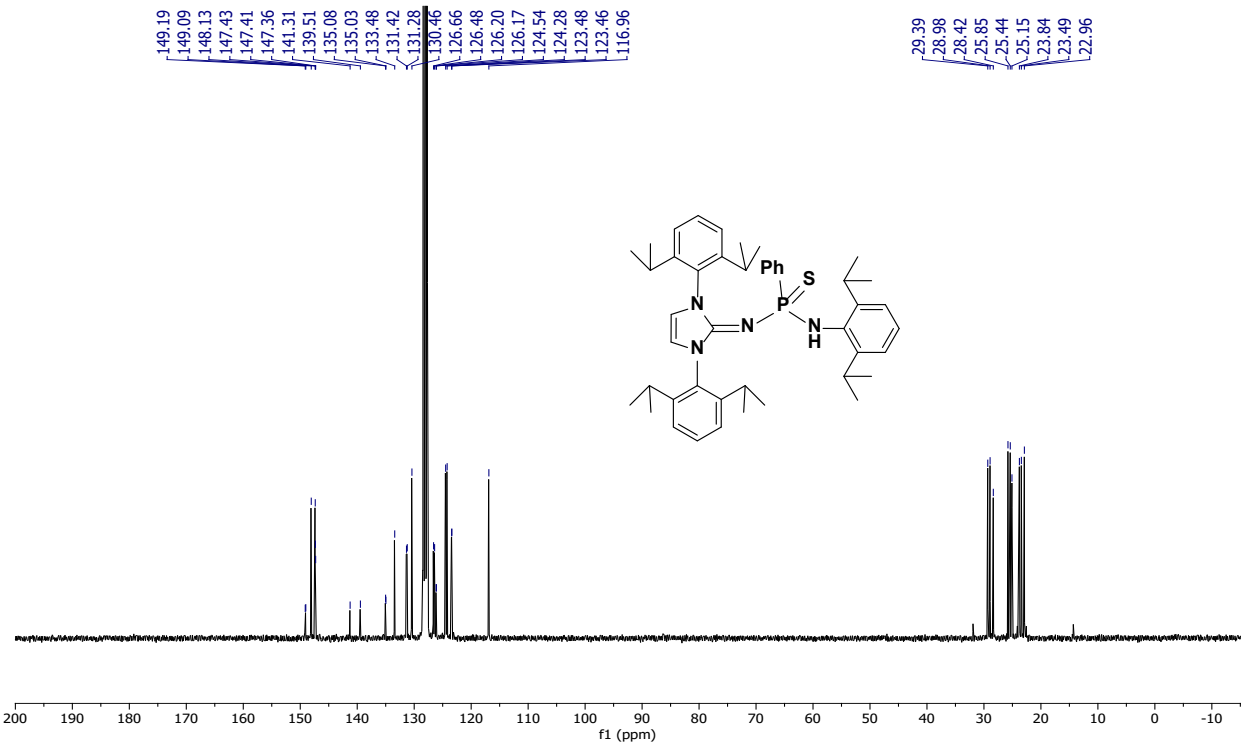


**Figure S13**. $^{13}C\{^{1}H\}$ NMR (75 MHz, $C_6D_6$, 298 K) spectrum of **2a-H**.

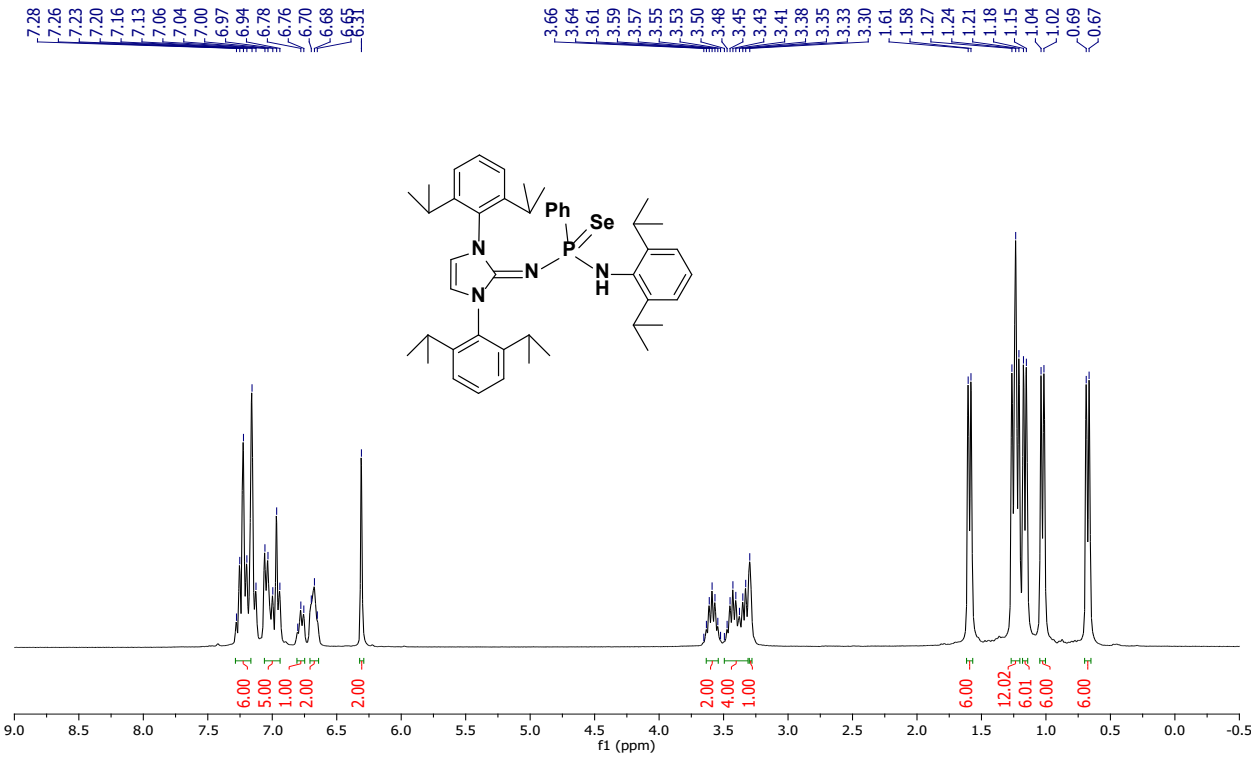


**Figure S14**. $^{1}H$ NMR (300 MHz, $C_6D_6$, 298 K) spectrum of **2b-H**.

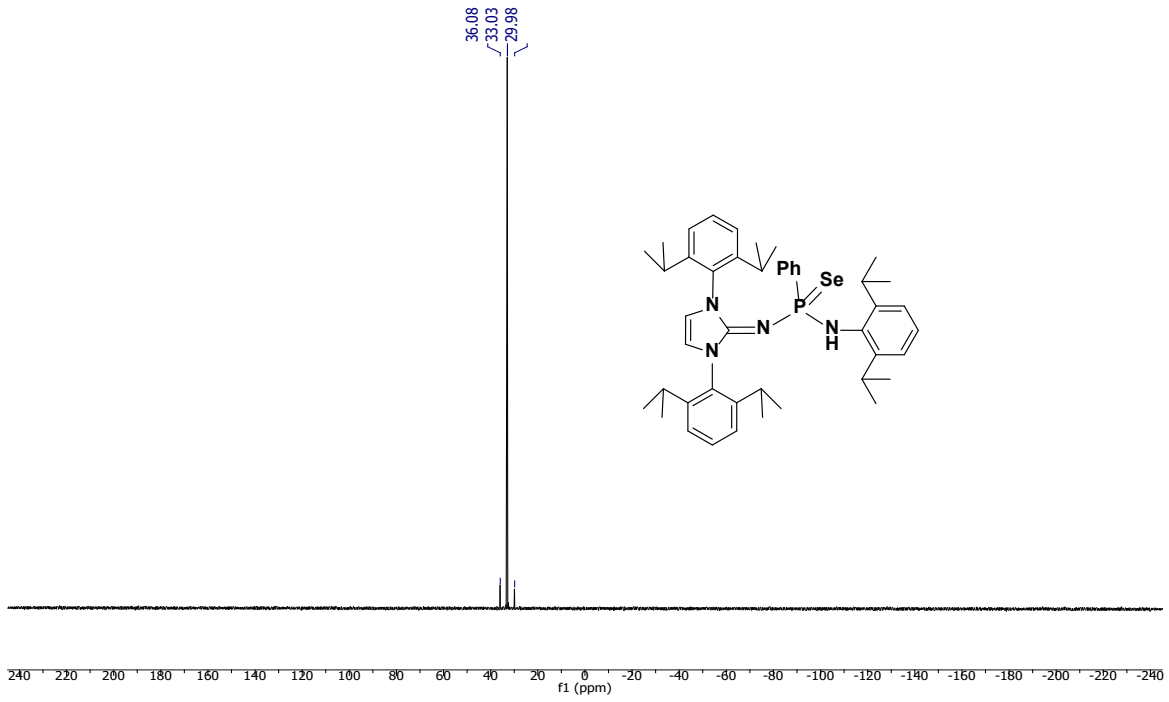


**Figure S15**. $^{31}P\{^{1}H\}$ NMR (121.5 MHz, $C_6D_6$, 298 K) spectrum of **2b-H**.

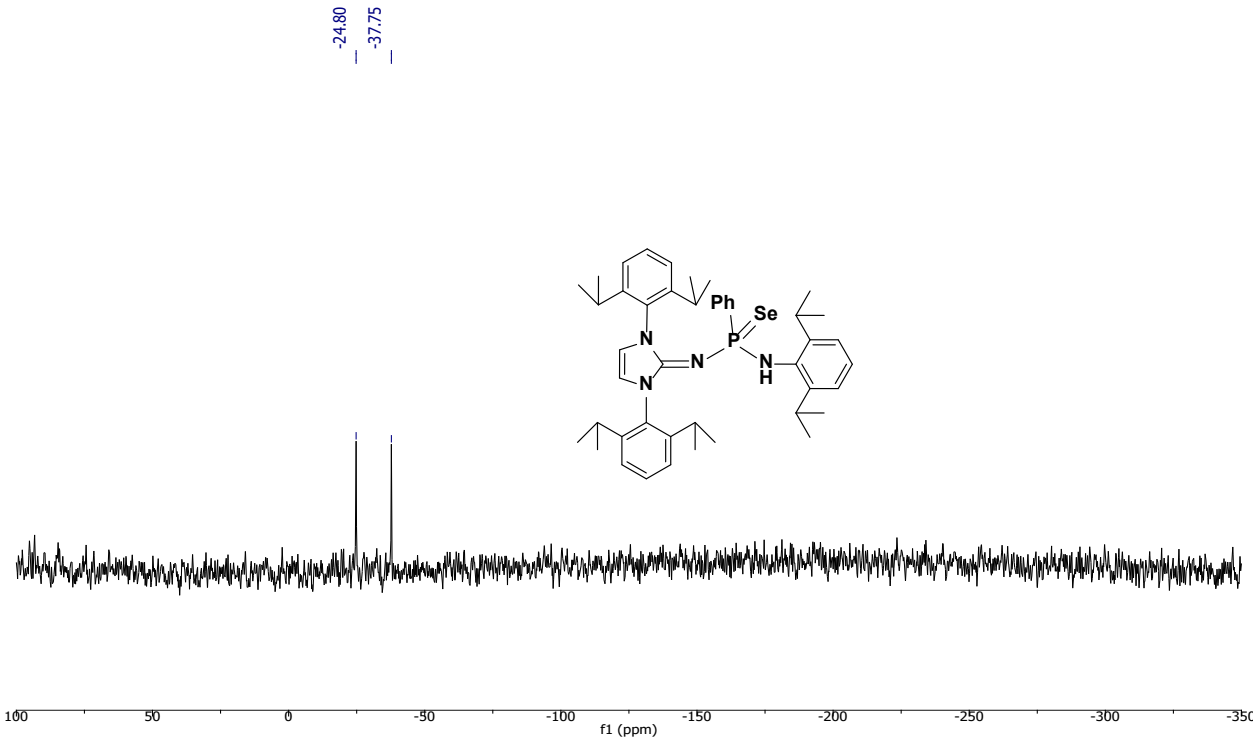


**Figure S16**. $^{77}Se\{^{1}H\}$ NMR (57.36 MHz, $C_6D_6$, 298 K) spectrum of **2b-H**.

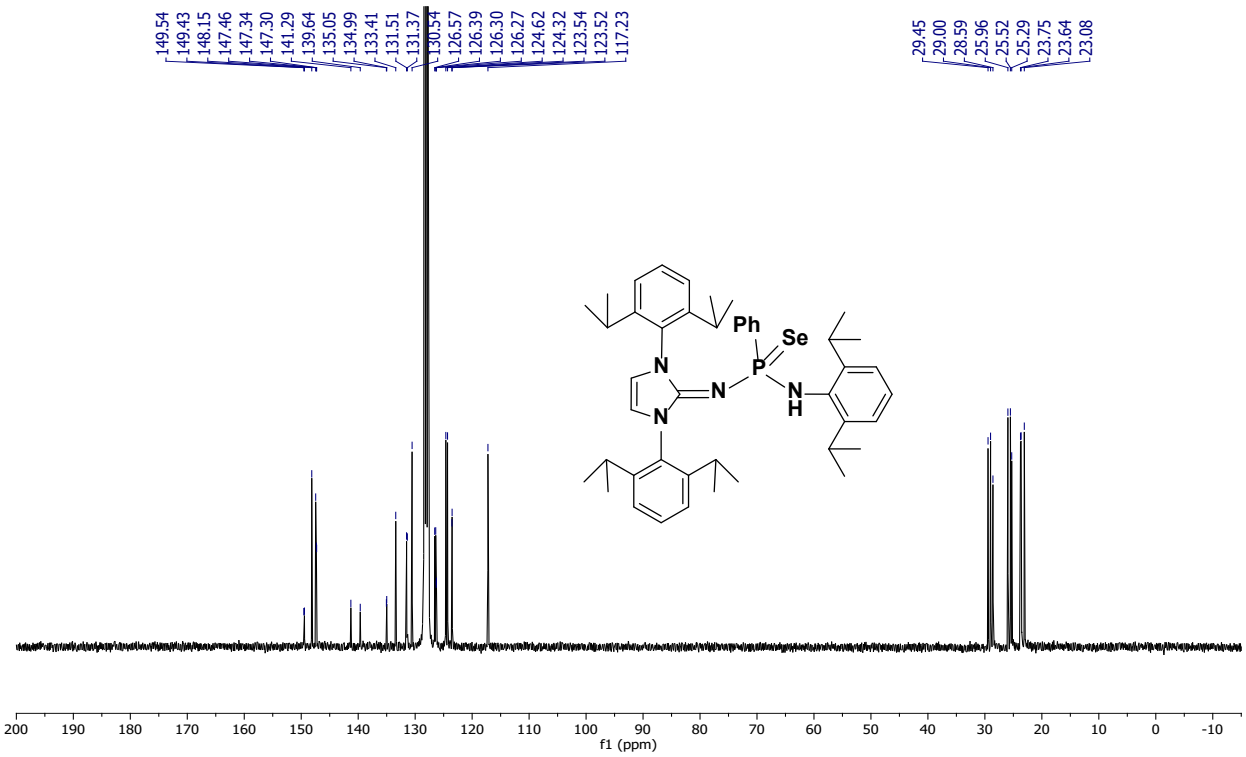


**Figure S17**. $^{13}C\{^{1}H\}$ NMR (75 MHz, $C_6D_6$, 298 K) spectrum of **2b-H**.

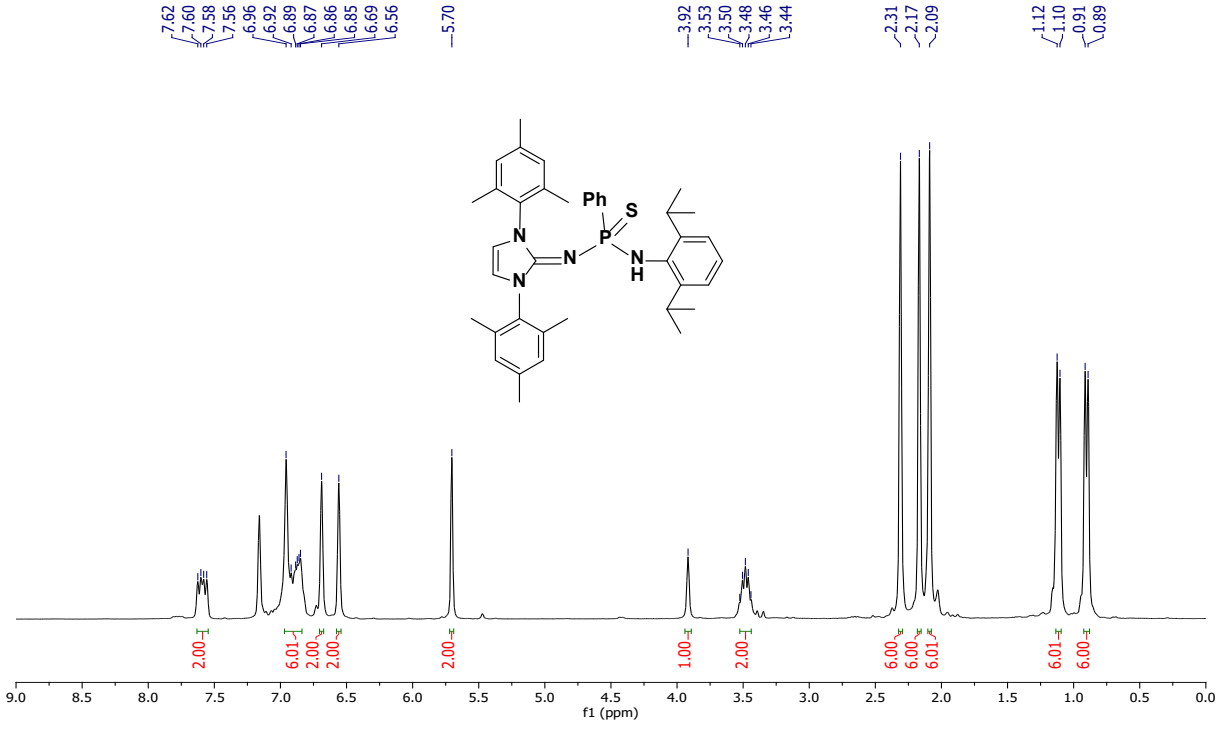


**Figure S18**. $^{1}H$ NMR (300 MHz, $C_6D_6$, 298 K) spectrum of **3a-H**.

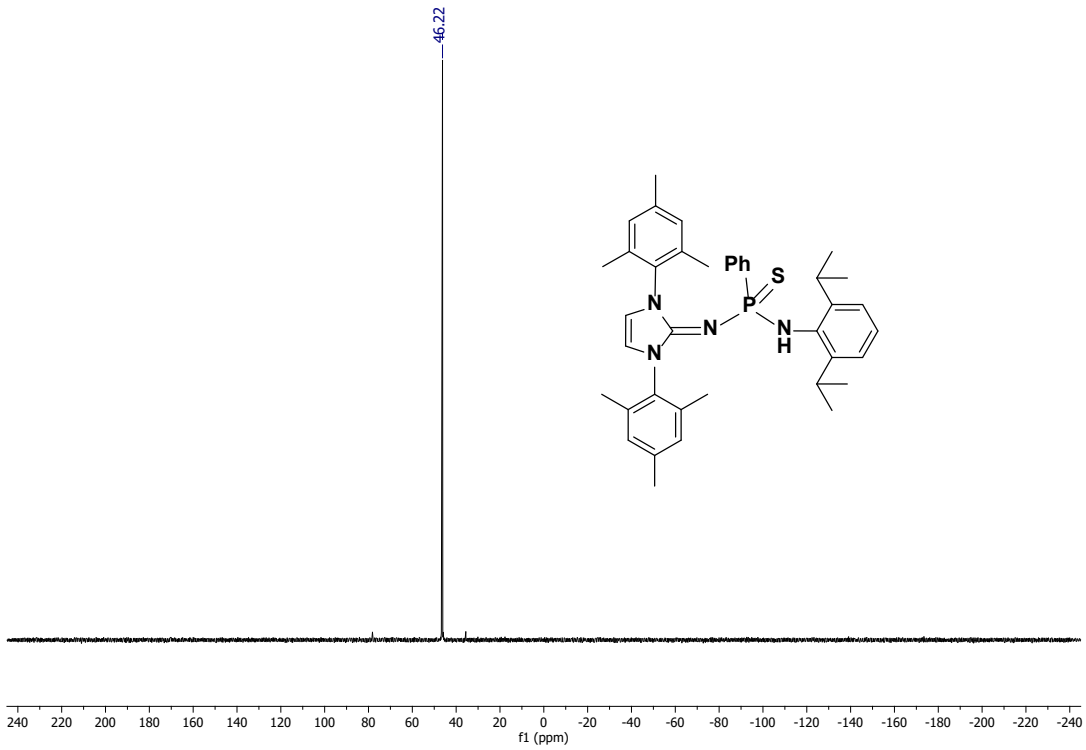


**Figure S19**. $^{31}P\{^{1}H\}$ NMR (121.5 MHz, $C_6D_6$, 298 K) spectrum of **3a-H**.

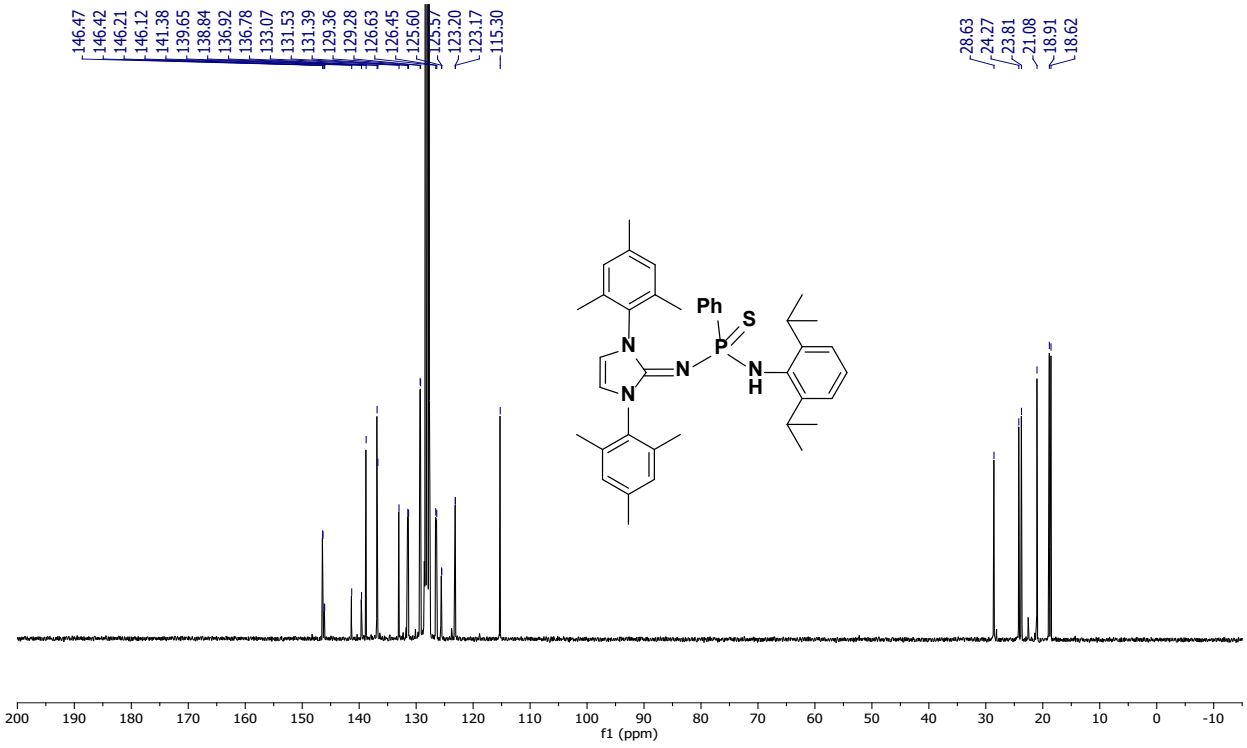


**Figure S20**. $^{13}C\{^{1}H\}$ NMR (75 MHz, $C_6D_6$, 298 K) spectrum of **3a-H**.

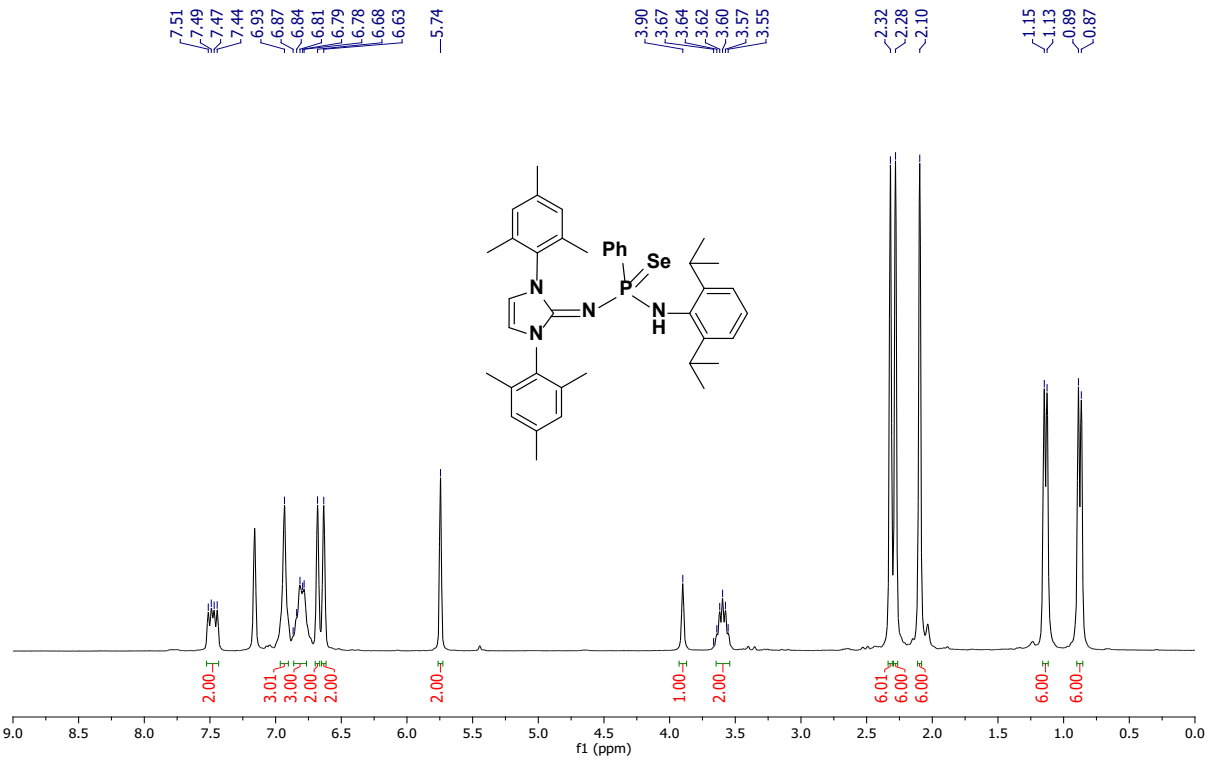


**Figure S21**. $^{1}$H NMR (300 MHz, $C_6D_6$, 298 K) spectrum of **3b-H**.


**Figure S22**. $^{31}$P{$^{1}$H} NMR (121.5 MHz, $C_6D_6$, 298 K) spectrum of **3b-H**.

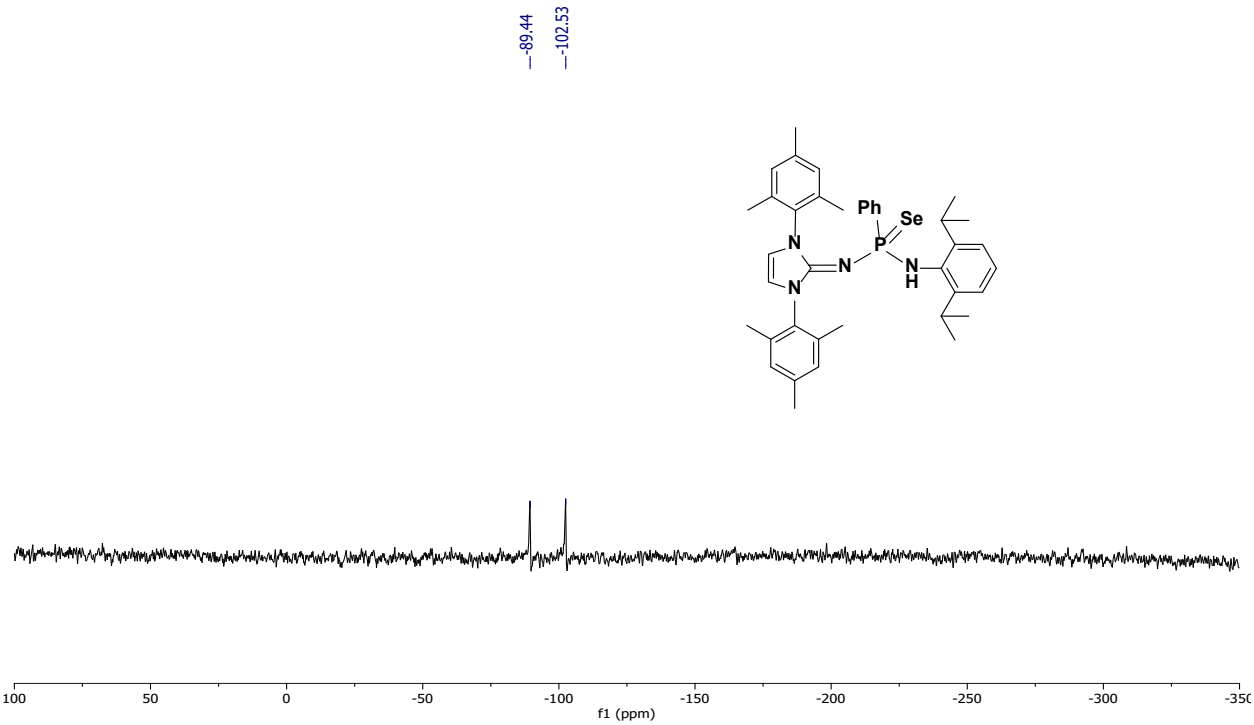


**Figure S23**. $^{77}Se\{^{1}H\}$ NMR (57.36 MHz, $C_6D_6$, 298 K) spectrum of **3b-H**.

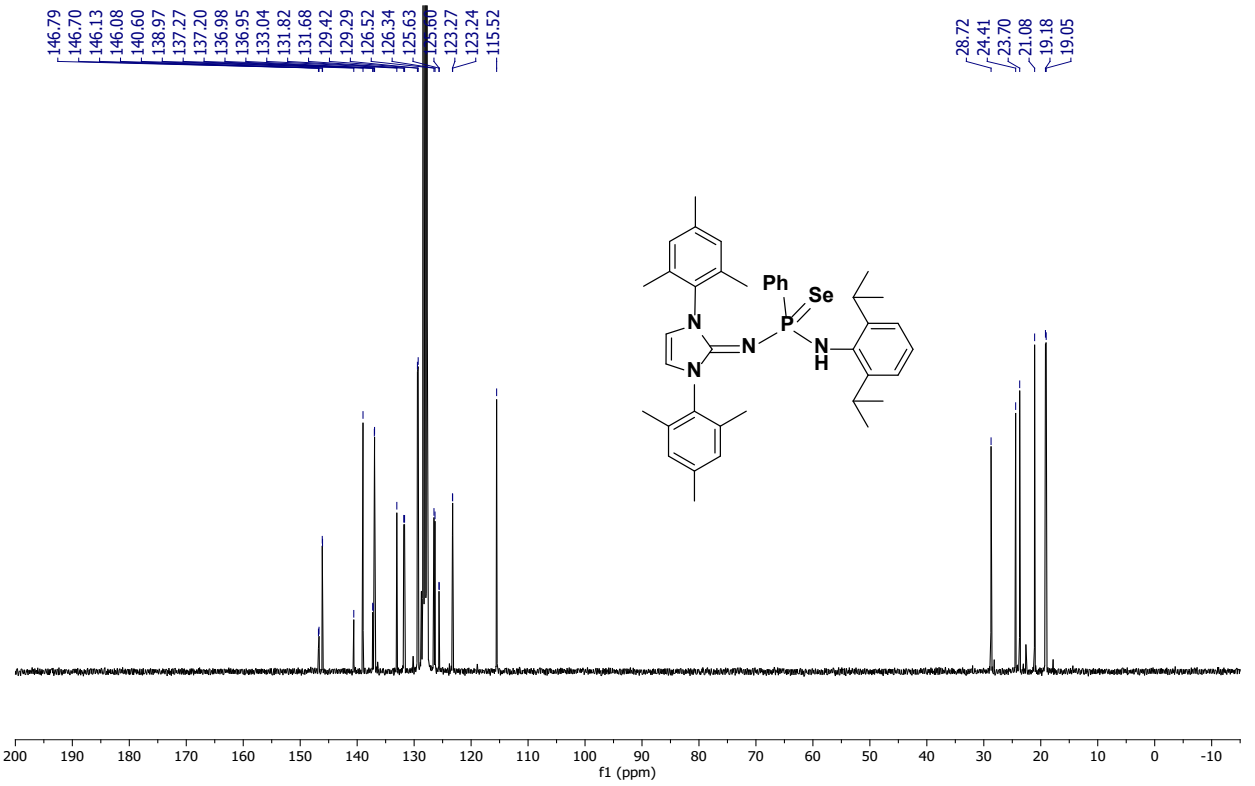


**Figure S24**. $^{13}C\{^{1}H\}$ NMR (75 MHz, $C_6D_6$, 298 K) spectrum of **3b-H**.

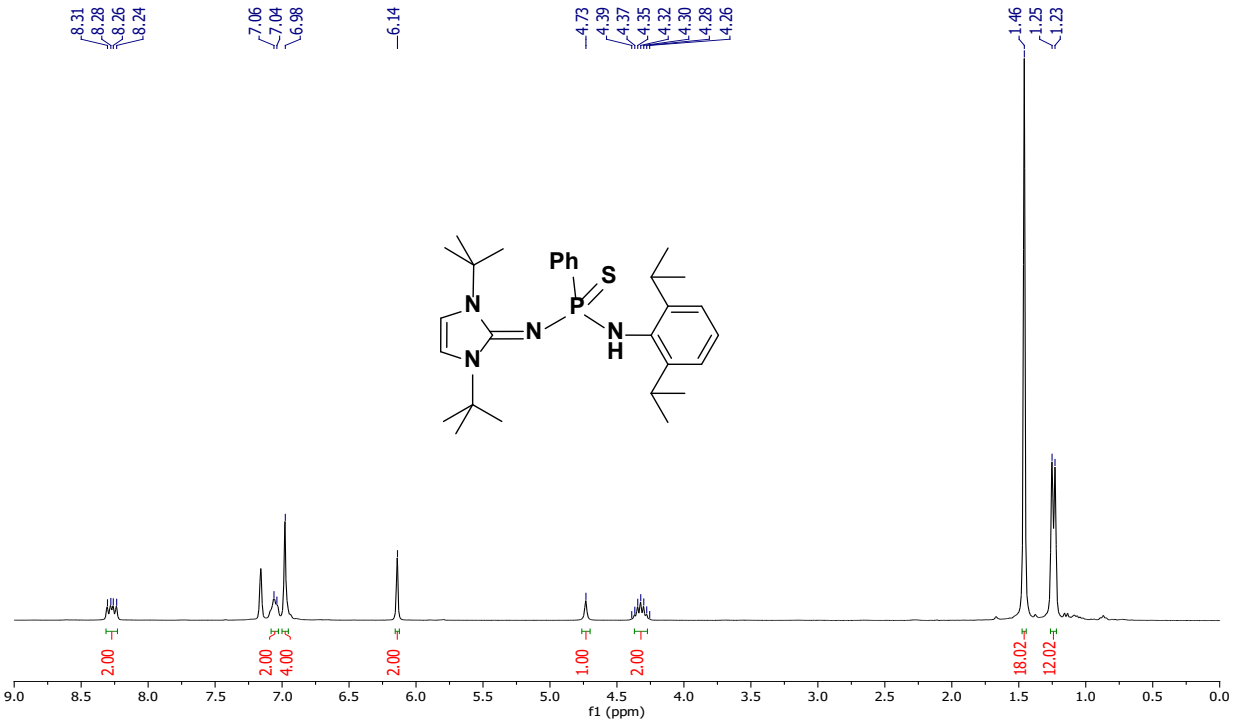


**Figure S25**. $^{1}$H NMR (300 MHz, $C_6D_6$, 298 K) spectrum of **4a-H**.

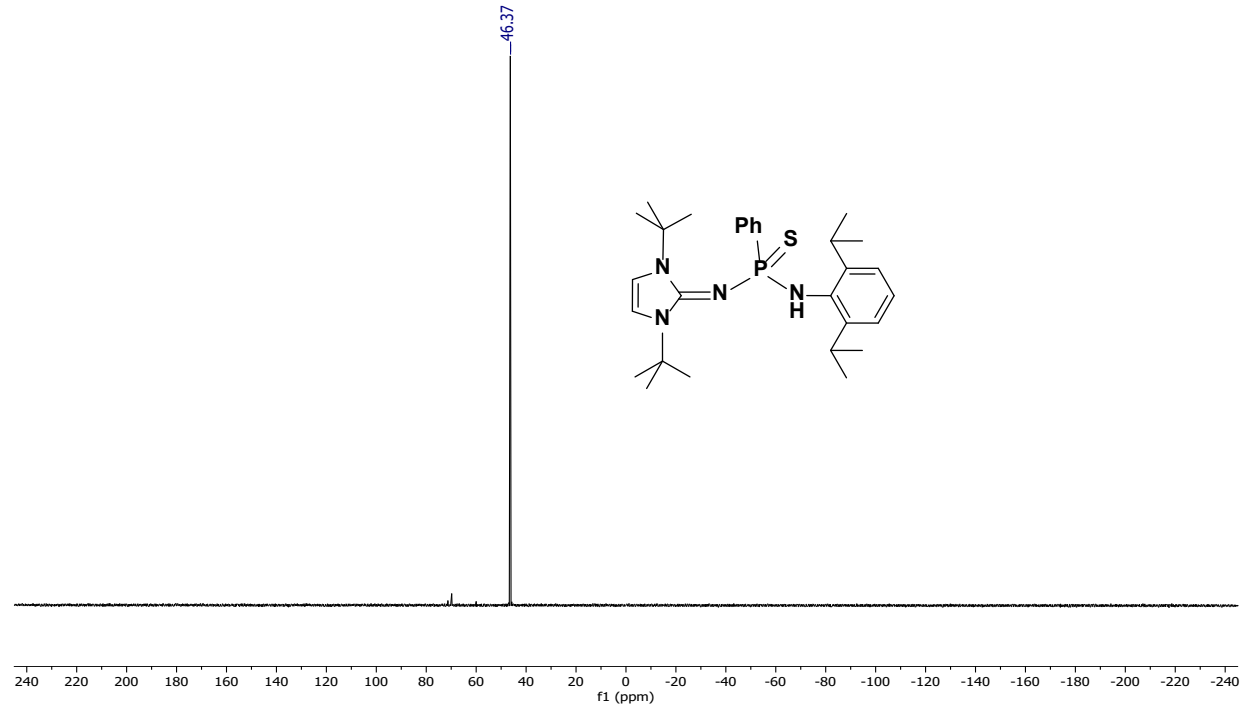


**Figure S26**. $^{31}$P{$^{1}$H} NMR (121.5 MHz, $C_6D_6$, 298 K) spectrum of **4a-H**.

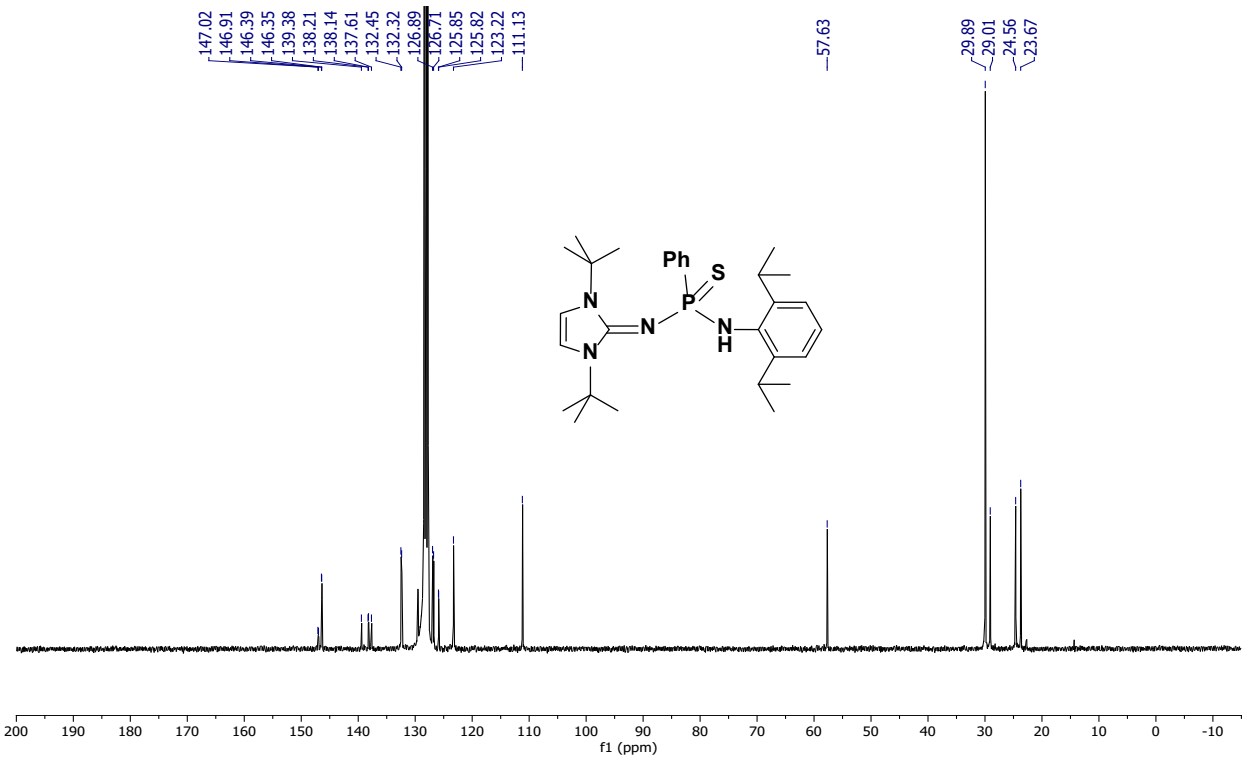


**Figure S27**. $^{13}C\{^{1}H\}$ NMR (75 MHz, $C_6D_6$, 298 K) spectrum of **4a-H**.

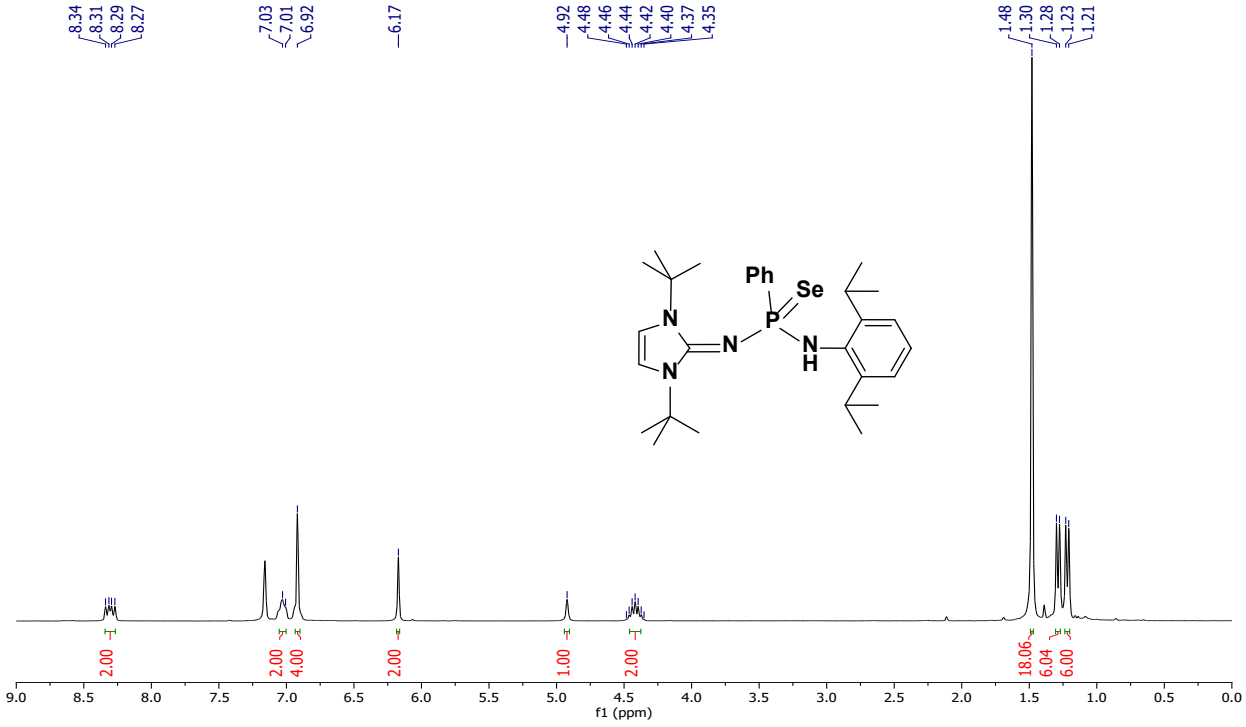


**Figure S28**. $^{1}H$ NMR (300 MHz, $C_6D_6$, 298 K) spectrum of **4b-H**.

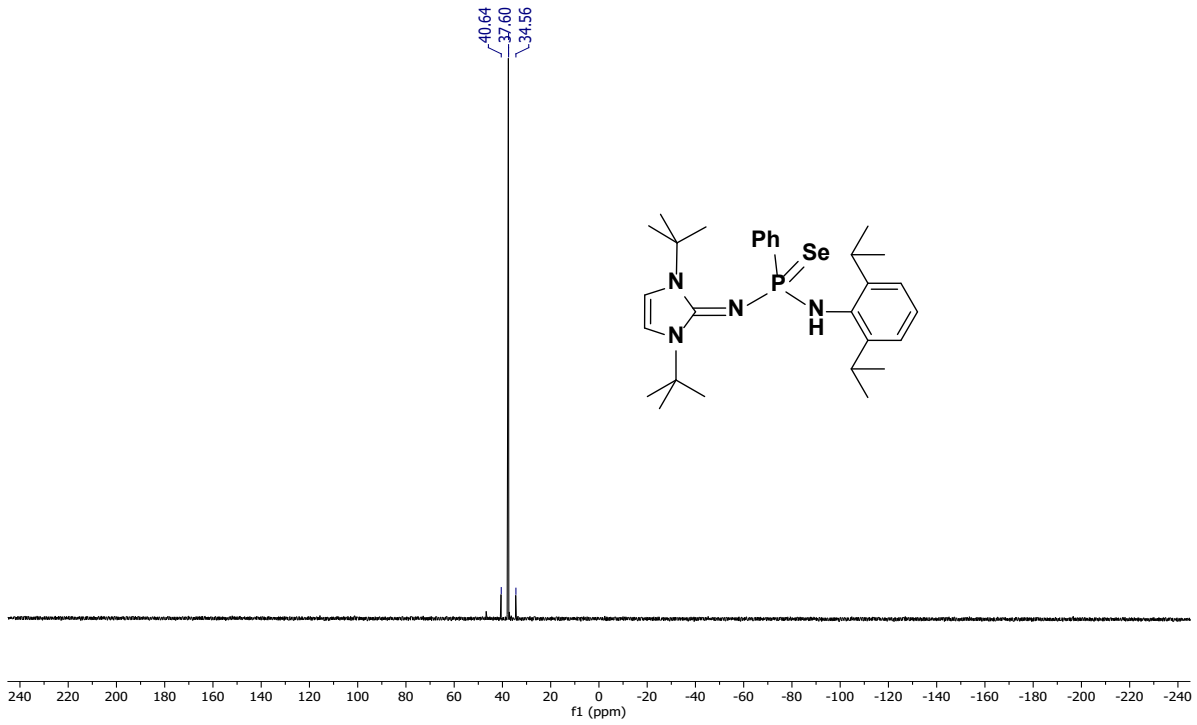


**Figure S29**. $^{31}P\{^{1}H\}$ NMR (121.5 MHz, $C_6D_6$, 298 K) spectrum of **4b-H**.

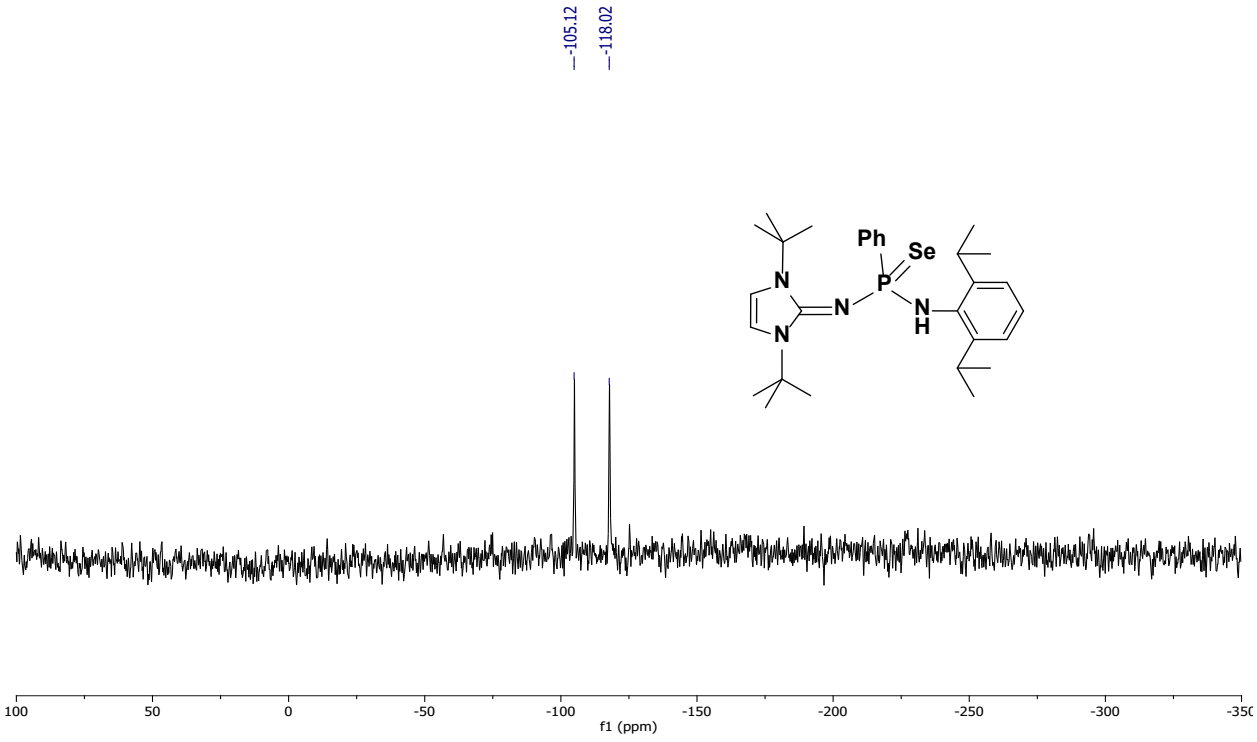


**Figure S30**. $^{77}Se\{^{1}H\}$ NMR (57.36 MHz, $C_6D_6$, 298 K) spectrum of **4b-H**.

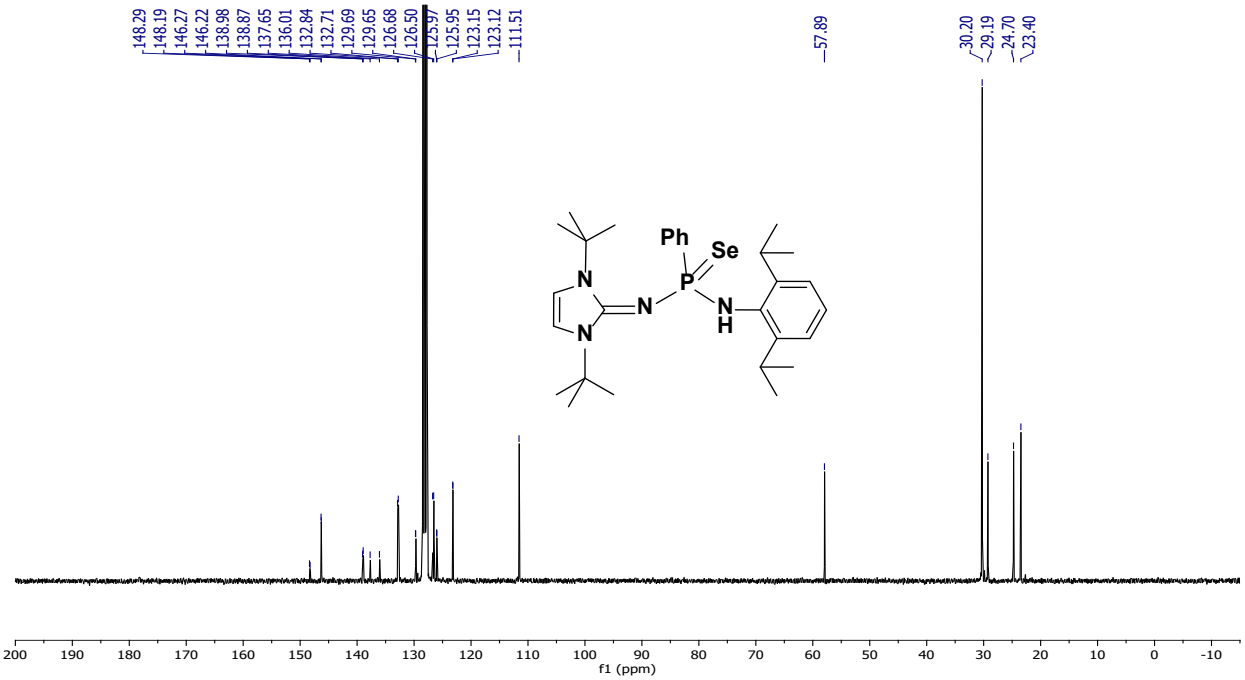


**Figure S31**. $^{13}C\{^{1}H\}$ NMR (75 MHz, $C_6D_6$, 298 K) spectrum of **4b-H**.

## 4. NMR spectra of metal complexes 5a, 5b, 6a, 6b, 7a and 7b:

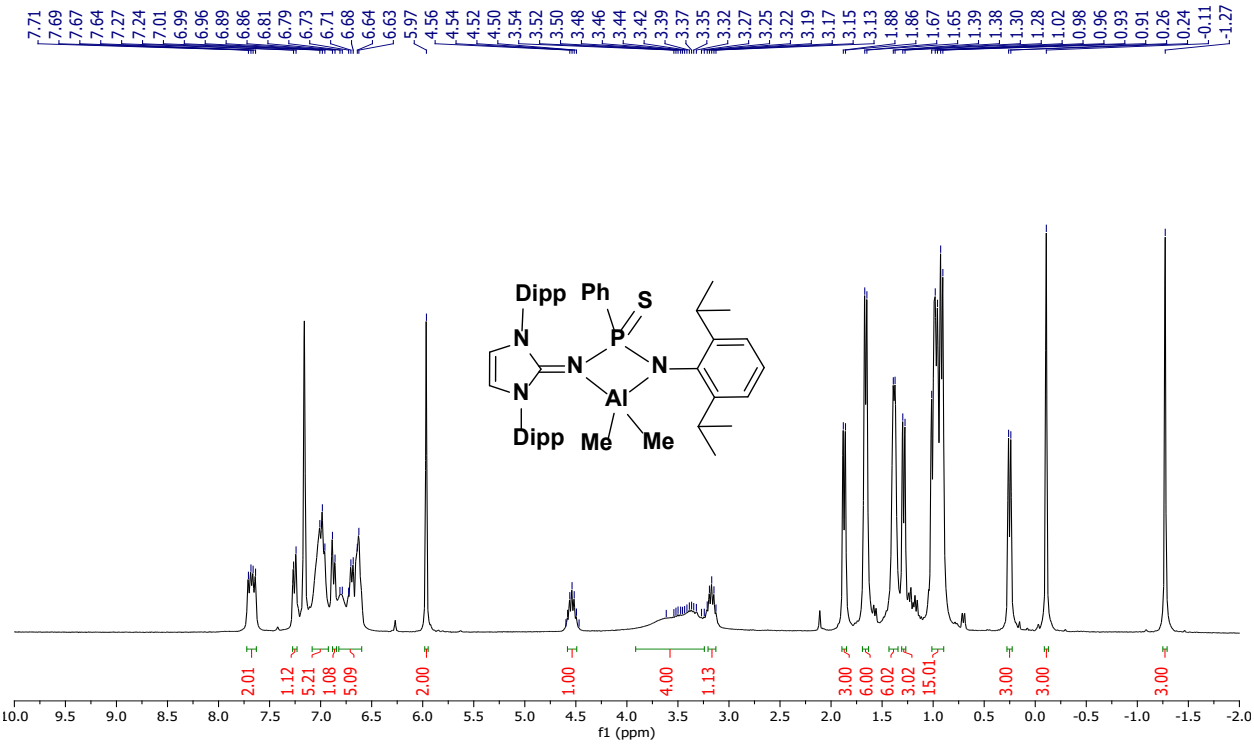


**Figure S32**. $^{1}H$ NMR (300 MHz, $C_6D_6$, 298 K) spectrum of **5a**.

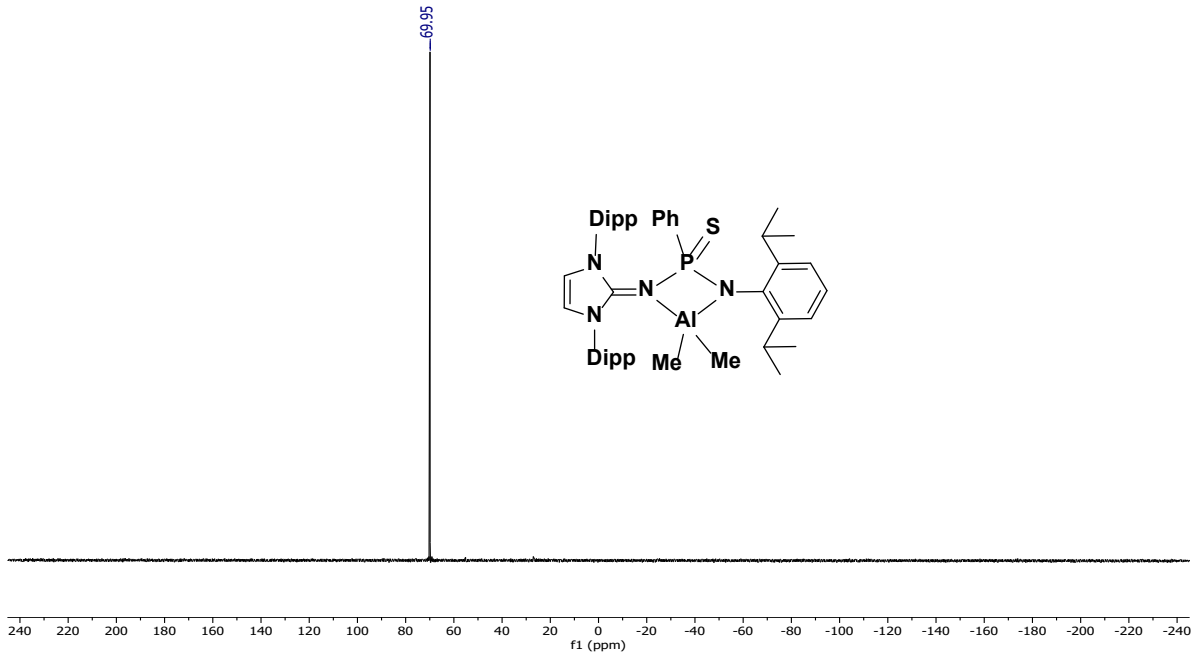


**Figure S33**. $^{31}P\{^{1}H\}$ NMR (121.5 MHz, $C_6D_6$, 298 K) spectrum of **5a**.

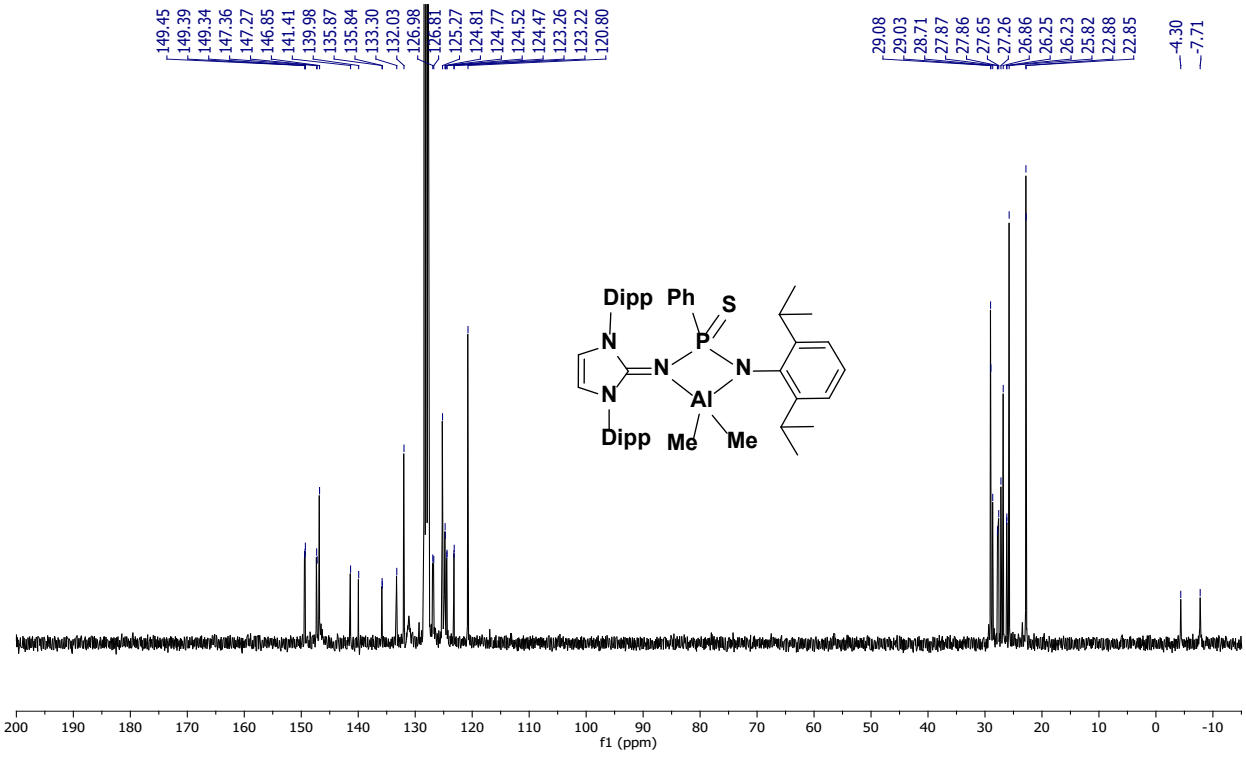


**Figure S34**. $^{13}C\{^{1}H\}$ NMR (75 MHz, $C_6D_6$, 298 K) spectrum of **5a**.

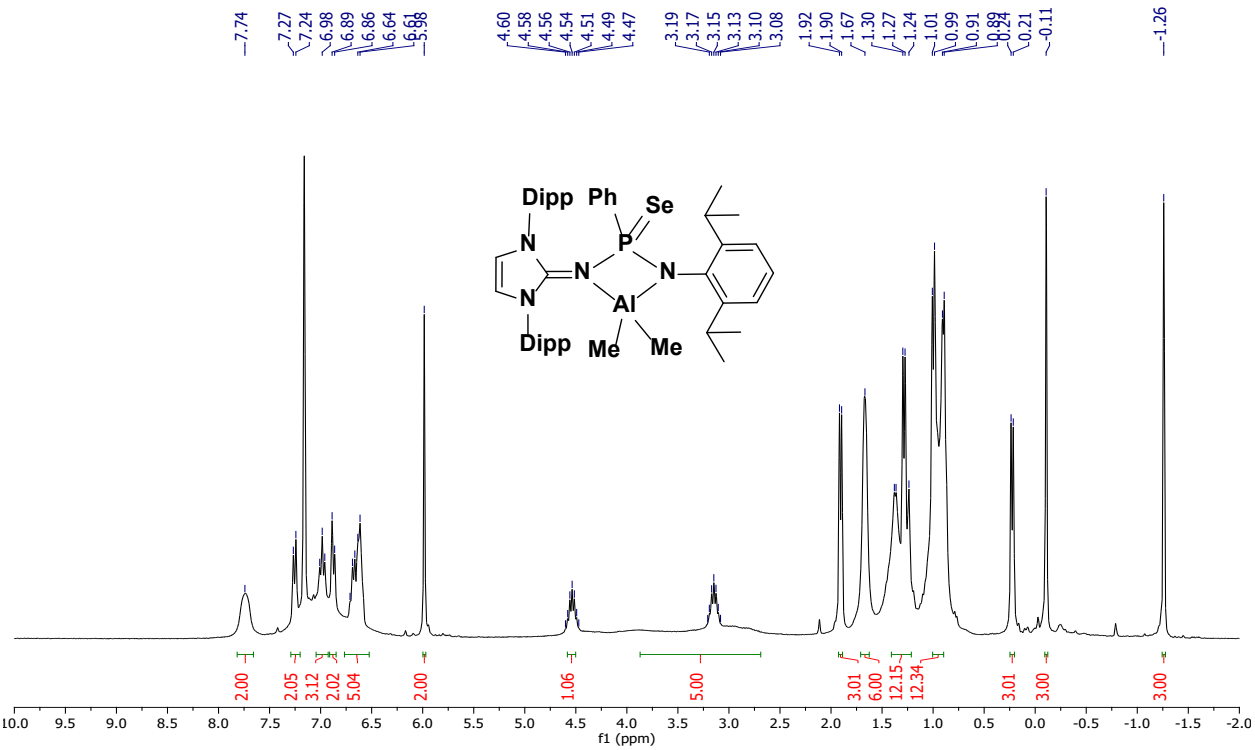


**Figure S35**. $^{1}H$ NMR (300 MHz, $C_6D_6$, 298 K) spectrum of **5b**.

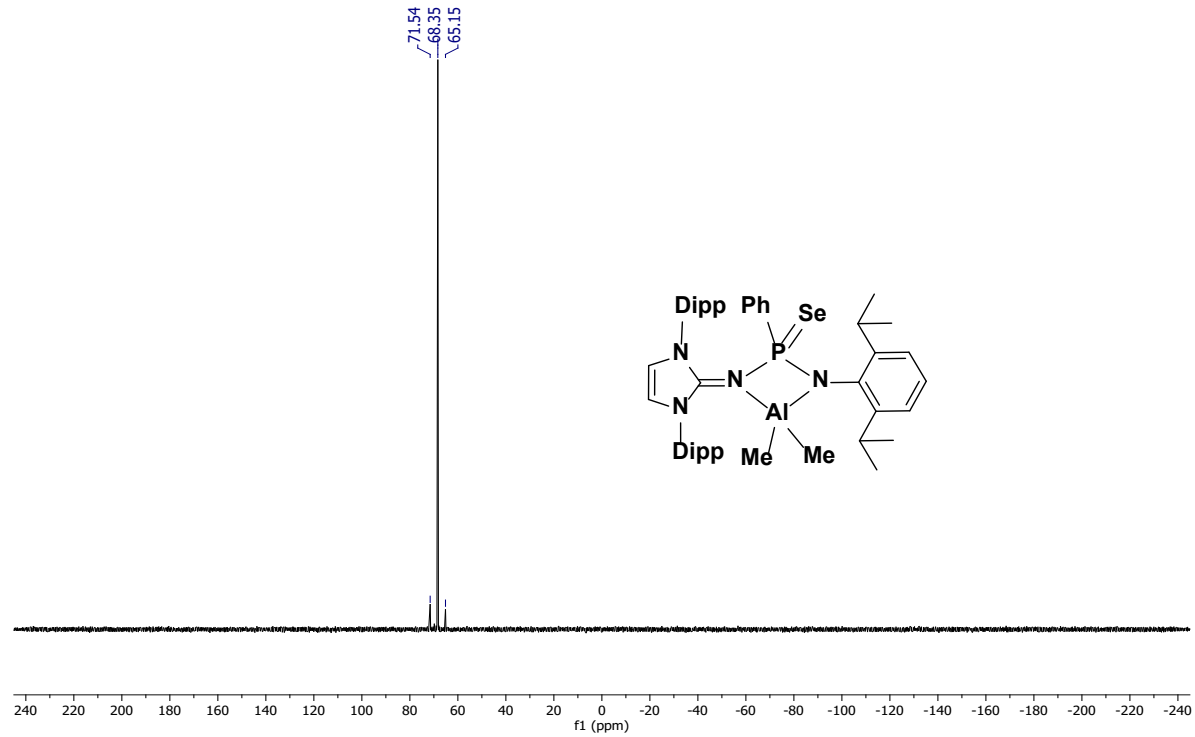


**Figure S36**. $^{31}P\{^{1}H\}$ NMR (121.5 MHz, $C_6D_6$, 298 K) spectrum of **5b**.

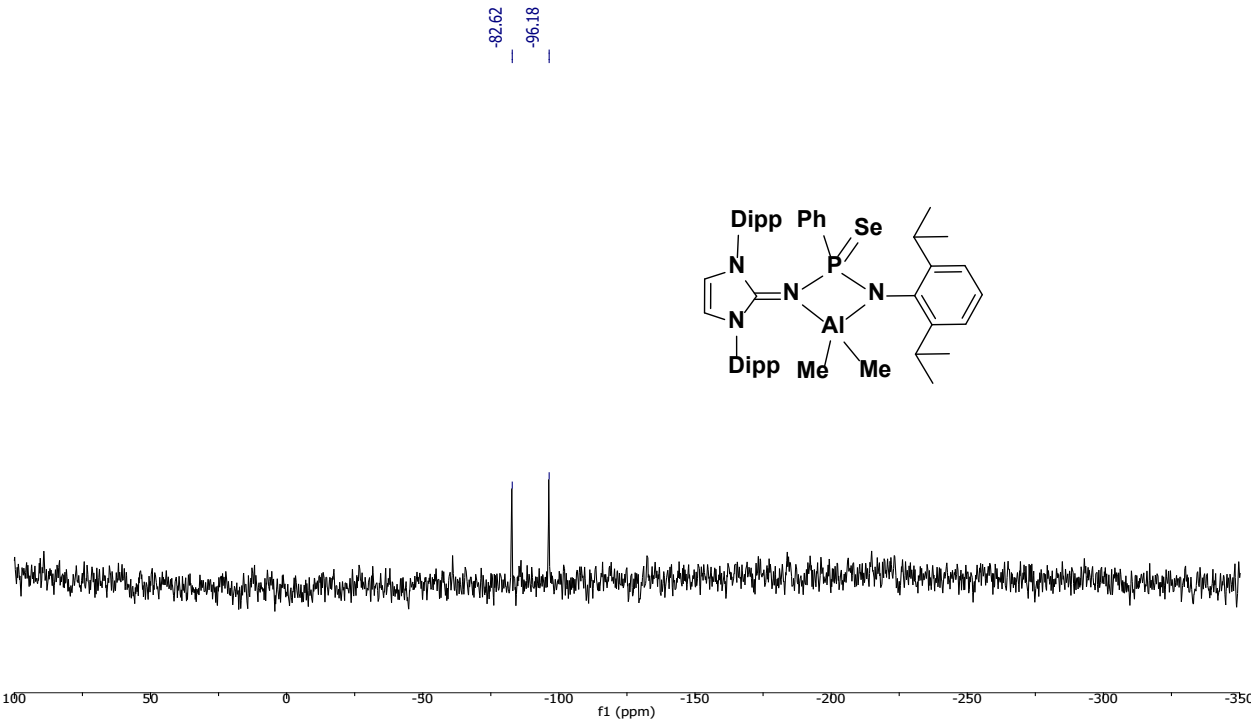


**Figure S37**. $^{77}Se\{^{1}H\}$ NMR (57.36 MHz, $C_6D_6$, 298 K) spectrum of **5b**.

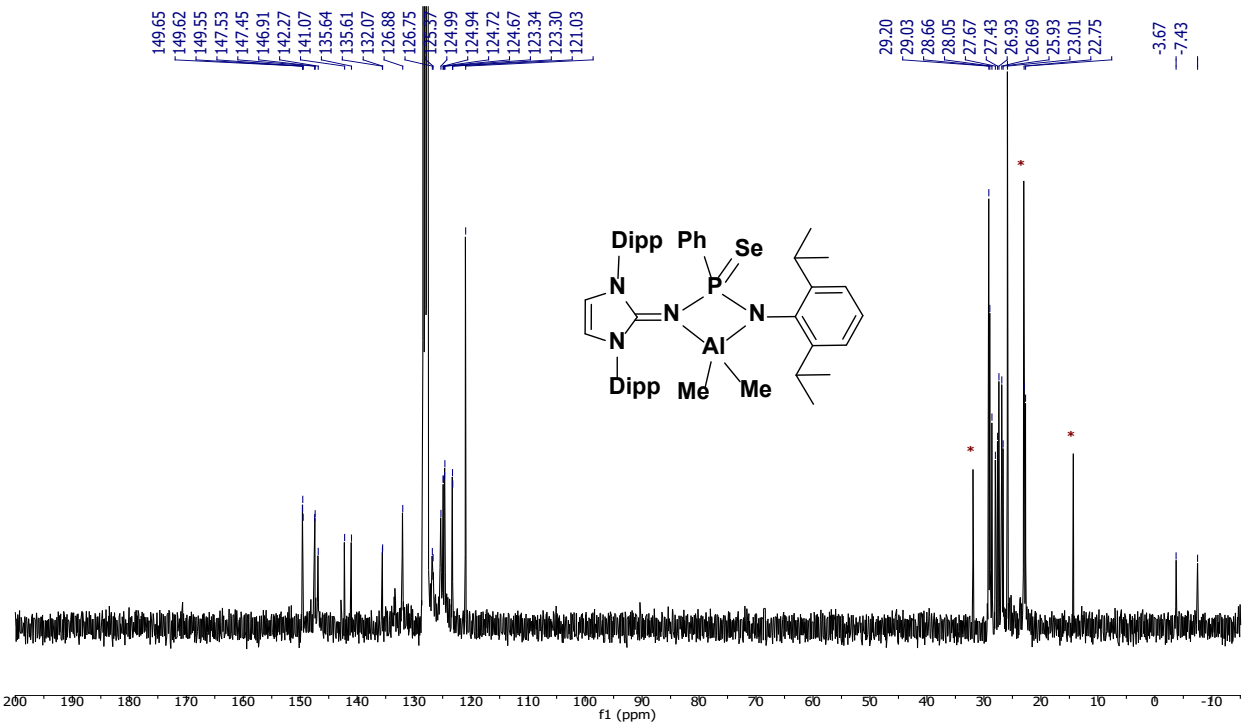


**Figure S38**. $^{13}C\{^{1}H\}$ NMR (75 MHz, $C_6D_6$, 298 K) spectrum of **5b** (* n-Hexane).

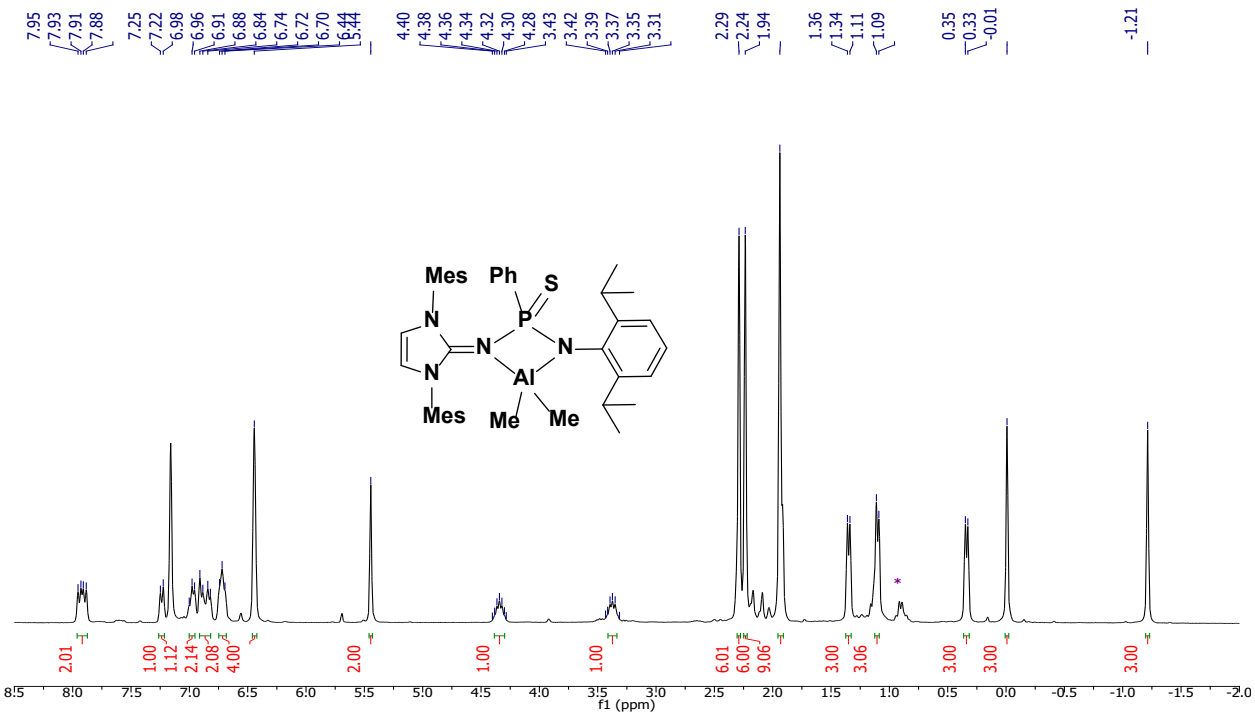


**Figure S39**. $^{1}H$ NMR (300 MHz, $C_6D_6$, 298 K) spectrum of **6a** (* n-Hexane)**.**

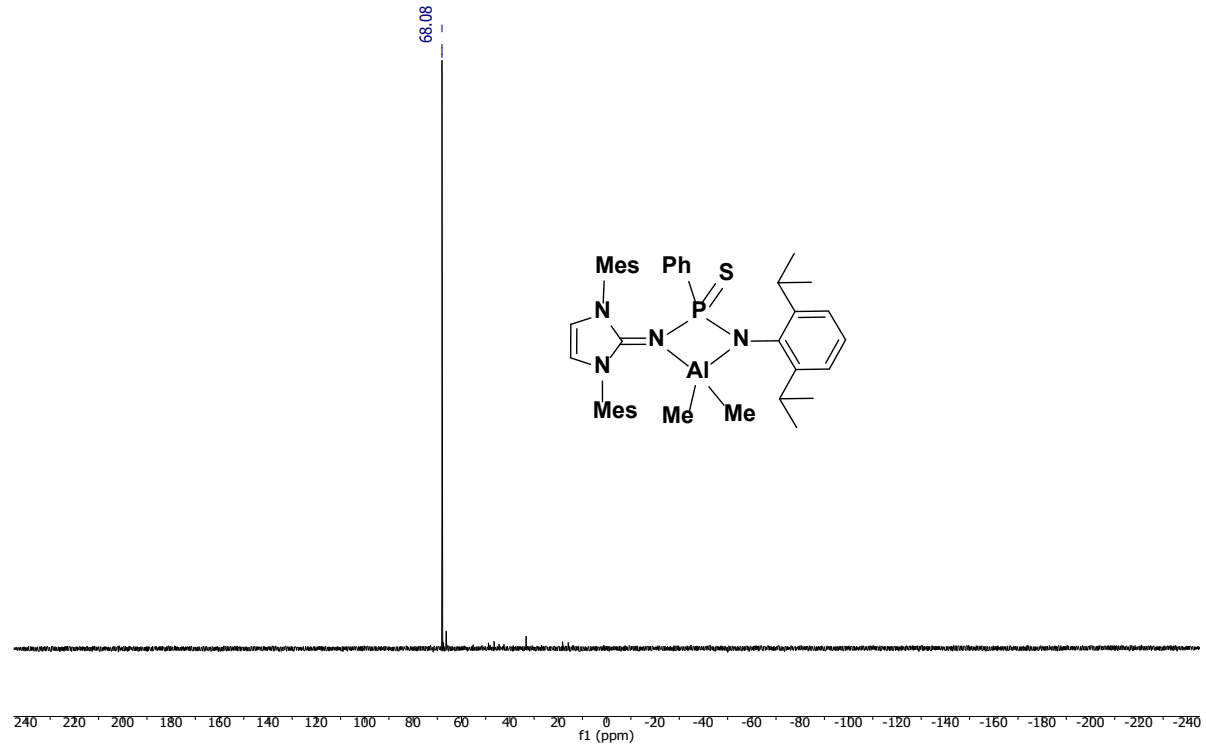


**Figure S40**. $^{31}P\{^{1}H\}$ NMR (121.5 MHz, $C_6D_6$, 298 K) spectrum of **6a**.

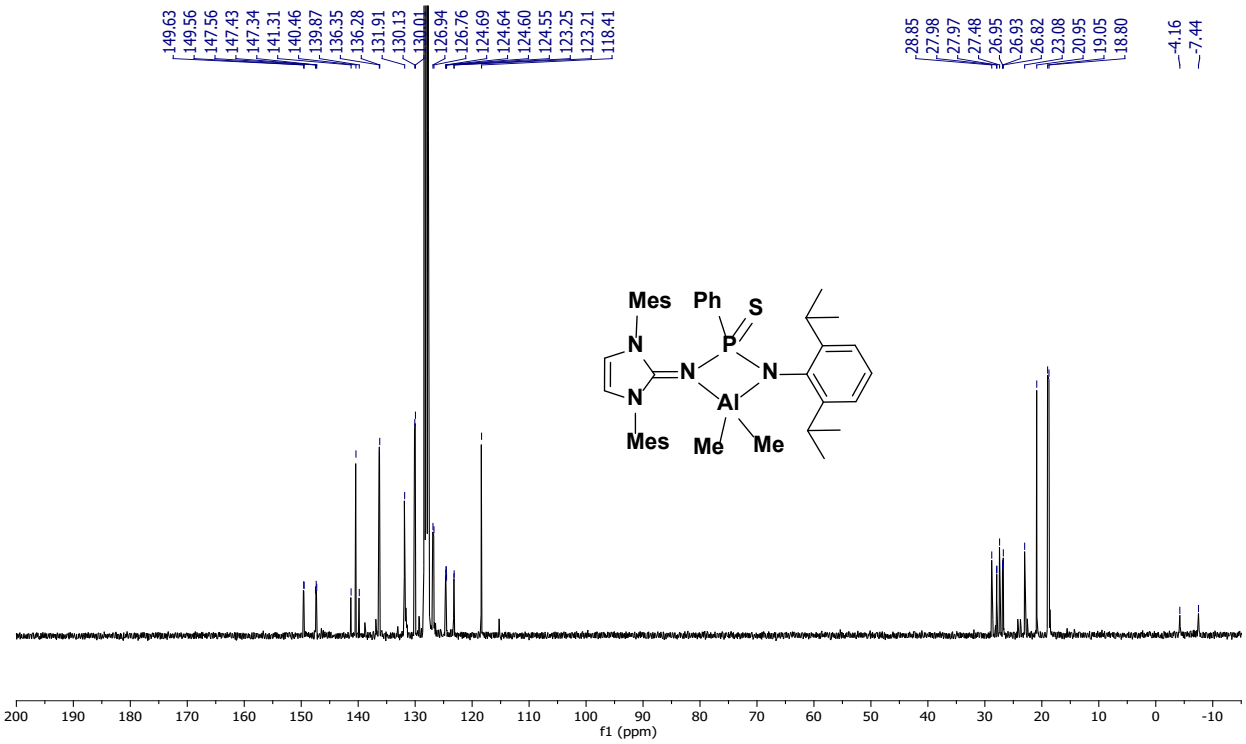


**Figure S41**. $^{13}C\{^{1}H\}$ NMR (75 MHz, $C_6D_6$, 298 K) spectrum of **6a**.

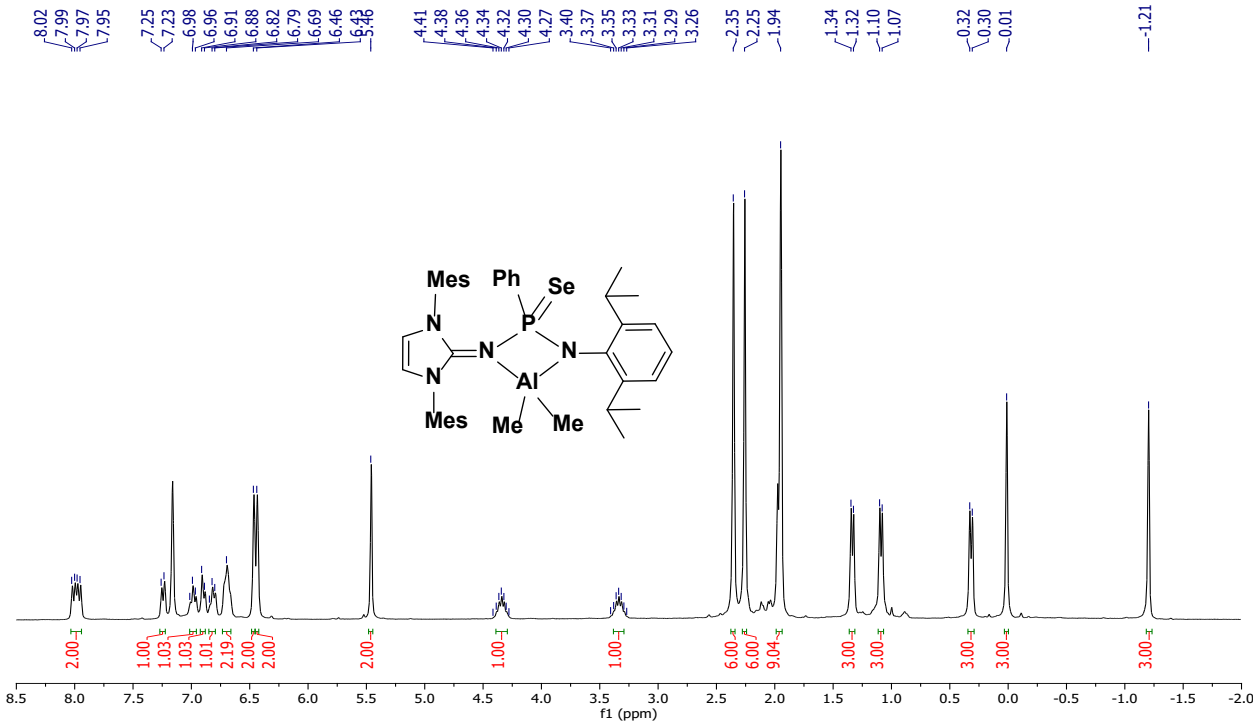


**Figure S42**. $^{1}H$ NMR (300 MHz, $C_6D_6$, 298 K) spectrum of **6b**.

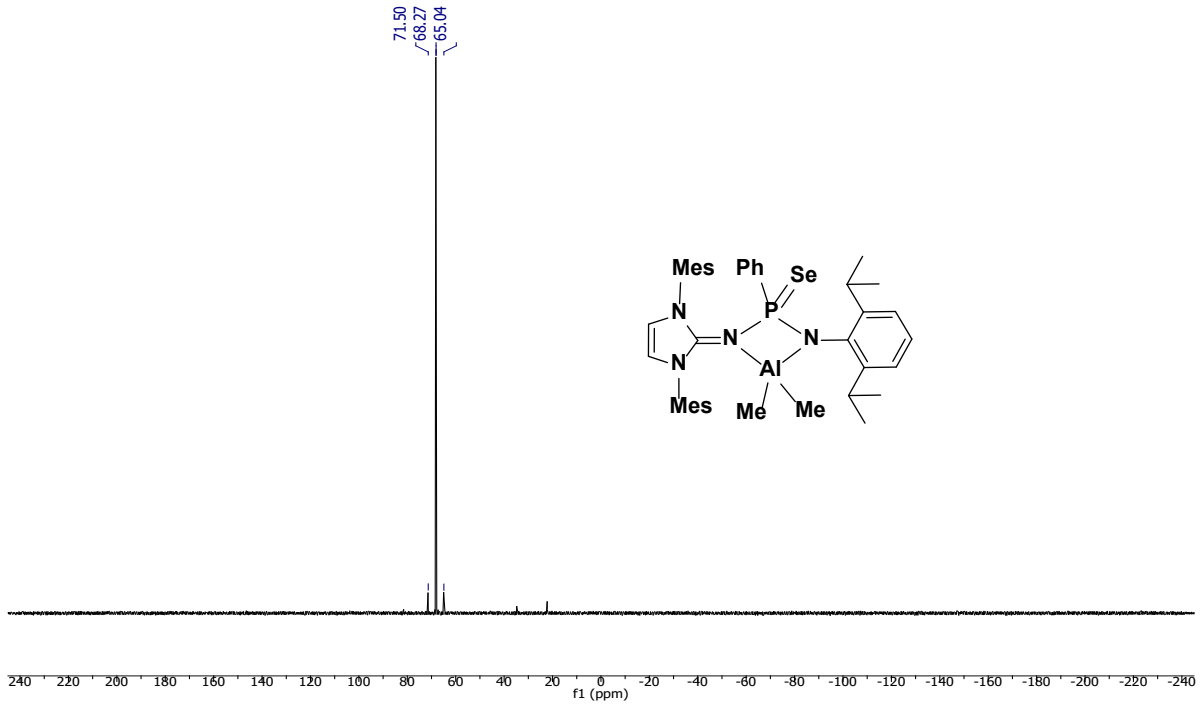


**Figure S43**. $^{31}P\{^{1}H\}$ NMR (121.5 MHz, $C_6D_6$, 298 K) spectrum of **6b**.

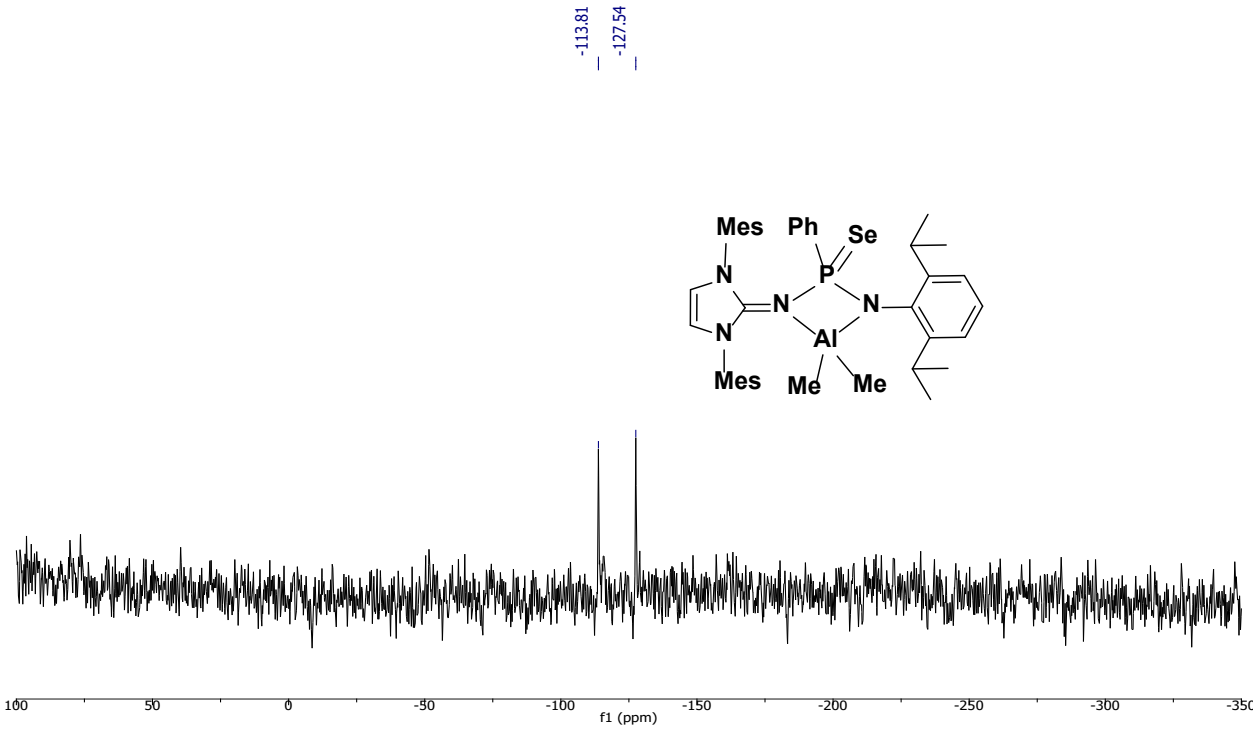


**Figure S44**. $^{77}Se\{^{1}H\}$ NMR (57.36 MHz, $C_6D_6$, 298 K) spectrum of **6b**.

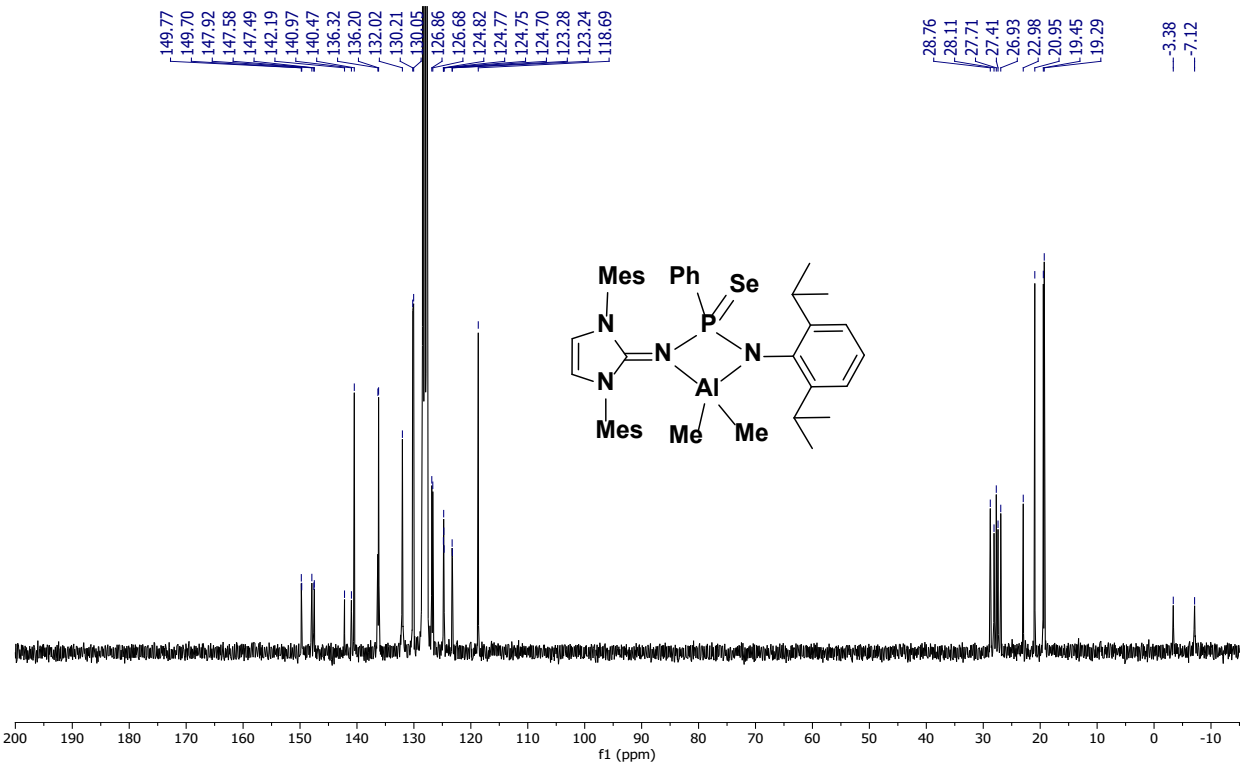


**Figure S45**. $^{13}C\{^{1}H\}$ NMR (75 MHz, $C_6D_6$, 298 K) spectrum of **6b**.

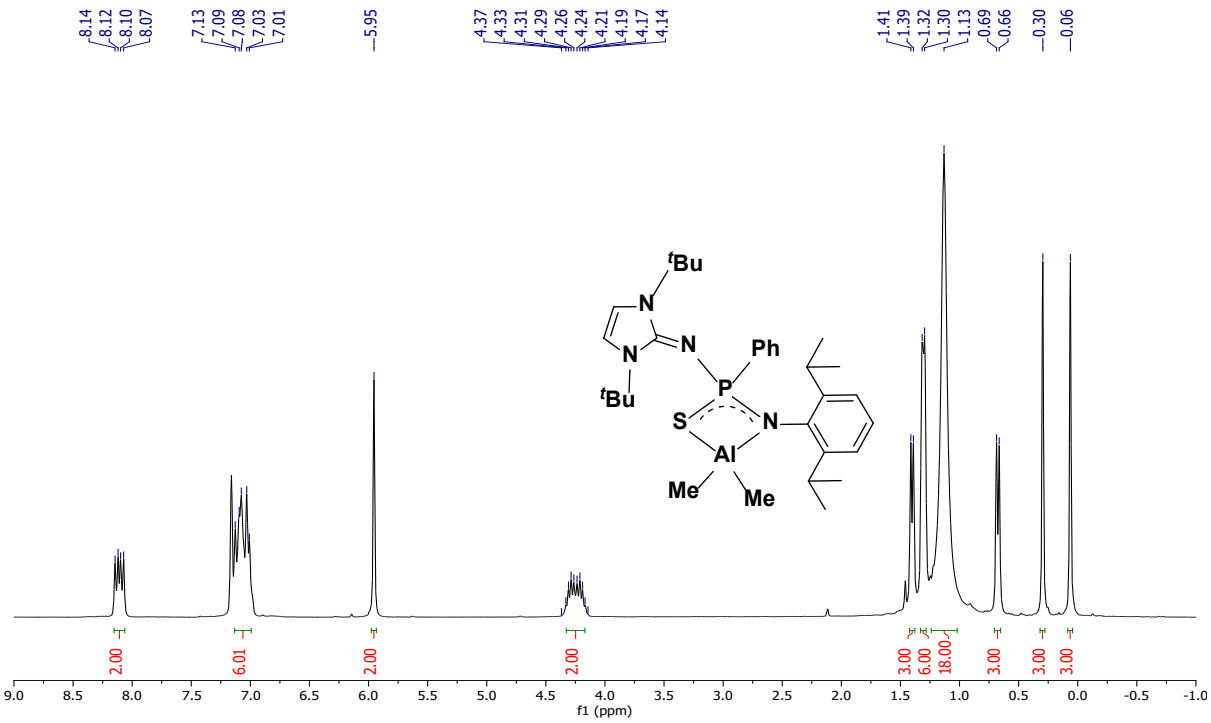


**Figure S46**. $^{1}H$ NMR (300 MHz, $C_6D_6$, 298 K) spectrum of **7a**.

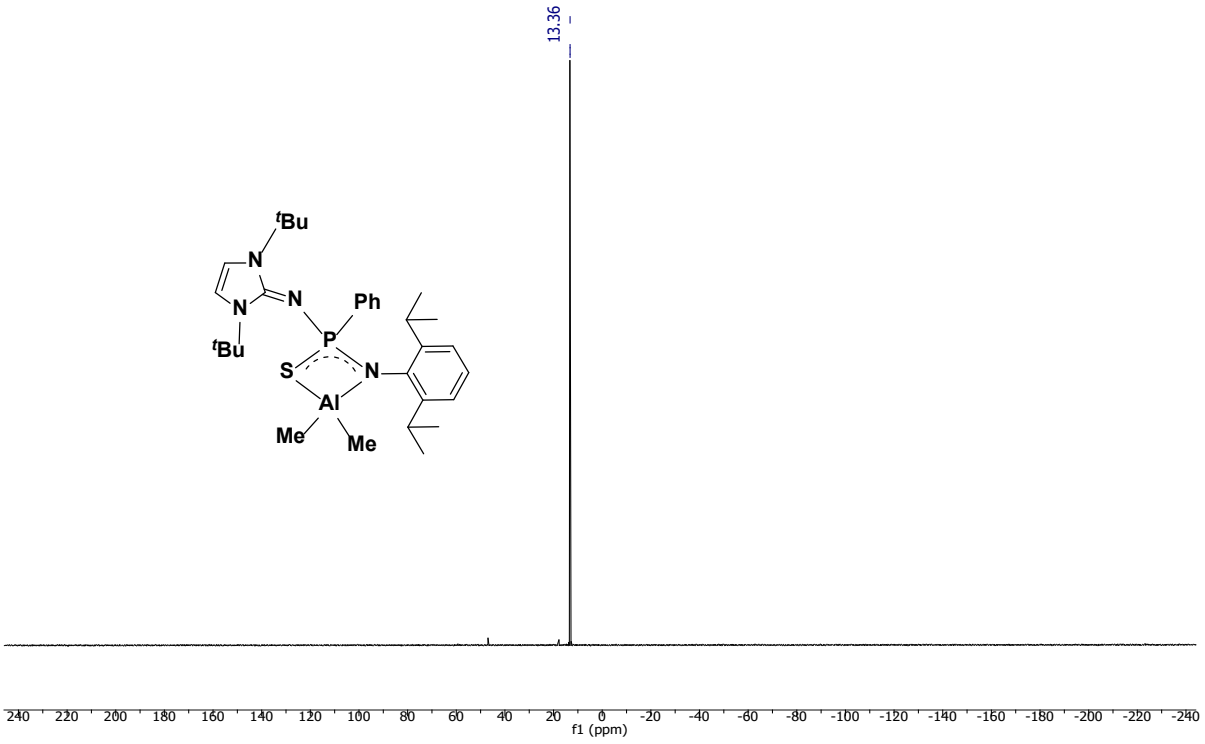


**Figure S47**. $^{31}P\{^{1}H\}$ NMR (121.5 MHz, $C_6D_6$, 298 K) spectrum of **7a**.

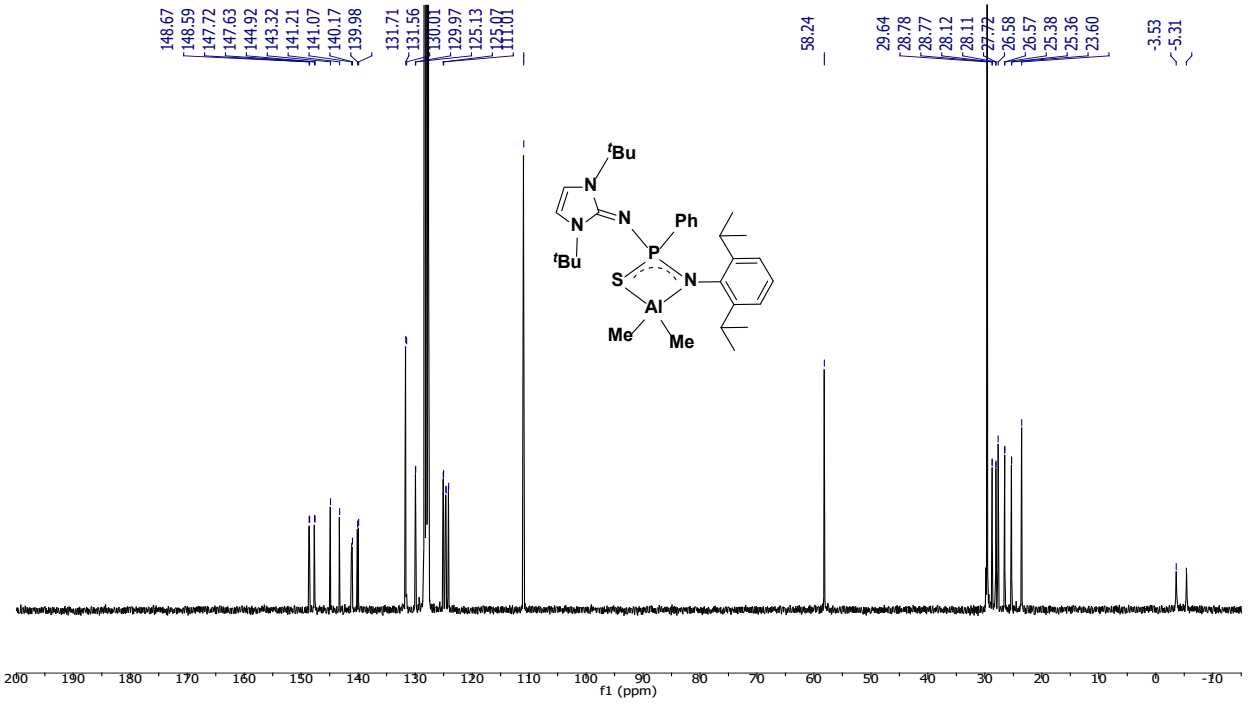


**Figure S48**. $^{13}C\{^{1}H\}$ NMR (75 MHz, $C_6D_6$, 298 K) spectrum of **7a**.

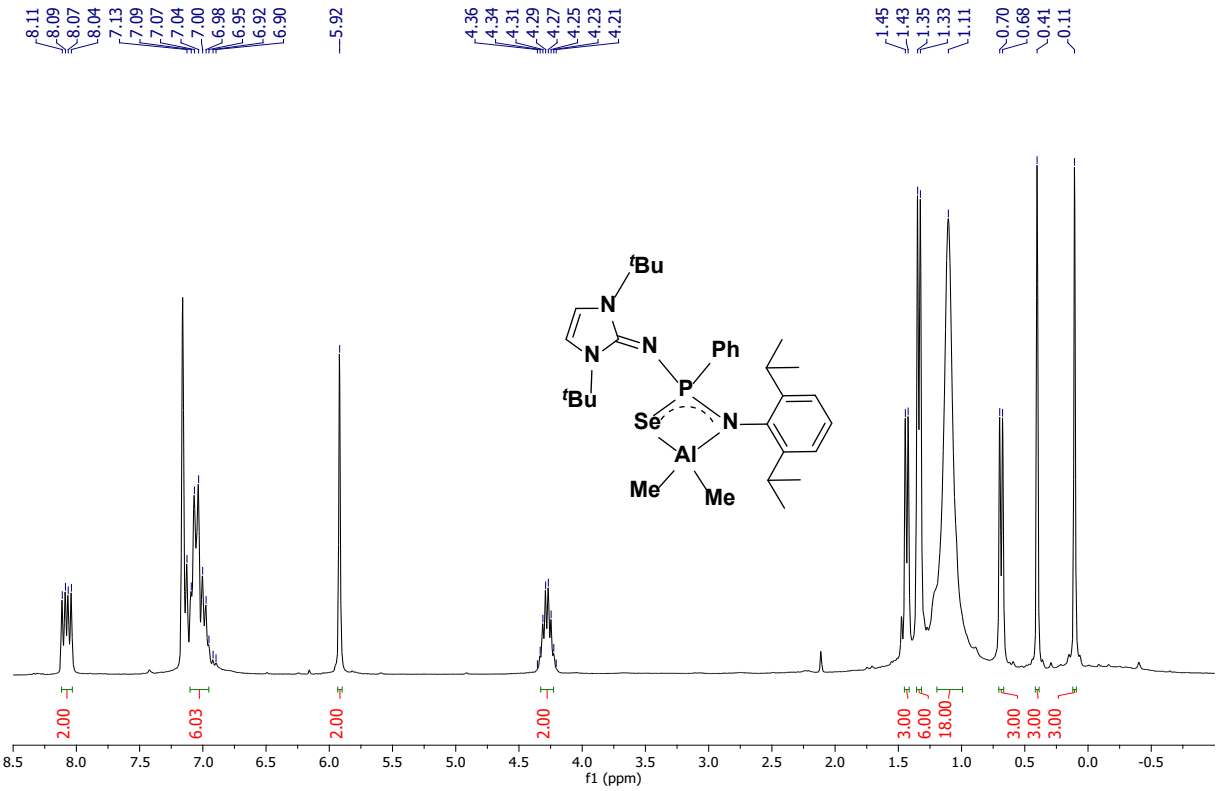


**Figure S49**. $^{1}H$ NMR (300 MHz, $C_6D_6$, 298 K) spectrum of **7b**.

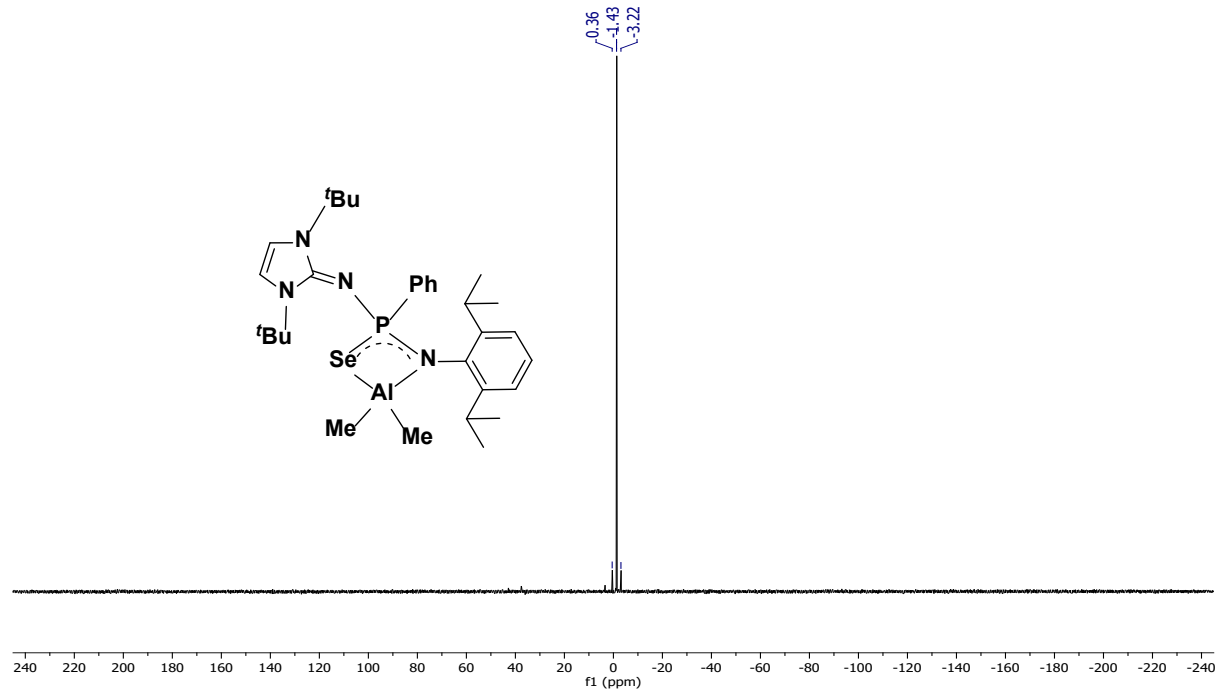


**Figure S50**. $^{31}P\{^{1}H\}$ NMR (121.5 MHz, $C_6D_6$, 298 K) spectrum of **7b**.

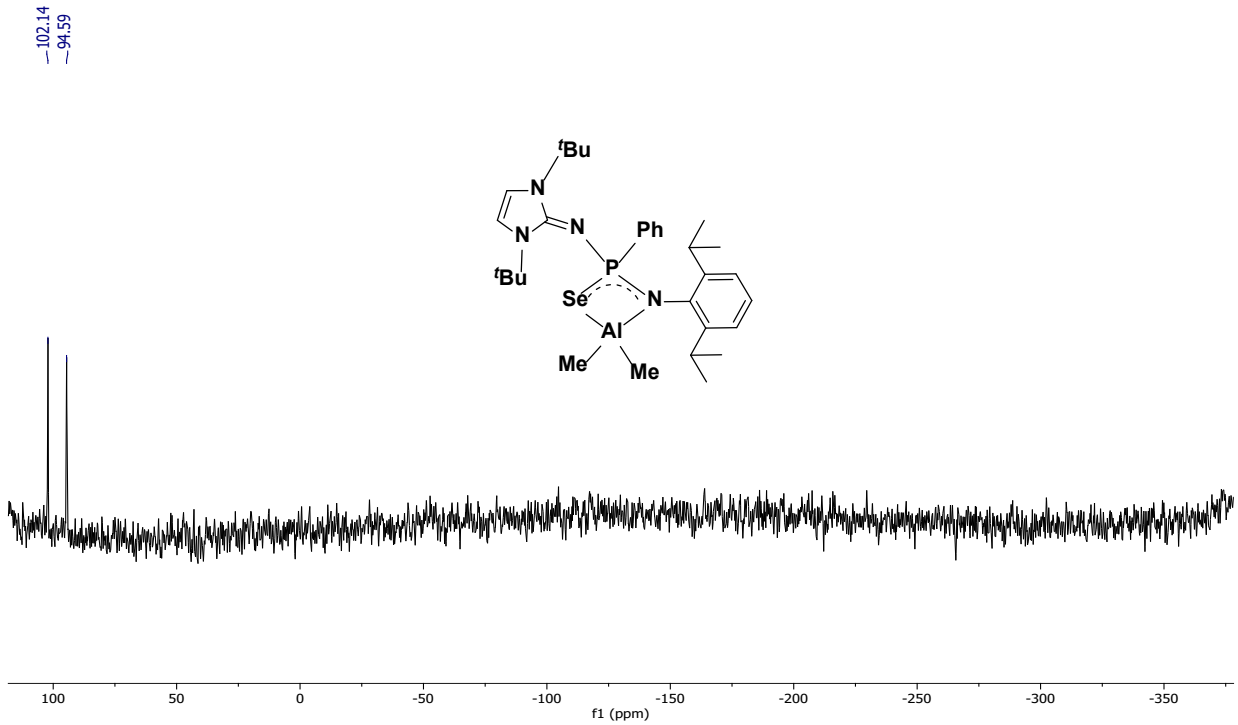


**Figure S51**. $^{77}Se\{^{1}H\}$ NMR (57.36 MHz, $C_6D_6$, 298 K) spectrum of **7b**.

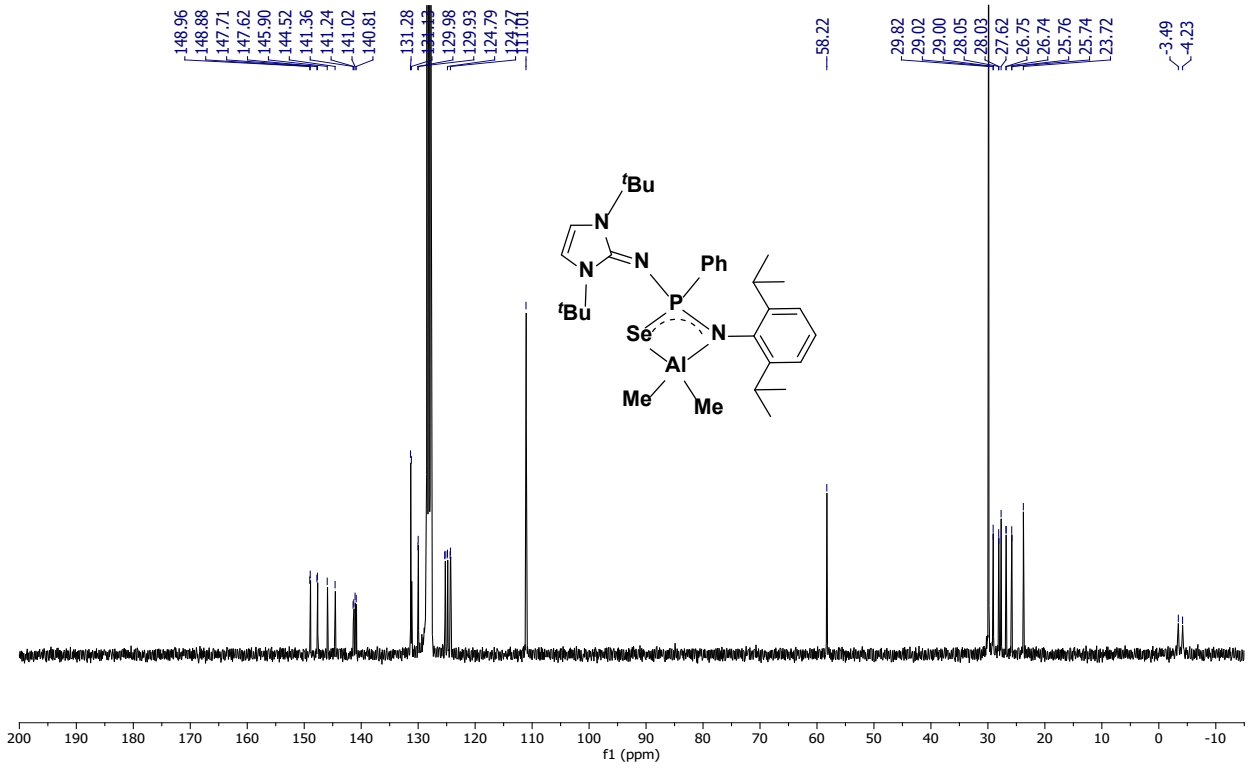


**Figure S52**. $^{13}C\{^{1}H\}$ NMR (75 MHz, $C_6D_6$, 298 K) spectrum of **7b**.

## 5. Catalytic hydroboration of nitriles

### General catalytic procedure for the hydroboration of nitriles

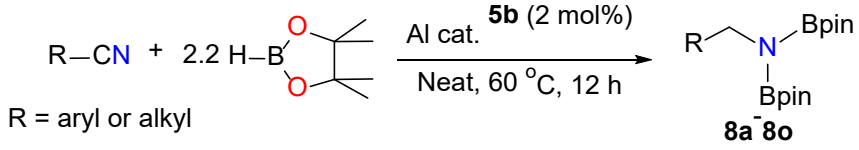


Inside the glove box, the Al catalyst **5b** (2 mol %) and pinacolborane (HBpin, 1.1 mmol, 2.2 equiv) was added to a Schlenk tube followed by the addition of nitriles (0.5 mmol, 1 equiv). The Schlenk tube was taken out from the glove box and the reaction mixture was stirred at 60 °C for 12 hours. Finally, volatiles of the mixture were removed under the reduced pressure to obtain the hydroboration product. The yield was calculated from $^{1}$H NMR spectroscopy with the help of 1,3,5-trimethoxy benzene as the internal standard. The progress of the reaction was monitored by $^{1}$H NMR, which indicated the completion of the reaction by the appearance of a new R-C*H*$_2$-N(Bpin)$_2$ resonance.

### NMR data of *N*,*N*-diborylamines

*N*-benzyl-4,4,5,5-tetramethyl-N-(4,4,5,5-tetramethyl-1,3,2-dioxaborolan-2-yl)-1,3,2-dioxaborolan-2-amine (**8a**)[3].

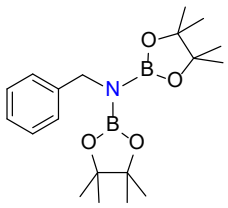


Yield: 98%. $^{1}$H NMR (400 MHz, $CDCl_3$, 298 K): $\delta_H$ (ppm) 7.40-7.38 (m, 1H, Ar-*H*), 7.29-7.24 (m, 2H, Ar-*H*), 7.15-7.10 (m, 2H, Ar-*H*), 4.04 (s, 2H, C*H*$_2$), 1.17 (s, 24H, Bpin-C*H*$_3$). $^{11}$B{$^{1}$H} NMR (128.4 MHz, $CDCl_3$, 298 K): $\delta_B$ (ppm) 25.3. $^{13}$C{$^{1}$H} NMR (100 MHz, $CDCl_3$, 298 K): $\delta_c$ (ppm) 142.9, 132.2, 128.4, 126.8, 126.6, 82.2, 45.3, 24.6.

4,4,5,5-tetramethyl-*N*-(2-methylbenzyl)-*N*-(4,4,5,5-tetramethyl-1,3,2-dioxaborolan-2-yl)-1,3,2-dioxaborolan-2-amine **(8b)**[4].

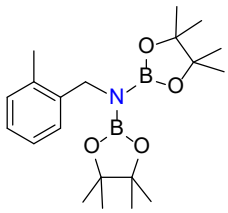

Yield: 97%. $^{1}$H NMR (400 MHz, $CDCl_3$, 298 K): $\delta_H$ (ppm) 7.49 (d, *J* = 8 Hz, 1H, Ar-*H*), 7.38 (t, *J* = 8 Hz, 1H, Ar-*H*), 7.23-7.15 (m, 2H, Ar-*H*), 3.90 (s, 2H, C*H*$_2$), 2.45 (s, 3H, C*H*$_3$), 1.13 (s, 24H, Bpin-C*H*$_3$). $^{11}$B{$^{1}$H} NMR (128.4 MHz, $CDCl_3$, 298 K): $\delta_B$ (ppm) 25.8. $^{13}$C{$^{1}$H} NMR (100 MHz, $CDCl_3$, 298 K): $\delta_c$ (ppm) 141.9, 135.9, 132.6, 132.4, 130.2, 126.2, 82.2, 31.6, 24.7, 20.4.

4,4,5,5-tetramethyl-*N*-(4-(methylthio)benzyl)-*N*-(4,4,5,5-tetramethyl-1,3,2-dioxaborolan-2-yl)-1,3,2-dioxaborolan-2-yl)-1,3,2-dioxaborolan-3-amine **(8c)**[5].

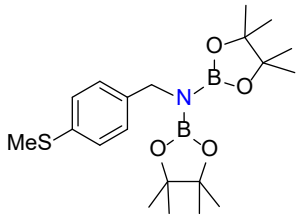

Yield: 95%. $^{1}$H NMR (400 MHz, $CDCl_3$, 298 K): $\delta_H$ (ppm) 7.41 (d, *J* = 8 Hz, 2H, Ar-*H*), 7.15 (d, *J* = 8 Hz, 2H, Ar-*H*), 3.96 (s, 2H, C*H*$_2$), 2.39 (s, 3H, S-C*H*$_3$), 1.14 (s, 24H, Bpin-C*H*$_3$). $^{11}$B{$^{1}$H} NMR (128.4 MHz, $CDCl_3$, 298 K): $\delta_B$ (ppm) 25.5. $^{13}$C{$^{1}$H} NMR (100 MHz, $CDCl_3$, 298 K): $\delta_c$ (ppm) 146.1, 139.9, 131.9, 125.4, 82.5, 44.6, 24.5, 14.5.

*N*-(4-(dimethylamino)benzyl)-4,4,5,5-tetramethyl-*N*-(4,4,5,5-tetramethyl-1,3,2-dioxaborolan-2-yl)-1,3,2-dioxaborolan-2-amine **(8d)**[6].

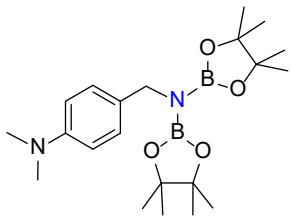

Yield: 97%. $^{1}$H NMR (400 MHz, $CDCl_3$, 298 K): $\delta_H$ (ppm) 7.13 (d, *J* = 8 Hz, 2H, Ar-*H*), 6.56 (t, *J* = 6 Hz, 2H, Ar-*H*), 4.05 (s, 2H, C*H*$_2$), 2.80 (s, 6H, N-C*H*$_3$), 1.12 (s, 24H, Bpin-C*H*$_3$). $^{11}$B{$^{1}$H} NMR (128.4 MHz, $CDCl_3$, 298 K): $\delta_B$ (ppm) 25.7. $^{13}$C{$^{1}$H} NMR (100 MHz, $CDCl_3$, 298 K): $\delta_c$ (ppm) 149.4, 131.8, 128.7, 112.6, 82.2, 46.6, 40.9, 24.6.

*N*-(4-fluorobenzyl)-4,4,5,5-tetramethyl-*N*-(4,4,5,5-tetramethyl-1,3,2-dioxaborolan-2-yl)-1,3,2-dioxaborolan-2-amine **(8e)**[4].

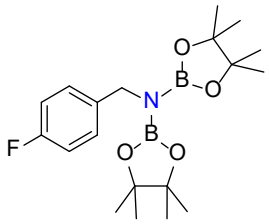


Yield: 98%. $^{1}$H NMR (400 MHz, $CDCl_3$, 298 K): $\delta_H$ (ppm) 7.21-7.18 (m, 2H, Ar-*H*), 6.86-6.83 (m, 1H, Ar-*H*), 4.10 (s, 2H, C*H*$_2$), 1.12 (s, 24H, Bpin-C*H*$_3$). $^{11}$B{$^{1}$H} NMR (128.4 MHz, $CDCl_3$, 298 K): $\delta_B$ (ppm) 25.9. $^{13}$C{$^{1}$H} NMR (100 MHz, $CDCl_3$, 298 K): $\delta_c$ (ppm) 162.8, 138.9, 134.8, 129.3, 82.5, 46.7, 24.6.

*N*-(4-chlorobenzyl)-4,4,5,5-tetramethyl-*N*-(4,4,5,5-tetramethyl-1,3,2-dioxaborolan-2-yl)-1,3,2-dioxaborolan-2-amine **(8f)**[4].

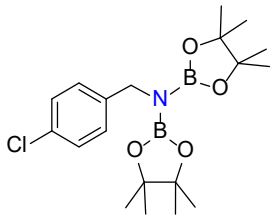


Yield: 96%. $^{1}$H NMR (400 MHz, $CDCl_3$, 298 K): $\delta_H$ (ppm) 7.61-7.59 (m, 2H, Ar-*H*), 7.47-7.46 (m, 1H, Ar-*H*), 4.17 (s, 2H, C*H*$_2$), 1.19 (s, 24H, Bpin-C*H*$_3$). $^{11}$B{$^{1}$H} NMR (128.4 MHz, $CDCl_3$, 298 K): $\delta_B$ (ppm) 25.6. $^{13}$C{$^{1}$H} NMR (150 MHz, $CDCl_3$, 298 K): $\delta_c$ (ppm) 133.5, 129.8, 129.1, 128.0, 82.6, 46.8, 24.6.

*N*-(4-bromobenzyl)-4,4,5,5-tetramethyl-*N*-(4,4,5,5-tetramethyl-1,3,2-dioxaborolan-2-yl)-1,3,2-dioxaborolan-2-amine **(8g)**[4].

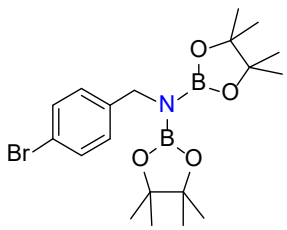

Yield: 96%. $^{1}$H NMR (400 MHz, $CDCl_3$, 298 K): $\delta_H$ (ppm) 7.76-7.74 (m, 2H, Ar-*H*), 7.29-7.27 (m, 2H, Ar-*H*), 4.08 (s, 2H, C*H*$_2$), 1.11 (s, 24H, Bpin-C*H*$_3$). $^{11}$B{$^{1}$H} NMR (128.4 MHz, $CDCl_3$, 298 K): $\delta_B$ (ppm) 25.6. $^{13}$C{$^{1}$H} NMR (100 MHz, $CDCl_3$, 298 K): $\delta_c$ (ppm) 142.8, 138.6, 133.2, 129.7, 82.5, 46.8, 24.6.

*N*-(4-iodobenzyl)-4,4,5,5-tetramethyl-*N*-(4,4,5,5-tetramethyl-1,3,2-dioxaborolan-2-yl)-1,3,2-dioxaborolan-2-yl)-1,3,2-dioxaborolan-2-amine **(8h)**[5].

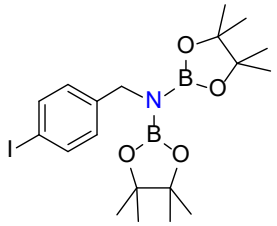

Yield: 97%. $^{1}$H NMR (400 MHz, $CDCl_3$, 298 K): $\delta_H$ (ppm) 7.55-7.53 (q, 2H, Ar-*H*), 7.45-7.43 (q, 2H, Ar-*H*), 4.08 (s, 2H, C*H*$_2$), 1.11 (s, 24H, Bpin-C*H*$_3$). $^{11}$B{$^{1}$H} NMR (128.4 MHz, $CDCl_3$, 298 K): $\delta_B$ (ppm) 25.7. $^{13}$C{$^{1}$H} NMR (100 MHz, $CDCl_3$, 298 K): $\delta_c$ (ppm) 142.14, 133.5, 132.7, 111.3, 82.5, 46.74, 24.6.

4,4,5,5-tetramethyl-*N*-(4,4,5,5-tetramethyl-1,3,2-dioxaborolan-2-yl)-*N*-(4-(trifluoromethyl)benz-yl)-1,3,2-dioxaborolan-2-amine **(8i)**[4].

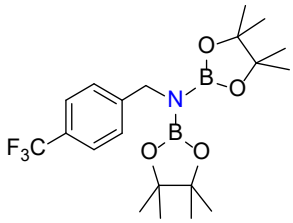

Yield: 96%. $^{1}$H NMR (400 MHz, $CDCl_3$, 298 K): $\delta_H$ (ppm) 7.48-7.41 (m, 2H, Ar-*H*), 7.33-7.29 (m, 2H, Ar-*H*), 4.19 (s, 2H, C*H*$_2$), 1.17 (s, 24H, Bpin-C*H*$_3$). $^{11}$B{$^{1}$H} NMR (128.4 MHz, $CDCl_3$, 298 K): $\delta_B$ (ppm) 25.9. $^{13}$C{$^{1}$H} NMR (100 MHz, $CDCl_3$, 298 K): $\delta_c$ (ppm) 147.2, 132.8, 127.7, 126.9, 125.3, 82.6, 44.9, 24.6.

*N*-(4-methoxyphenethyl)-4,4,5,5-tetramethyl-*N*-(4,4,5,5-tetramethyl-1,3,2-dioxaborolan-2-yl)-1,3,2-dioxaborolan-2-amine **(8j)**[7].

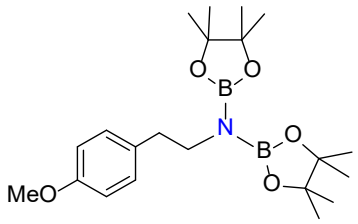


Yield: 98%. $^{1}$H NMR (400 MHz, $CDCl_3$, 298 K): $\delta_H$ (ppm) 7.02-6.99 (t, 2H, Ar-*H*), 6.72-6.99 (q, 2H, Ar-*H*), 3.65 (s, 3H, O-C*H*$_3$), 3.17 (t, *J* = 8 Hz, 2H, C*H*$_2$), 2.56 (t, 2H, *J* = 8 Hz, C*H*$_2$), 1.08 (s, 24H, Bpin-C*H*$_3$). $^{11}$B{$^{1}$H} NMR (128.4 MHz, $CDCl_3$, 298 K): $\delta_B$ (ppm) 25.51. $^{13}$C{$^{1}$H} NMR (100 MHz, $CDCl_3$, 298 K): $\delta_c$ (ppm) 157.8, 132.6, 130.2, 113.6, 82.0, 55.3, 45.4, 38.5, 24.5.

*N*-(4-fluorophenethyl)-4,4,5,5-tetramethyl-*N*-(4,4,5,5-tetramethyl-1,3,2-dioxaborolan-2-yl)-1,3,2-dioxaborolan-2-yl)-1,3,2-dioxaborolan-2-amine **(8k)**[7].

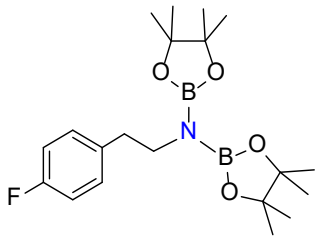


Yield: 94%. $^{1}$H NMR (400 MHz, $CDCl_3$, 298 K): $\delta_H$ (ppm) 7.22-7.18 (m, 2H, Ar-*H*), 6.99-6.95 (m, 2H, Ar-*H*), 3.18 (t, *J* = 8 Hz, 2H, C*H*$_2$), 2.59 (t, *J* = 6 Hz, 2H, C*H*$_2$), 1.08 (s, 24H, Bpin-C*H*$_3$). $^{11}$B{$^{1}$H} NMR (128.4 MHz, $CDCl_3$, 298 K): $\delta_B$ (ppm) 25.8. $^{13}$C{$^{1}$H} NMR (100 MHz, $CDCl_3$, 298 K): $\delta_c$ (ppm) 163.7, 136.1, 130.7, 129.8, 129.7, 116.2, 82.1, 45.2, 38.5, 24.5.

*N*-(2,2-diphenylethyl)-4,4,5,5-tetramethyl-*N*-(4,4,5,5-tetramethyl-1,3,2-dioxaborolan-2-yl)-1,3,2-dioxaborolan-2-yl)-1,3,2-dioxaborolan-2-amine **(8l)**[8].

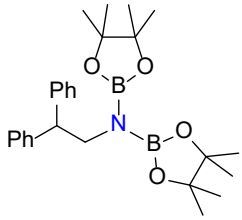


Yield: 94%. $^{1}$H NMR (400 MHz, $CDCl_3$, 298 K): $\delta_H$ (ppm) 7.20-7.17 (m, 8H, Ar-*H*), 7.09-7.07 (m, 2H, Ar-*H*), 4.16 (t, *J* = 4 Hz, 1H, C*H*$_2$), 3.64 (d, *J* = 8 Hz, 1H, Ph$_2$(C*H*)), 1.10 (s, 24H, Bpin-C*H*$_3$). $^{11}$B{$^{1}$H} NMR (128.4 MHz, $CDCl_3$, 298 K): $\delta_B$ (ppm) 25.7. $^{13}$C{$^{1}$H} NMR (100 MHz,

$CDCl_3$, 298 K): $\delta_c$ (ppm) 143.4, 136.0, 129.3, 128.8, 128.3, 128.2, 127.8, 126.1, 82.2, 48.5, 42.7, 24.5.

4,4,5,5-tetramethyl-*N*-(4,4,5,5-tetramethyl-1,3,2-dioxaborolan-2-yl)-*N*-(thiophen-2-ylmethyl)-1,3,2-dioxaborolan-2-amine **(8m)**[9].

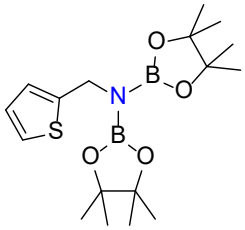

Yield: 97%. $^1$H NMR (400 MHz, $CDCl_3$, 298 K): $\delta_H$ (ppm) 7.10-7.08 (m, 1H, Ar-*H*), 6.92-6.91 (m,1H, Ar-*H*), 6.87-6.85(m, 1H, Ar-*H*), 4.37 (s, 2H, C$H_2$), 1.22 (s, 24H, Bpin-C$H_3$). $^{11}$B{$^1$H} NMR (128.4 MHz, $CDCl_3$, 298 K): $\delta_B$ (ppm) 25.5. $^{13}$C{$^1$H} NMR (100 MHz, $CDCl_3$, 298 K): $\delta_c$ (ppm) 146.9, 126.2, 124.6, 123.6, 82.6, 42.2, 24.6.

*N*-(2-methoxyethyl)-4,4,5,5-tetramethyl-*N*-(4,4,5,5-tetramethyl-1,3,2-dioxaborolan-2-yl)-1,3,2-dioxaborolan-2-amine **(8n)**[7].

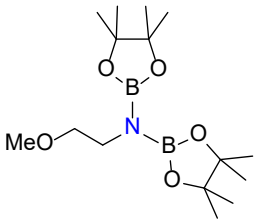

Yield: 98%. $^1$H NMR (400 MHz, $CDCl_3$, 298 K): $\delta_H$ (ppm) 3.23 (t, $J$ = 6 Hz, 5H, C$H_2$ and O-C$H_3$), 3.13 (t, $J$ = 6 Hz, 2H, C$H_2$), 1.14 (s, 24H, Bpin-C$H_3$). $^{11}$B{$^1$H} NMR (128.4 MHz, $CDCl_3$, 298 K): $\delta_B$ (ppm) 25.9. $^{13}$C{$^1$H} NMR (100 MHz, $CDCl_3$, 298 K): $\delta_c$ (ppm) 82.2, 74.2, 58.6, 42.8, 24.5.

*N*,*N'*-(1,4-phenylenebis(methylene))bis(4,4,5,5-tetramethyl-*N*-(4,4,5,5-tetramethyl-1,3,2-dioxaborolan-2-yl)-1,3,2-dioxaborolan-2-amine) **(8o)**[4].

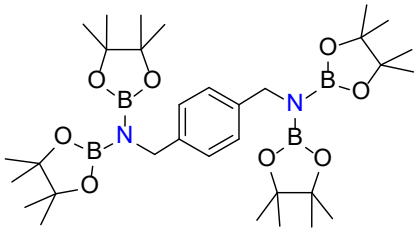

Yield: 97%. $^{1}$H NMR (400 MHz, $CDCl_3$, 298 K): $\delta_H$ (ppm) 7.79 (s, 4H, Ar-*H*), 4.18 (s, 4H, C*H*$_2$), 1.18 (s, 48H, Bpin-C*H*$_3$). $^{11}$B{$^{1}$H} NMR (128.4 MHz, $CDCl_3$, 298 K): $\delta_B$ (ppm) 25.8. $^{13}$C{$^{1}$H} NMR (100 MHz, $CDCl_3$, 298 K): $\delta_c$ (ppm) 140.8, 132.9, 127.0, 116.9, 82.4, 47.1, 24.6.

**General procedure for the primary ammonium salt**

With the hydroboration product of the nitriles, 0.05 M HCl solution was added and stirred for 4 h at room temperature. Further primary ammonium salts were extracted from the water layer of a water-DCM mixture.

**NMR data of primary ammonium salt**

Benzyl ammonium salt **(9a)**[4].

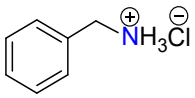

Yield: 90%. $^{1}$H NMR (400 MHz, $D_2O$, 298 K): $\delta_H$ (ppm) 7.40-7.39 (m, 5H, Ar-*H*), 4.10 (s, 2H, C*H*$_2$). $^{13}$C{$^{1}$H} NMR (100 MHz, $D_2O$, 298 K): $\delta_c$ (ppm) 132.6, 129.2, 128.8, 43.1.

*o*-tolylmethanaminium chloride **(9b)**[4].

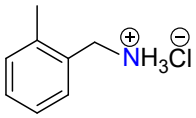

Yield: 88%. $^{1}$H NMR (400 MHz, $D_2O$, 298 K): $\delta_H$ (ppm) 7.25-7.16 (m, 4H, Ar-*H*), 4.08 (s, 2H, C*H*$_2$), 2.24 (s, 3H, C*H*$_3$). $^{13}$C{$^{1}$H} NMR (100 MHz, $D_2O$, 298 K): $\delta_c$ (ppm) 137.2, 130.8, 129.4, 129.1, 126.6, 40.4, 18.07.

(4-bromophenyl)methanaminium chloride **(9c)**.

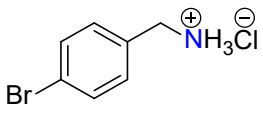

Yield: 89%. $^{1}$H NMR (400 MHz, $D_2O$, 298 K): $\delta_H$ (ppm) 7.52 (d, *J* = 8 Hz, 2H, Ar-*H*), 7.25 (d, *J* = 8 Hz, 2H, Ar-*H*), 4.05 (s, 2H, C*H*$_2$). $^{13}$C{$^{1}$H} NMR (100 MHz, $D_2O$, 298 K): $\delta_c$ (ppm) 132.1, 131.7, 130.7, 122.7, 42.5.

(4-iodophenyl)methanaminium chloride **(9d)**[10].

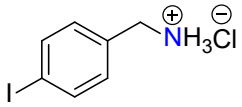


Yield: 90%. $^{1}$H NMR (400 MHz, $D_2O$, 298 K): $\delta_H$ (ppm) 7.75 (d, *J* = 8 Hz, 2H, Ar-*H*), 7.13 (d, *J* = 8 Hz, 2H, Ar-*H*), 4.05 (s, 2H, C*H*$_2$). $^{13}$C{$^{1}$H} NMR (100 MHz, $D_2O$, 298 K): $\delta_c$ (ppm) 138.2, 132.2, 130.7, 94.6, 42.6.

2-(4-fluorophenyl)ethanaminium chloride **(9e)**.

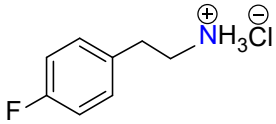


Yield: 85%. $^{1}$H NMR (400 MHz, $D_2O$, 298 K): $\delta_H$ (ppm) 7.21 (t, *J* = 6 Hz, 2H, Ar-*H*), 7.03 (t, *J* = 10 Hz, 2H, Ar-*H*), 3.16 (t, *J* = 8 Hz, 2H, C*H*$_2$), 2.88 (t, *J* = 8 Hz, 2H, C*H*$_2$). $^{13}$C{$^{1}$H} NMR (100 MHz, $D_2O$, 298 K): $\delta_c$ (ppm) 132.3, .130.6, 130.5, 115.7, 115.5, 40.6, 31.9.

## 6. Catalytic hydroboration of alkynes

### General catalytic procedure for the hydroboration of alkynes

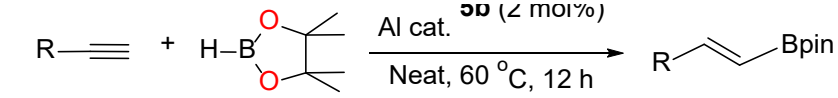


R = aryl or alkyl

**10a-10l**

Inside the glove box, the Al catalyst **5b** (2 mol %) and HBpin (0.5 mmol, 1 equiv) was added to a Schlenk tube followed by the addition of alkynes (0.5 mmol, 1 equiv). The Schlenk tube was taken out from the glove box and the reaction mixture was stirred at 60 °C for 12 hours. Finally, volatiles of the mixture were removed under the reduced pressure to obtain the hydroboration product. The

yield was calculated from $^{1}$H NMR spectroscopy with the help of 1,3,5-trimethoxy benzene as the internal standard.

**NMR data of vinylboronates**

(*E*)-4,4,5,5-tetramethyl-2-styryl-1,3,2-dioxaborolane **(10a)**[11].

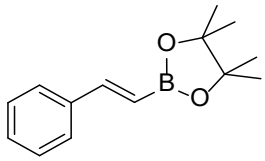

Yield: 97%. $^{1}$H NMR (400 MHz, $CDCl_3$, 298 K): $\delta_H$ (ppm) 7.42-7.40 (m, 2H, Ar-*H*), 7.35-7.30 (d, *J* = 20 Hz, 1H, C*H*), 7.28-7.21 (m, 3H, Ar-*H*), 6.12-6.07 (d, *J* = 20 Hz, C*H*), 1.24 (s, 12H, Bpin-C$H_3$). $^{11}$B{$^{1}$H} NMR (128.4 MHz, $CDCl_3$, 298 K): $\delta_B$ (ppm) 30.5. $^{13}$C{$^{1}$H} NMR (100 MHz, $CDCl_3$, 298 K): $\delta_c$ (ppm) 149.6, 137.6, 129.0, 128.7, 127.2, 83.5, 24.9.

(*E*)-4,4,5,5-tetramethyl-2-(3-methylstyryl)-1,3,2-dioxaborolane **(10b)**[8].

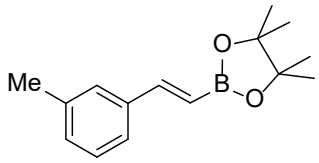

Yield: 95%. $^{1}$H NMR (400 MHz, $CDCl_3$, 298 K): $\delta_H$ (ppm) 7.32-7.27 (d, *J* = 20 Hz, C*H*), 7.22-7.21 (m, 2H, C$H_2$), 7.17-7.12 (m, 2H, C$H_2$), 6.10-6.05 (d, *J* = 20 Hz, C*H*), 2.26 (s, 3H, C$H_3$), 1.23 (s, 12H, Bpin-C$H_3$). $^{11}$B{$^{1}$H} NMR (128.4 MHz, $CDCl_3$, 298 K): $\delta_B$ (ppm) 30.0. $^{13}$C{$^{1}$H} NMR (100 MHz, $CDCl_3$, 298 K): $\delta_c$ (ppm) 149.8, 138.2, 137.6, 129.8, 129.7, 128.6, 127.9, 124.4, 83.4, 24.9, 21.5.

(*E*)-2-(4-methoxystyryl)-4,4,5,5-tetramethyl-1,3,2-dioxaborolane **(10c)**[11].

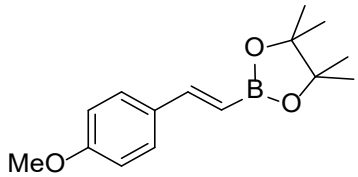

Yield: 96%. $^{1}$H NMR (400 MHz, $CDCl_3$, 298 K): $\delta_H$ (ppm) 7.36-7.33 (m, 2H, Ar-*H*), 7.30-7.25 (d, *J* = 20 Hz, 1H, C*H*), 6.79-6.74 (m, 2H, Ar-*H*), 5.96-5.91 (d, *J* = 20 Hz, 1H, C*H*), 3.71 (s, 3H, O-C*H*$_3$), 1.22 (s, 12H, Bpin-C*H*$_3$). $^{11}$B{$^{1}$H} NMR (128.4 MHz, $CDCl_3$, 298 K): $\delta_B$ (ppm) 30.2. $^{13}$C{$^{1}$H} NMR (100 MHz, $CDCl_3$, 298 K): $\delta_c$ (ppm) 160.4, 149.2, 130.5, 128.6, 114.0, 83.3, 55.3, 24.9.

(*E*)-2-(3-fluorostyryl)-4,4,5,5-tetramethyl-1,3,2-dioxaborolane **(10d)**.

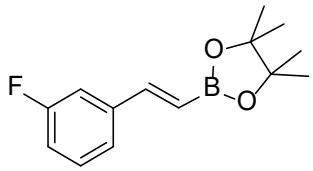


Yield: 95%. $^{1}$H NMR (400 MHz, $CDCl_3$, 298 K): $\delta_H$ (ppm) 7.29-7.24 (d, *J* = 20 Hz, 1H, C*H*), 7.22-7.18 (m, 1H, Ar-*H*), 7.17-7.15 (m, 1H, Ar-*H*), 7.11-7.08 (m, 1H, Ar-*H*), 6.92-6.90 (m, 1H, Ar-*H*), 6.11-6.06 (d, *J* = 20 Hz, 1H, C*H*), 1.23 (s, 12H, Bpin-C*H*$_3$). $^{11}$B{$^{1}$H} NMR (128.4 MHz, $CDCl_3$, 298 K): $\delta_B$ (ppm) 30.1. $^{13}$C{$^{1}$H} NMR (100 MHz, $CDCl_3$, 298 K): $\delta_c$ (ppm) 164.3, 148.1, 139.9, 130.0, 123.01, 115.8, 115.6, 113.4, 113.2, 83.5, 24.8.

(*E*)-2-(2-bromostyryl)-4,4,5,5-tetramethyl-1,3,2-dioxaborolane **(10e)**.

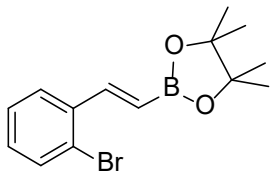


Yield: 95%. $^{1}$H NMR (400 MHz, $CDCl_3$, 298 K): $\delta_H$ (ppm) 7.72-7.68 (d, *J* = 16 Hz, 1H, C*H*), 7.61-7.58 (m, 1H, Ar-*H*), 7.54-7.52 (m, 1H, Ar-*H*), 7.29-7.26 (m, 1H, Ar-*H*), 7.14-7.10 (m, 1H, Ar-*H*), 6.14-6.09 (d, *J* = 20 Hz, 1H, C*H*), 1.30 (s, 12H, Bpin-C*H*$_3$). $^{11}$B{$^{1}$H} NMR (128.4 MHz, $CDCl_3$, 298 K): $\delta_B$ (ppm) 29.7. $^{13}$C{$^{1}$H} NMR (100 MHz, $CDCl_3$, 298 K): $\delta_c$ (ppm) 147.6, 134.2, 133.2, 132.6, 130.1, 127.6, 127.4, 127.1, 83.6, 24.9.

(*E*)-4,4,5,5-tetramethyl-2-(2-(thiophen-3-yl)vinyl)-1,3,2-dioxaborolane **(10f)**[10].

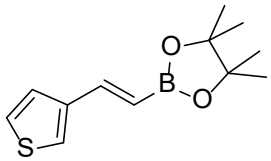

Yield: 94%. $^{1}$H NMR (400 MHz, $CDCl_3$, 298 K): $\delta_H$ (ppm) 7.33-7.29 (d, $J$ = 16 Hz, 1H, C*H*), 7.24-7.22 (m, 2H, Ar-*H*), 7.20-7.18 (m, 1H, Ar-*H*), 5.90-5.85 (d, $J$ = 20 Hz, 1H, C*H*), 1.23 (s, 12H, Bpin-C$H_3$). $^{11}$B{$^{1}$H} NMR (128.4 MHz, $CDCl_3$, 298 K): $\delta_B$ (ppm) 30.3. $^{13}$C{$^{1}$H} NMR (100 MHz, $CDCl_3$, 298 K): $\delta_c$ (ppm) 143.3, 128.4, 126.3, 125.1, 83.5, 24.9.

(*E*)-2-(2-cyclohexylvinyl)-4,4,5,5-tetramethyl-1,3,2-dioxaborolane **(10g)**[8].

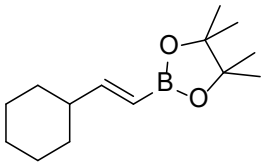

Yield: 94%. $^{1}$H NMR (400 MHz, $CDCl_3$, 298 K): $\delta_H$ (ppm) 6.61-6.55 (dd, $J$ = 4 Hz, 1H, C*H*), 5.40-5.35 (dd, $J$ = 4 Hz, 1H, C*H*), 1.88-1.84 (m, 1H, Cyclohexyl-C*H*), 1.76-1.70 (m, 6H, C$H_2$), 1.27 (s, 12H, Bpin-C$H_3$), 1.21-1.17 (m, 4H, C$H_2$). $^{11}$B{$^{1}$H} NMR (128.4 MHz, $CDCl_3$, 298 K): $\delta_B$ (ppm) 29.8. $^{13}$C{$^{1}$H} NMR (100 MHz, $CDCl_3$, 298 K): $\delta_c$ (ppm) 160.0, 83.1, 43.4, 32.0, 26.3, 26.1, 24.9.

(*E*)-2-(2-cyclopentavinyl)-4,4,5,5-tetramethyl-1,3,2-dioxaborolane **(10h)**[8].

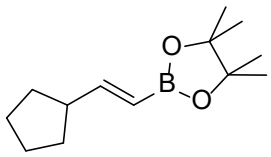

Yield. 97%. $^{1}$H NMR (400 MHz, $CDCl_3$, 298 K): $\delta_H$ (ppm) 6.57-6.50 (dd, 1H, C*H*), 5.35-5.30 (dd, 1H, C*H*), 2.49-2.38 (m, 1H, Cyclopentyl-C*H*), 1.73-1.67 (m, 2H, C$H_2$), 1.59-1.53 (m, 2H, C$H_2$), 1.52-1.45 (m, 2H, C$H_2$), 1.32-1.27 (m, 2H, C$H_2$), 1.19 (s, 12H, Bpin-C$H_3$). $^{11}$B{$^{1}$H} NMR (128.4 MHz, $CDCl_3$, 298 K): $\delta_B$ (ppm) 29.6. $^{13}$C{$^{1}$H} NMR (100 MHz, $CDCl_3$, 298 K): $\delta_c$ (ppm) 159.0, 83.1, 46.3, 32.5, 25.4, 24.9.

(*E*)-2-(2-(cyclohex-1-en-1-yl)vinyl)-4,4,5,5-tetramethyl-1,3,2-dioxaborolane **(10i)**[11].

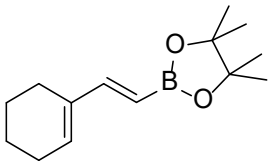

Yield. 96%. $^{1}$H NMR (400 MHz, $CDCl_3$, 298 K): $\delta_H$ (ppm) 6.97-6.94 (d, *J* = 12 Hz, 1H, C*H*), 5.89 (t, *J* = 4 Hz, 1H, Cyclohexenyl-C*H*), 5.37-5.34 (d, *J* = 12 Hz, 1H, C*H*), 2.08-2.07 (d, 4H, C$H_2$), 1.61-1.58 (m, 2H, C$H_2$), 1.53-1.50 (m, 2H, C$H_2$), 1.20 (s, 12H, Bpin-C$H_3$). $^{11}$B{$^{1}$H} NMR (128.4 MHz, $CDCl_3$, 298 K): $\delta_B$ (ppm) 30.3. $^{13}$C{$^{1}$H} NMR (100 MHz, $CDCl_3$, 298 K): $\delta_c$ (ppm) 153.4, 137.3, 134.4, 83.1, 26.3, 24.9, 23.9, 22.5, 22.4.

(*E*)-2-(2-(cyclohex-1-en-1-yl)vinyl)-4,4,5,5-tetramethyl-1,3,2-dioxaborolane **(10j)**[8].

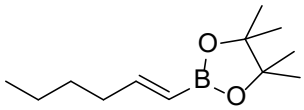

Yield. 93%. $^{1}$H NMR (400 MHz, $CDCl_3$, 298 K): $\delta_H$ (ppm) 6.96-6.93 (d, *J* = 12 Hz, 1H, C*H*), 5.37-5.34 (d, *J* = 12 Hz, 1H, C*H*), 2.07-2.05 (m, 5H, C$H_2$), 1.60-1.56 (m, 2H, C$H_2$), 1.53-1.49 (m, 2H, C$H_2$), 1.20 (s, 12H, Bpin-C$H_3$). $^{11}$B{$^{1}$H} NMR (128.4 MHz, $CDCl_3$, 298 K): $\delta_B$ (ppm) 29.7. $^{13}$C{$^{1}$H} NMR (100 MHz, $CDCl_3$, 298 K): $\delta_c$ (ppm) 154.9, 83.1, 35.6, 30.5, 24.9, 22.4, 14.1.

(*E*)-2-(5-chloropent-1-en-1-yl)-4,4,5,5-tetramethyl-1,3,2-dioxaborolane **(10k)**[8].

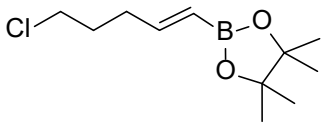

Yield: 95%. $^{1}$H NMR (400 MHz, $CDCl_3$, 298 K): $\delta_H$ (ppm) 6.55-6.47 (dt,1H, C*H*), 5.44-5.39 (d, *J* = 20 Hz, 1H, C*H*), 3.46 (t, *J* = 6 Hz, 2H, C$H_2$), 2.25-2.21 (m, 2H, C$H_2$), 1.84-1.79 (m, 2H, C$H_2$), 1.19 (s, 12H, Bpin-C$H_3$). $^{11}$B{$^{1}$H} NMR (128.4 MHz, $CDCl_3$, 298 K): $\delta_B$ (ppm) 29.7. $^{13}$C{$^{1}$H} NMR (100 MHz, $CDCl_3$, 298 K): $\delta_c$ (ppm) 152.2, 83.2, 44.4, 32.8, 31.1, 24.9.

(*E*)-trimethyl(2-(4,4,5,5-tetramethyl-1,3,2-dioxaborolan-2-yl)vinyl)ailane **(10l)**[8].

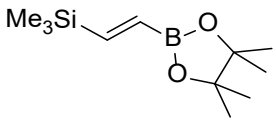

Yield: 95%. $^{1}$H NMR (400 MHz, $CDCl_3$, 298 K): $\delta_H$ (ppm) 7.12-7.09 (d, $J$ = 12 Hz, 1H, C*H*), 6.24-6.21 (d, $J$ = 12 Hz, 1H, C*H*), 1.26 (s, 12H, Bpin-C$H_3$), 0.06 (s, 9H, Si(C$H_3$)$_3$). $^{11}$B{$^{1}$H} NMR (128.4 MHz, $CDCl_3$, 298 K): $\delta_B$ (ppm) 29.7. $^{13}$C{$^{1}$H} NMR (100 MHz, $CDCl_3$, 298 K): $\delta_c$ (ppm) 157.9, 131.4, 83.5, 24.9, -1.76.

## 7. Catalytic hydroboration of alkenes

### General catalytic procedure for the hydroboration of alkenes

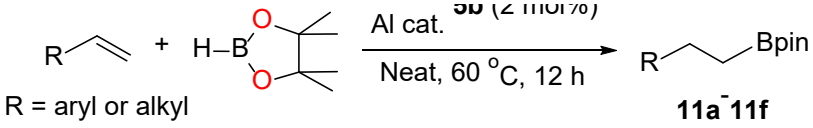


Inside the glove box, the Al catalyst **5b** (2 mol %) and HBpin (0.5 mmol, 1 equiv) was added to a Schlenk tube followed by the addition of alkenes (0.5 mmol, 1 equiv). The Schlenk tube was taken out from the glove box and the reaction mixture was stirred at 60 °C for 12 hours. Finally, volatiles of the mixture were removed under the reduced pressure to obtain the hydroboration product. The yield was calculated from $^{1}$H NMR spectroscopy with the help of 1,3,5-trimethoxy benzene as the internal standard.

### NMR data of alkyl boronates

4,4,5,5-tetramethyl-2-phenethyl-1,3,2-dioxaborolane **(11a)**[12].

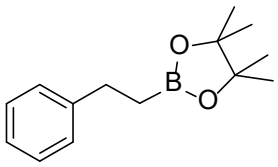

Yield: 96%. $^{1}$H NMR (400 MHz, $CDCl_3$, 298 K): $\delta_H$ (ppm) 7.19-7.12 (m, 5H, Ar-*H*), 2.67 (t, $J$ = 8 Hz, 2H, C$H_2$), 1.13 (s, 12H, Bpin-C$H_3$), 1.06 (t, $J$ = 10 Hz, 2H, C$H_2$). $^{11}$B{$^{1}$H} NMR (128.4 MHz, $CDCl_3$, 298 K): $\delta_B$ (ppm) 33.8. $^{13}$C{$^{1}$H} NMR (100 MHz, $CDCl_3$, 298 K): $\delta_c$ (ppm) 144.5, 128.3, 128.1, 125.6, 83.2, 30.1, 24.9.

2-(4-methoxyphenethyl)-4,4,5,5-tetramethyl-1,3,2-dioxaborolane **(11b)**[13].

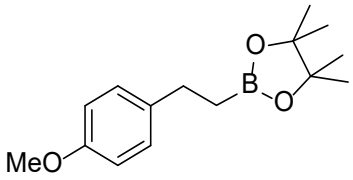


Yield: 93%. $^{1}$H NMR (400 MHz, $CDCl_3$, 298 K): $\delta_H$ (ppm) 7.05 (d, *J* = 8 Hz, 2H, Ar-*H*), 6.73 (d, *J* = 8 Hz, 2H, Ar-*H*), 3.68 (s, 3H, O-C*H*$_3$), 2.61 (t, *J* = 8 Hz, 2H, C*H*$_2$), 1.14 (s, 12H, Bpin-C*H*$_3$), 1.03 (t, *J* = 6 Hz, 2H, C*H*$_2$). $^{11}$B{$^{1}$H} NMR (128.4 MHz, $CDCl_3$, 298 K): $\delta_B$ (ppm) 33.2. $^{13}$C{$^{1}$H} NMR (100 MHz, $CDCl_3$, 298 K): $\delta_c$ (ppm) 157.7, 136.7, 128.9, 113.7, 83.2, 55.4, 29.2, 24.9.

2-(4-methylphenethyl)-4,4,5,5-tetramethyl-1,3,2-dioxaborolane **(11c)**[12].

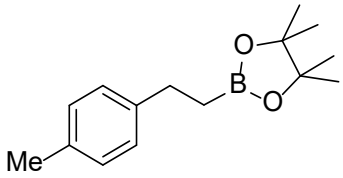


Yield: 96%. $^{1}$H NMR (400 MHz, $CDCl_3$, 298 K): $\delta_H$ (ppm) 7.03-7.02 (t, 2H, Ar-*H*), 6.99-6.98 (d, 2H, Ar-*H*), 2.63 (t, *J* = 6 Hz, 2H, C*H*$_2$), 2.22 (s, 3H, C*H*$_3$) 1.14 (s, 12H, Bpin-C*H*$_3$), 1.05 (t, *J* = 6 Hz, 2H, C*H*$_2$). $^{11}$B{$^{1}$H} NMR (128.4 MHz, $CDCl_3$, 298 K): $\delta_B$ (ppm) 33.8. $^{13}$C{$^{1}$H} NMR (100 MHz, $CDCl_3$, 298 K): $\delta_c$ (ppm) 141.5, 134.9, 128.9, 127.9, 83.2, 29.6, 24.9, 21.1.

2-(4-fluorophenethyl)-4,4,5,5-tetramethyl-1,3,2-dioxaborolane **(11d)**[12].

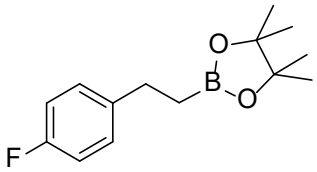


Yield: 96%. $^{1}$H NMR (400 MHz, $CDCl_3$, 298 K): $\delta_H$ (ppm) 7.09-7.06 (m, 2H, Ar-*H*), 6.87-6.83 (m, 2H, Ar-*H*), 2.63 (t, *J* = 8 Hz, 2H, C*H*$_2$), 1.13 (s, 12H, Bpin-C*H*$_3$), 1.04 (t, *J* = 8 Hz, 2H, C*H*$_2$). $^{11}$B{$^{1}$H} NMR (128.4 MHz, $CDCl_3$, 298 K): $\delta_B$ (ppm) 33.9. $^{13}$C{$^{1}$H} NMR (100 MHz, $CDCl_3$, 298 K): $\delta_c$ (ppm) 162.4, 129.5, 128.3, 115.0, 114.8, 83.2, 29.3, 24.9, 24.6.

2-(4-chlorophenethyl)-4,4,5,5-tetramethyl-1,3,2-dioxaborolane **(11e)**[12].

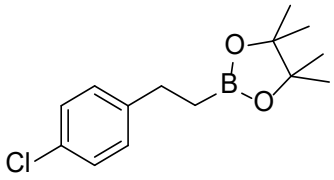


Yield: 97%. $^{1}$H NMR (400 MHz, $CDCl_3$, 298 K): $\delta_H$ (ppm) 7.13-7.12 (m, 2H, Ar-*H*), 7.05-7.04 (m, 2H, Ar-*H*), 2.63 (t, *J* = 6 Hz, 2H, C*H*$_2$), 1.12 (s, 12H, Bpin-C*H*$_3$), 1.03 (t, *J* = 6 Hz, 2H, C*H*$_2$). $^{11}$B{$^{1}$H} NMR (128.4 MHz, $CDCl_3$, 298 K): $\delta_B$ (ppm) 33.6. $^{13}$C{$^{1}$H} NMR (100 MHz, $CDCl_3$, 298 K): $\delta_c$ (ppm) 142.9, 129.5, 128.3, 127.5, 117.8, 83.3, 29.4, 24.9.

2-(6-bromohexyl)-4,4,5,5-tetramethyl-1,3,2-dioxaborolane **(11f)**[12].

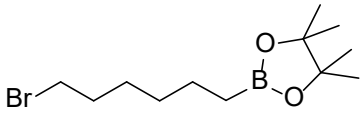


Yield: 96%. $^{1}$H NMR (400 MHz, $CDCl_3$, 298 K): $\delta_H$ (ppm) 3.35-3.31 (m, 2H, C*H*$_2$), 1.80-1.75 (m, 2H, C*H*$_2$), 1.38-1.32 (m, 4H, C*H*$_2$), 1.27-1.23 (m, 2H, C*H*$_2$), 1.17 (s, 12H, Bpin-C*H*$_3$), 0.71 (t, *J* = 6 Hz, 2H, C*H*$_2$). $^{11}$B{$^{1}$H} NMR (128.4 MHz, $CDCl_3$, 298 K): $\delta_B$ (ppm) 33.9. $^{13}$C{$^{1}$H} NMR (100 MHz, $CDCl_3$, 298 K): $\delta_c$ (ppm) 83.0, 34.1, 32.8, 31.5, 28.0, 24.9, 23.9.

## 8. NMR spectra of hydroboration products

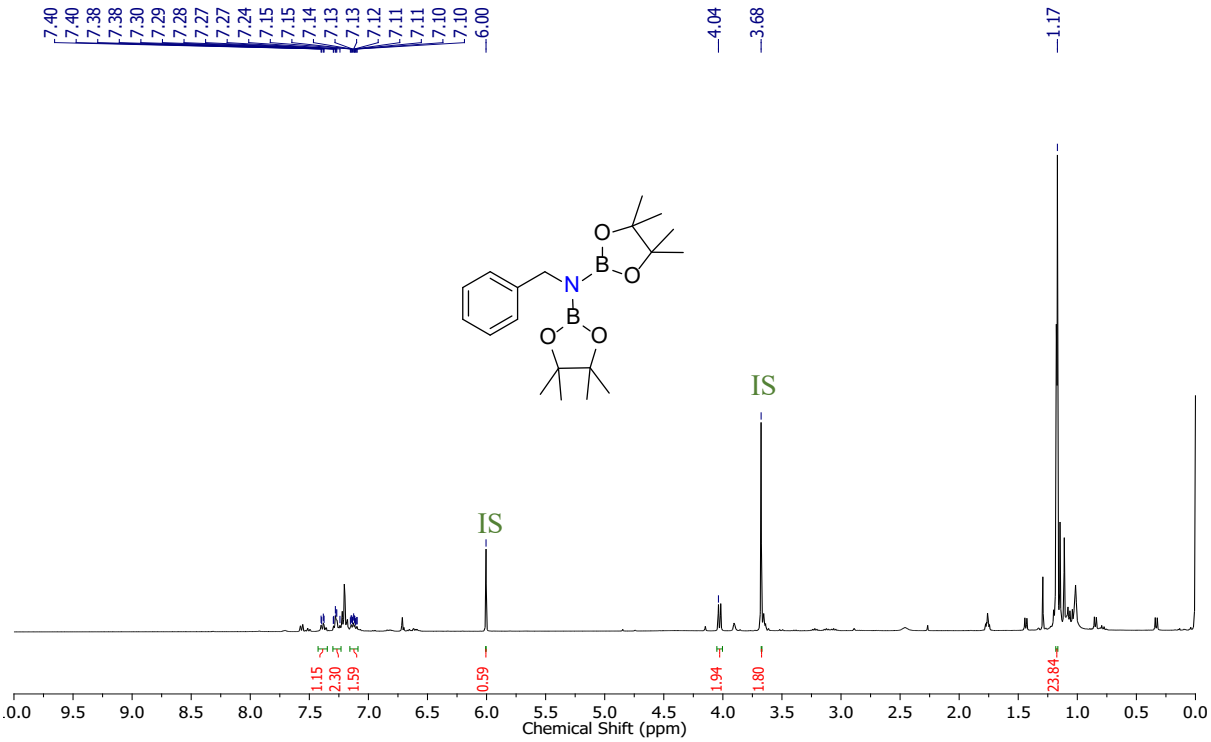


**Figure S53**. $^{1}$H NMR (400 MHz, $CDCl_3$, 298 K) spectrum of **8a**.

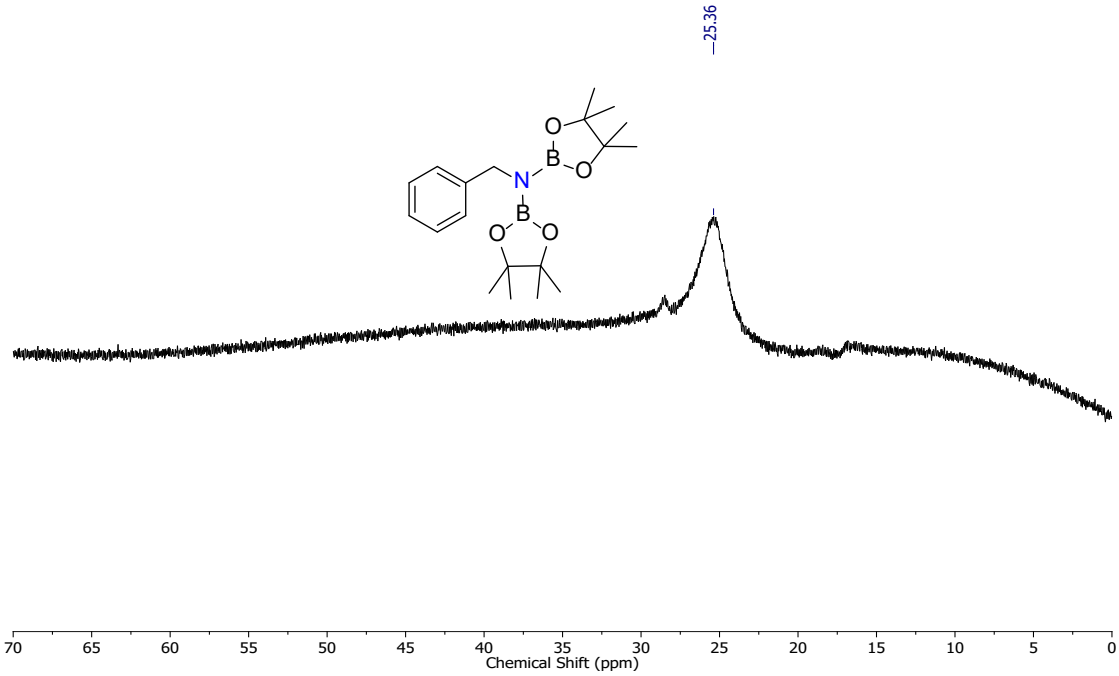


**Figure S54**. $^{11}B\{^{1}H\}$ NMR (128.4 MHz, $CDCl_3$, 298 K) spectrum of **8a**.

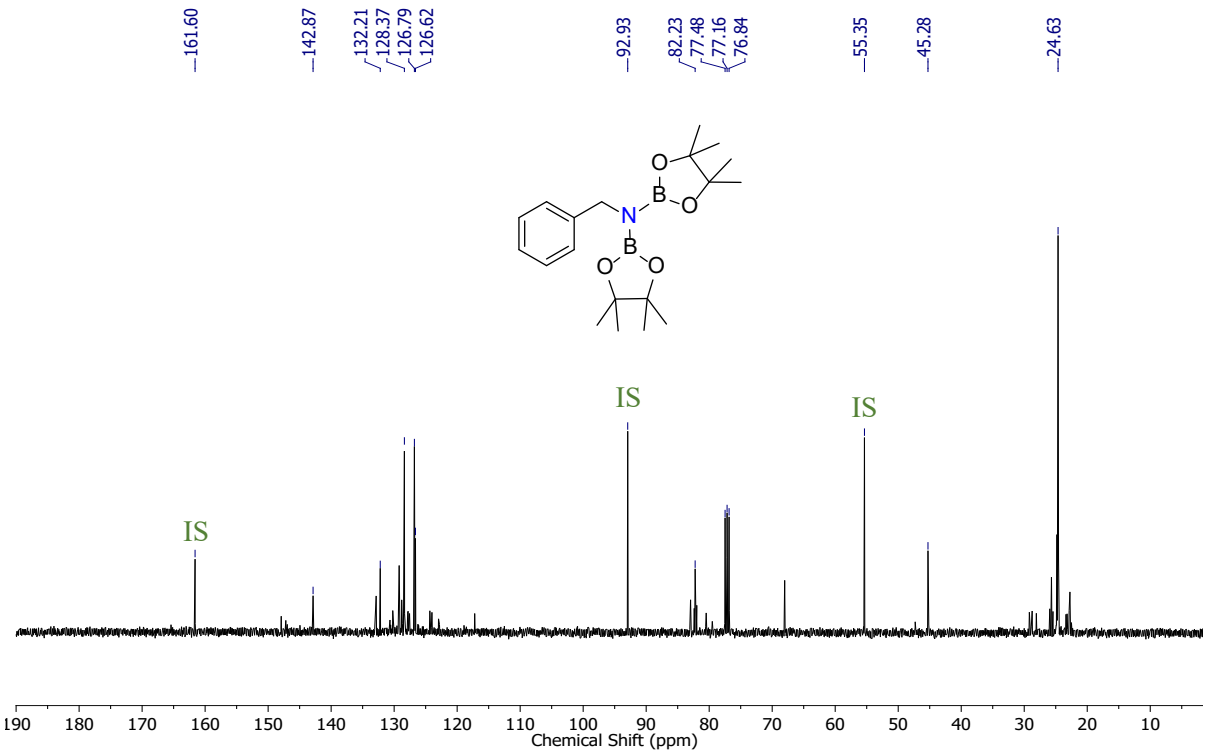


**Figure S55**. $^{13}C\{^{1}H\}$ NMR (100 MHz, $CDCl_3$, 298 K) spectrum of **8a**.

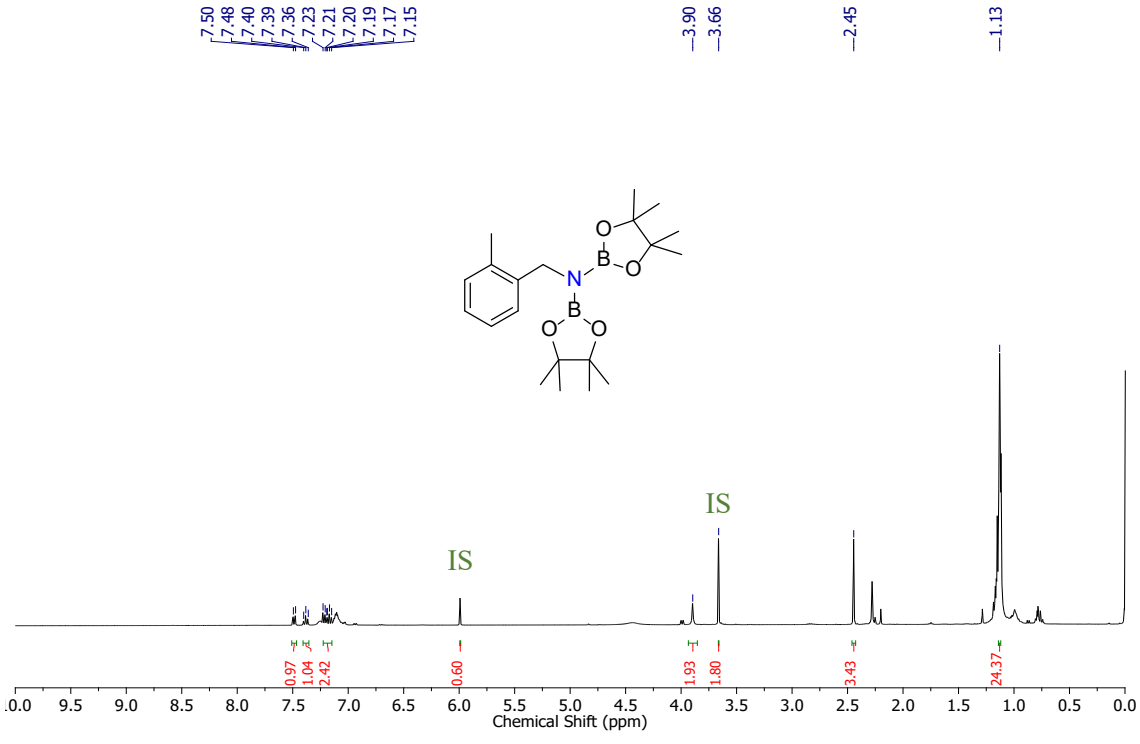


**Figure S56**. $^{1}H$ NMR (400 MHz, $CDCl_3$, 298 K) spectrum of **8b**.

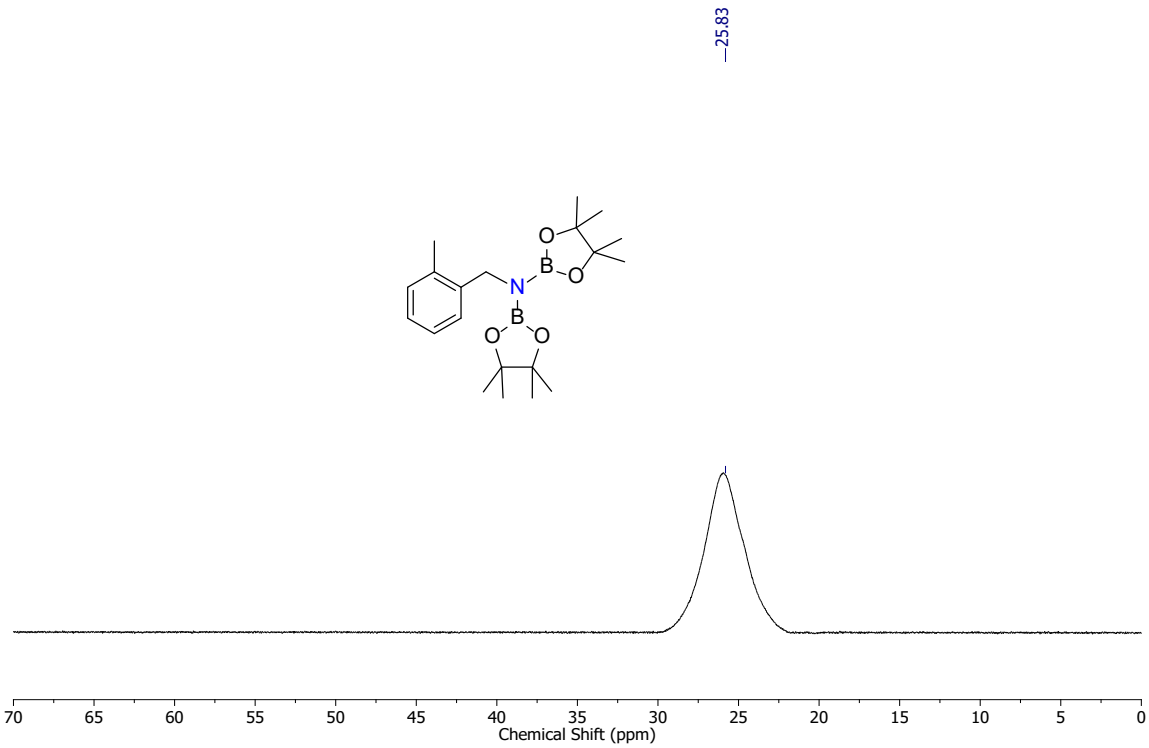


**Figure S57**. $^{11}B\{^{1}H\}$ NMR (128.4 MHz, $CDCl_3$, 298 K) spectrum of **8b**.

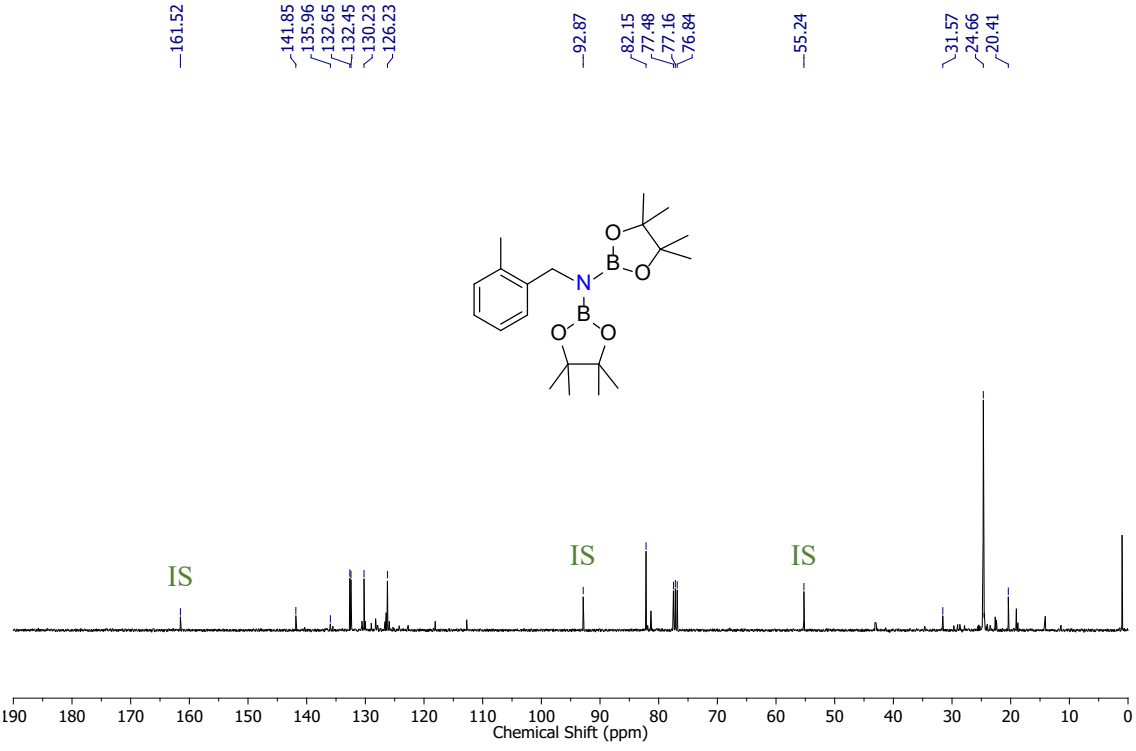


**Figure S58**. $^{13}C\{^{1}H\}$ NMR (100 MHz, $CDCl_3$, 298 K) spectrum of **8b**.

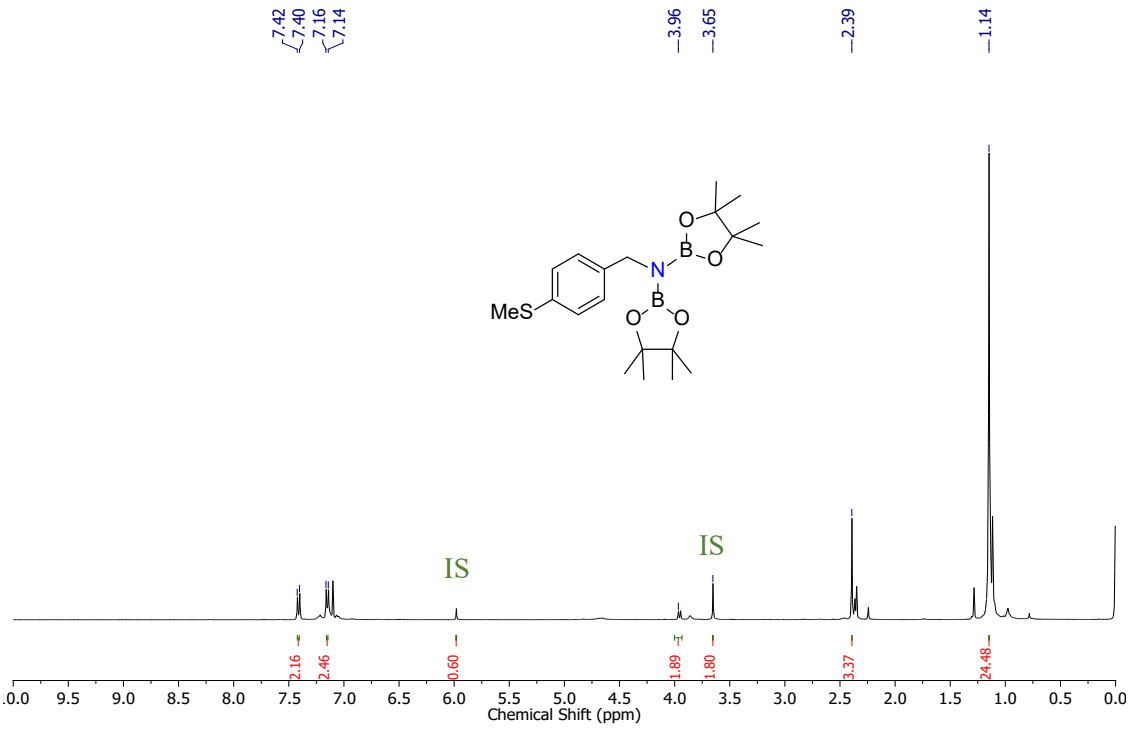


**Figure S59**. $^{1}H$ NMR (400 MHz, $CDCl_3$, 298 K) spectrum of **8c**.

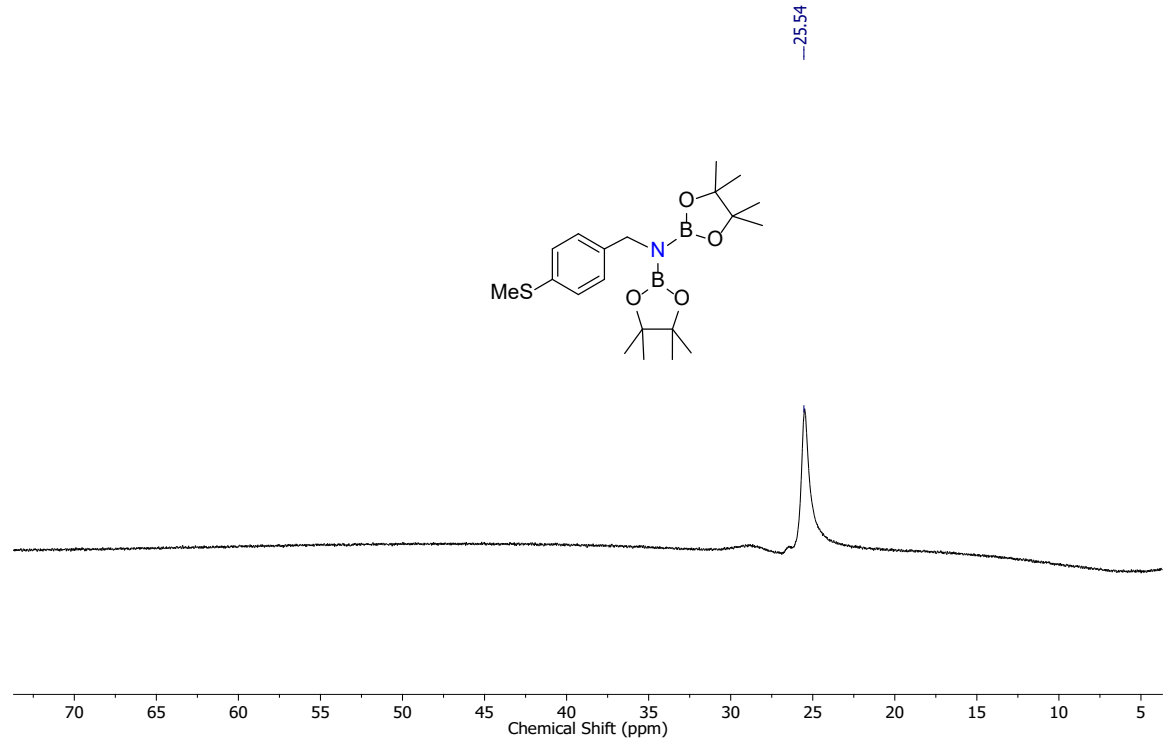


**Figure S60**. $^{11}B\{^{1}H\}$ NMR (128.4 MHz, $CDCl_3$, 298 K) spectrum of **8c**.

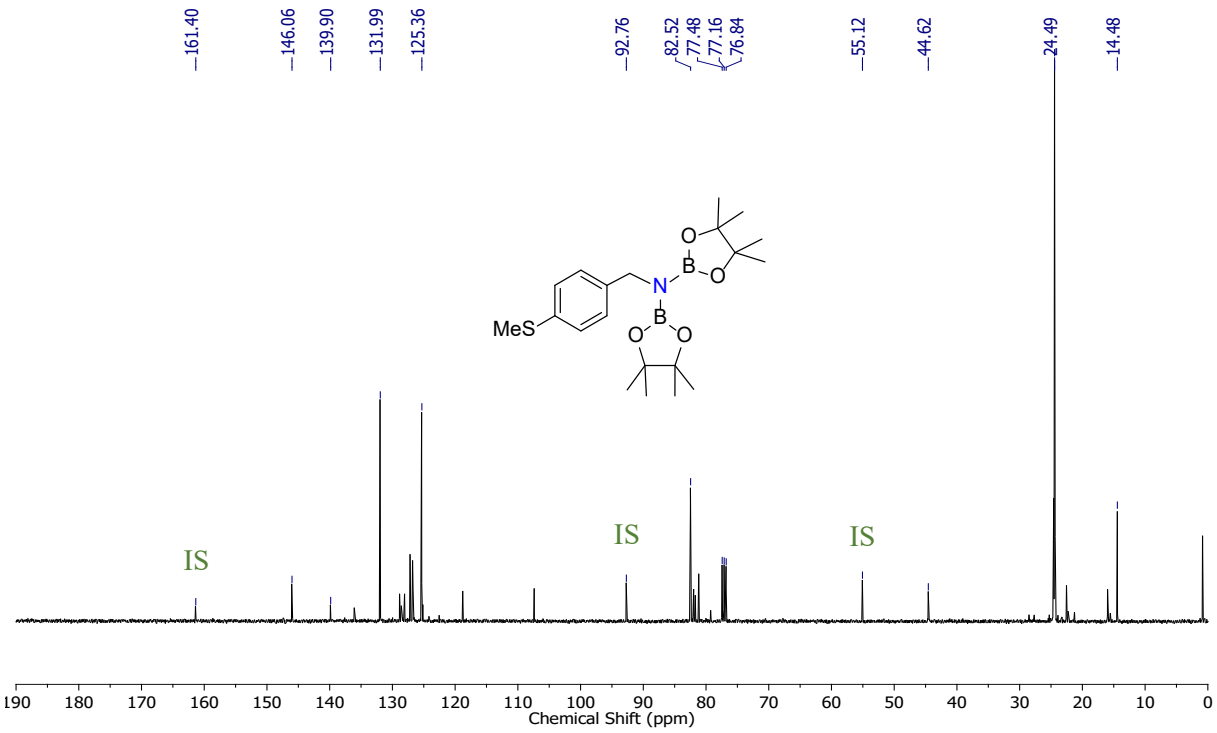


**Figure S61**. $^{13}C\{^{1}H\}$ NMR (100 MHz, $CDCl_3$, 298 K) spectrum of **8c**.

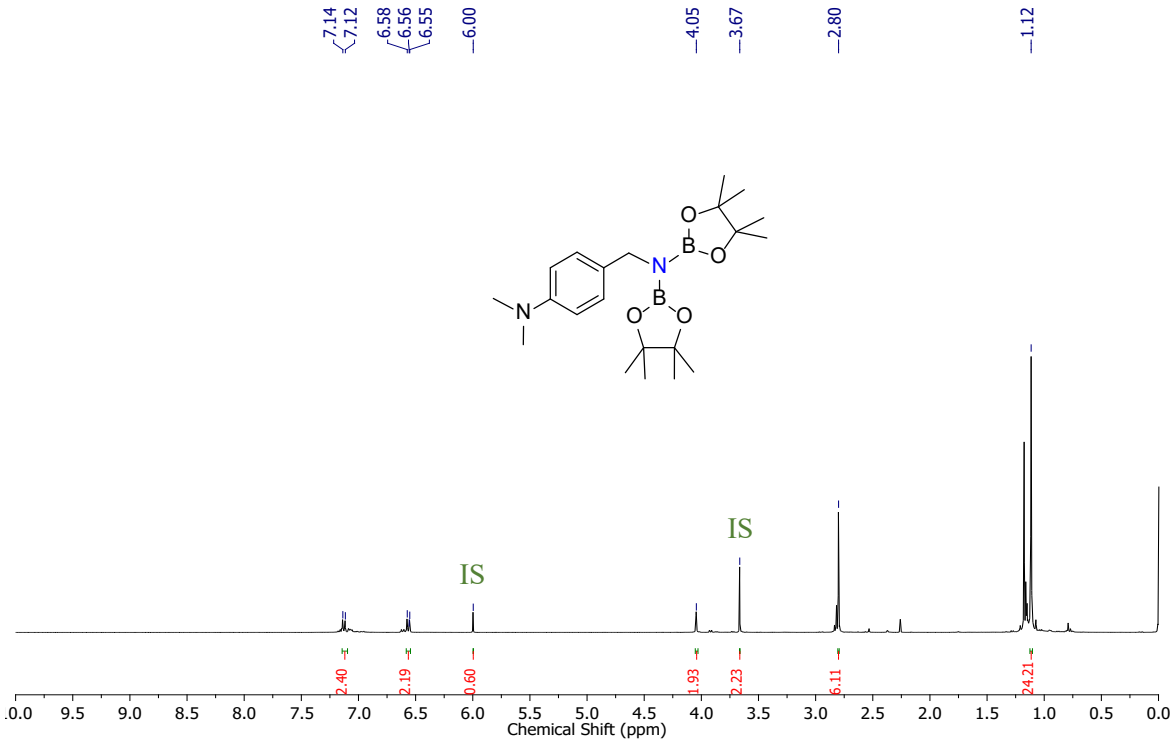


**Figure S62**. $^{1}H$ NMR (400 MHz, $CDCl_3$, 298 K) spectrum of **8d**.

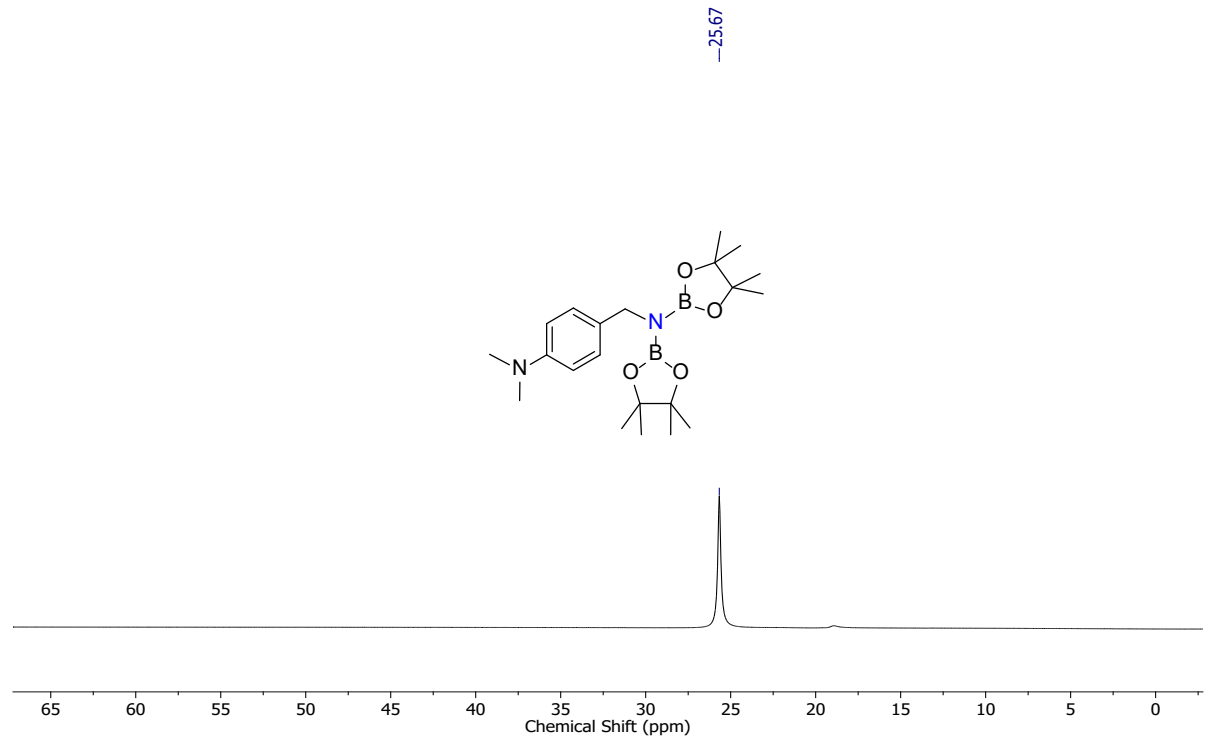


**Figure S63**. $^{11}B\{^{1}H\}$ NMR (128.4 MHz, $CDCl_3$, 298 K) spectrum of **8d**.

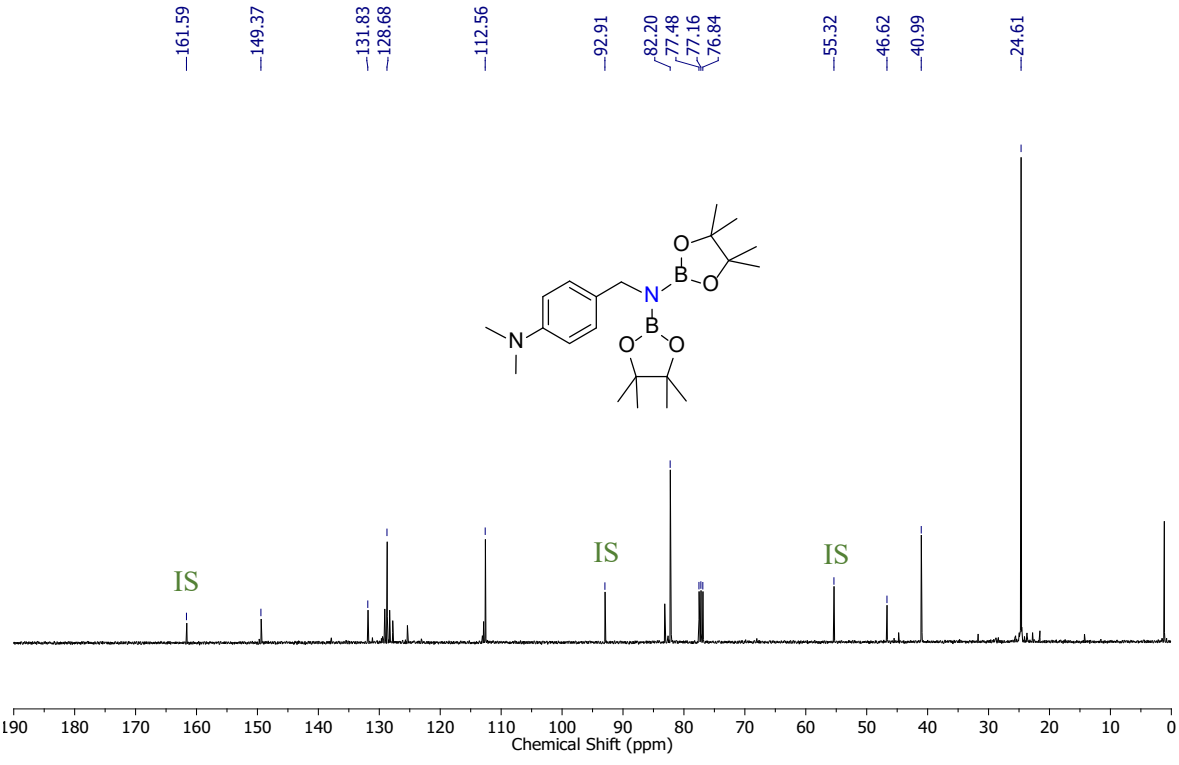


**Figure S64**. $^{13}C\{^{1}H\}$ NMR (100 MHz, $CDCl_3$, 298 K) spectrum of **8d**.

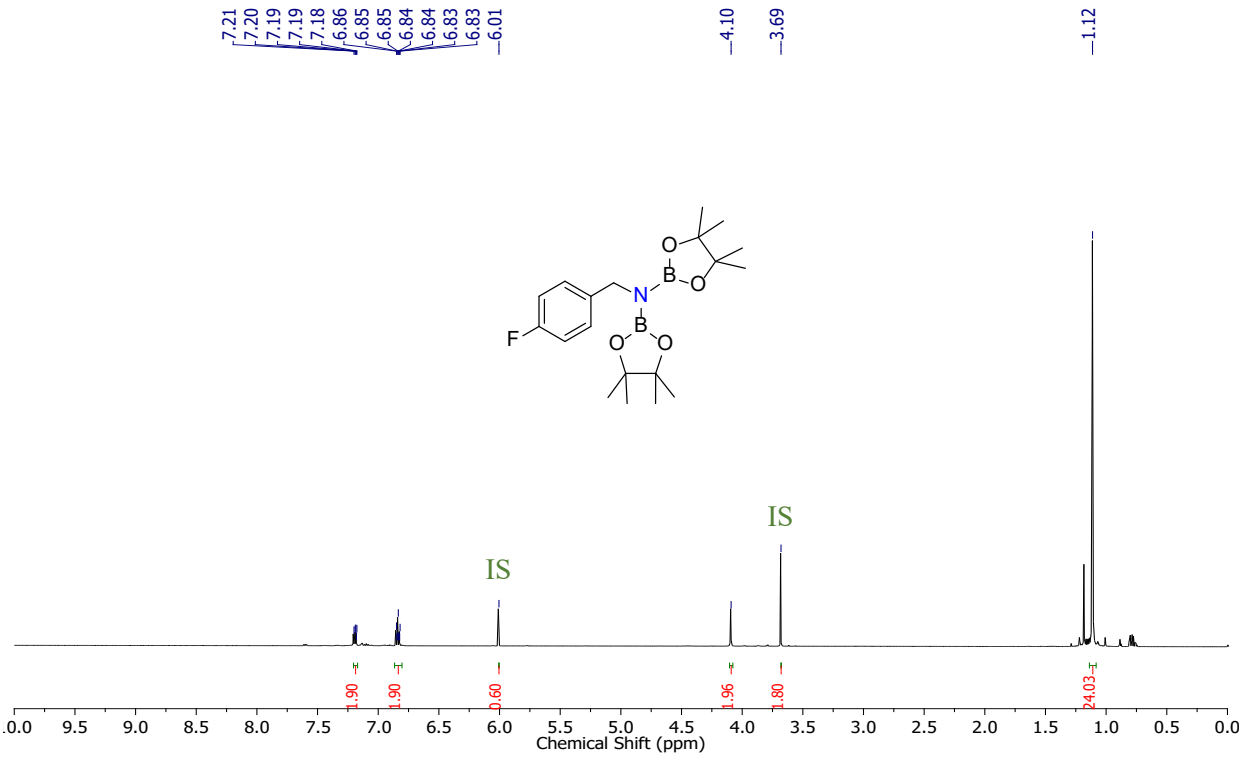


**Figure S65**. $^{1}H$ NMR (400 MHz, $CDCl_3$, 298 K) spectrum of **8e**.

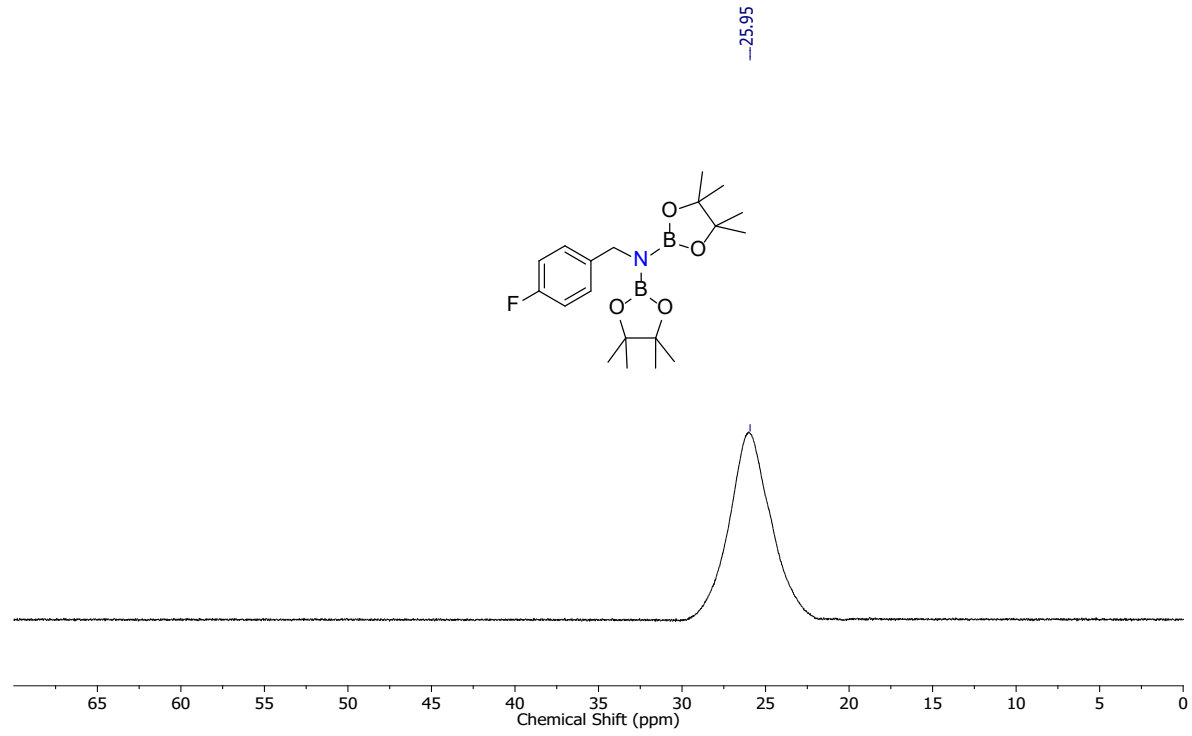


**Figure S66**. $^{11}B\{^{1}H\}$ NMR (128.4 MHz, $CDCl_3$, 298 K) spectrum of **8e**.

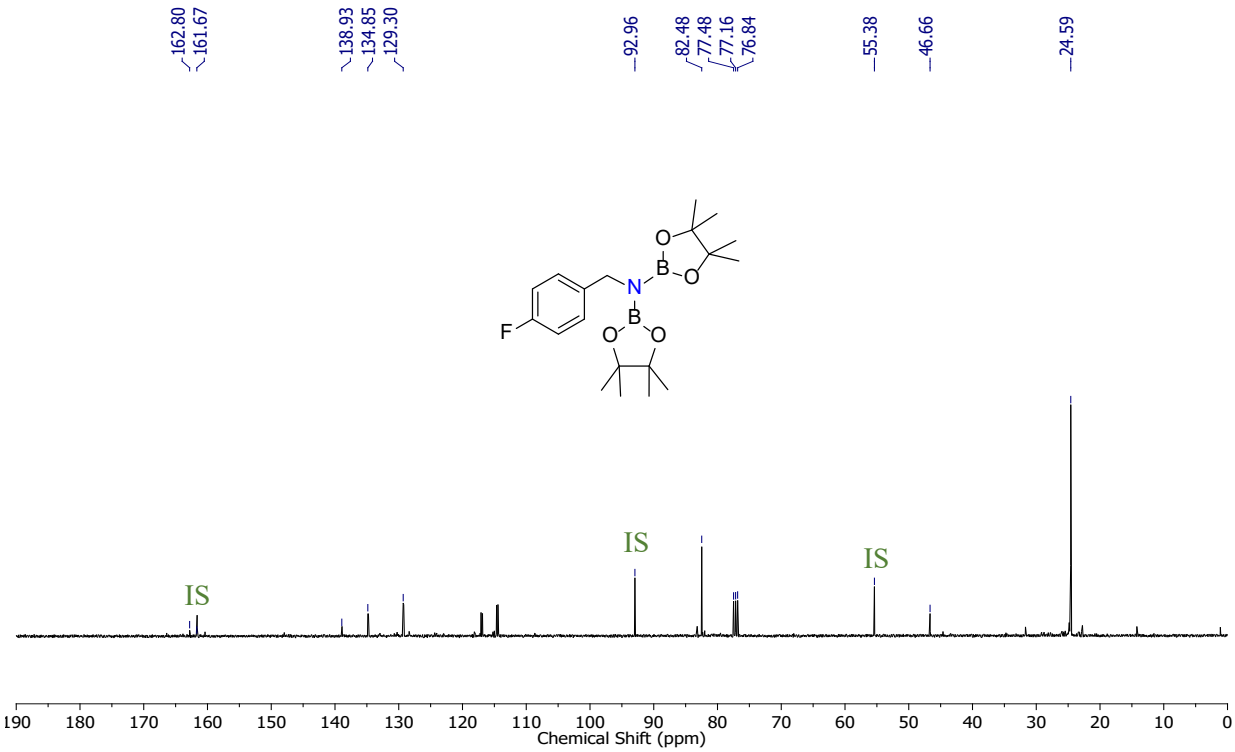


**Figure S67**. $^{13}C\{^{1}H\}$ NMR (100 MHz, $CDCl_3$, 298 K) spectrum of **8e**.

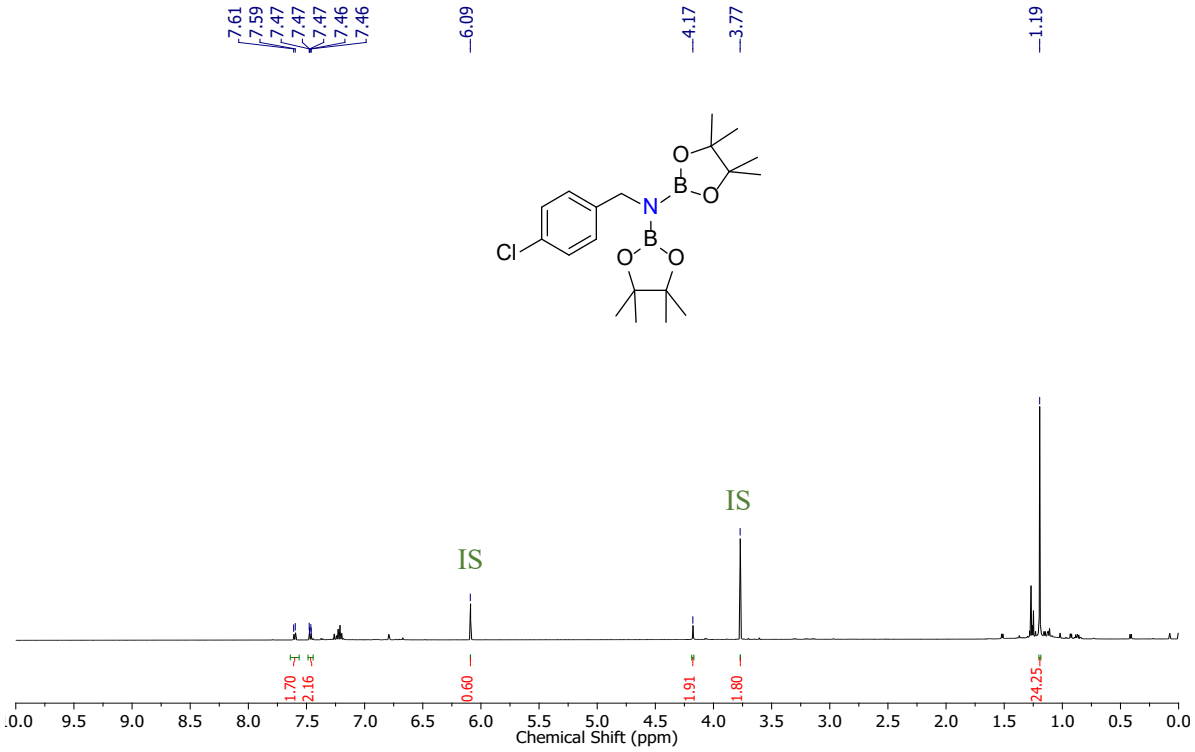


**Figure S68**. $^{1}H$ NMR (400 MHz, $CDCl_3$, 298 K) spectrum of **8f**.

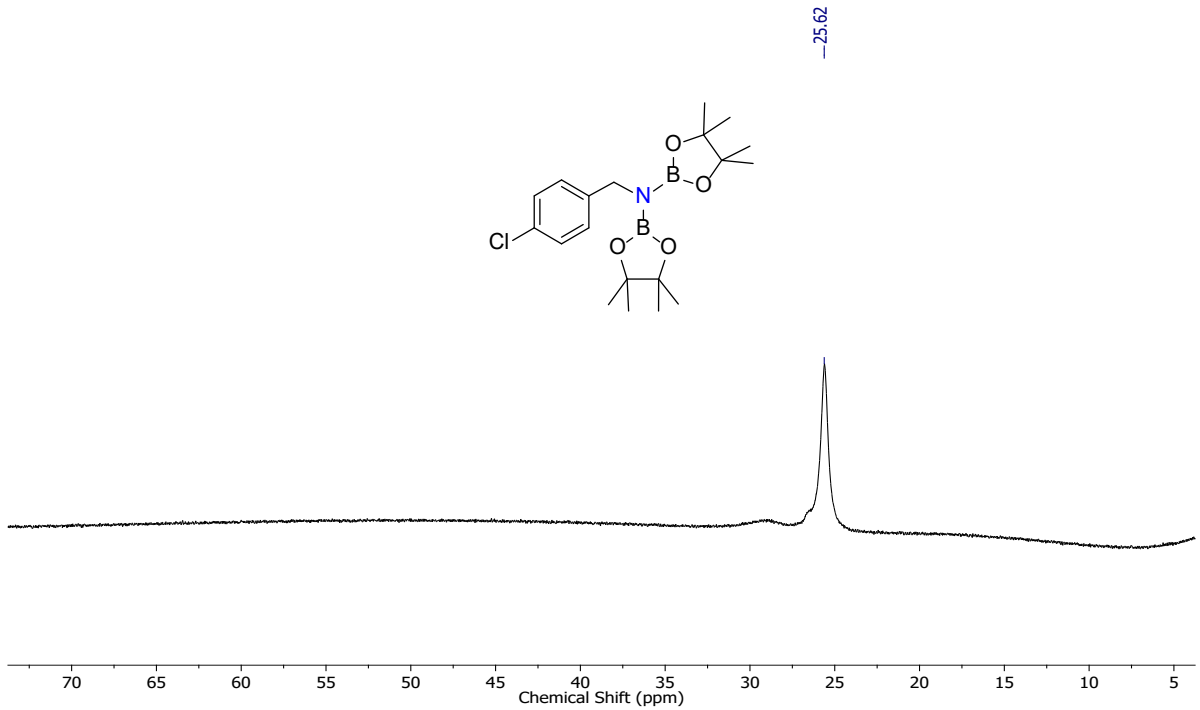


**Figure S69**. $^{11}B\{^{1}H\}$ NMR (128.4 MHz, $CDCl_3$, 298 K) spectrum of **8f**.

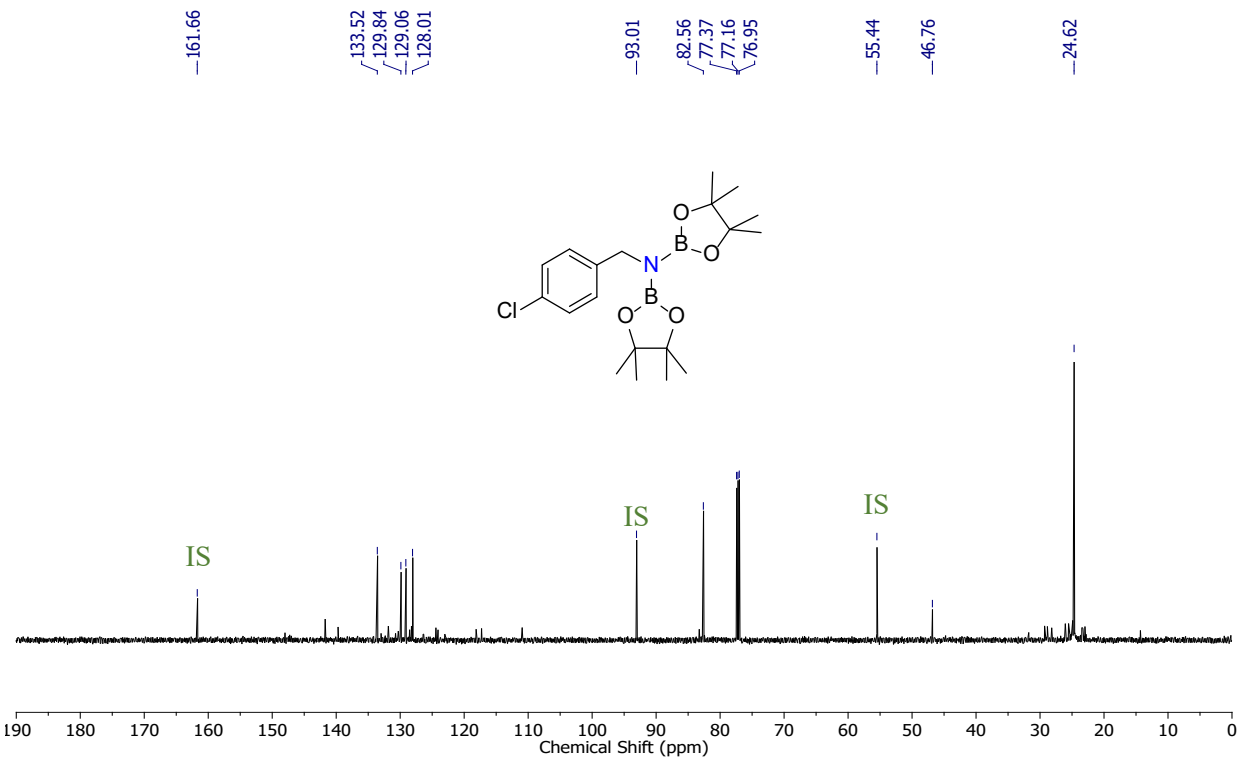


**Figure S70**. $^{13}C\{^{1}H\}$ NMR (100 MHz, $CDCl_3$, 298 K) spectrum of **8f**.

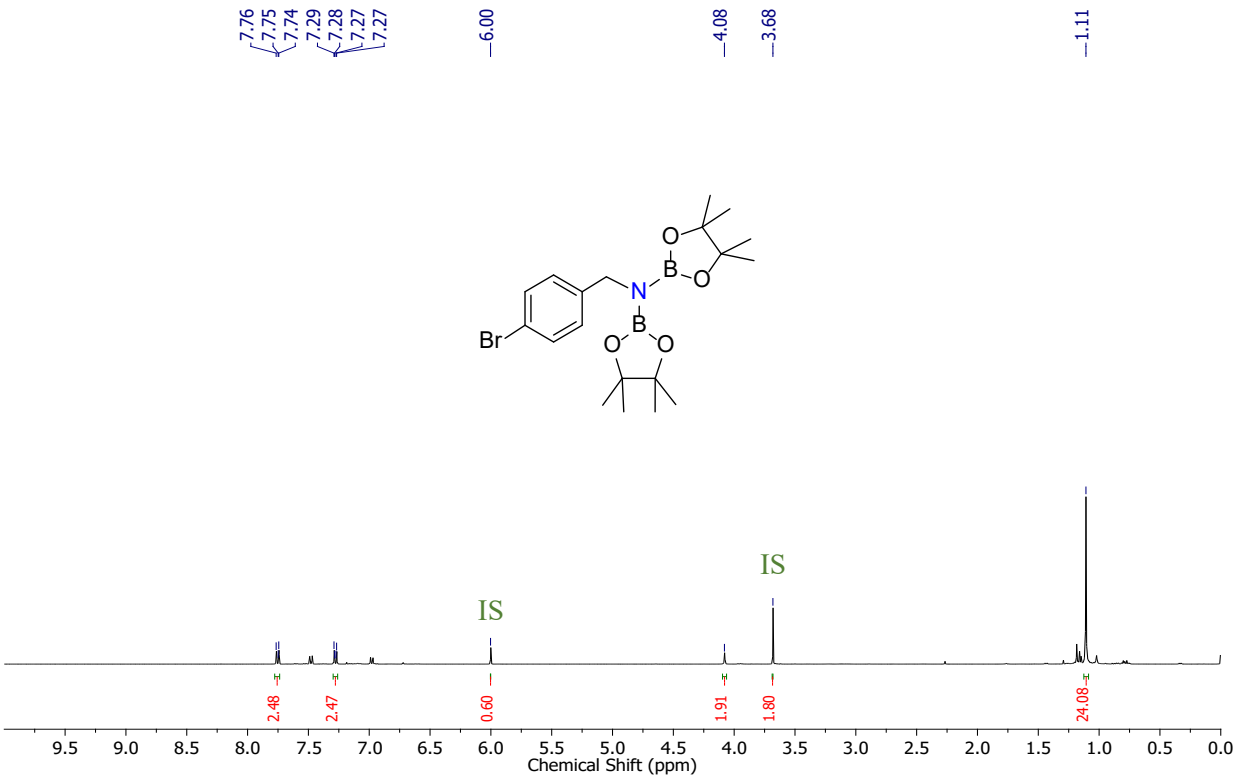


**Figure S71**. $^{1}H$ NMR (400 MHz, $CDCl_3$, 298 K) spectrum of **8g**.

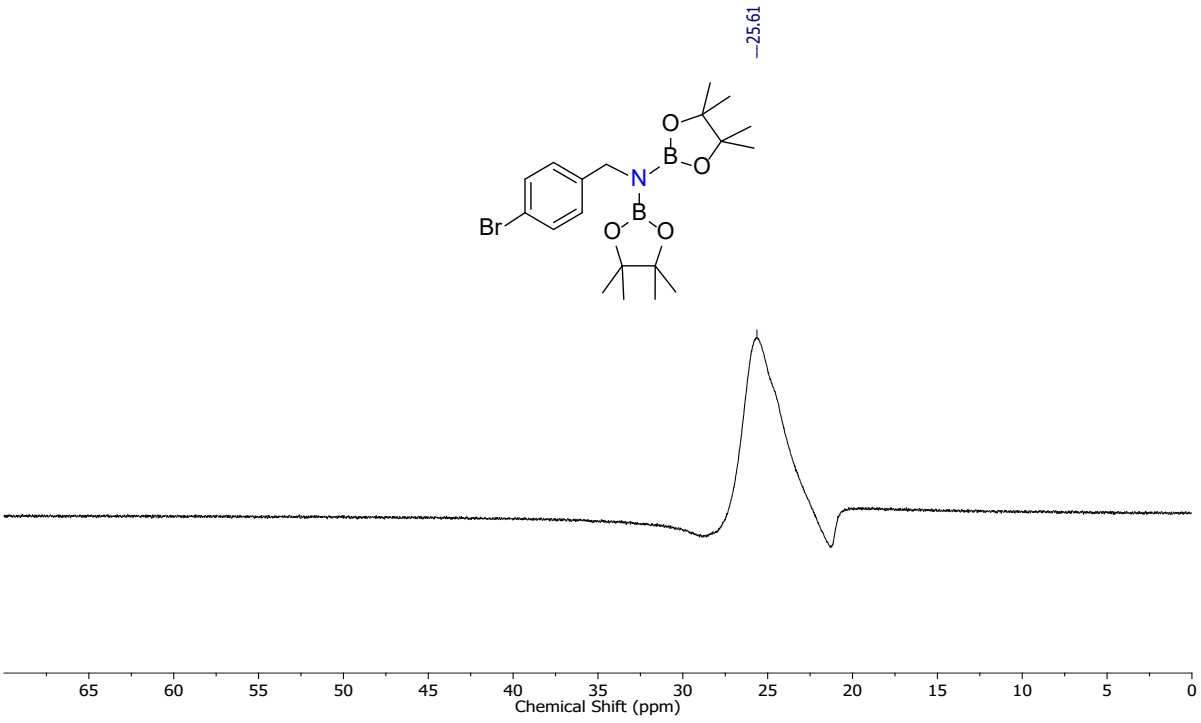


**Figure S72**. $^{11}B\{^{1}H\}$ NMR (128.4 MHz, $CDCl_3$, 298 K) spectrum of **8g**.

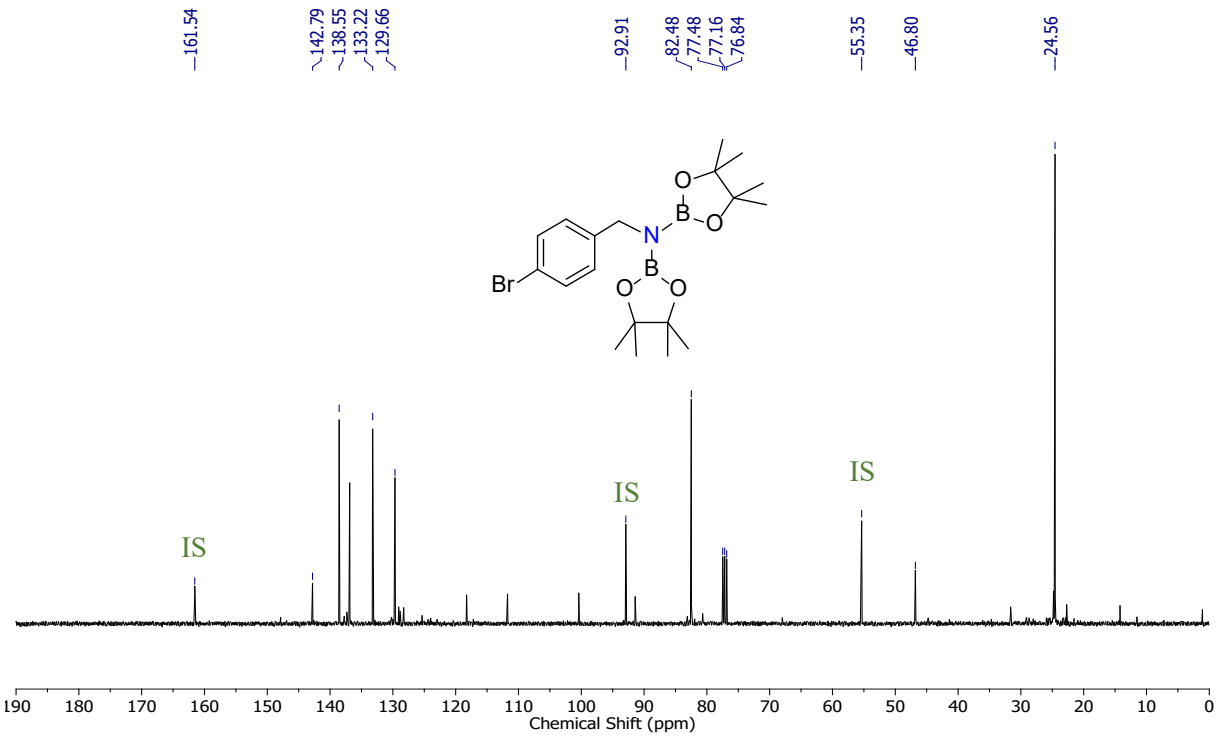


**Figure S73**. $^{13}C\{^{1}H\}$ NMR (100 MHz, $CDCl_3$, 298 K) spectrum of **8g**.

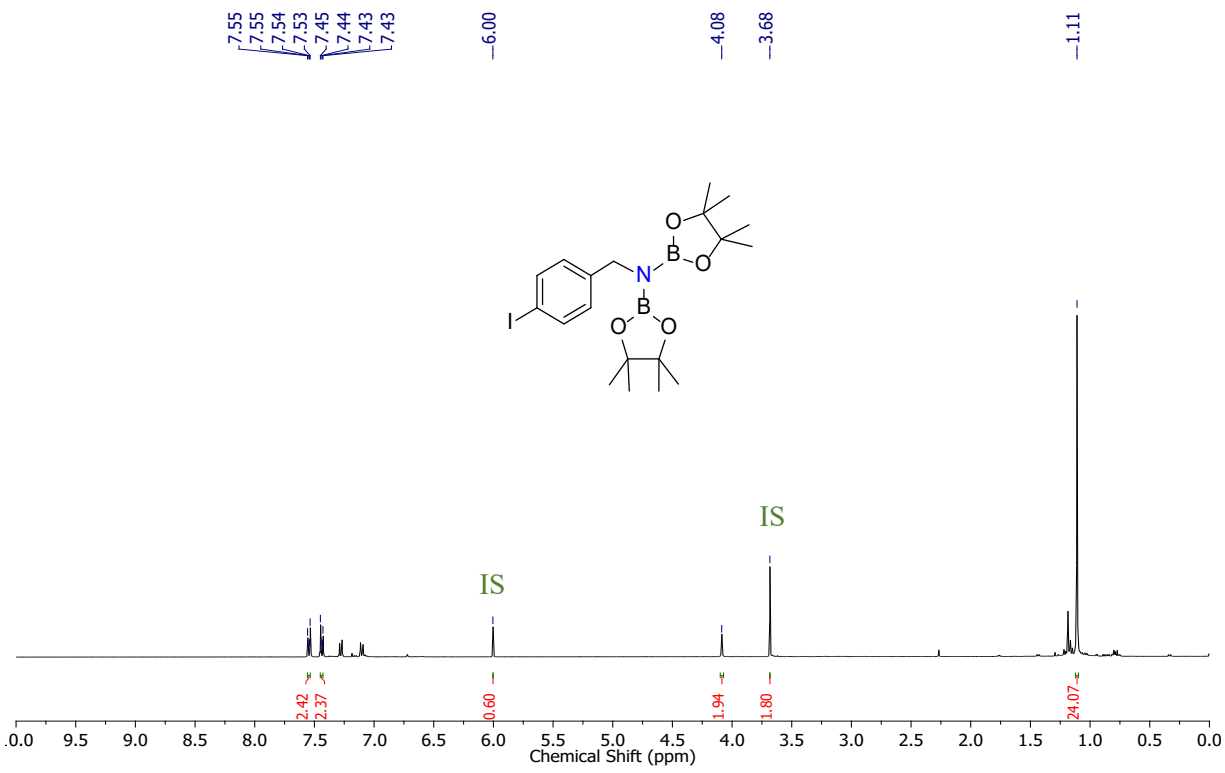


**Figure S74**. $^{1}H$ NMR (400 MHz, $CDCl_3$, 298 K) spectrum of **8h**.

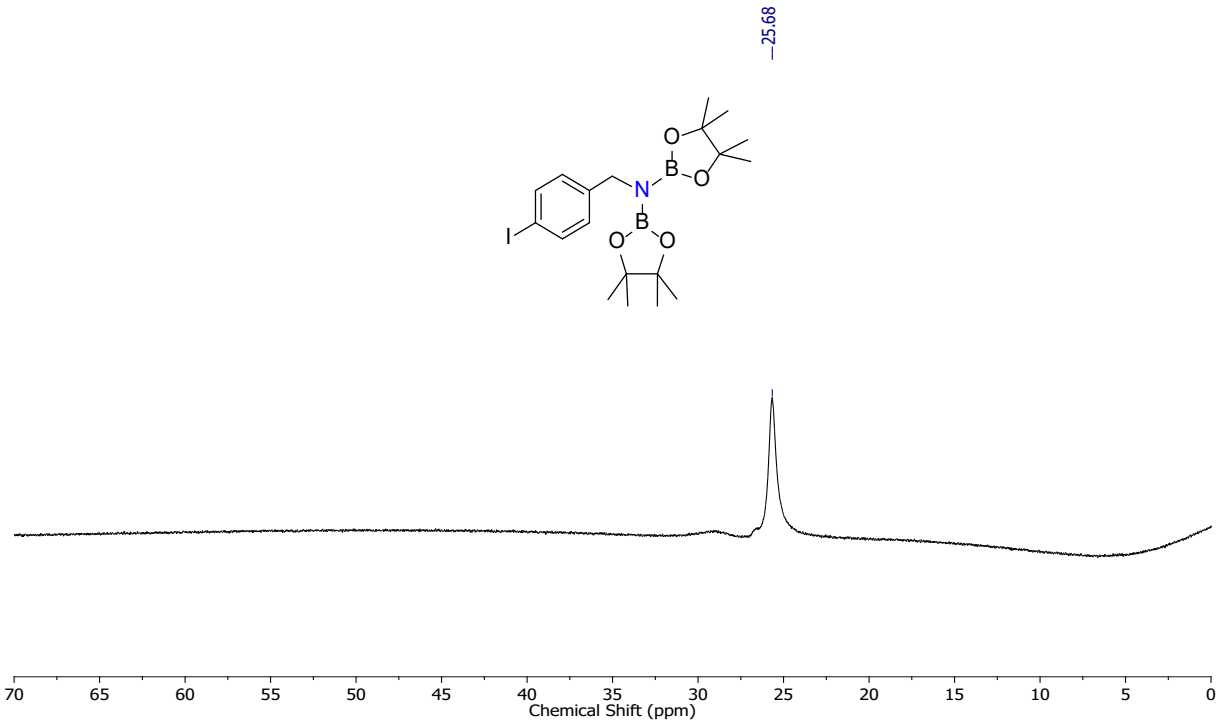


**Figure S75**. $^{11}B\{^{1}H\}$ NMR (128.4 MHz, $CDCl_3$, 298 K) spectrum of **8h**.

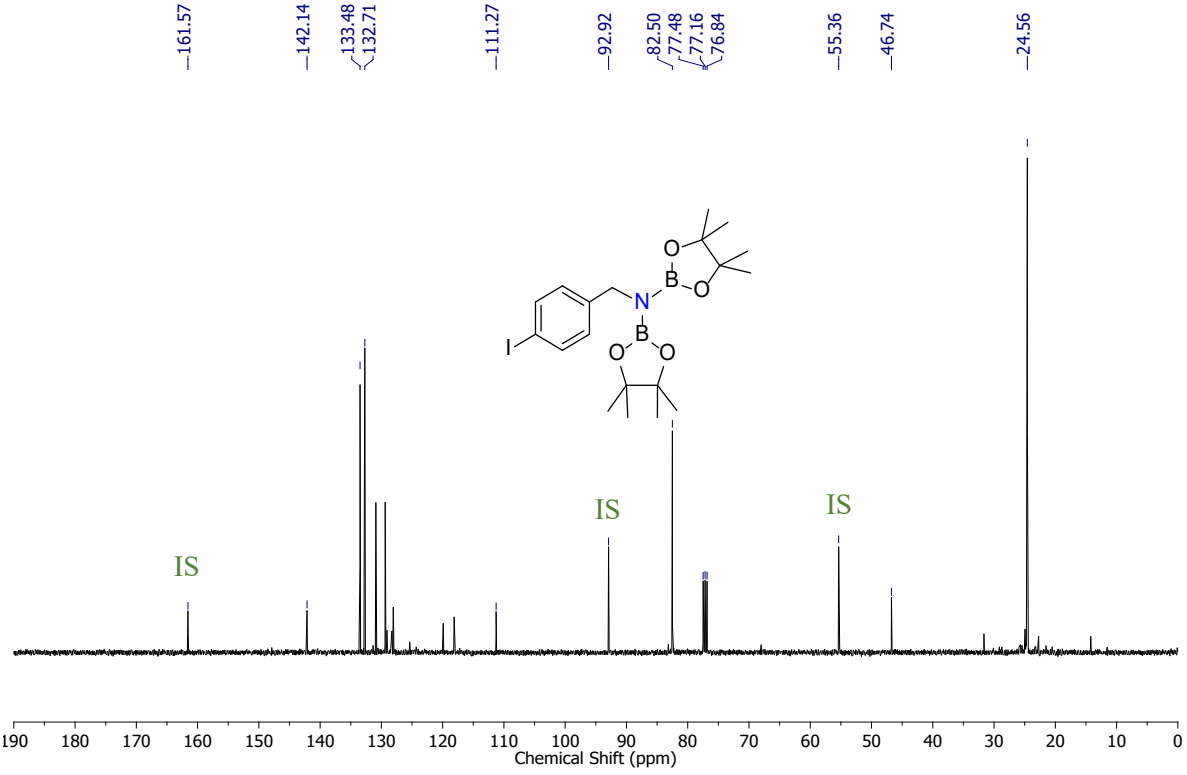


**Figure S76**. $^{13}C\{^{1}H\}$ NMR (100 MHz, $CDCl_3$, 298 K) spectrum of **8h**.

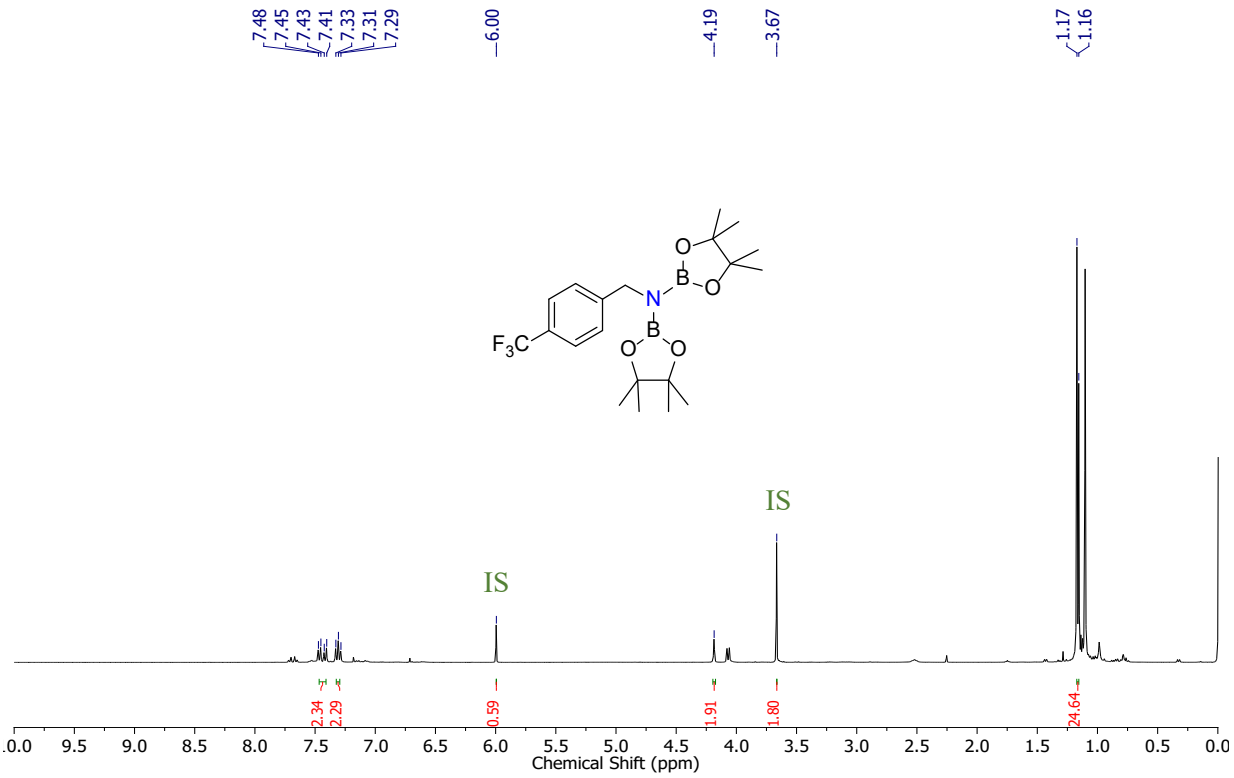


**Figure S77**. $^{1}H$ NMR (400 MHz, $CDCl_3$, 298 K) spectrum of **8i**.

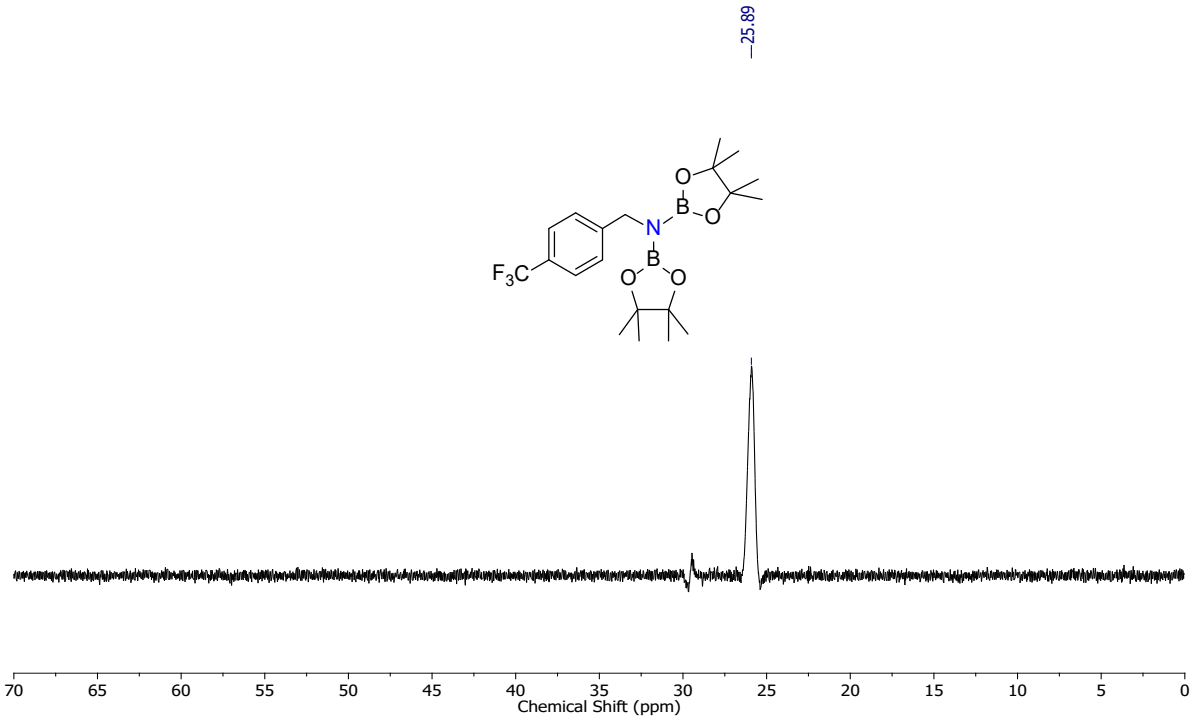


**Figure S78**. $^{11}B\{^{1}H\}$ NMR (128.4 MHz, $CDCl_3$, 298 K) spectrum of **8i**.

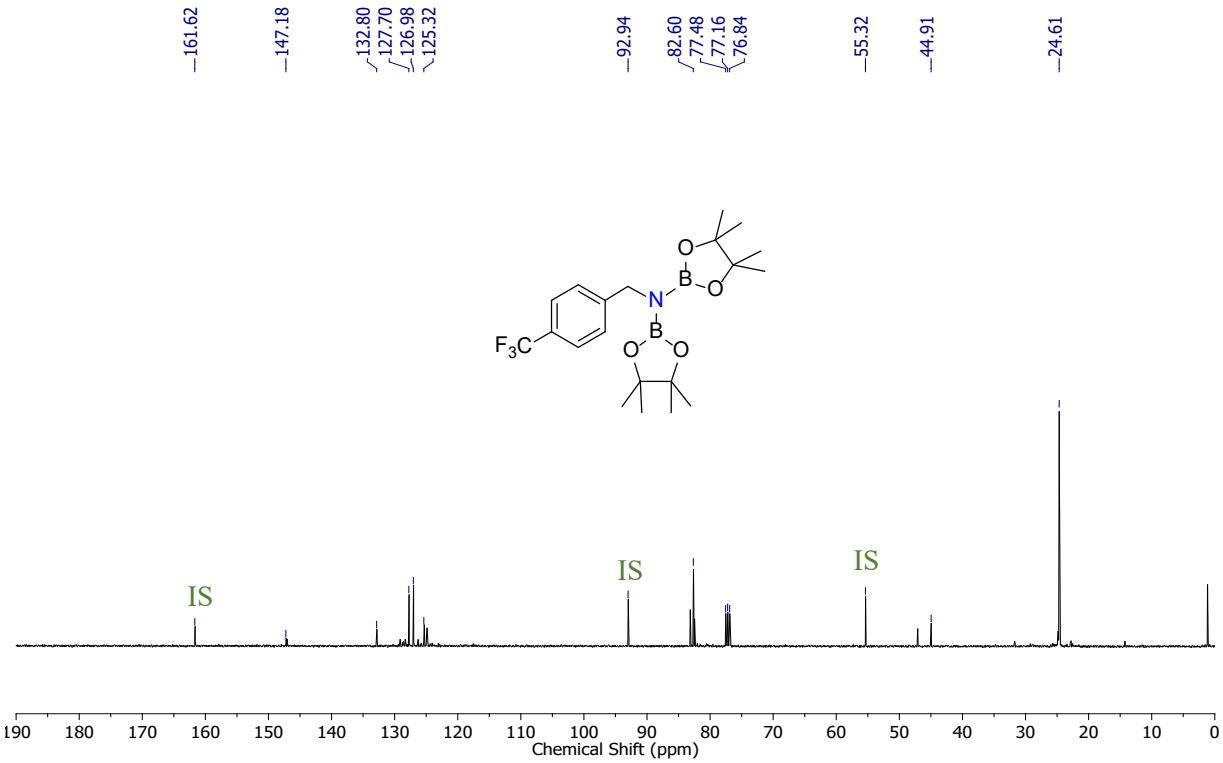


**Figure S79**. $^{13}C\{^{1}H\}$ NMR (100 MHz, $CDCl_3$, 298 K) spectrum of **8i**.

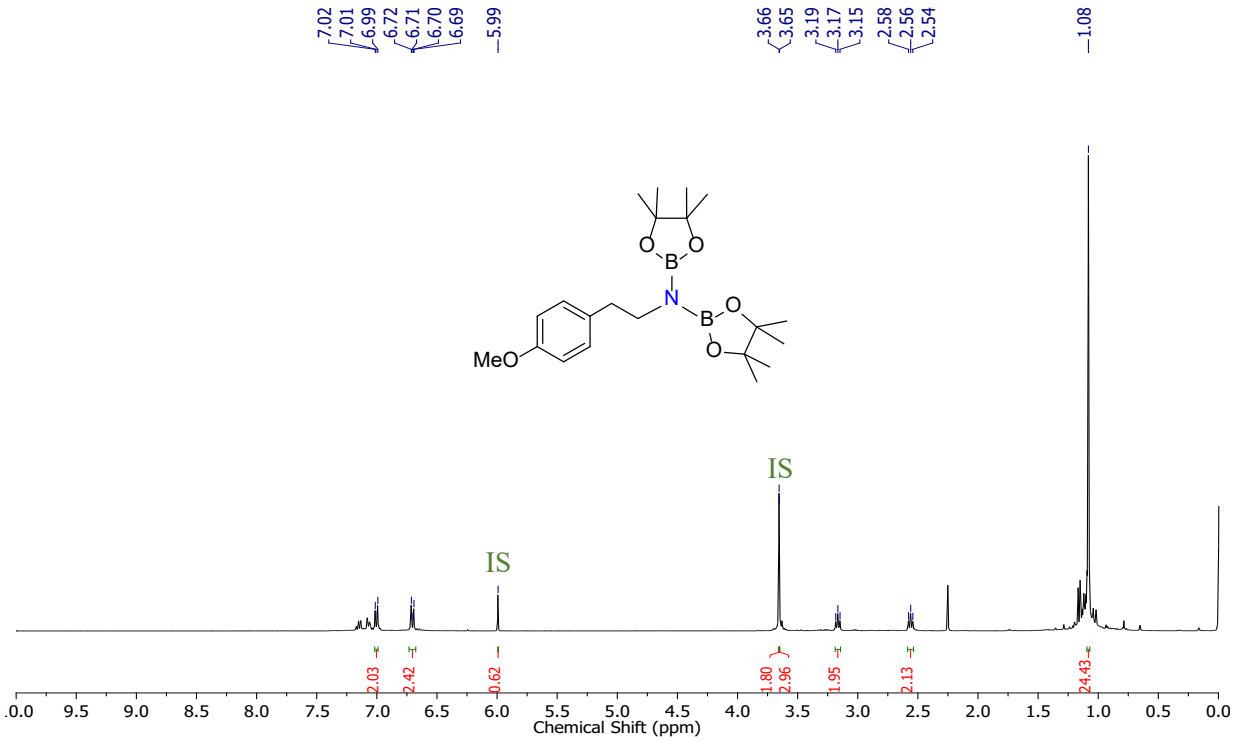


**Figure S80**. $^{1}H$ NMR (400 MHz, $CDCl_3$, 298 K) spectrum of **8j**.

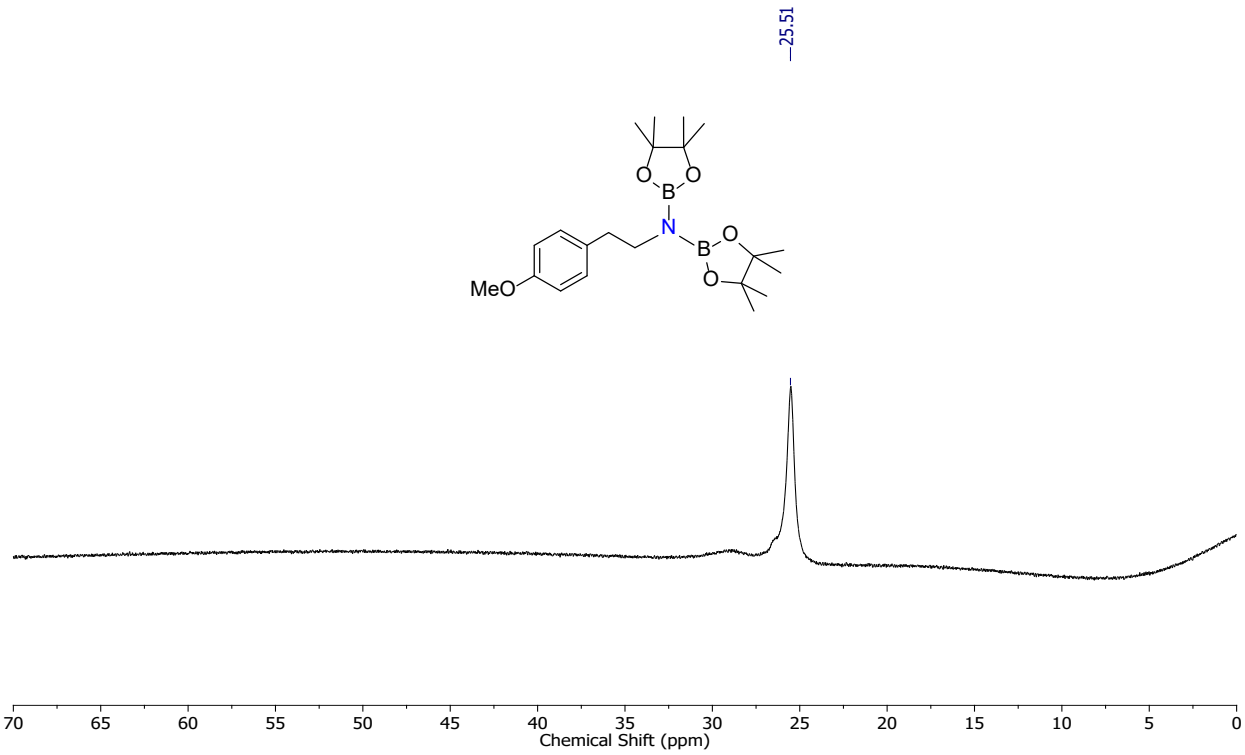


**Figure S81**. $^{11}B\{^{1}H\}$ NMR (128.4 MHz, $CDCl_3$, 298 K) spectrum of **8j**.

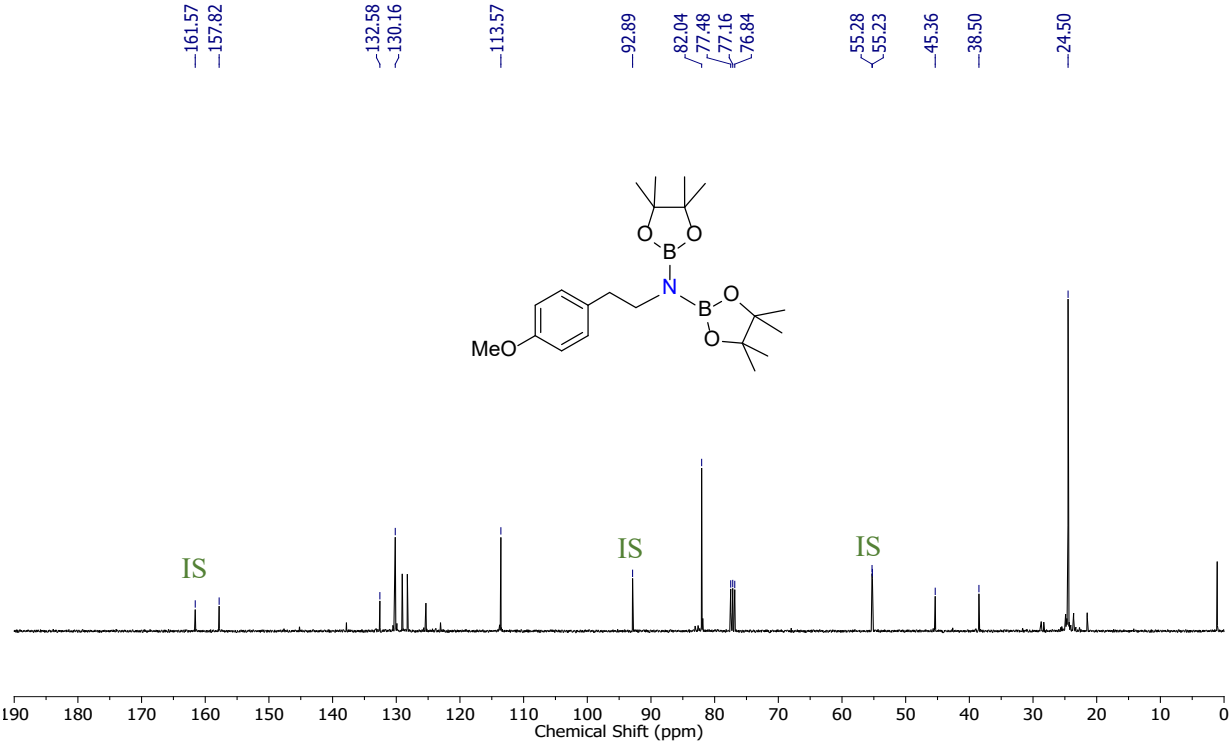


**Figure S82**. $^{13}C\{^{1}H\}$ NMR (100 MHz, $CDCl_3$, 298 K) spectrum of **8j**.

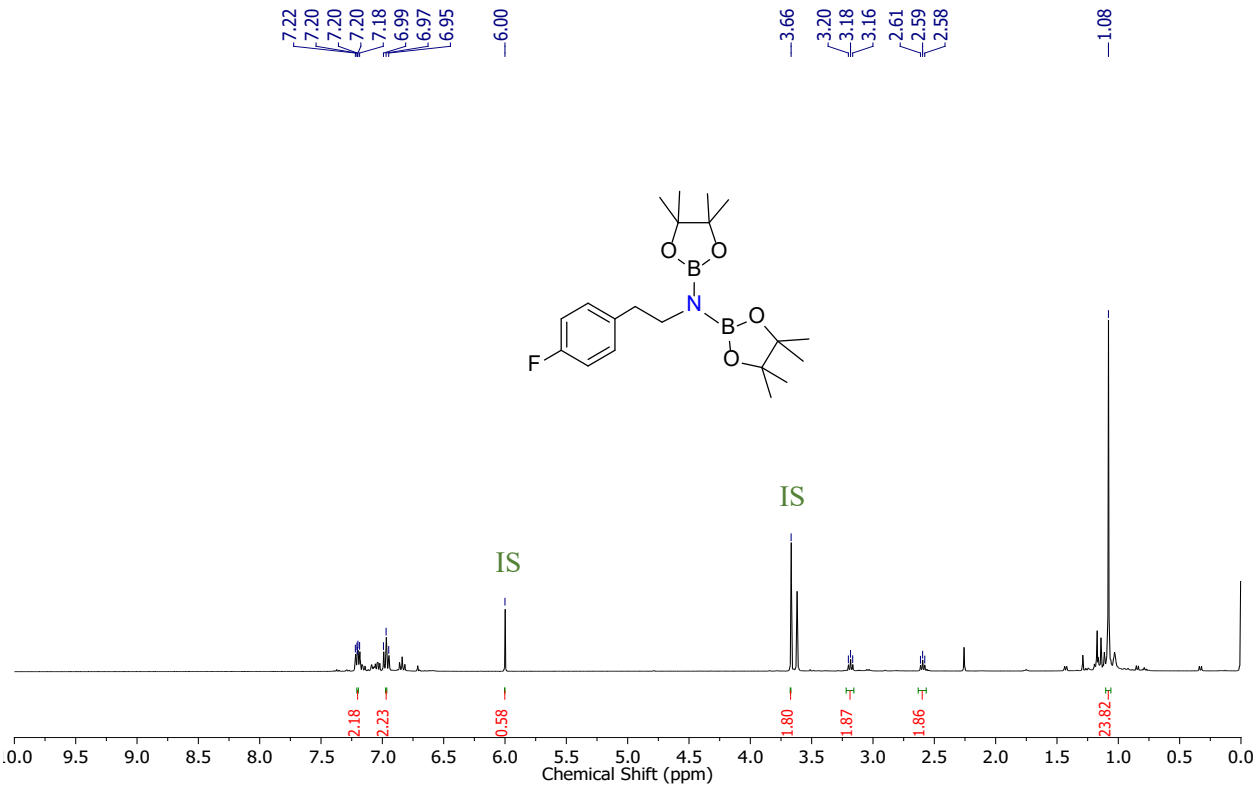


**Figure S83**. $^{1}H$ NMR (400 MHz, $CDCl_3$, 298 K) spectrum of **8k**.

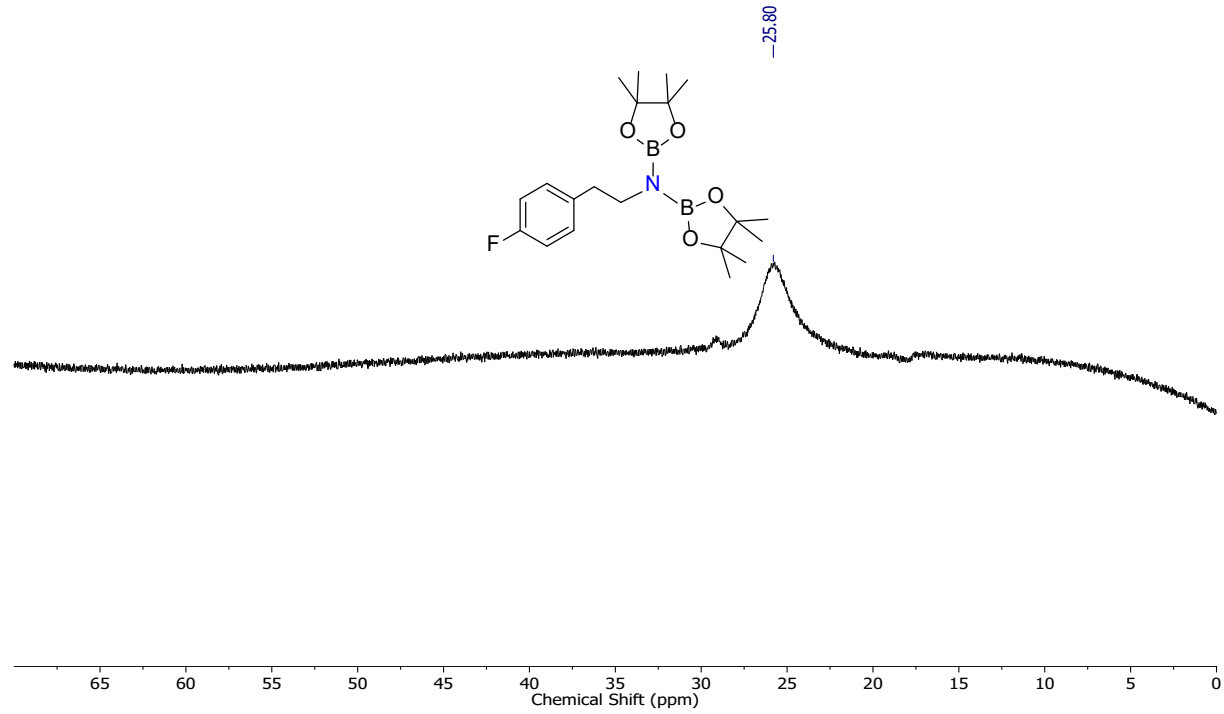


**Figure S84**. $^{11}B\{^{1}H\}$ NMR (128.4 MHz, $CDCl_3$, 298 K) spectrum of **8k**.

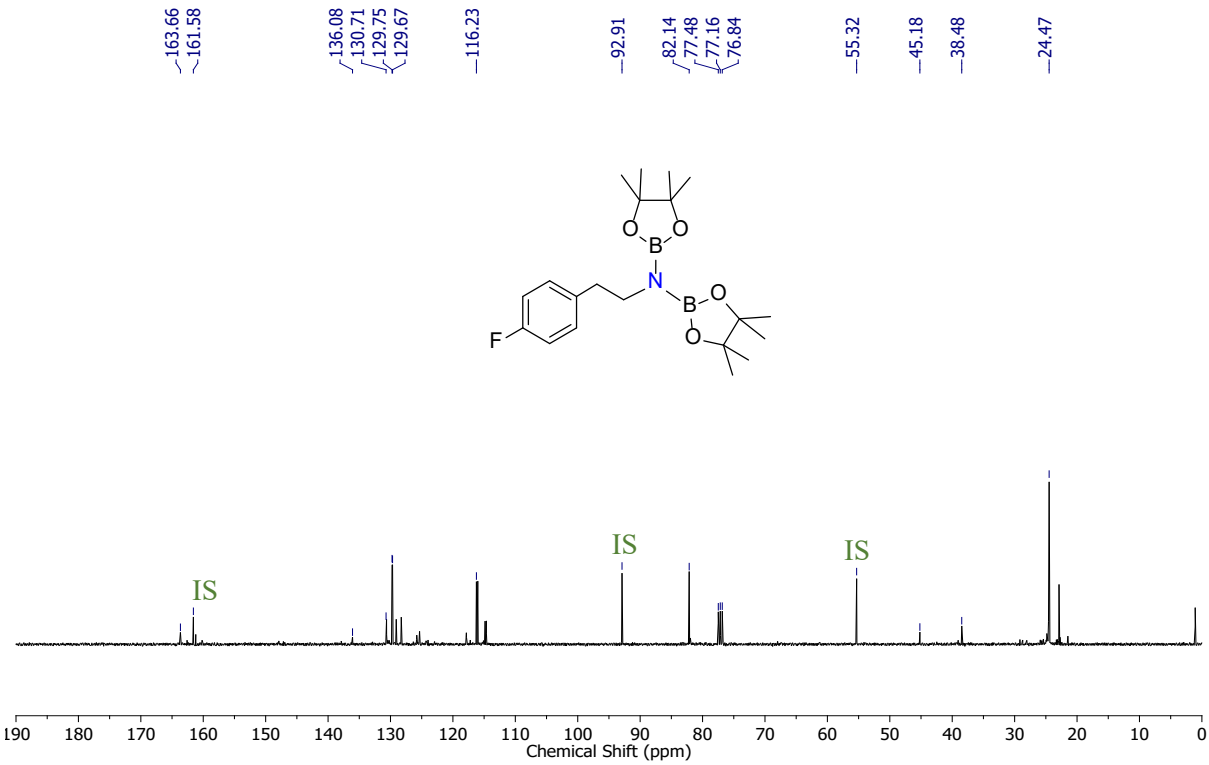


**Figure S85**. $^{13}C\{^{1}H\}$ NMR (100 MHz, $CDCl_3$, 298 K) spectrum of **8k**.

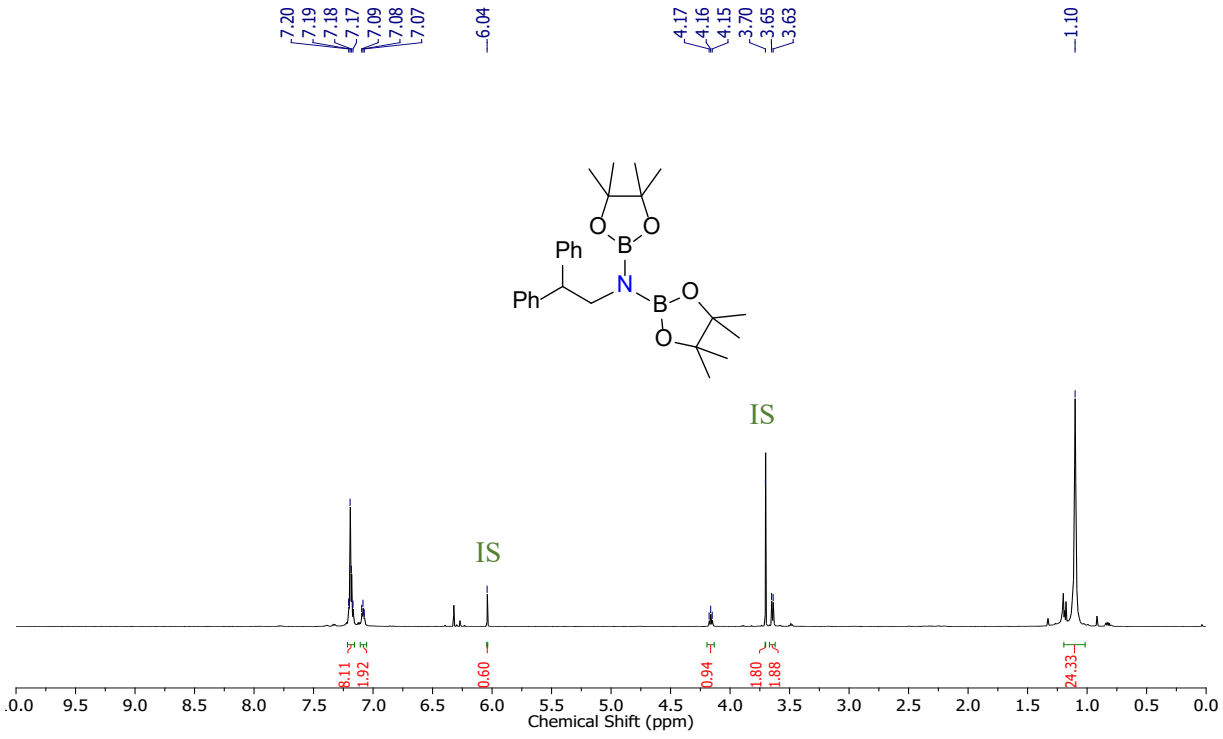


**Figure S86**. $^{1}H$ NMR (400 MHz, $CDCl_3$, 298 K) spectrum of **8l**.

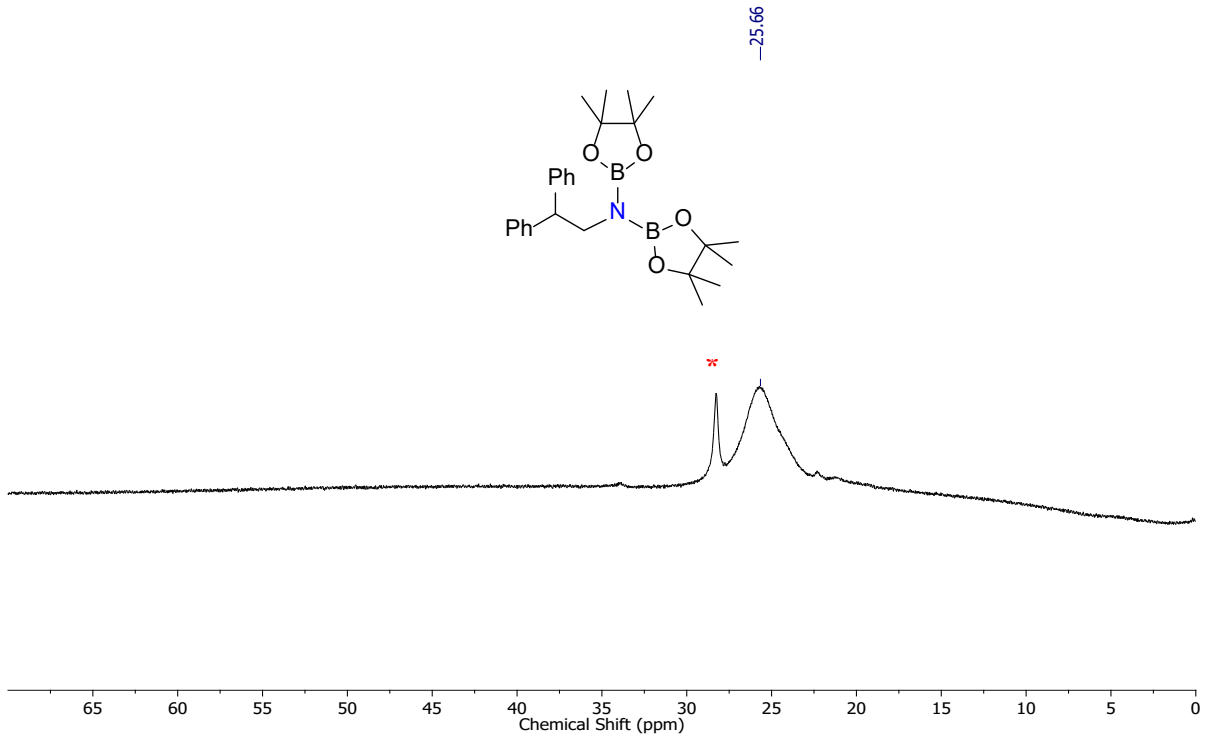


**Figure S87**. $^{11}B\{^{1}H\}$ NMR (128.4 MHz, $CDCl_3$, 298 K) spectrum of **8l** (* HBpin).

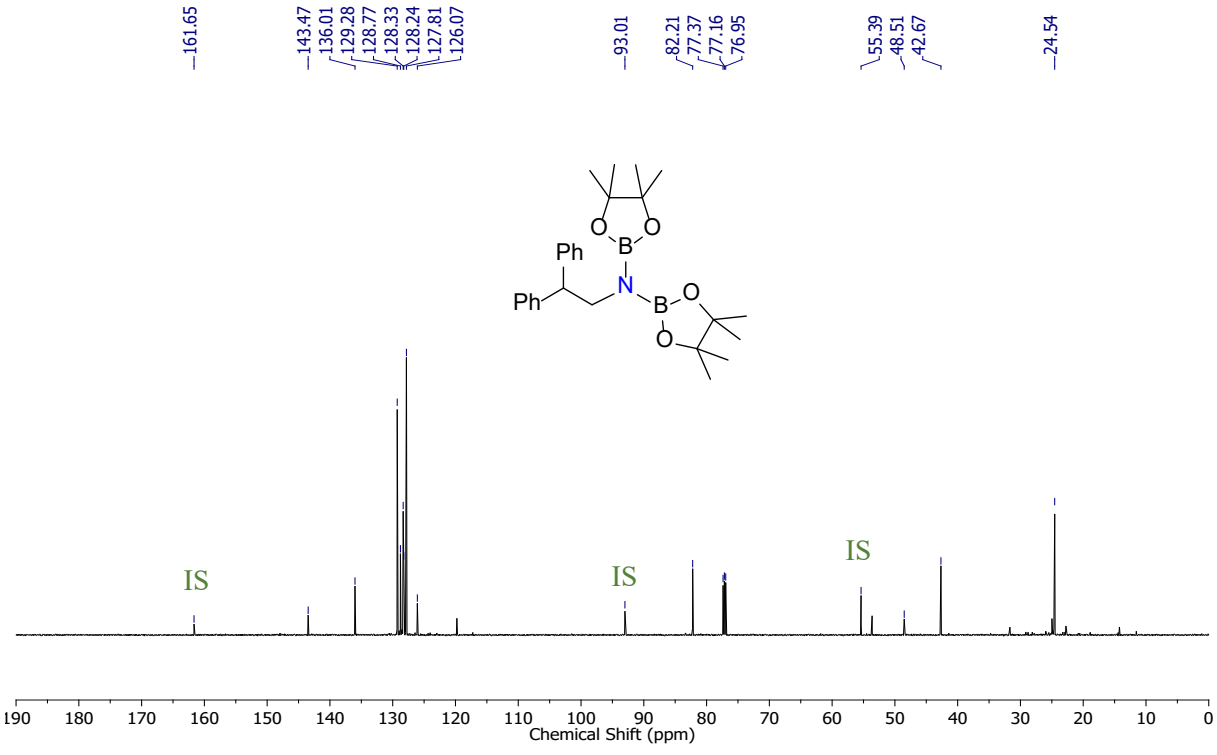


**Figure S88**. $^{13}C\{^{1}H\}$ NMR (100 MHz, $CDCl_3$, 298 K) spectrum of **8l**.

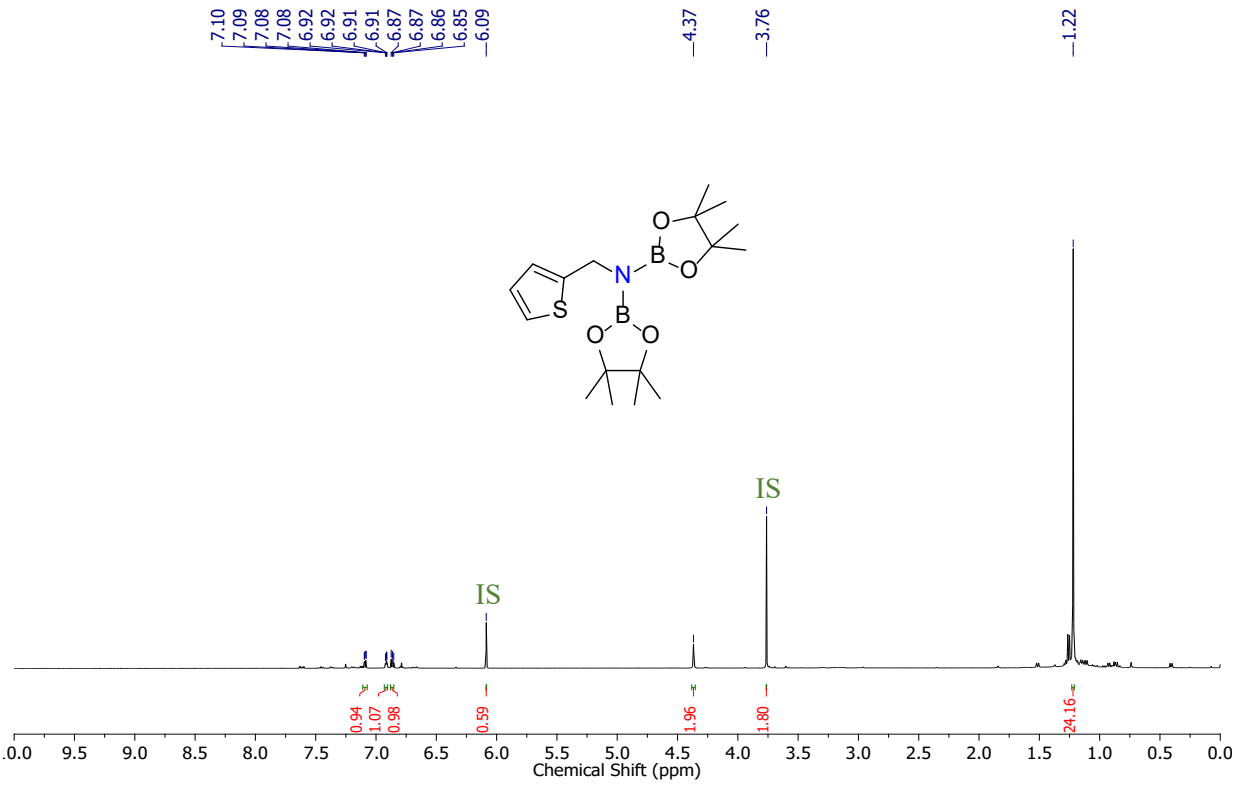


**Figure S89**. $^{1}H$ NMR (400 MHz, $CDCl_3$, 298 K) spectrum of **8m**.

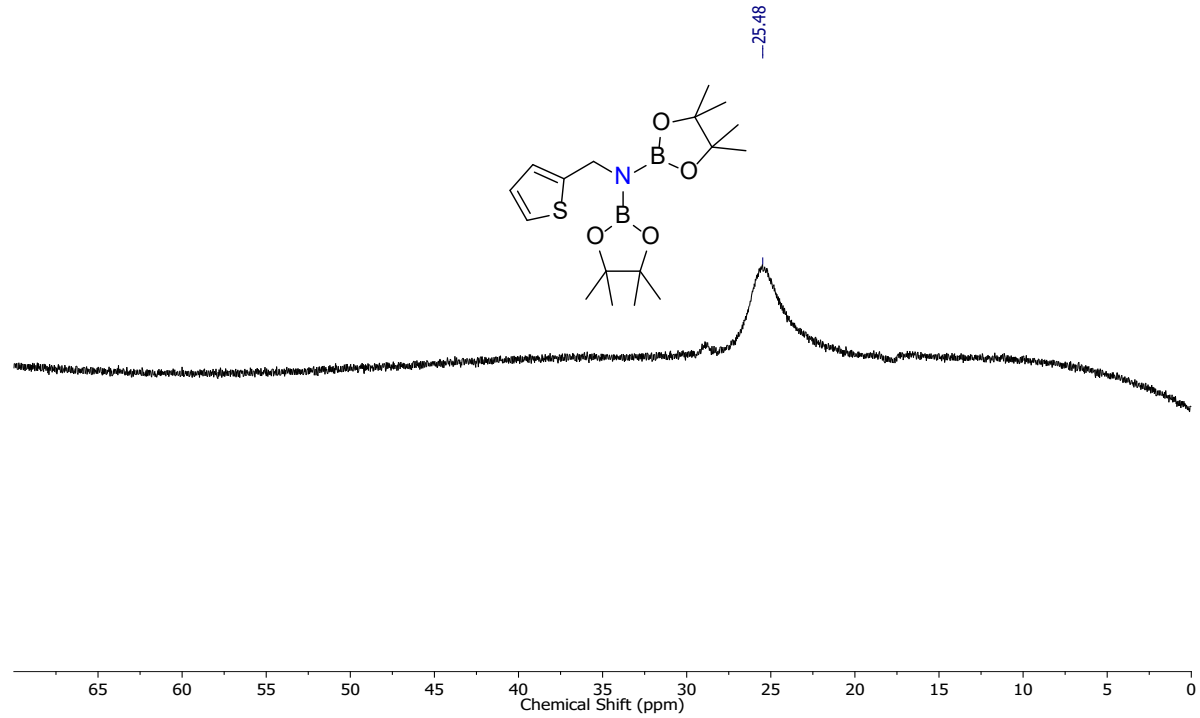


**Figure S90**. $^{11}B\{^{1}H\}$ NMR (128.4 MHz, $CDCl_3$, 298 K) spectrum of **8m**.

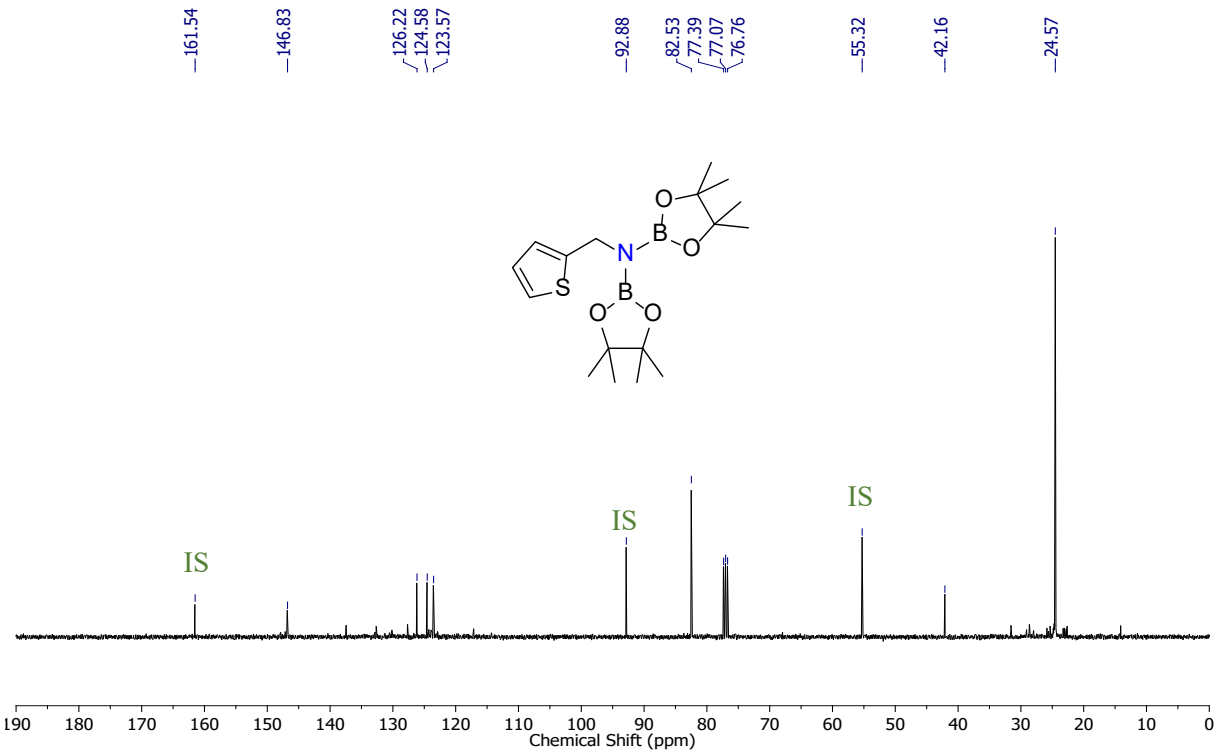


**Figure S91**. $^{13}C\{^{1}H\}$ NMR (100 MHz, $CDCl_3$, 298 K) spectrum of **8m**.

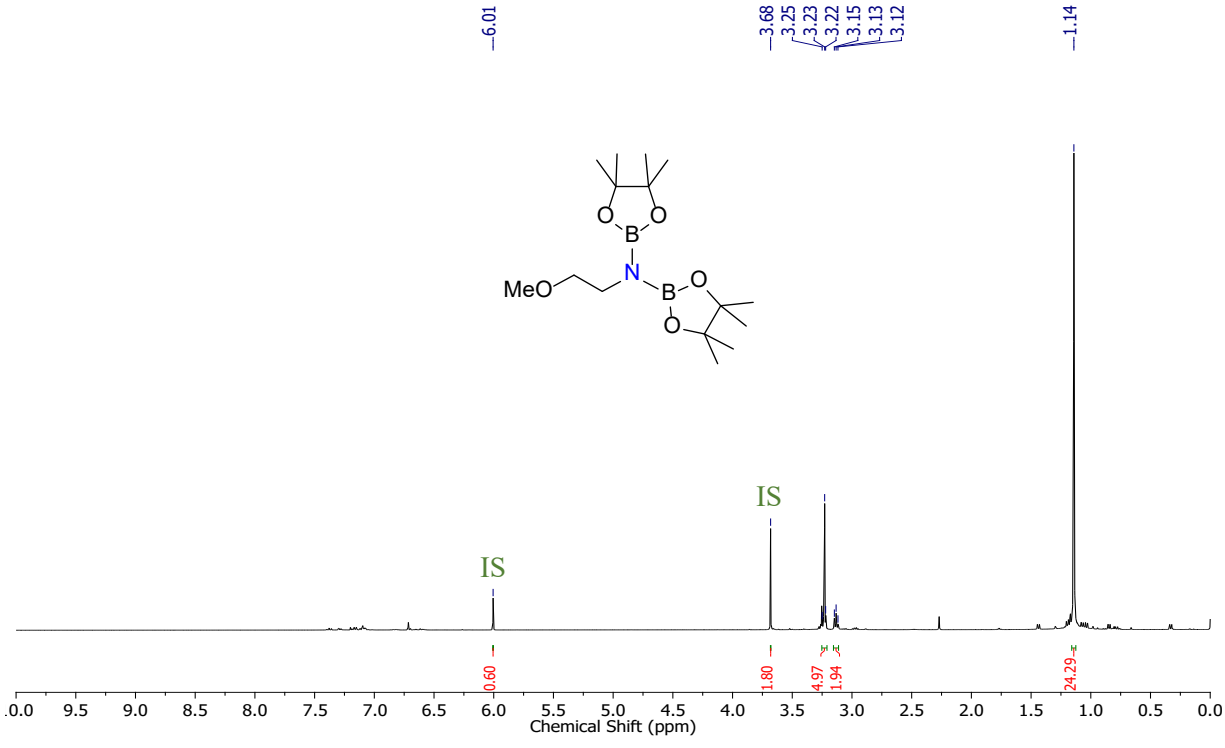


**Figure S92**. $^{1}H$ NMR (400 MHz, $CDCl_3$, 298 K) spectrum of **8n**.

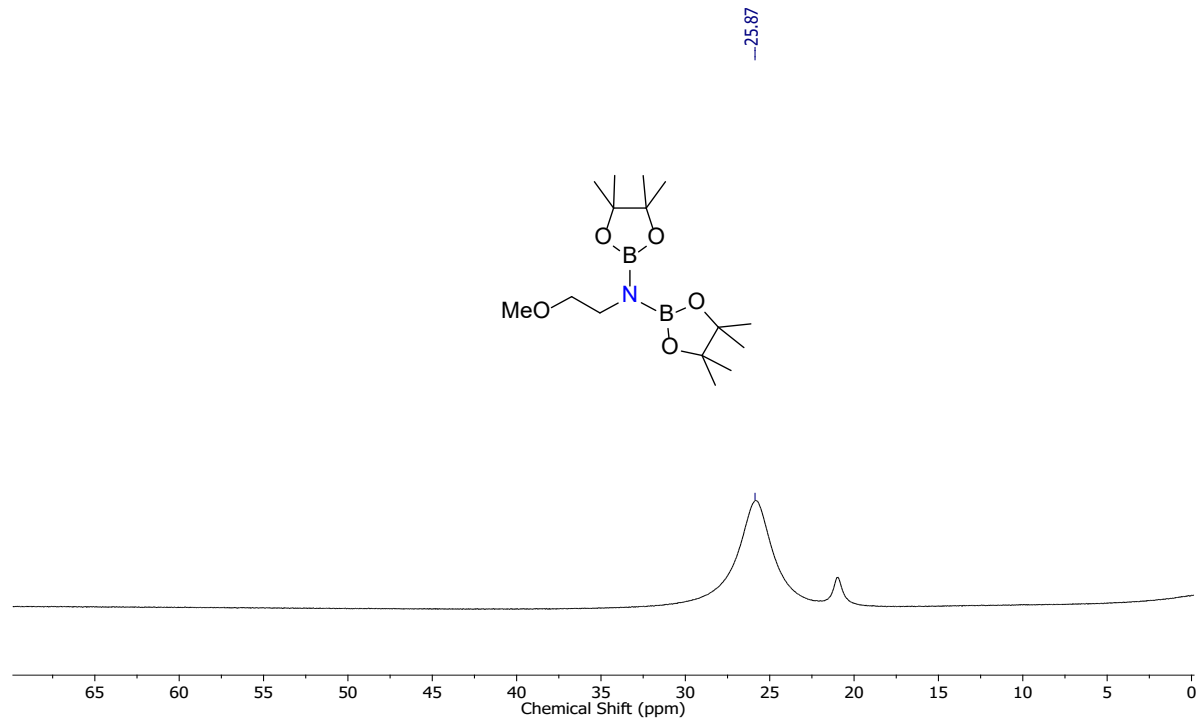


**Figure S93**. $^{11}B\{^{1}H\}$ NMR (128.4 MHz, $CDCl_3$, 298 K) spectrum of **8n**.

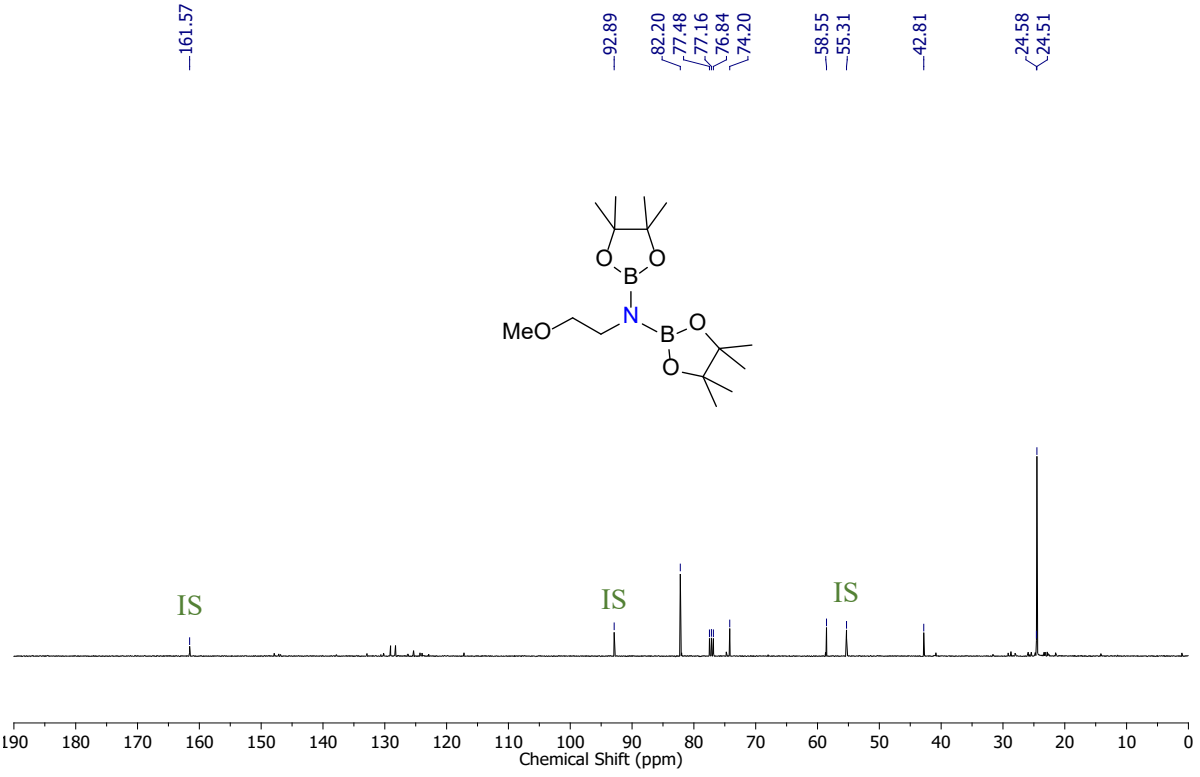


**Figure S94**. $^{13}C\{^{1}H\}$ NMR (100 MHz, $CDCl_3$, 298 K) spectrum of **8n**.

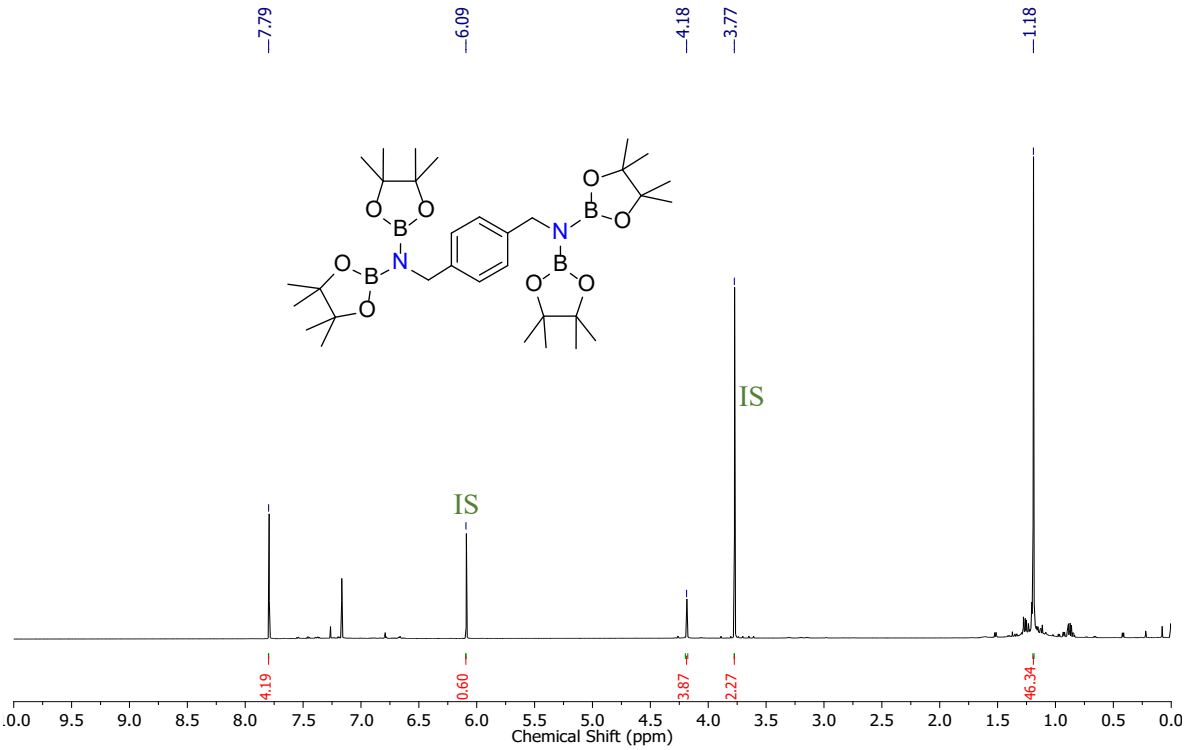


**Figure S95**. $^{1}H$ NMR (400 MHz, $CDCl_3$, 298 K) spectrum of **8o**.

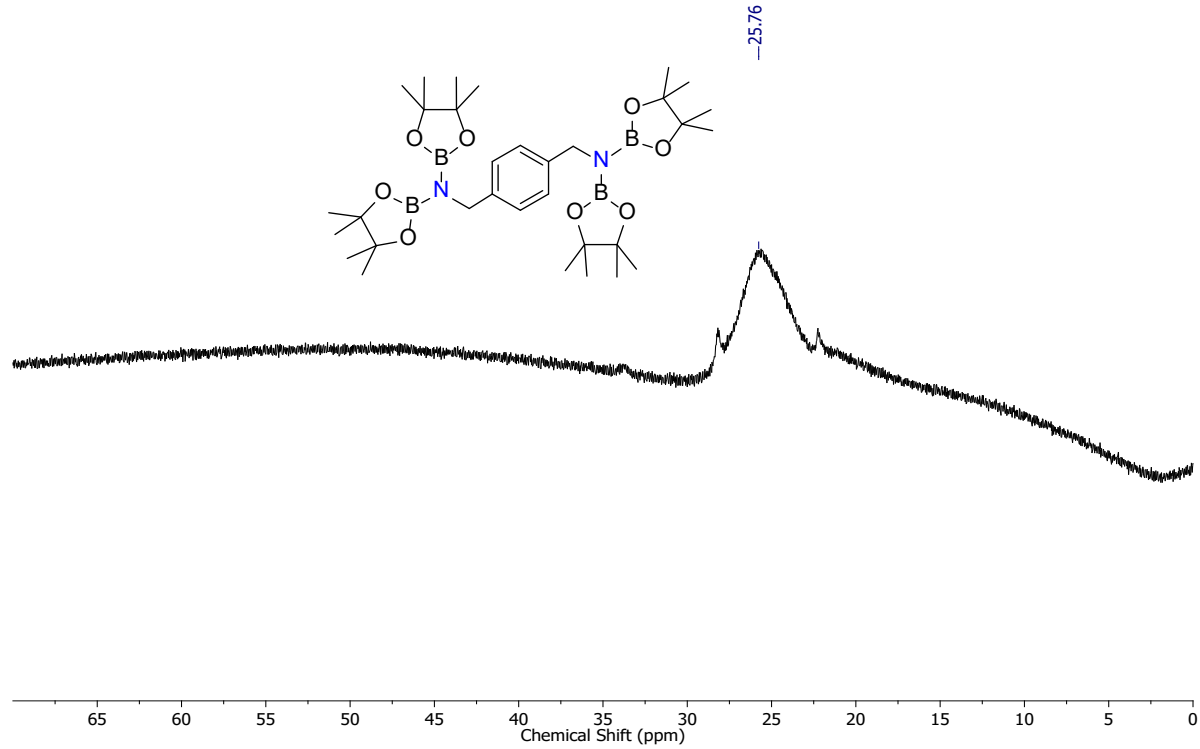


**Figure S96**. $^{11}B\{^{1}H\}$ NMR (128.4 MHz, $CDCl_3$, 298 K) spectrum of **8o**.

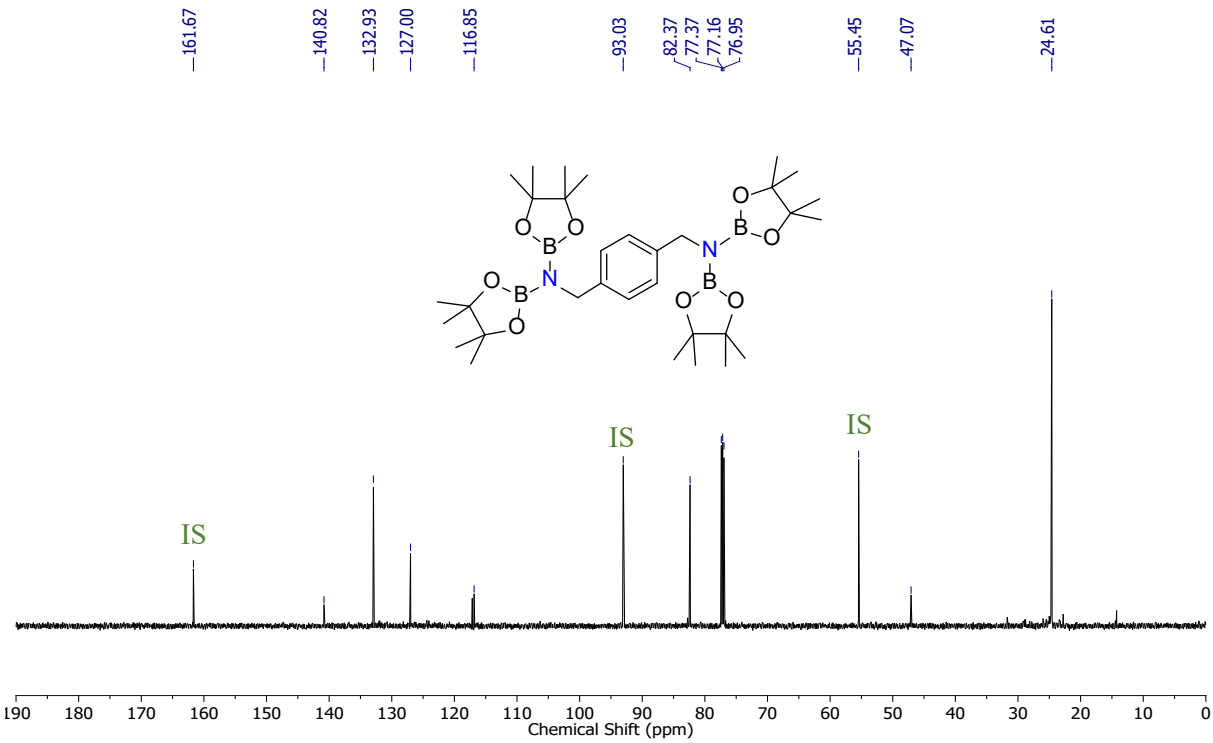


**Figure S97**. $^{13}C\{^{1}H\}$ NMR (100 MHz, $CDCl_3$, 298 K) spectrum of **8o**.

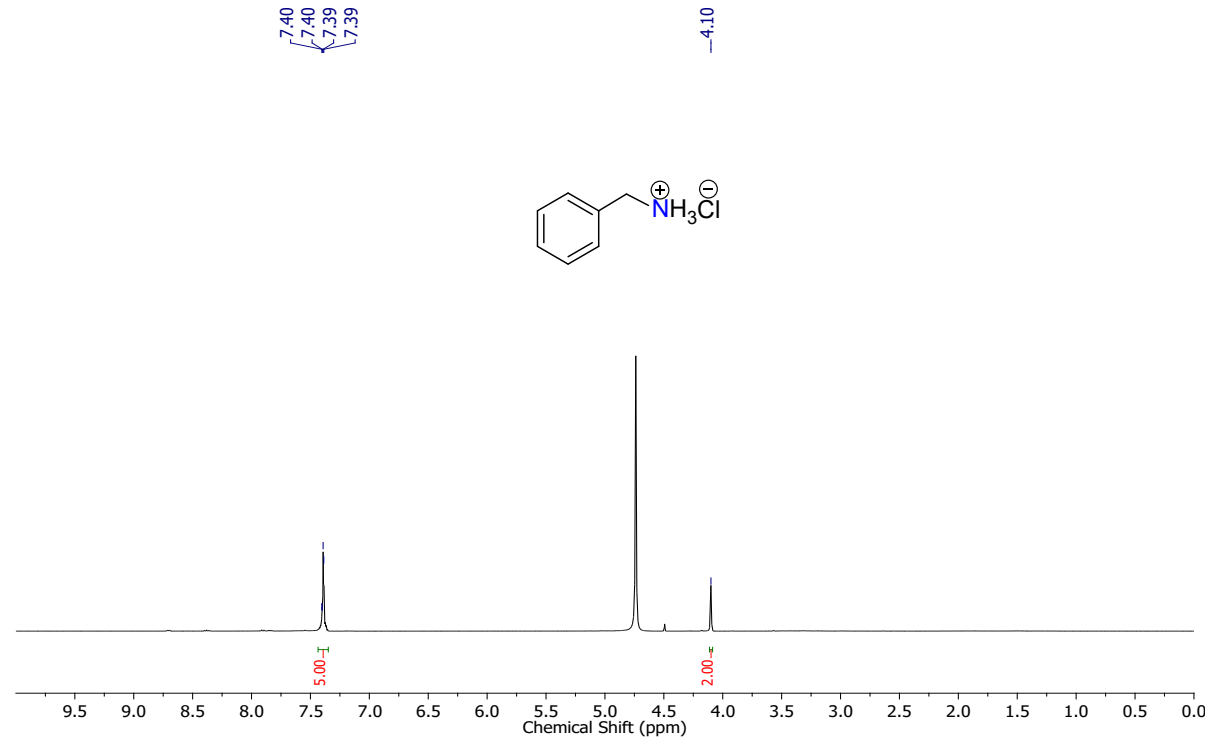


**Figure S98**. $^{1}H$ NMR (400 MHz, $CDCl_3$, 298 K) spectrum of **9a**.

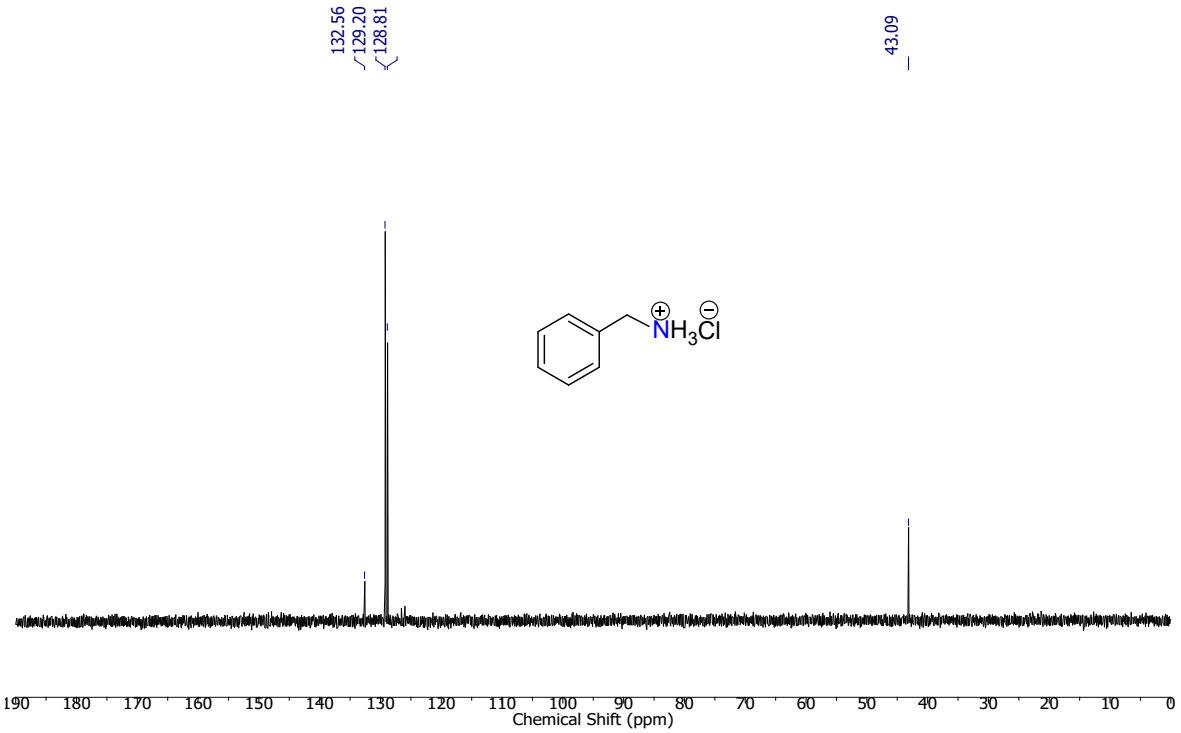


**Figure S99**. $^{13}C\{^{1}H\}$ NMR (100 MHz, $CDCl_3$, 298 K) spectrum of **9a**.

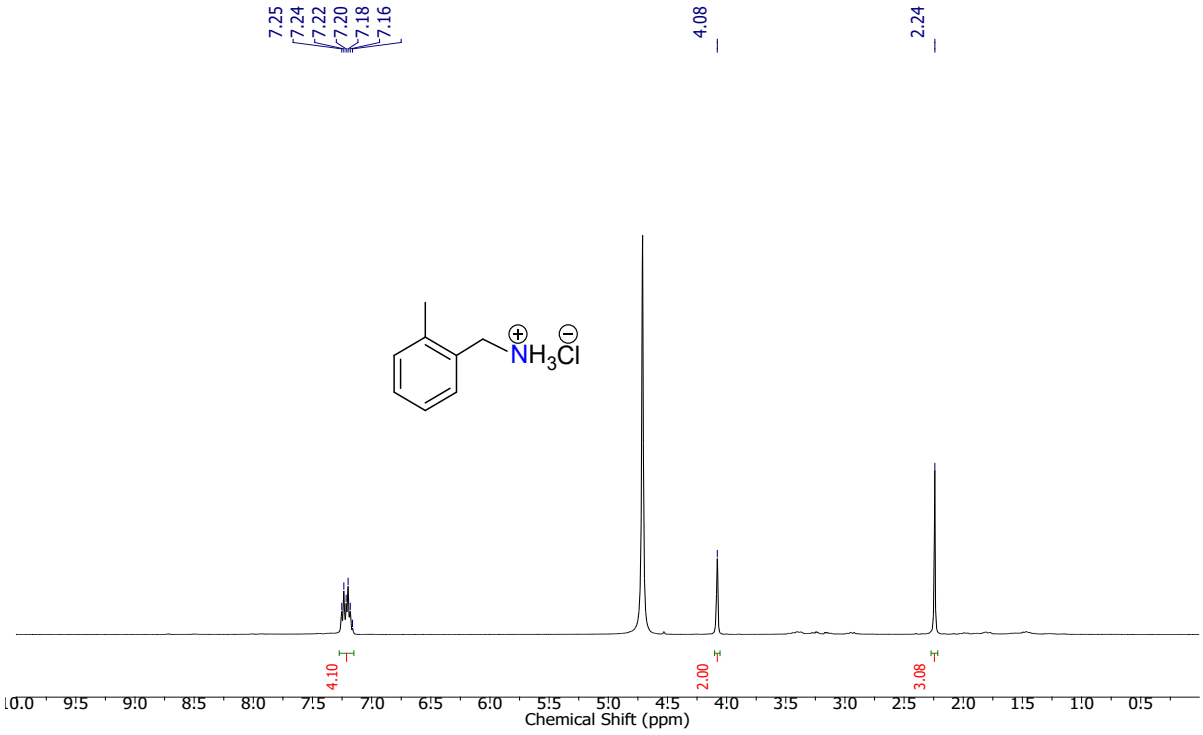


**Figure S100**. $^{1}H$ NMR (400 MHz, $CDCl_3$, 298 K) spectrum of **9b**.

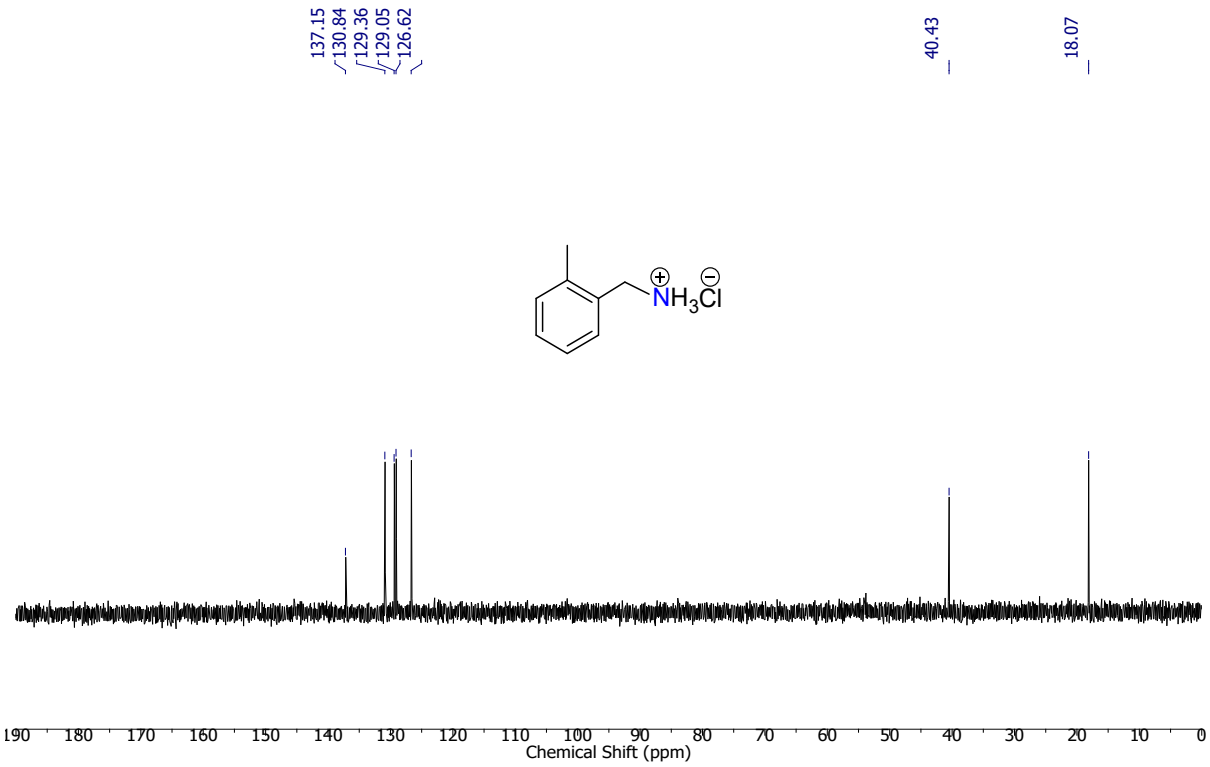


**Figure S101**. $^{13}C\{^{1}H\}$ NMR (100 MHz, $CDCl_3$, 298 K) spectrum of **9b**.

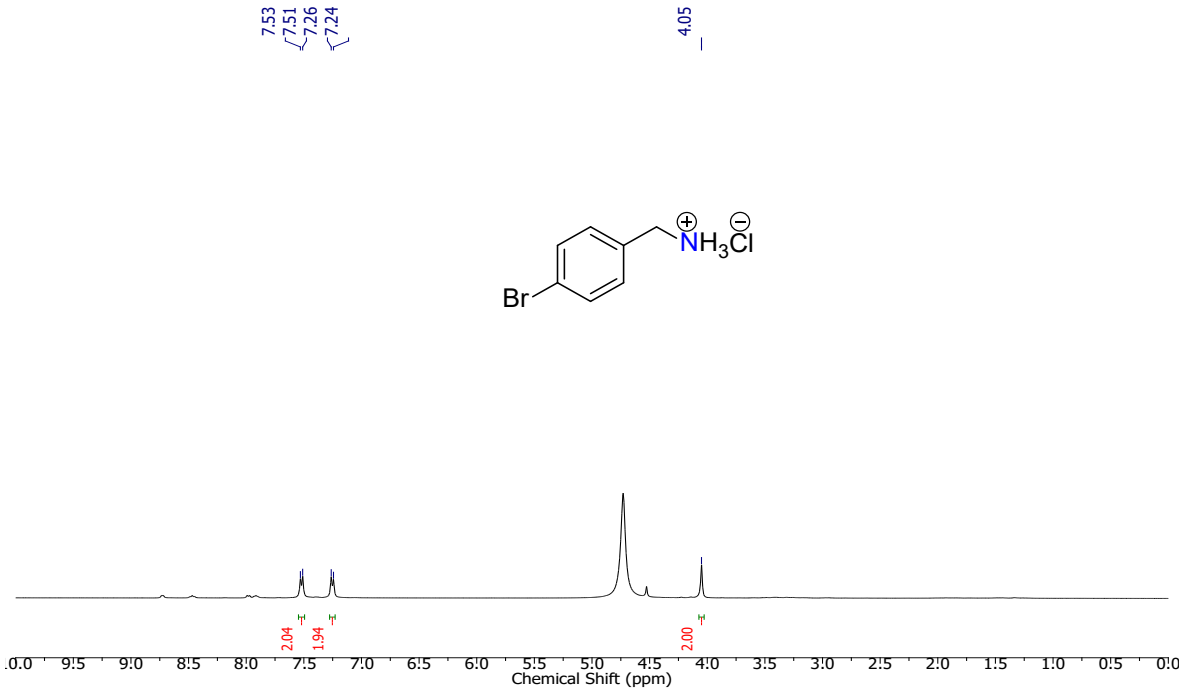


**Figure S102**. $^{1}H$ NMR (400 MHz, $CDCl_3$, 298 K) spectrum of **9c**.

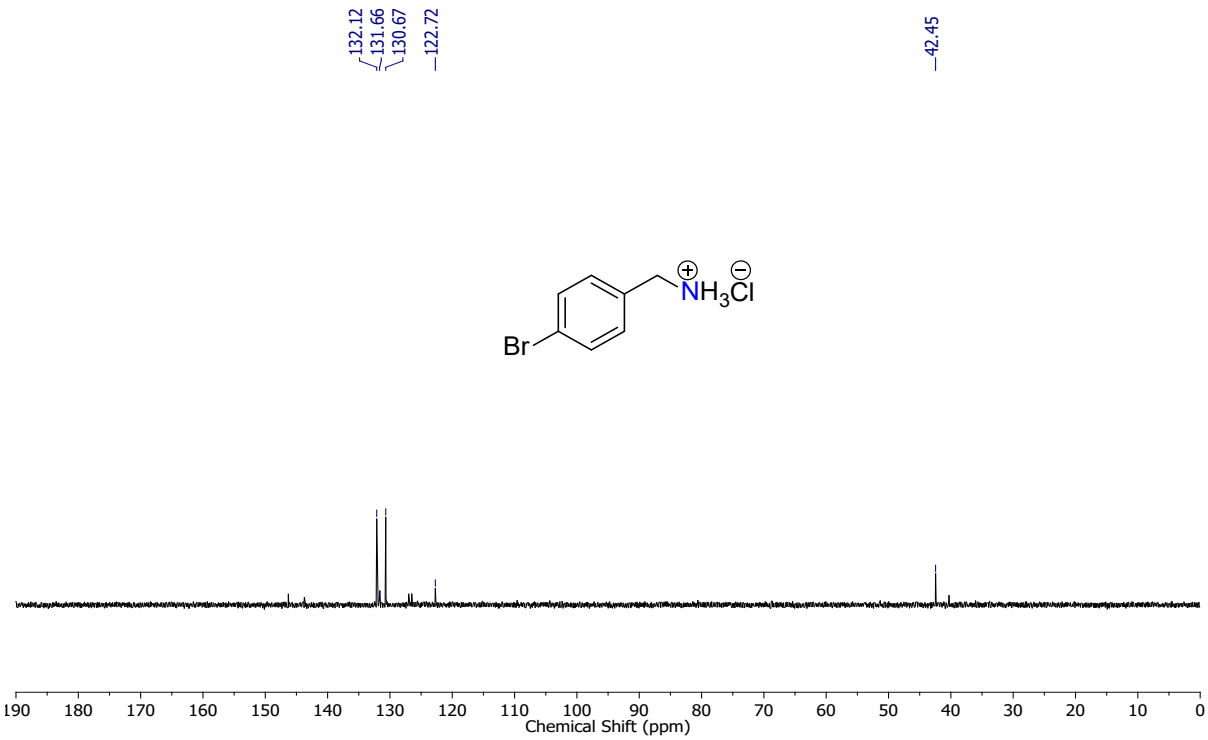


**Figure S103**. $^{13}C\{^{1}H\}$ NMR (100 MHz, $CDCl_3$, 298 K) spectrum of **9c**.

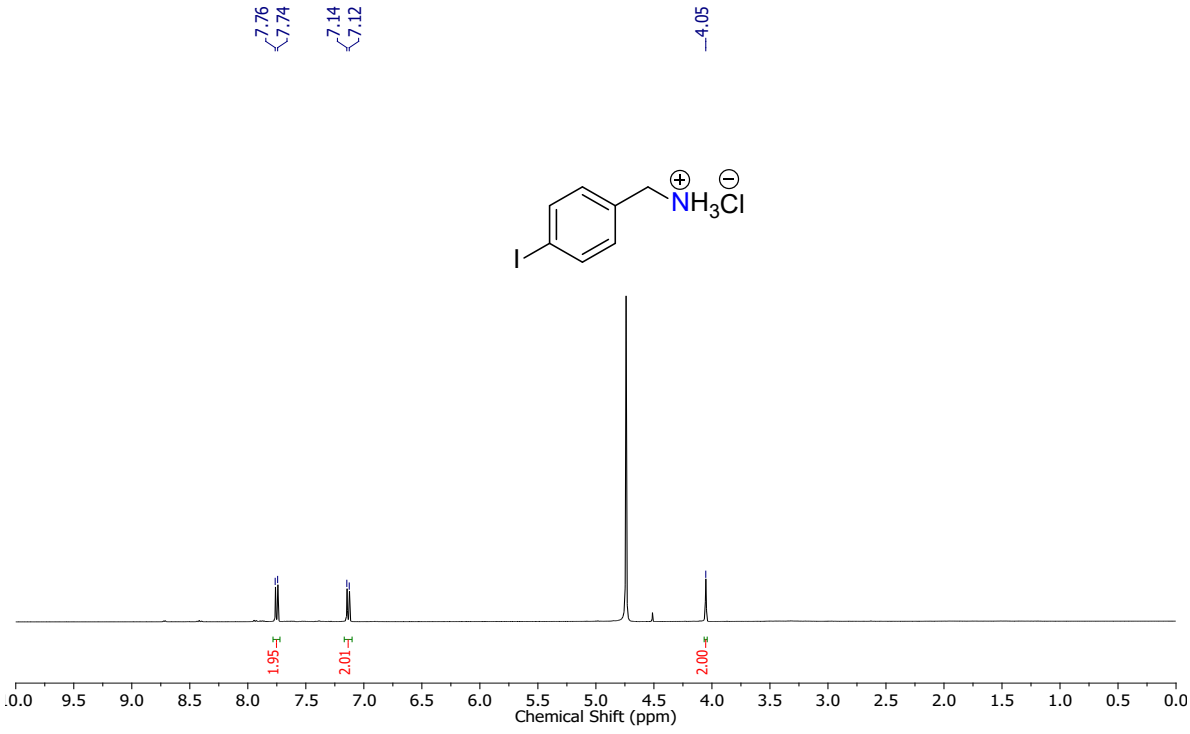


**Figure S104**. $^{1}H$ NMR (400 MHz, $CDCl_3$, 298 K) spectrum of **9d**.

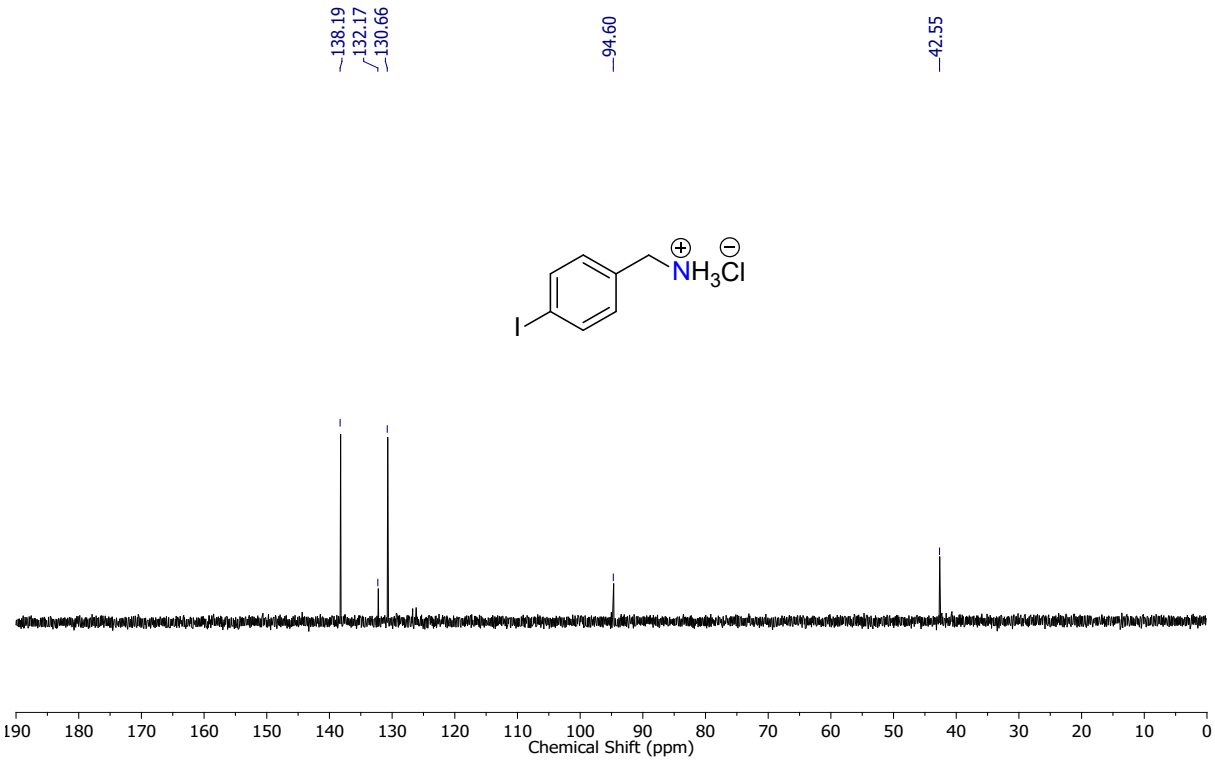


**Figure S105**. $^{13}C\{^{1}H\}$ NMR (100 MHz, $CDCl_3$, 298 K) spectrum of **9d**.

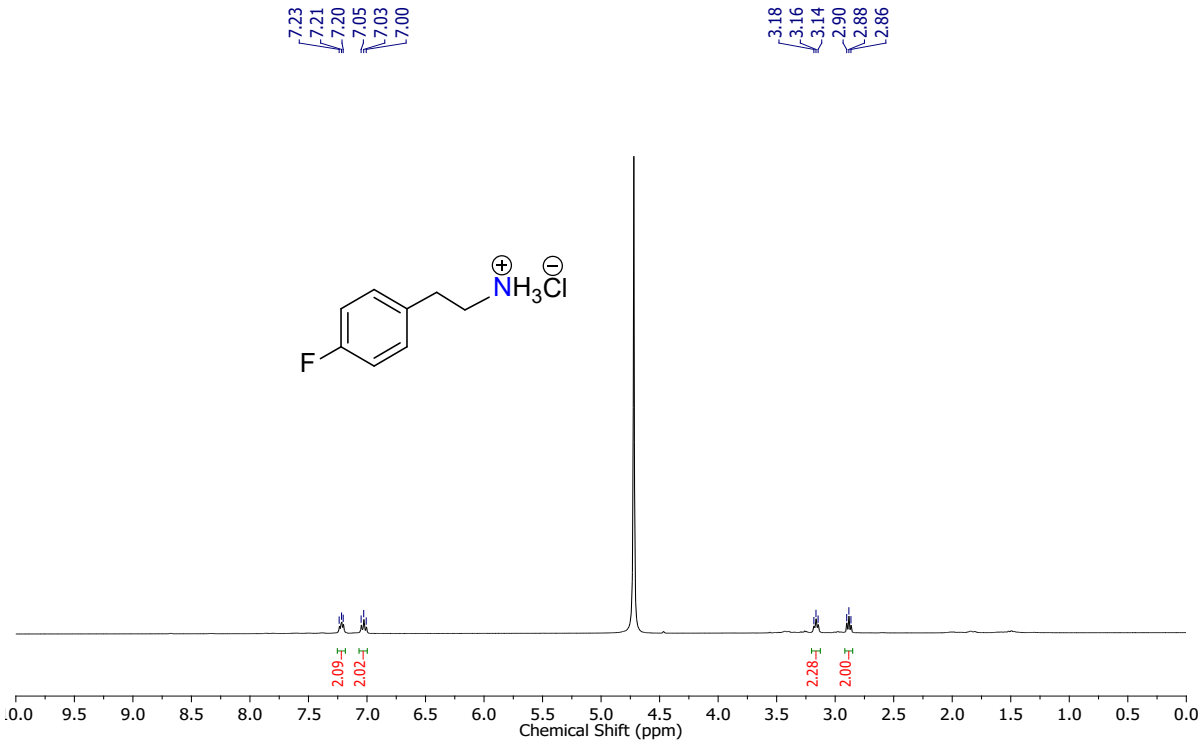


**Figure S106**. $^{1}H$ NMR (400 MHz, $CDCl_3$, 298 K) spectrum of **9e**.

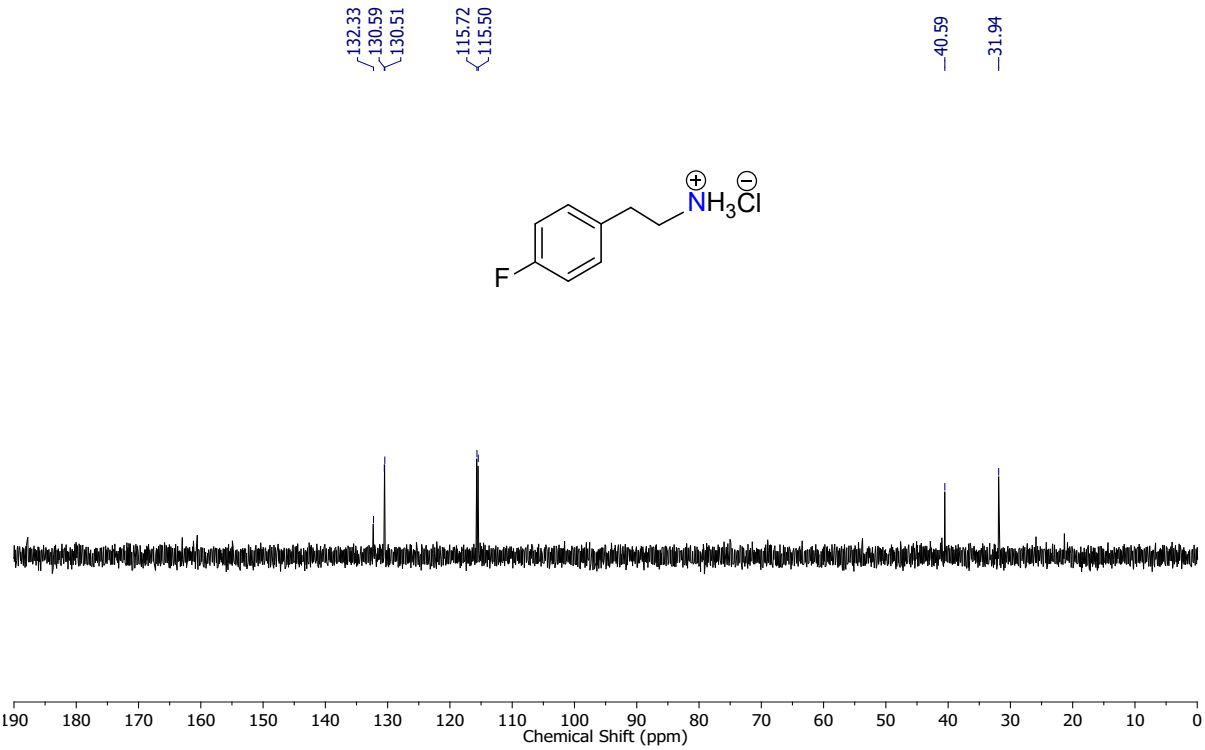


**Figure S107**. $^{13}C\{^{1}H\}$ NMR (100 MHz, $CDCl_3$, 298 K) spectrum of **9e**.

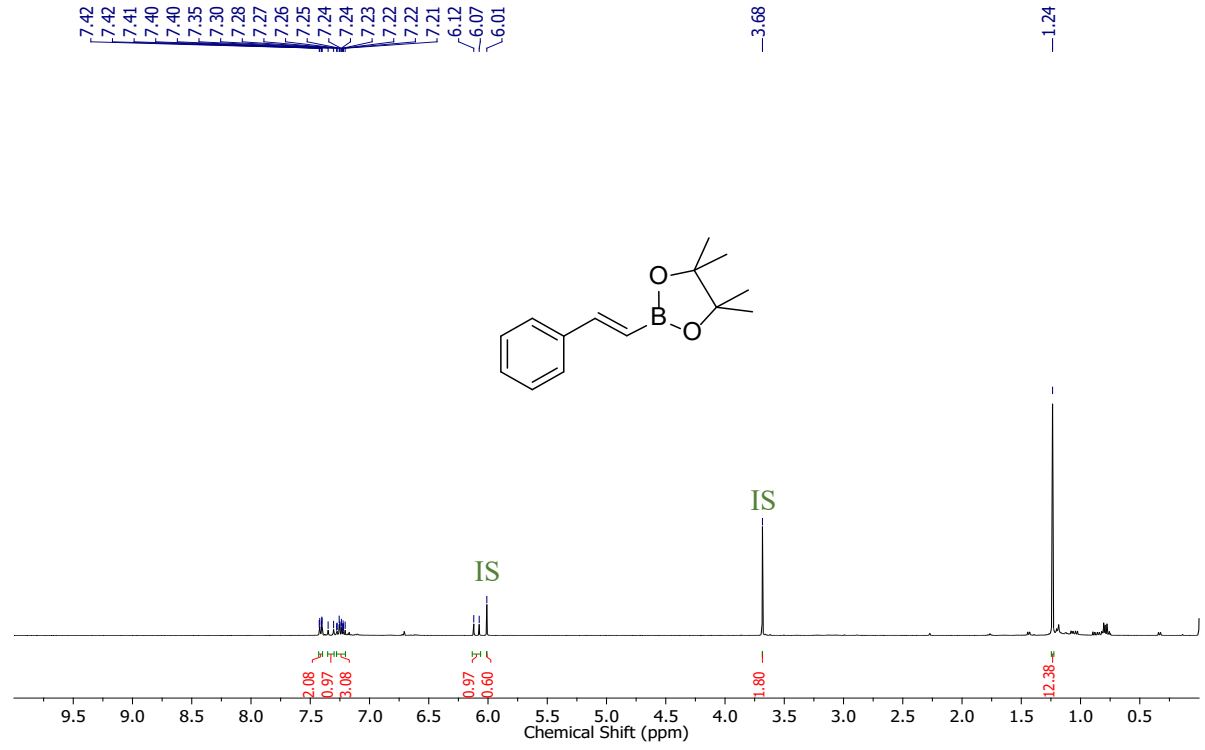


**Figure S108**. $^{1}H$ NMR (400 MHz, $CDCl_3$, 298 K) spectrum of **10a**.

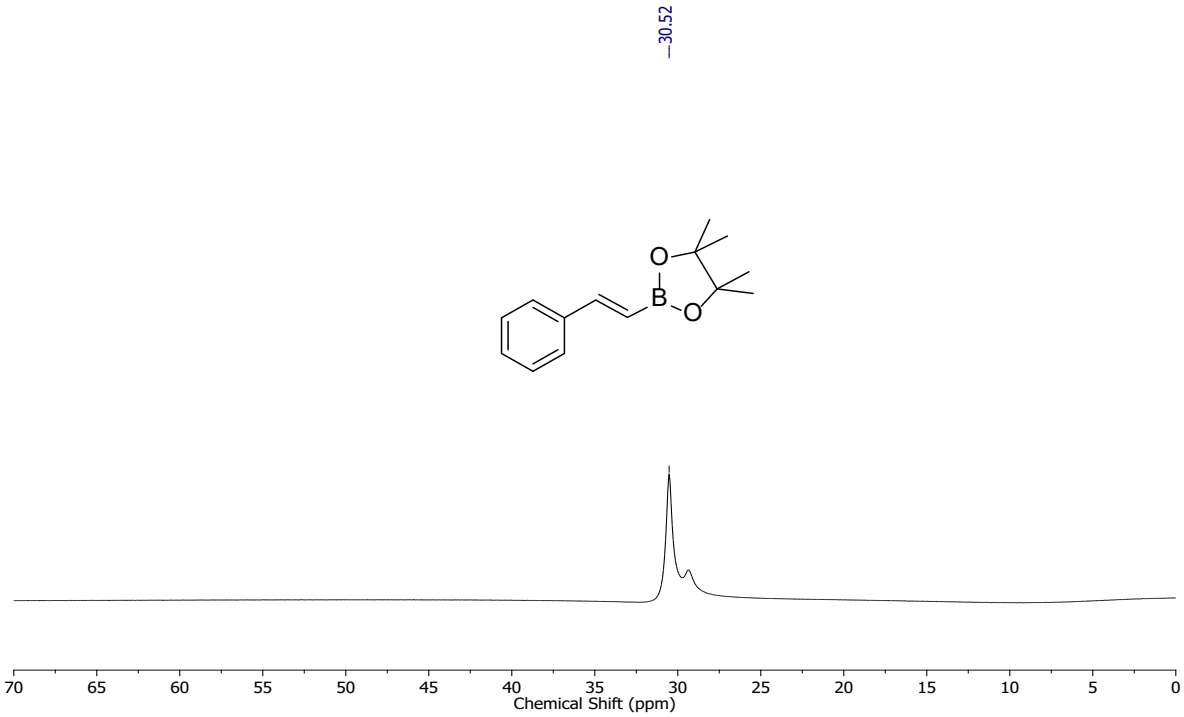


**Figure S109**. $^{11}B\{^{1}H\}$ NMR (128.4 MHz, $CDCl_3$, 298 K) spectrum of **10a**.

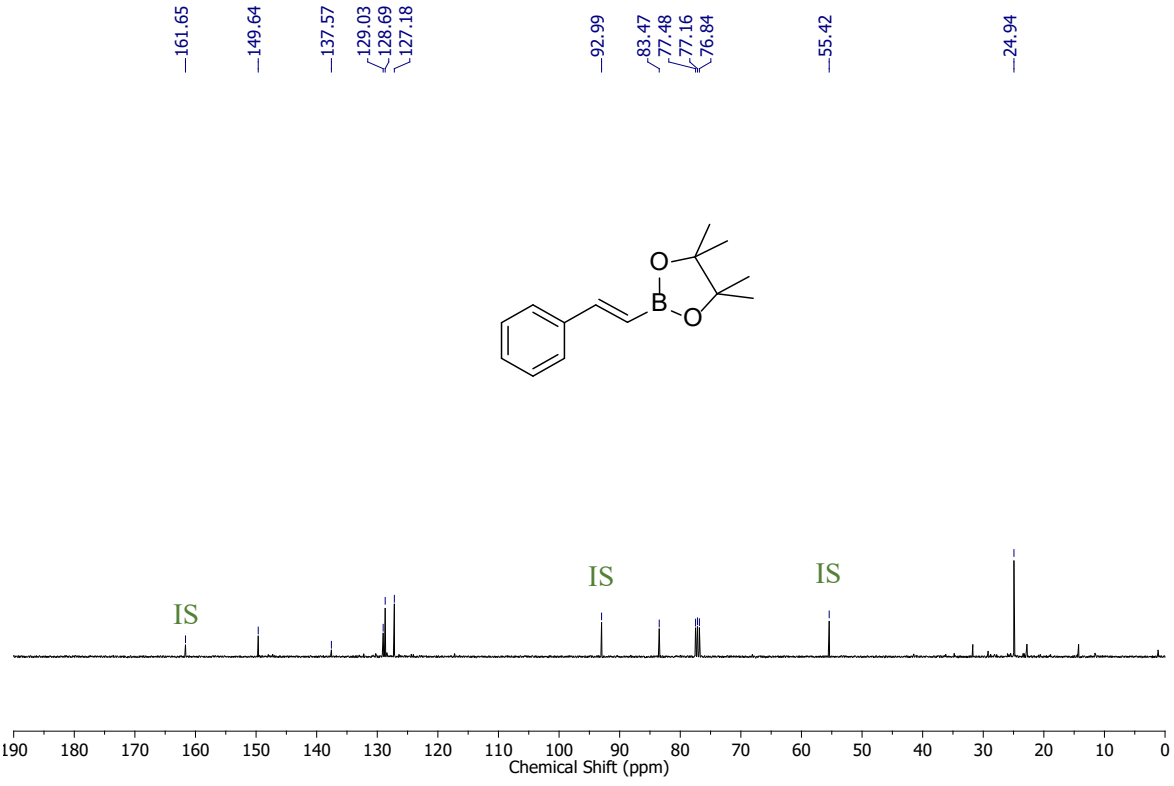


**Figure S110**. $^{13}C\{^{1}H\}$ NMR (100 MHz, $CDCl_3$, 298 K) spectrum of **10a**.

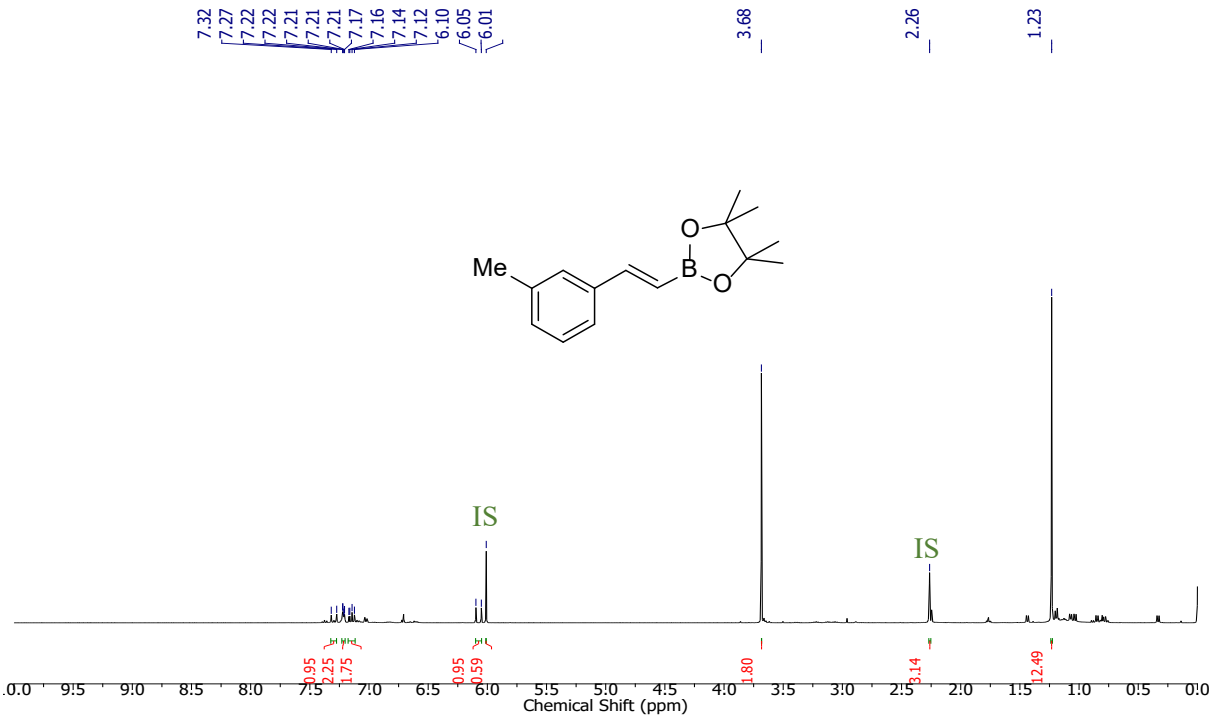


**Figure S111**. $^{1}H$ NMR (400 MHz, $CDCl_3$, 298 K) spectrum of **10b**.

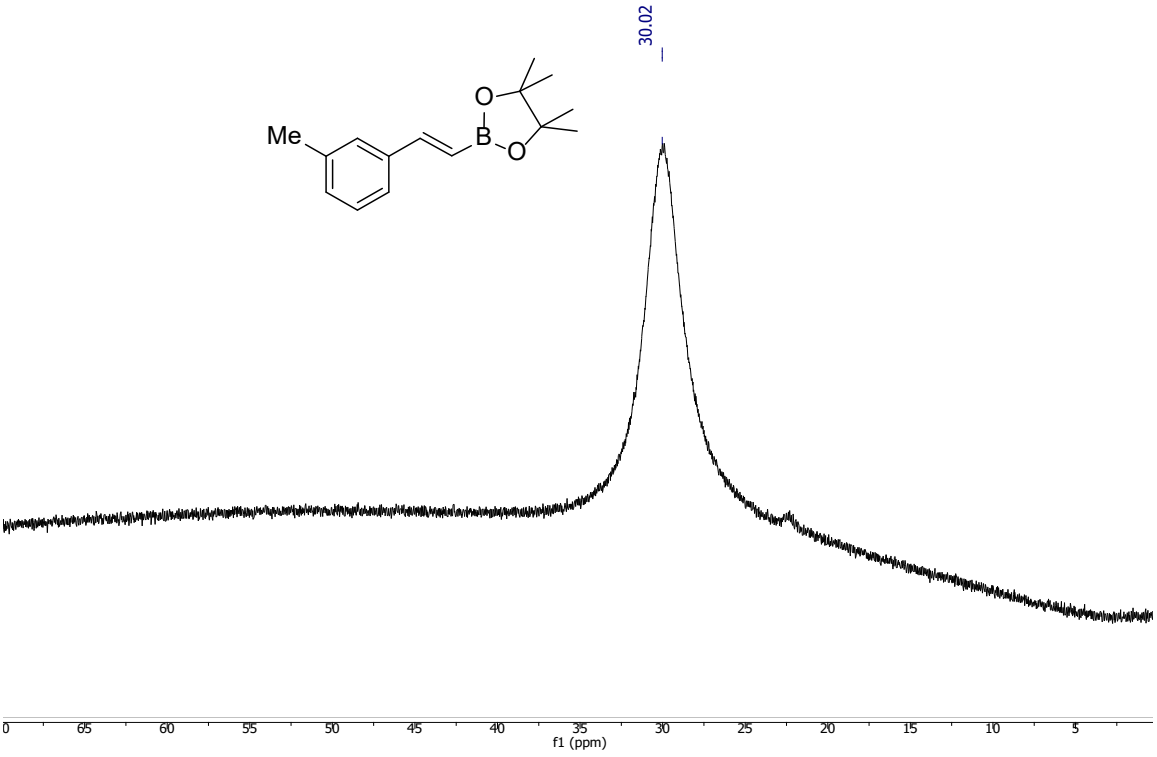


**Figure S112**. $^{11}B\{^{1}H\}$ NMR (128.4 MHz, $CDCl_3$, 298 K) spectrum of **10b**.

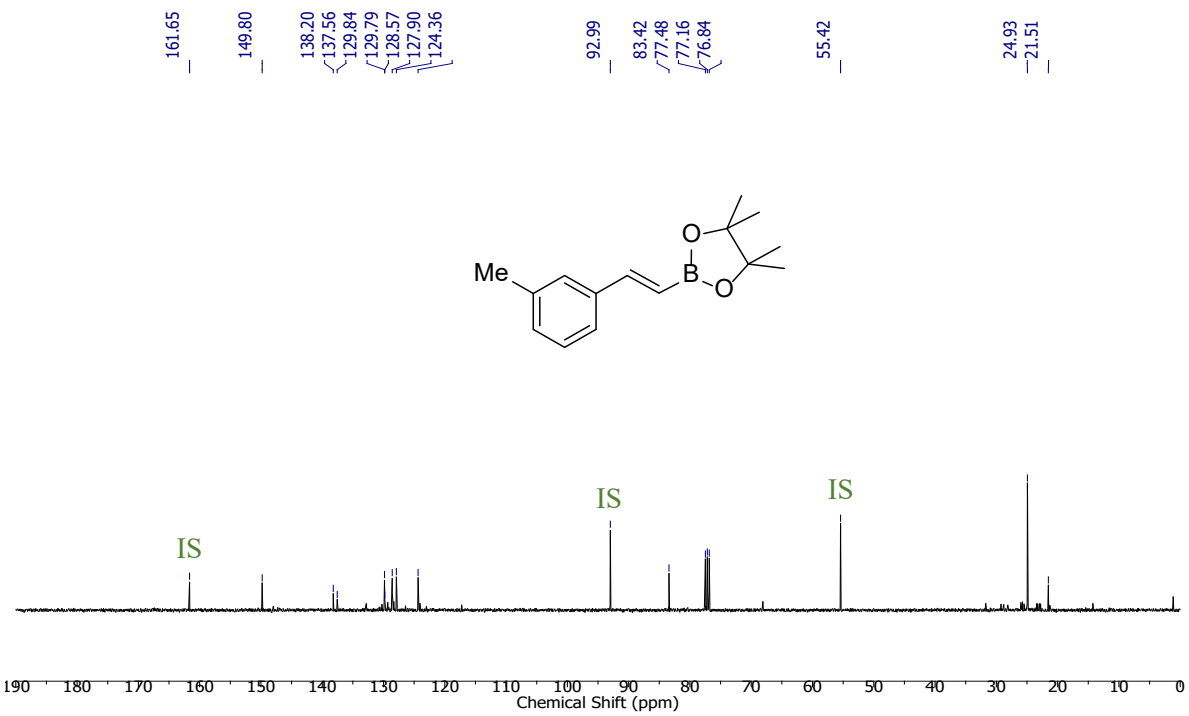


**Figure S113**. $^{13}C\{^{1}H\}$ NMR (100 MHz, $CDCl_3$, 298 K) spectrum of **10b**.

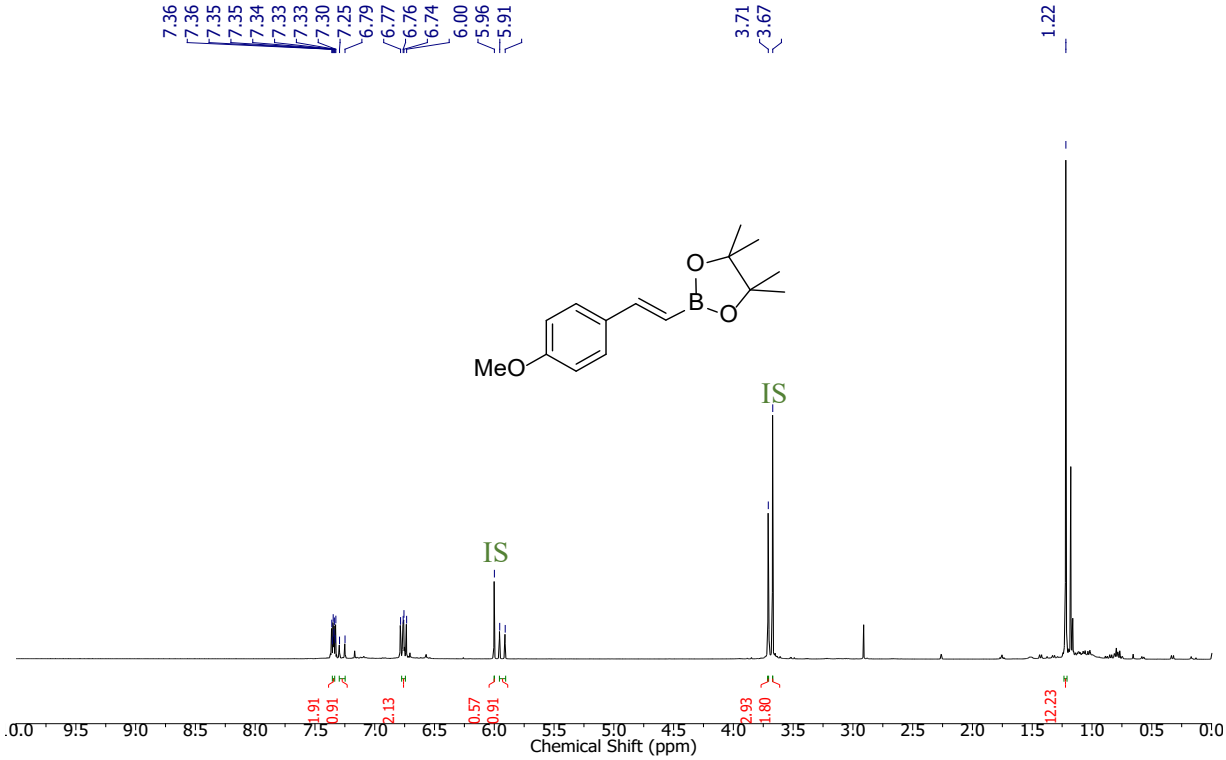


**Figure S114**. $^{1}H$ NMR (400 MHz, $CDCl_3$, 298 K) spectrum of **10c**.

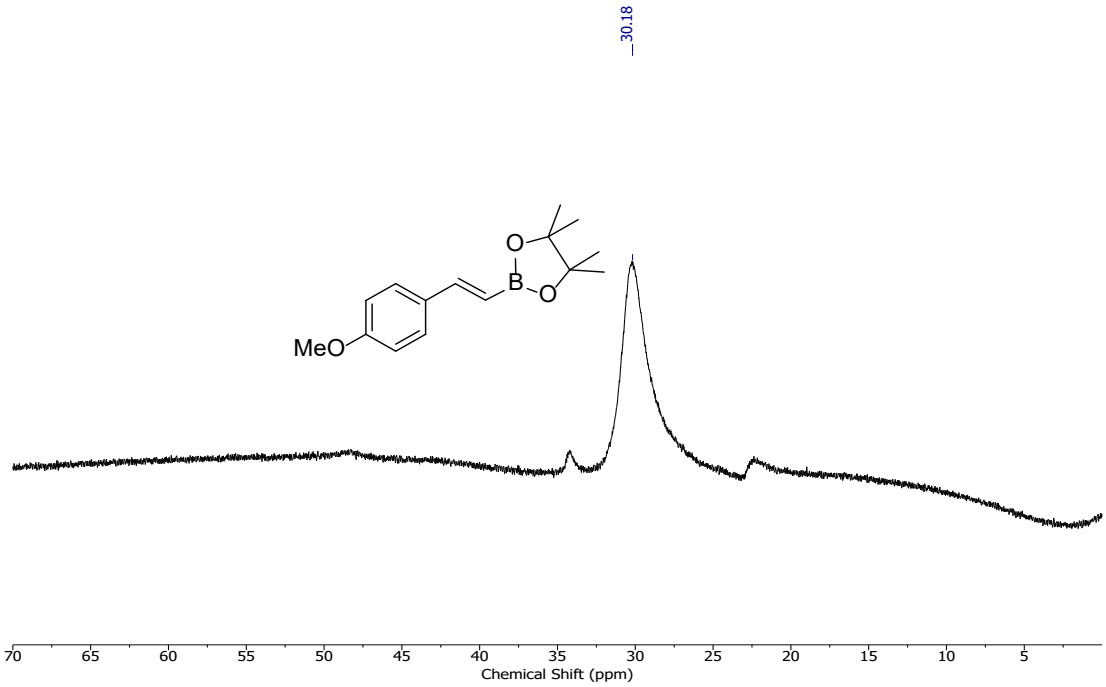


**Figure S115**. $^{11}B\{^{1}H\}$ NMR (128.4 MHz, $CDCl_3$, 298 K) spectrum of **10c**.

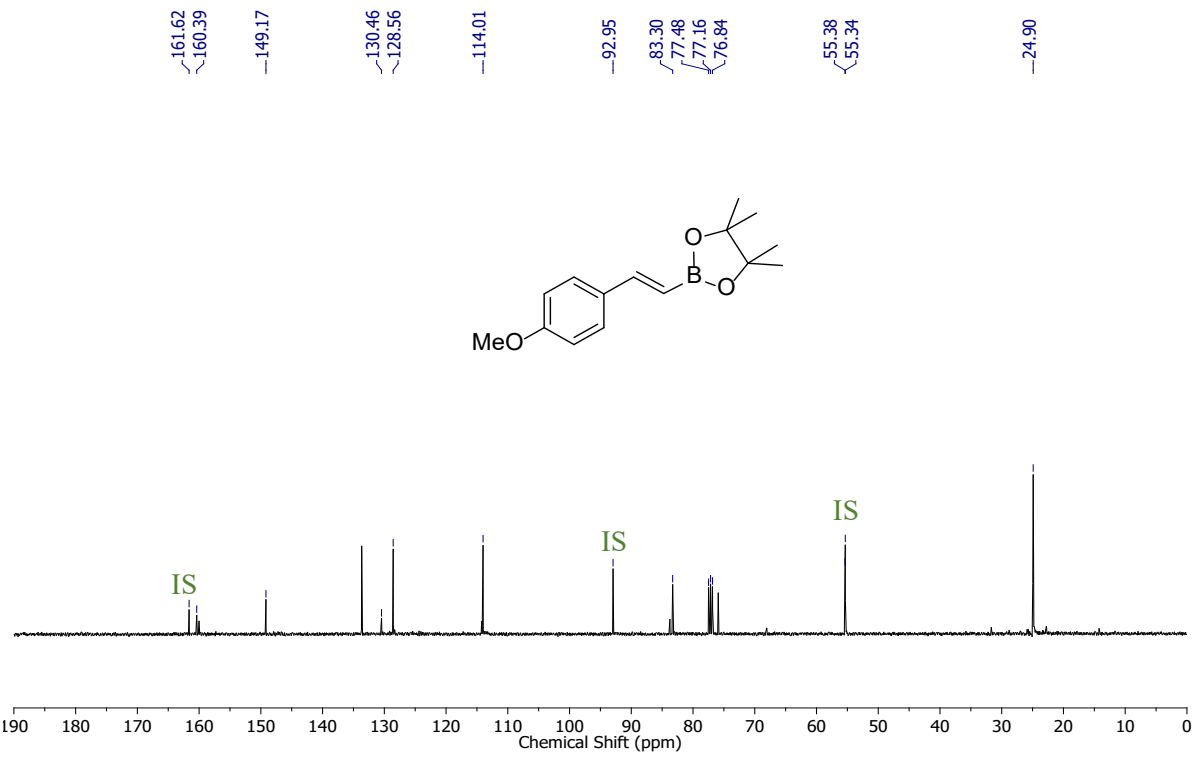


**Figure S116**. $^{13}C\{^{1}H\}$ NMR (100 MHz, $CDCl_3$, 298 K) spectrum of **10c**.

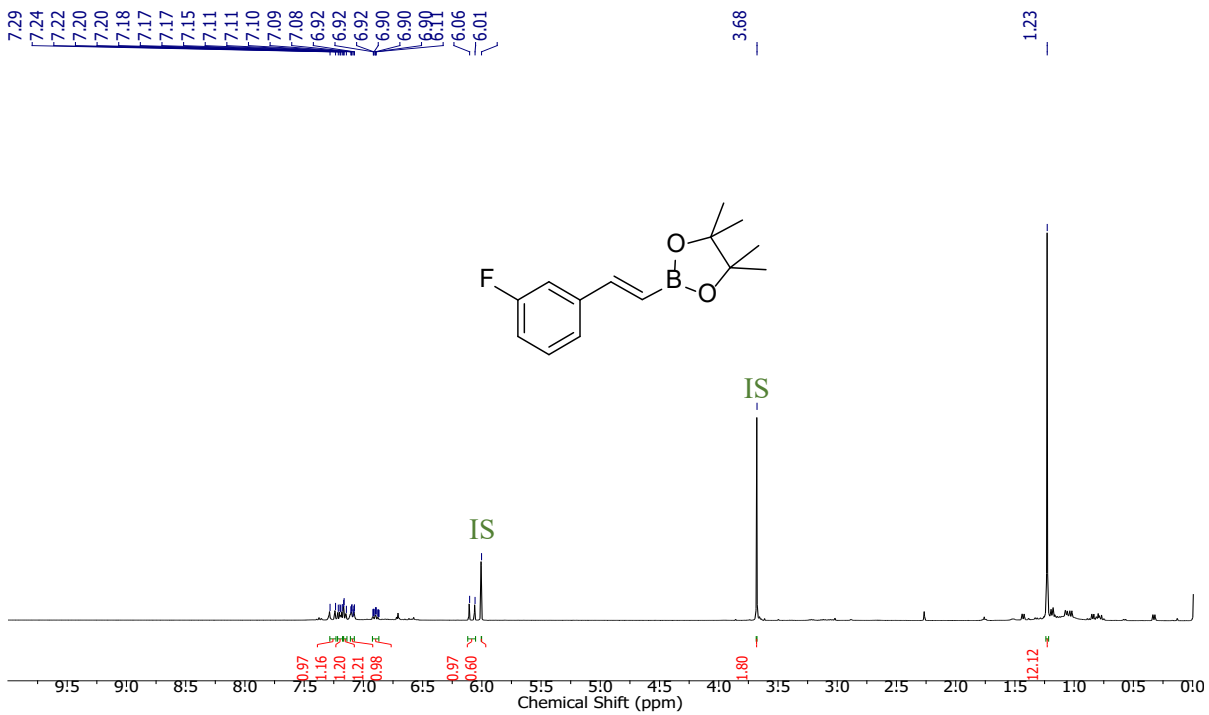


**Figure S117**. $^{1}H$ NMR (400 MHz, $CDCl_3$, 298 K) spectrum of **10d**.

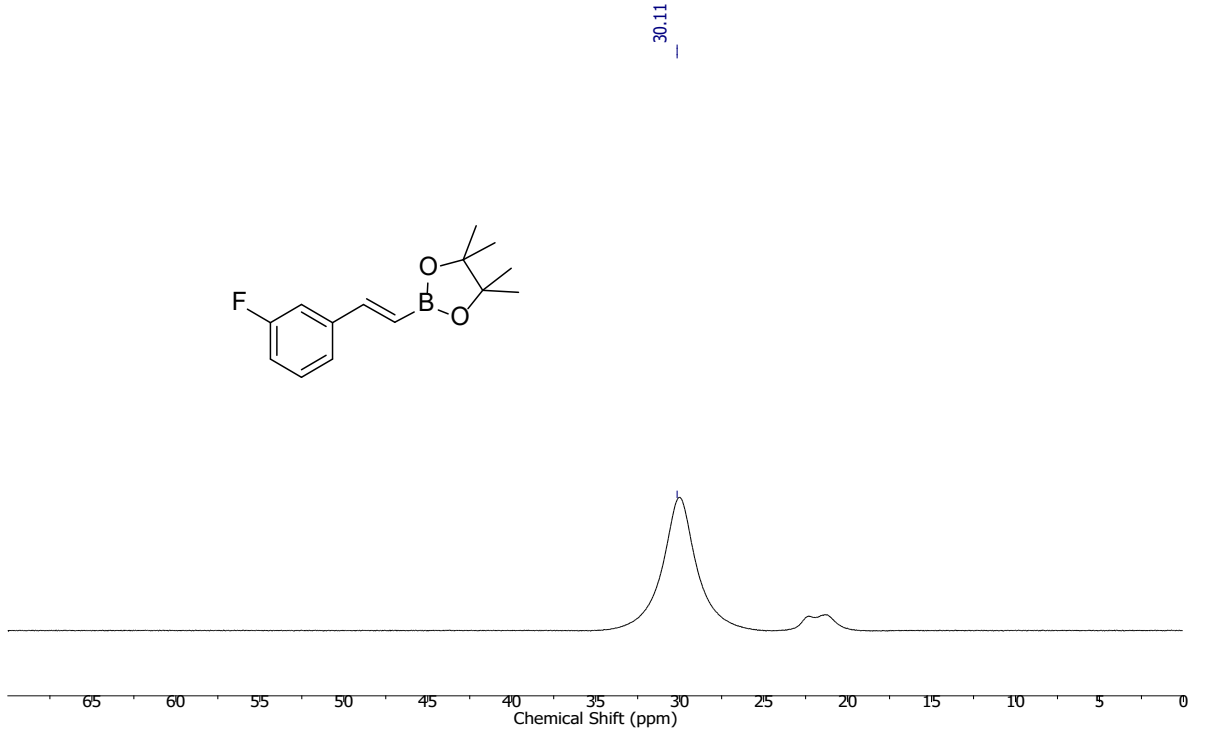


**Figure S118**. $^{11}B\{^{1}H\}$ NMR (128.4 MHz, $CDCl_3$, 298 K) spectrum of **10d**.

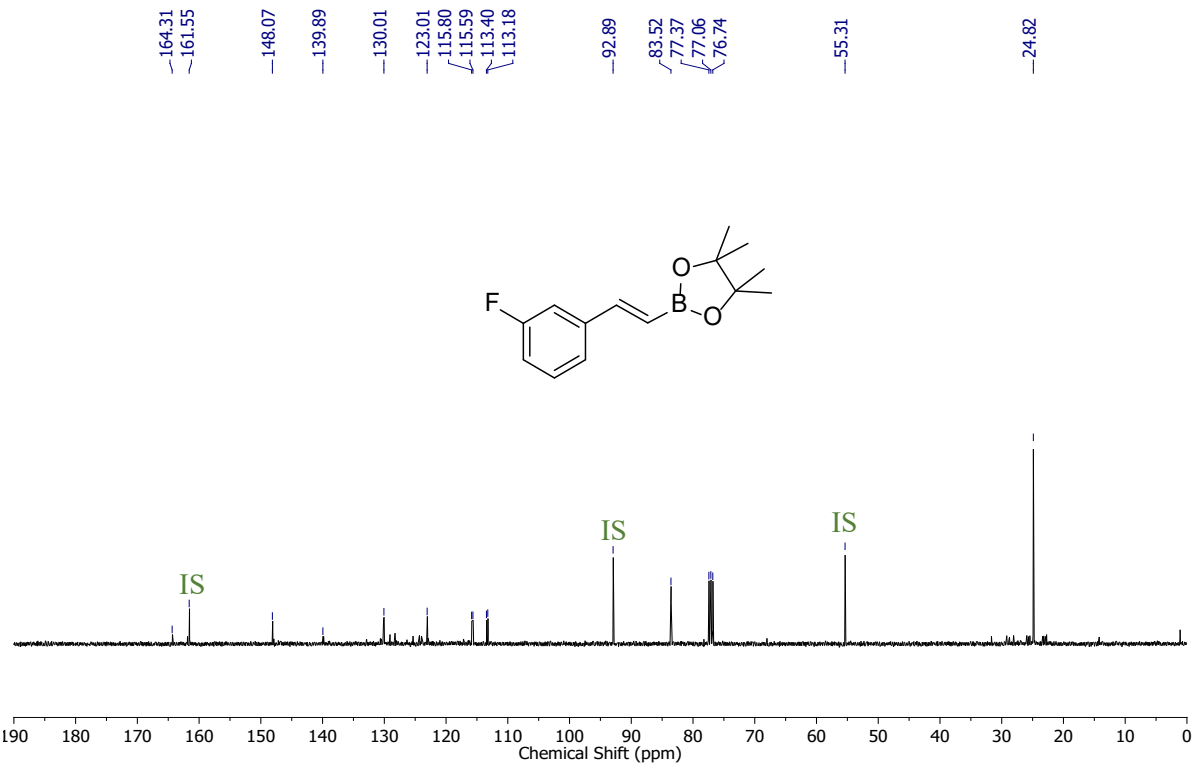


**Figure S119**. $^{13}C\{^{1}H\}$ NMR (100 MHz, $CDCl_3$, 298 K) spectrum of **10d**.

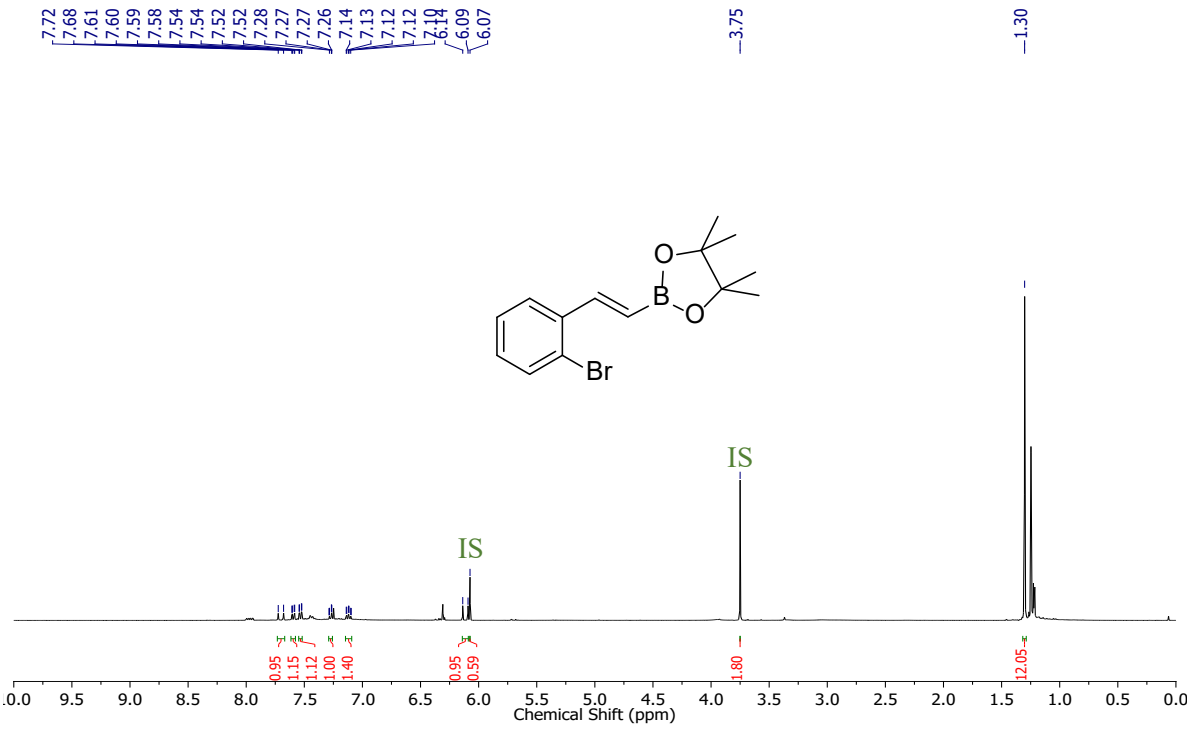


**Figure S120**. $^{1}H$ NMR (400 MHz, $CDCl_3$, 298 K) spectrum of **10e**.

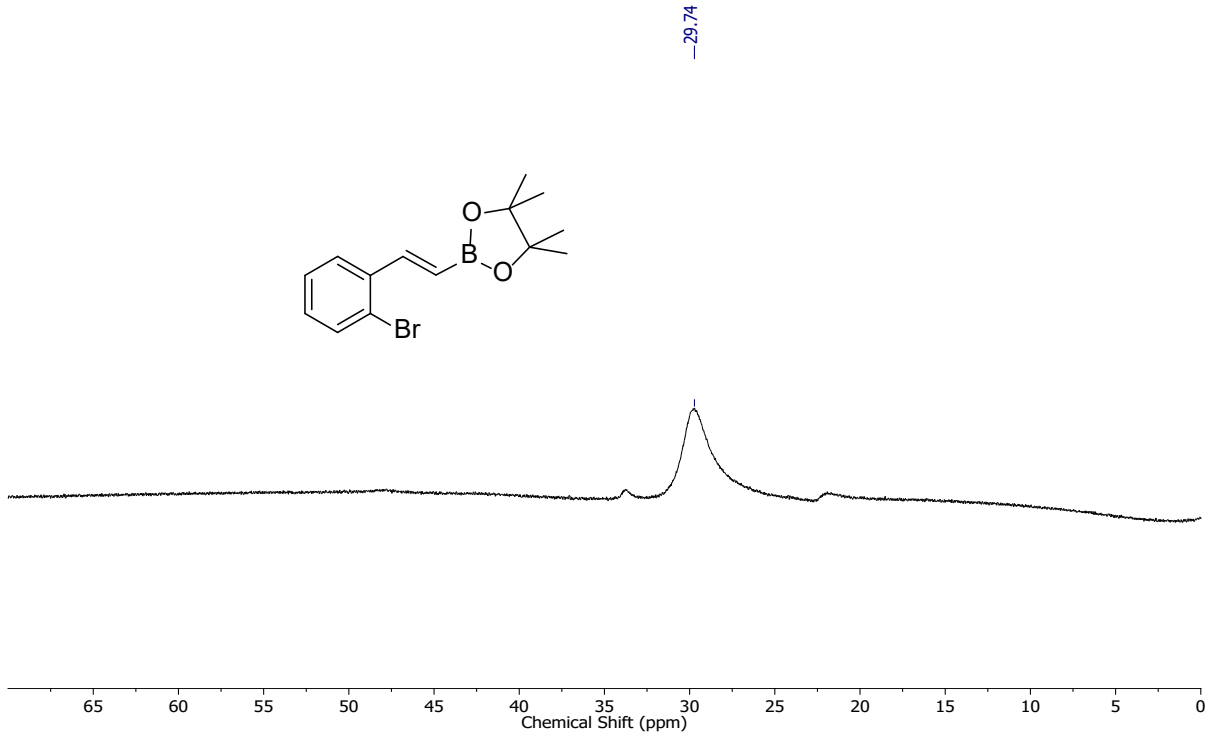


**Figure S121**. $^{11}B\{^{1}H\}$ NMR (128.4 MHz, $CDCl_3$, 298 K) spectrum of **10e**.

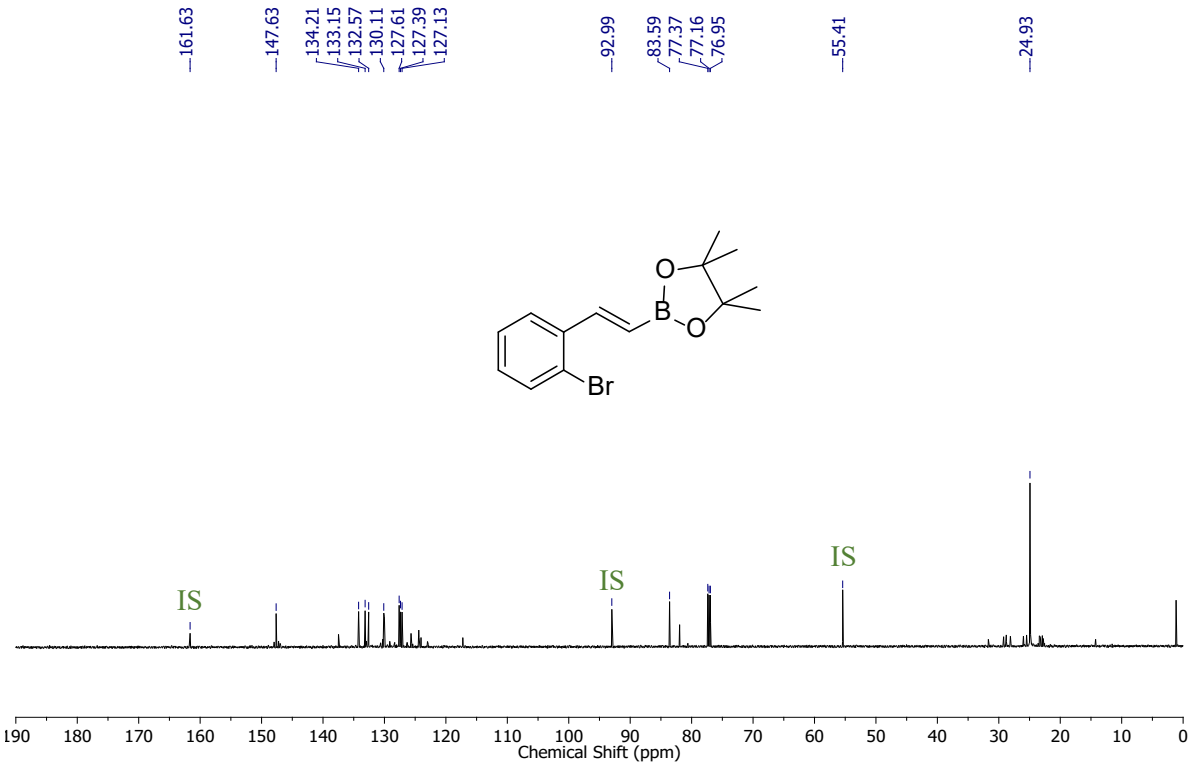


**Figure S122**. $^{13}C\{^{1}H\}$ NMR (100 MHz, $CDCl_3$, 298 K) spectrum of **10e**.

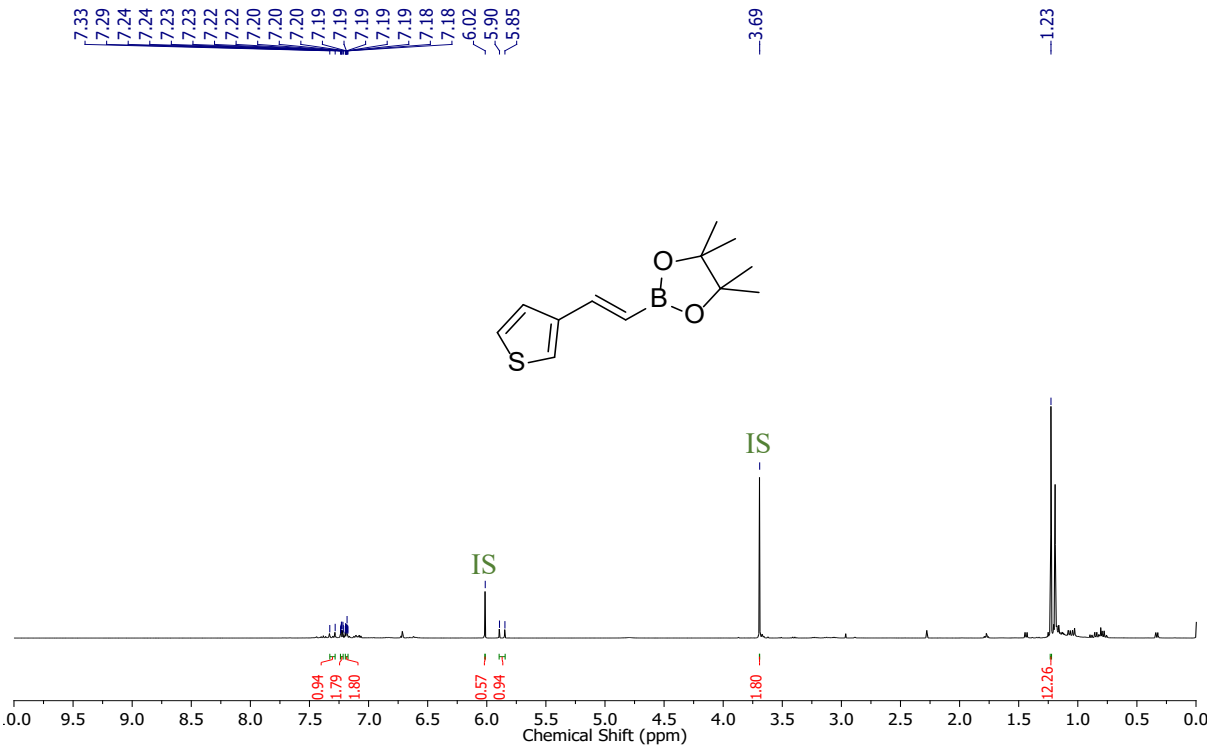


**Figure S123**. $^{1}H$ NMR (400 MHz, $CDCl_3$, 298 K) spectrum of **10f**.

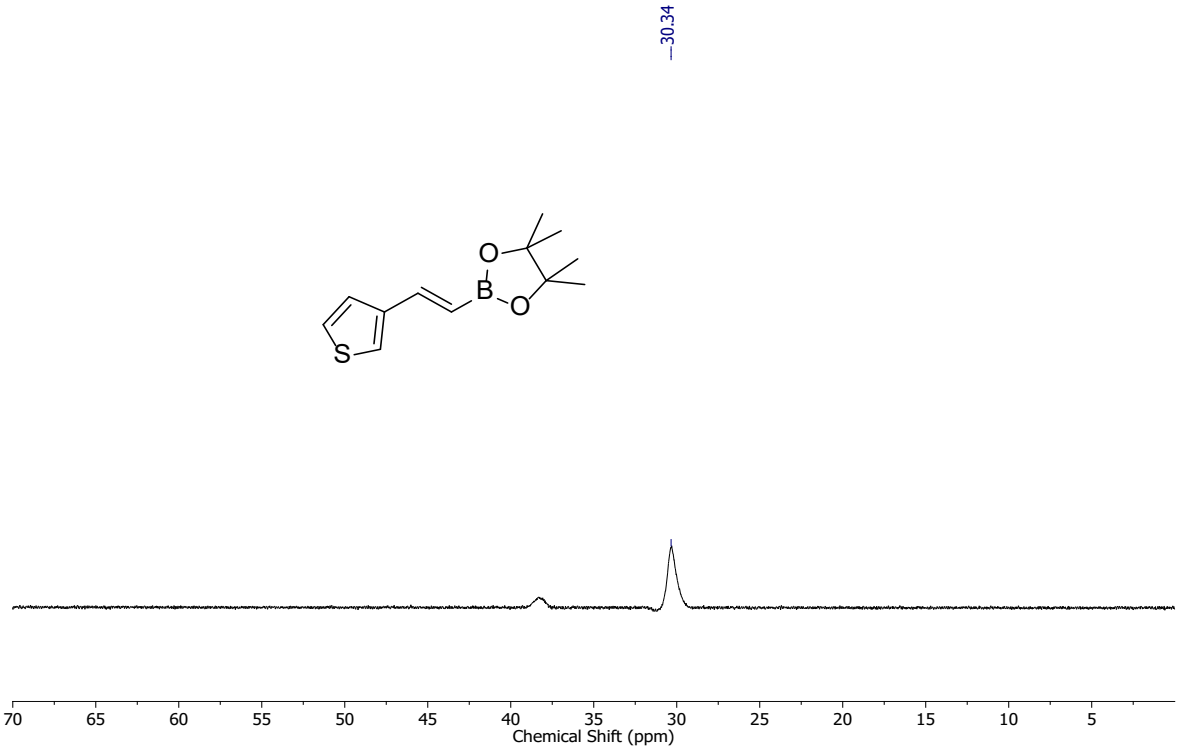


**Figure S124**. $^{11}B\{^{1}H\}$ NMR (128.4 MHz, $CDCl_3$, 298 K) spectrum of **10f**.

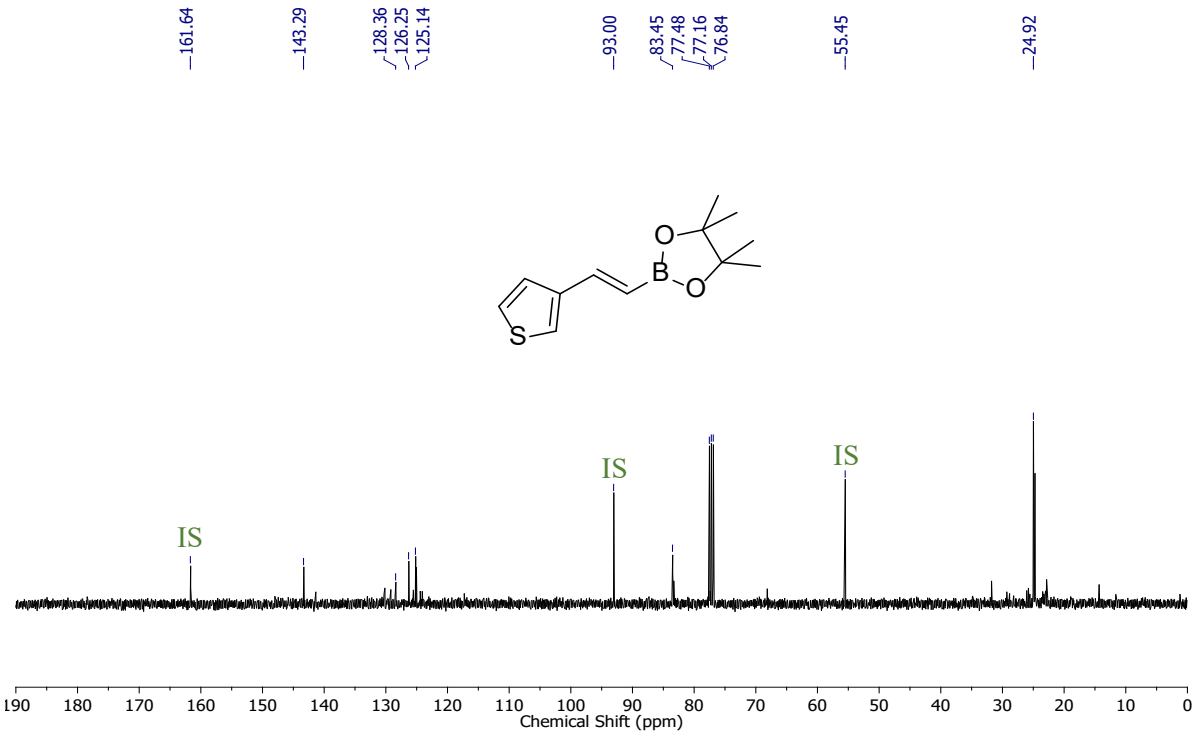


**Figure S125**. $^{13}C\{^{1}H\}$ NMR (100 MHz, $CDCl_3$, 298 K) spectrum of **10f**.

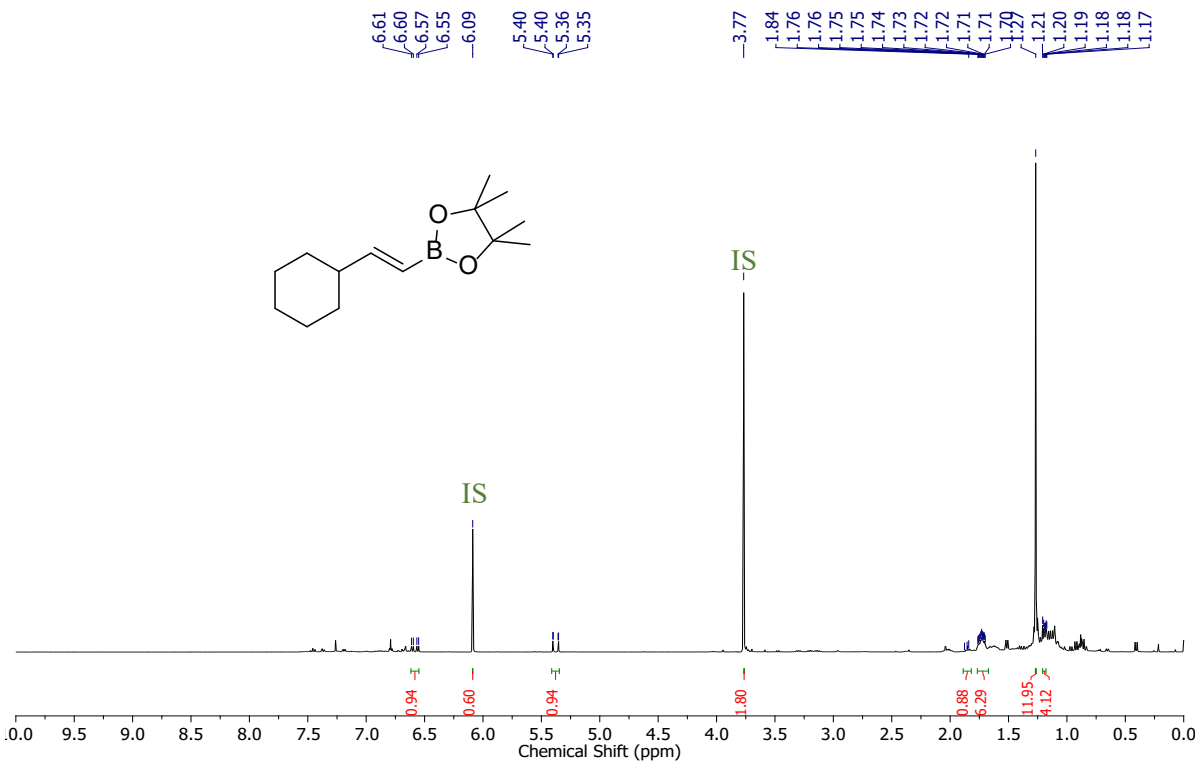


**Figure S126**. $^{1}H$ NMR (400 MHz, $CDCl_3$, 298 K) spectrum of **10g**.

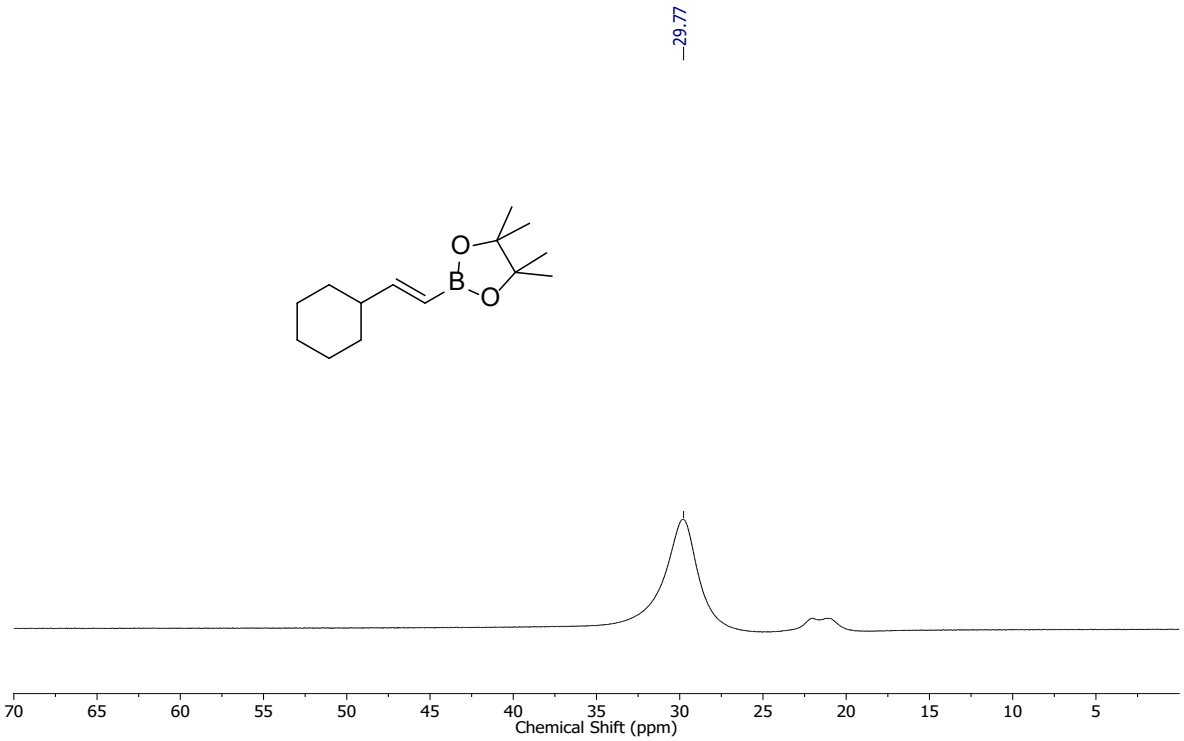


**Figure S127**. $^{11}B\{^{1}H\}$ NMR (128.4 MHz, $CDCl_3$, 298 K) spectrum of **10g**.

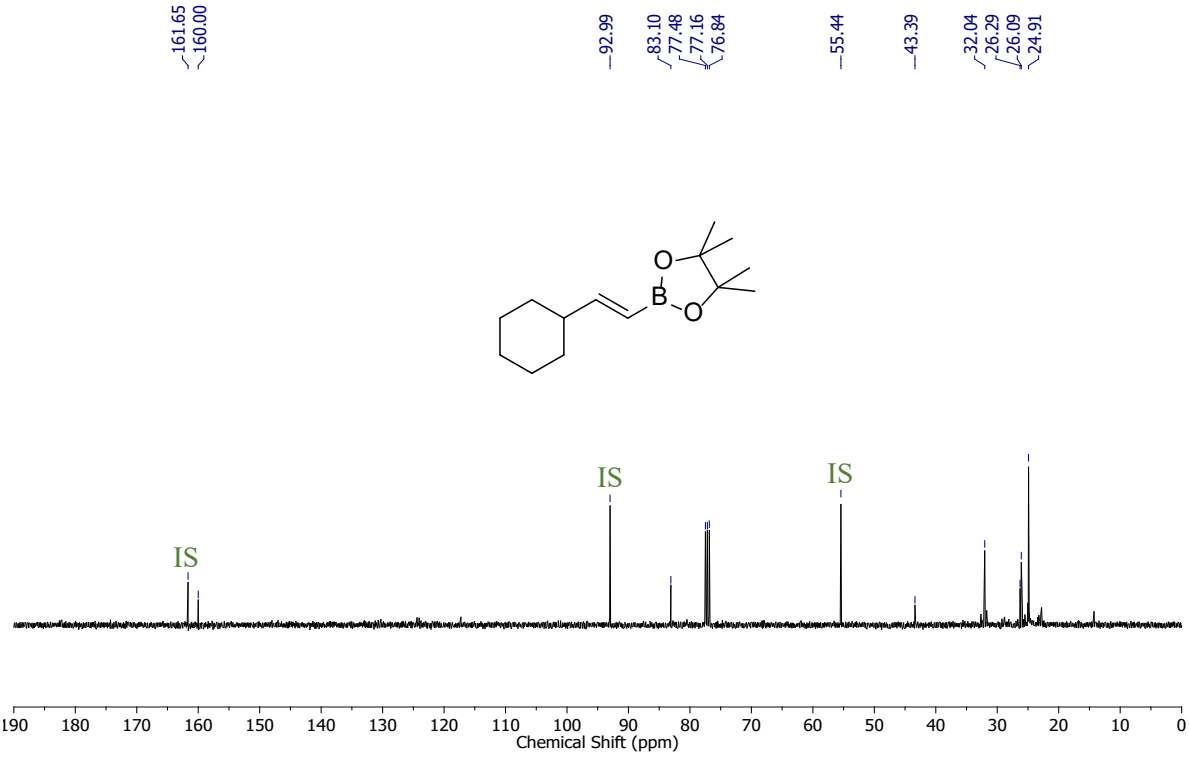


**Figure S128**. $^{13}C\{^{1}H\}$ NMR (100 MHz, $CDCl_3$, 298 K) spectrum of **10g**.

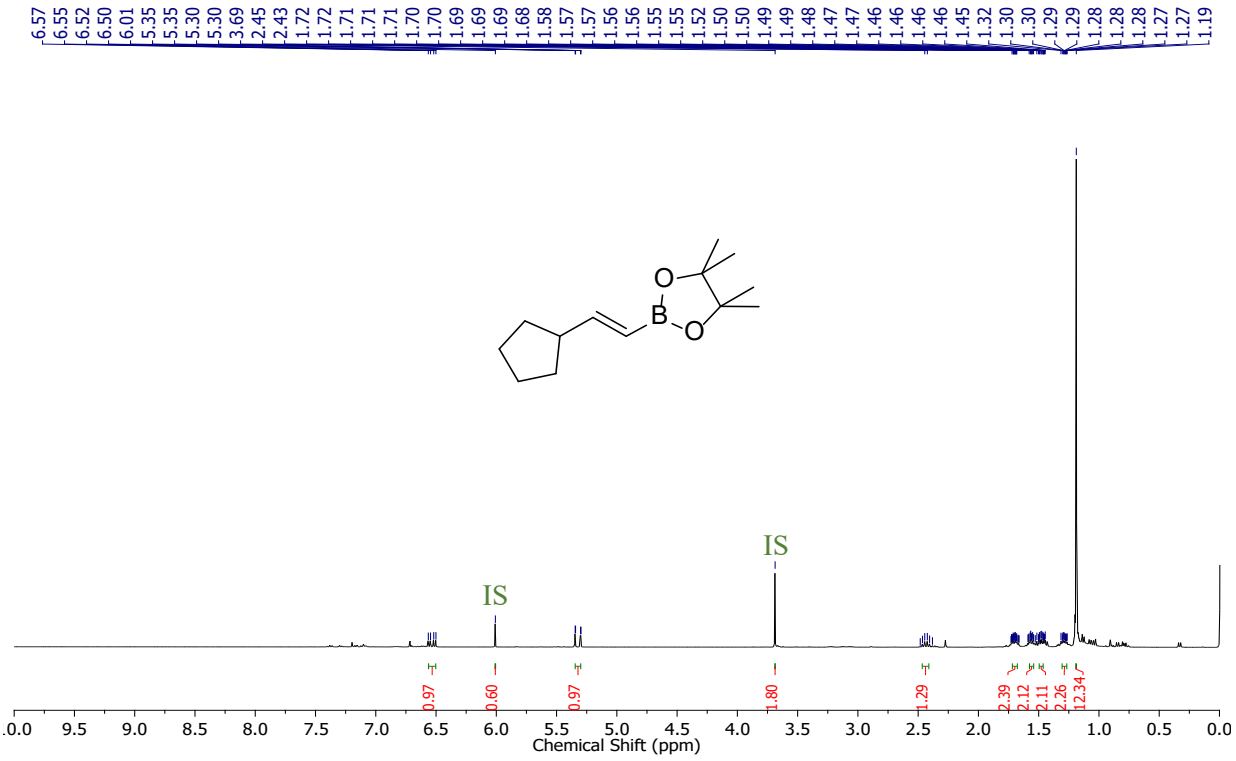


**Figure S129**. $^{1}H$ NMR (400 MHz, $CDCl_3$, 298 K) spectrum of **10h**.

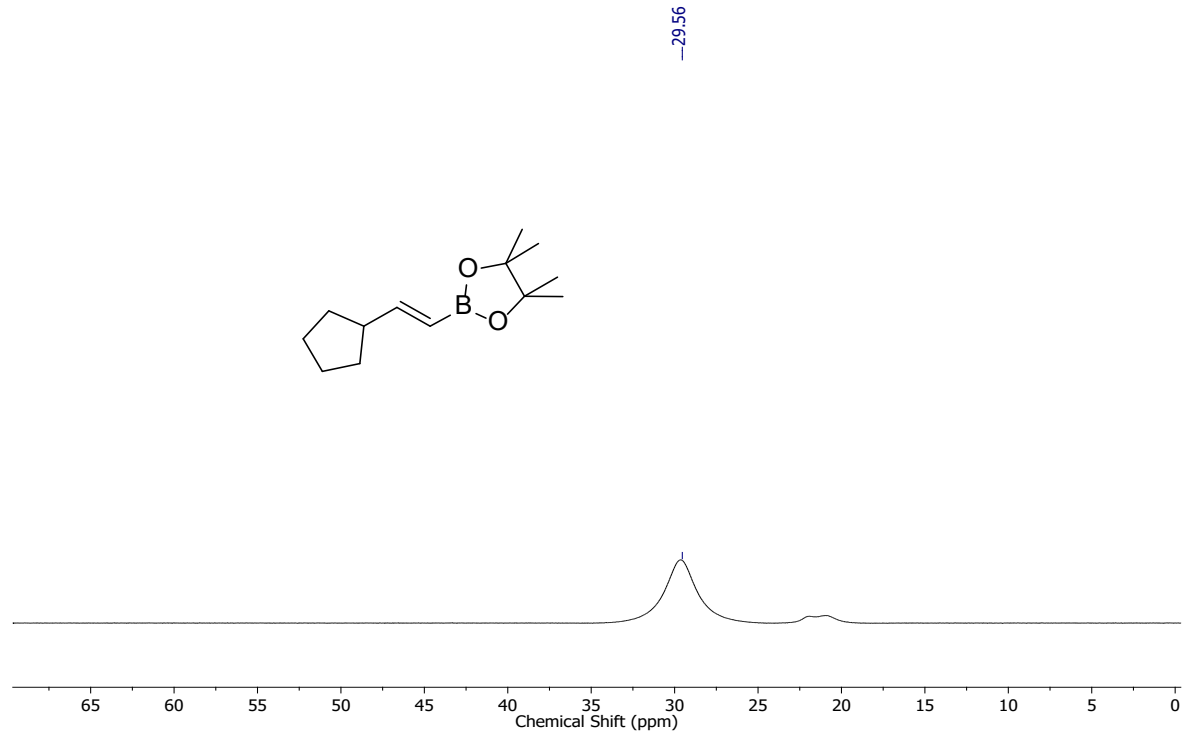


**Figure S130**. $^{11}B\{^{1}H\}$ NMR (128.4 MHz, $CDCl_3$, 298 K) spectrum of **10h**.

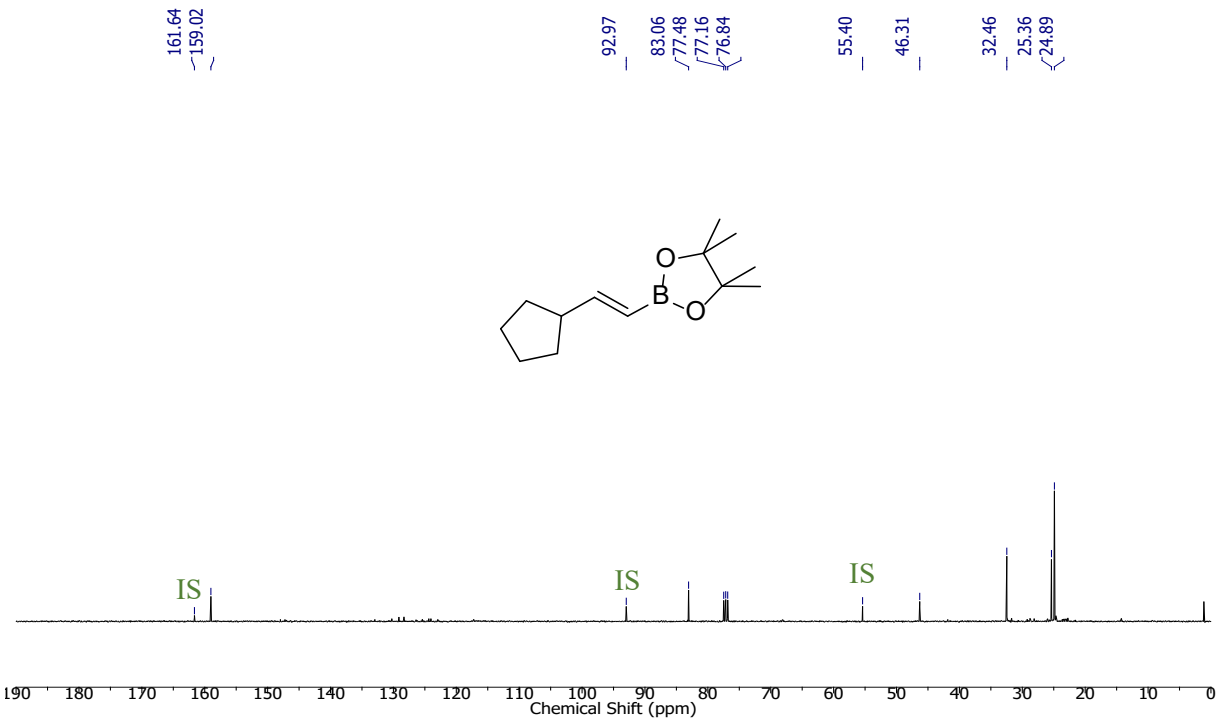


**Figure S131**. $^{13}C\{^{1}H\}$ NMR (100 MHz, $CDCl_3$, 298 K) spectrum of **10h**.

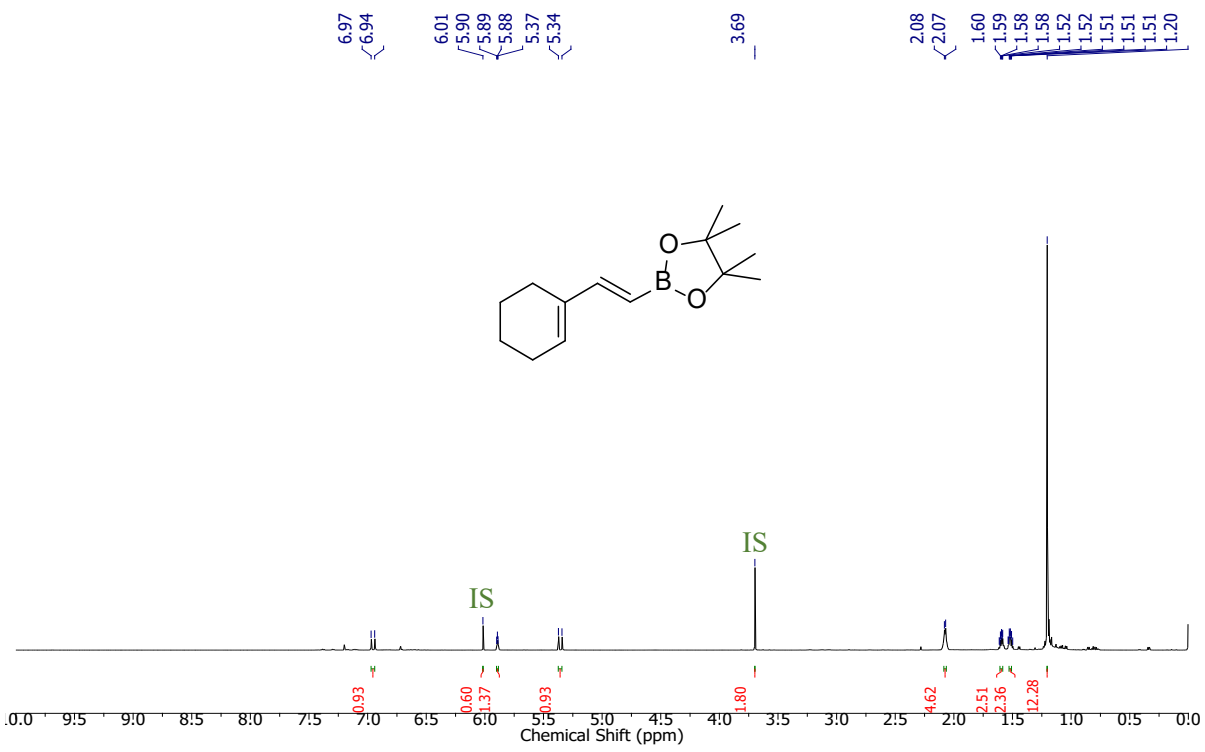


**Figure S132**. $^{1}H$ NMR (400 MHz, $CDCl_3$, 298 K) spectrum of **10i**.

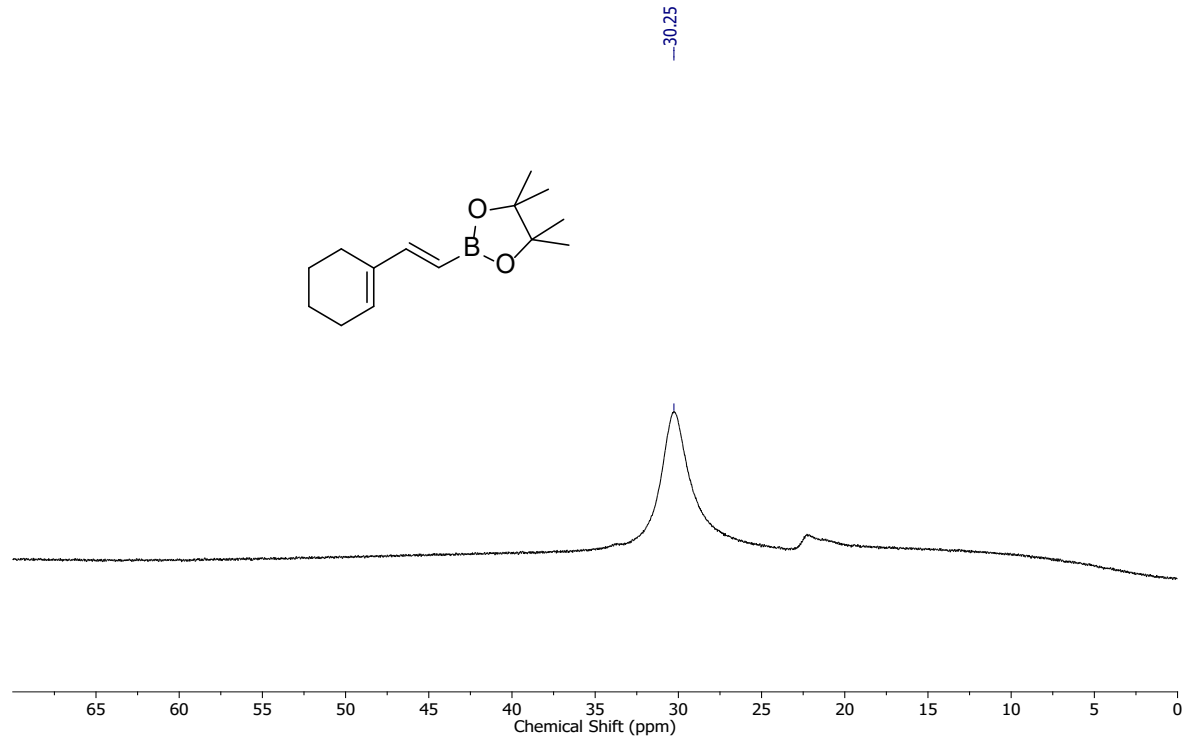


**Figure S133**. $^{11}B\{^{1}H\}$ NMR (128.4 MHz, $CDCl_3$, 298 K) spectrum of **10i**.

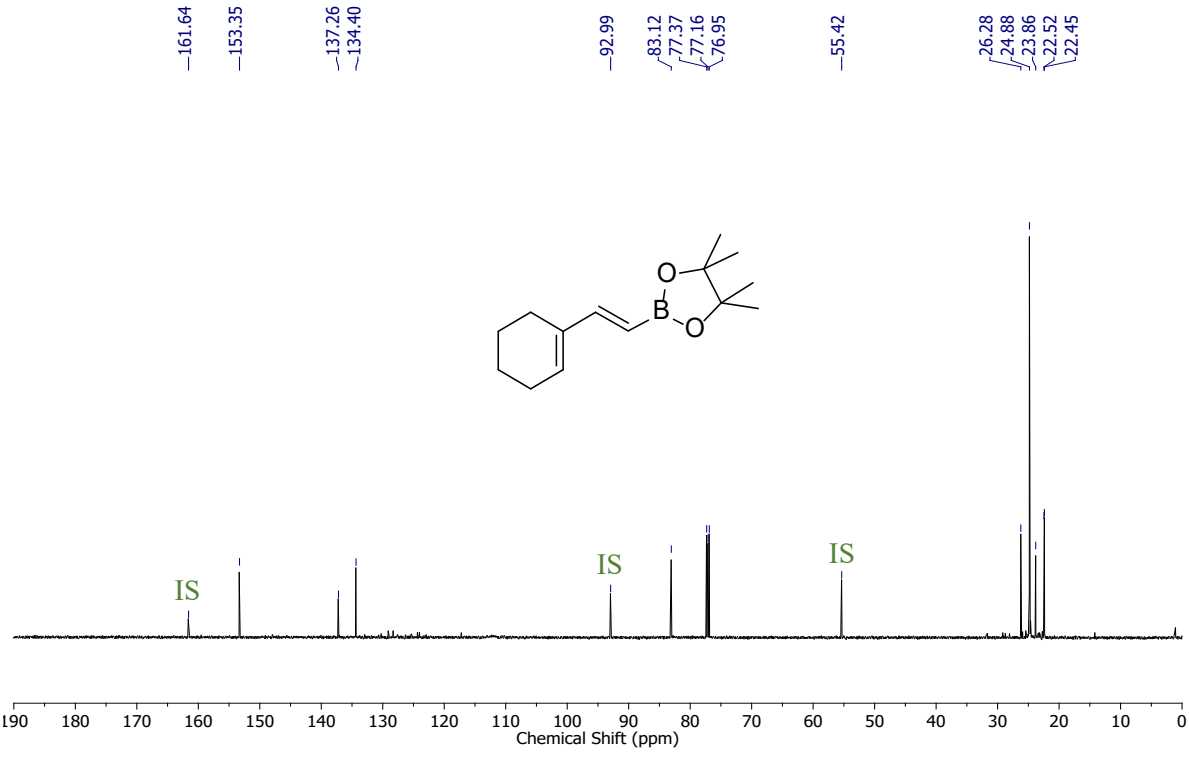


**Figure S134**. $^{13}C\{^{1}H\}$ NMR (100 MHz, $CDCl_3$, 298 K) spectrum of **10i**.

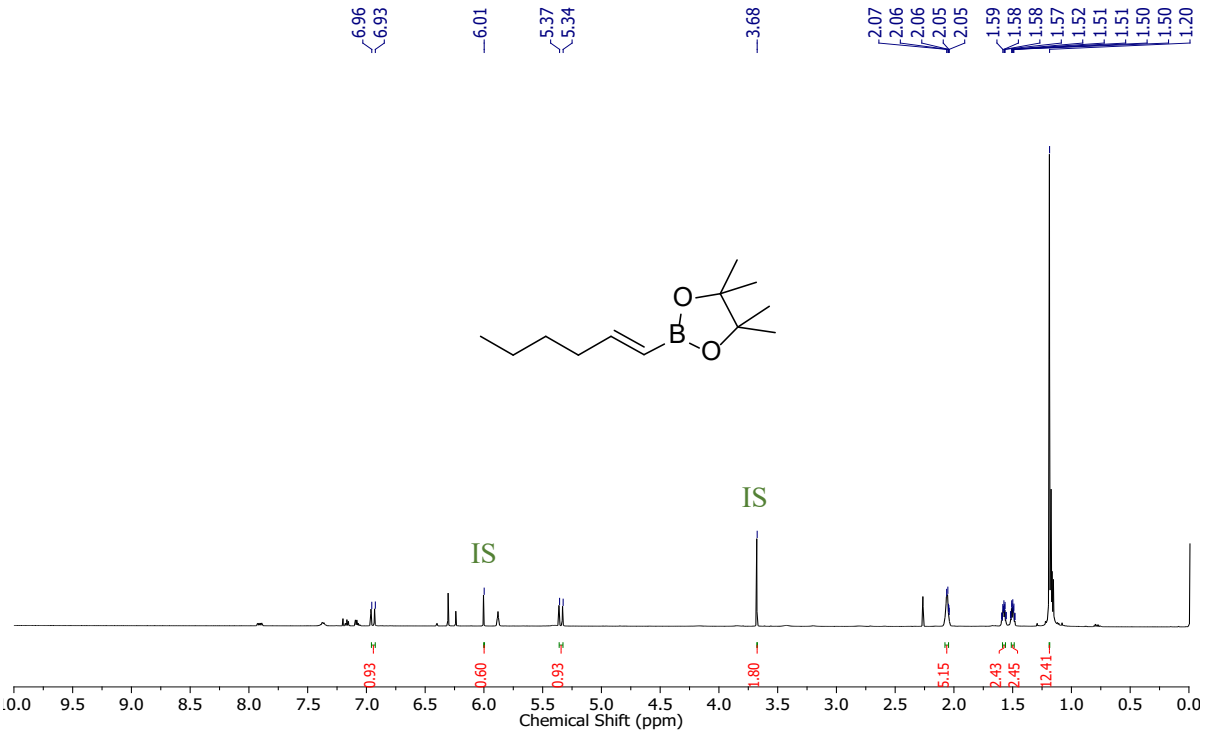


**Figure S135**. $^{1}H$ NMR (400 MHz, $CDCl_3$, 298 K) spectrum of **10j**.

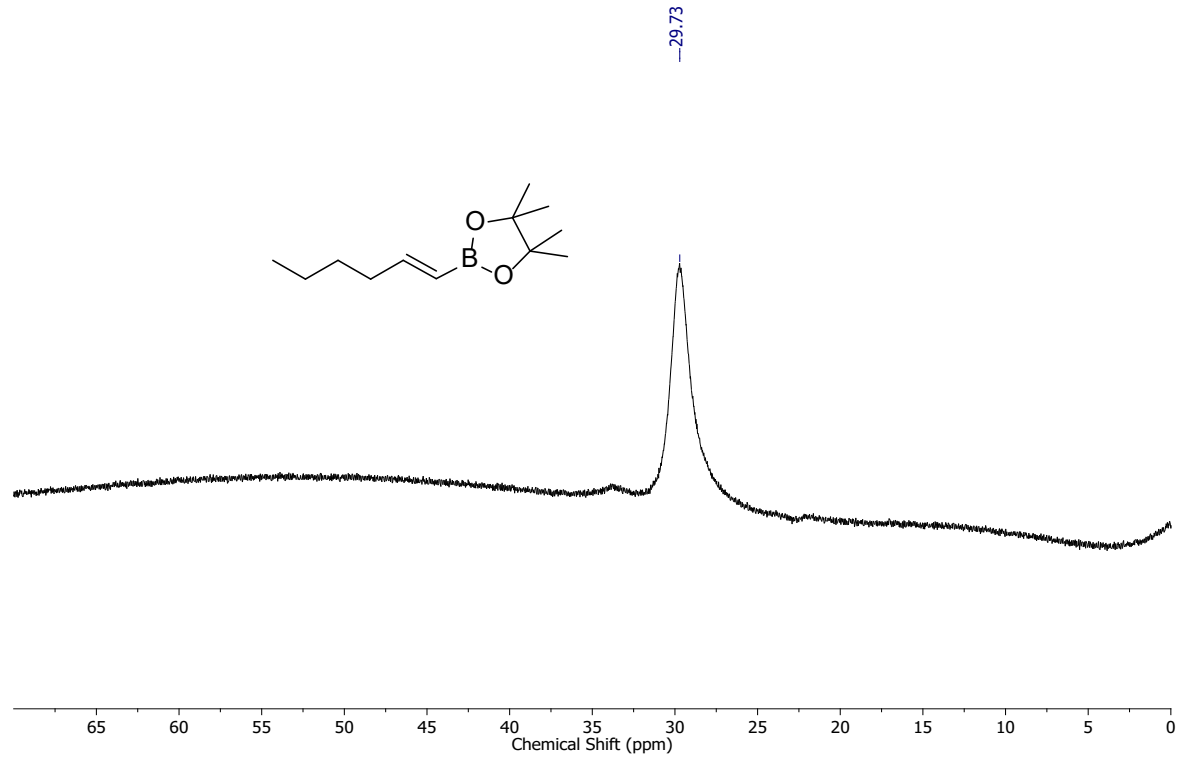


**Figure S136**. $^{11}B\{^{1}H\}$ NMR (128.4 MHz, $CDCl_3$, 298 K) spectrum of **10j**.

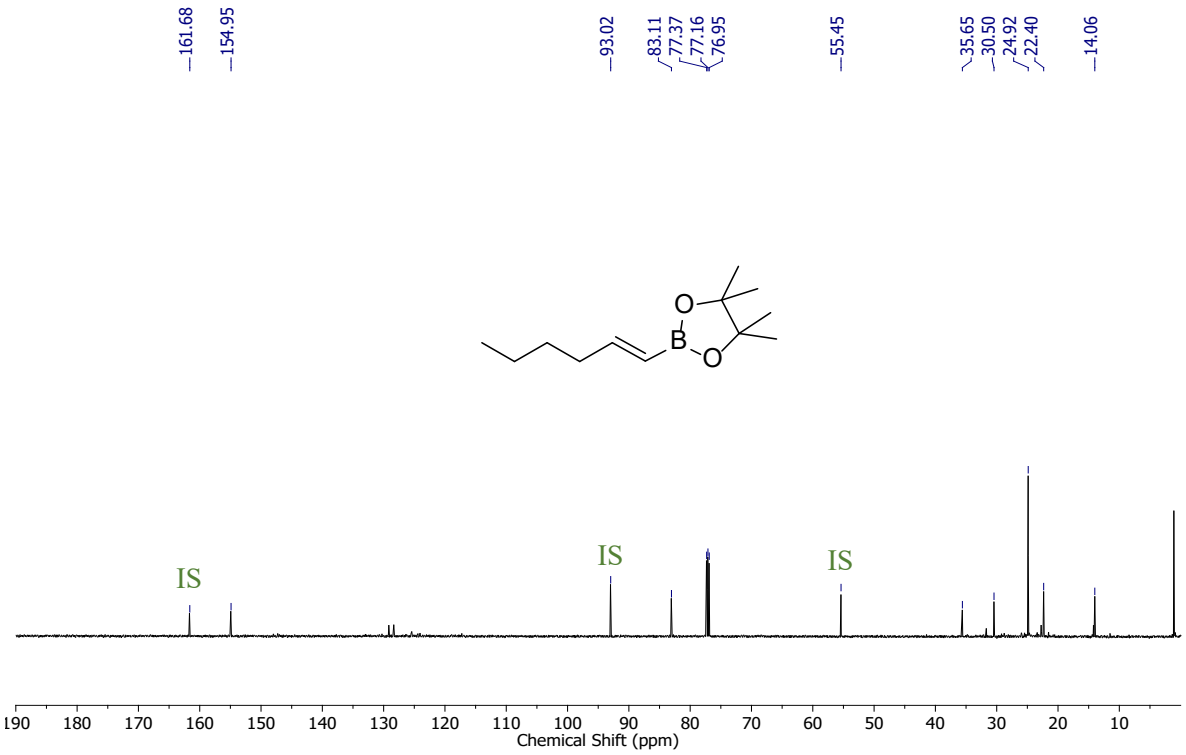


**Figure S137**. $^{13}C\{^{1}H\}$ NMR (100 MHz, $CDCl_3$, 298 K) spectrum of **10j**.

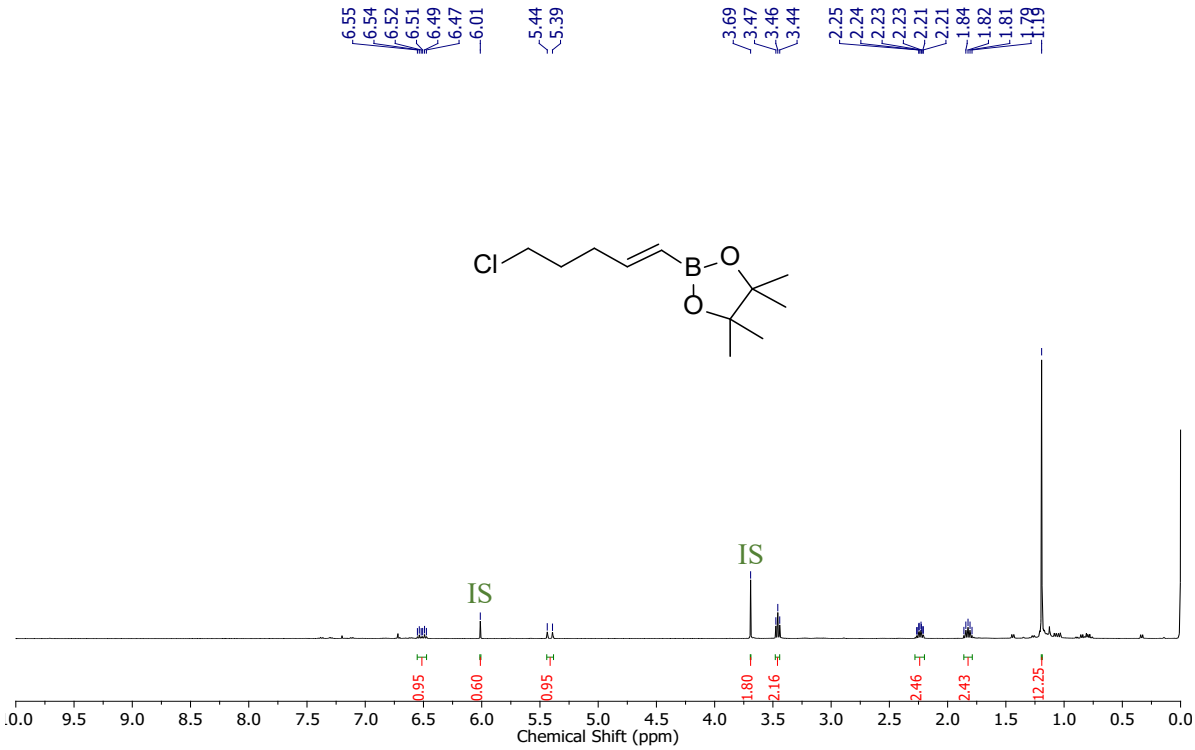


**Figure S138**. $^{1}H$ NMR (400 MHz, $CDCl_3$, 298 K) spectrum of **10k**.

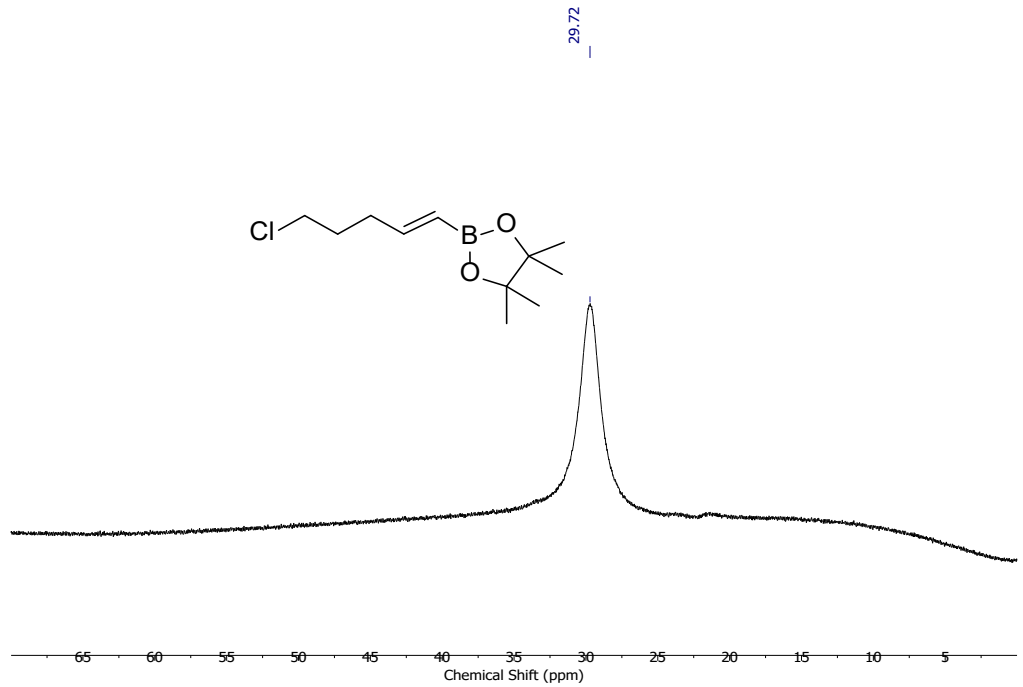


**Figure S139**. $^{11}B\{^{1}H\}$ NMR (128.4 MHz, $CDCl_3$, 298 K) spectrum of **10k**.

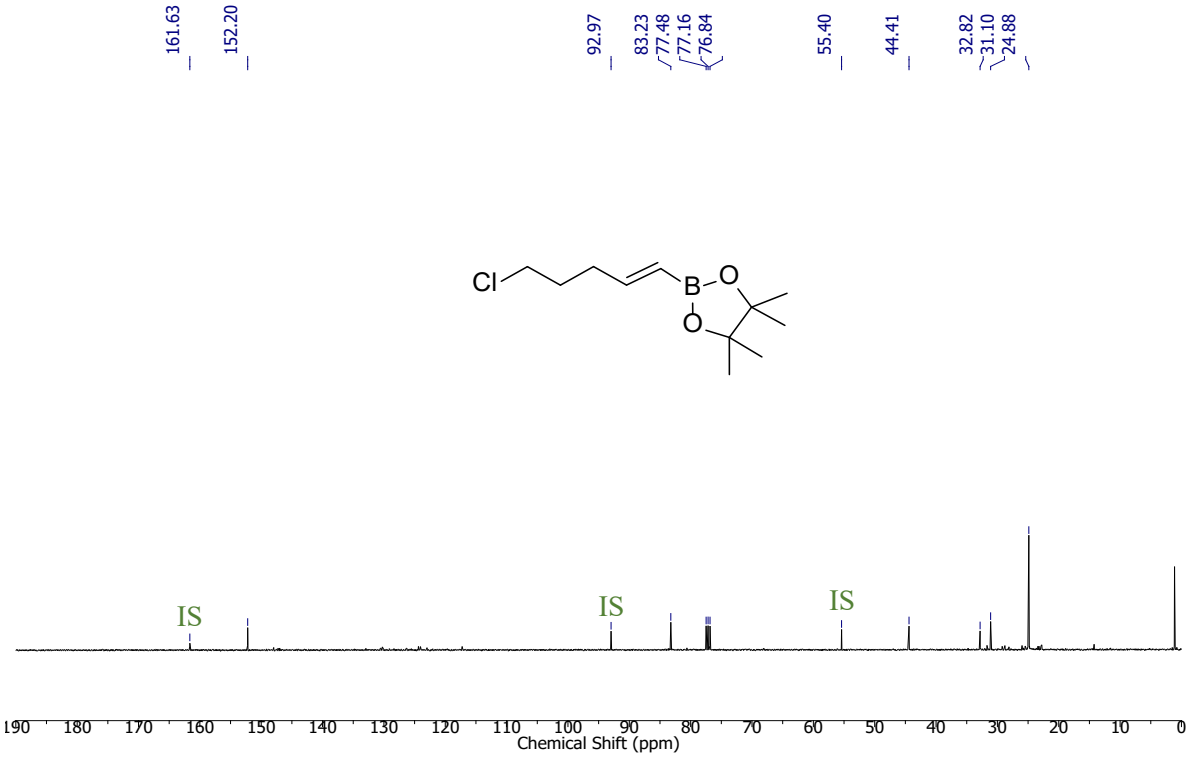


**Figure S140**. $^{13}C\{^{1}H\}$ NMR (100 MHz, $CDCl_3$, 298 K) spectrum of **10k**.

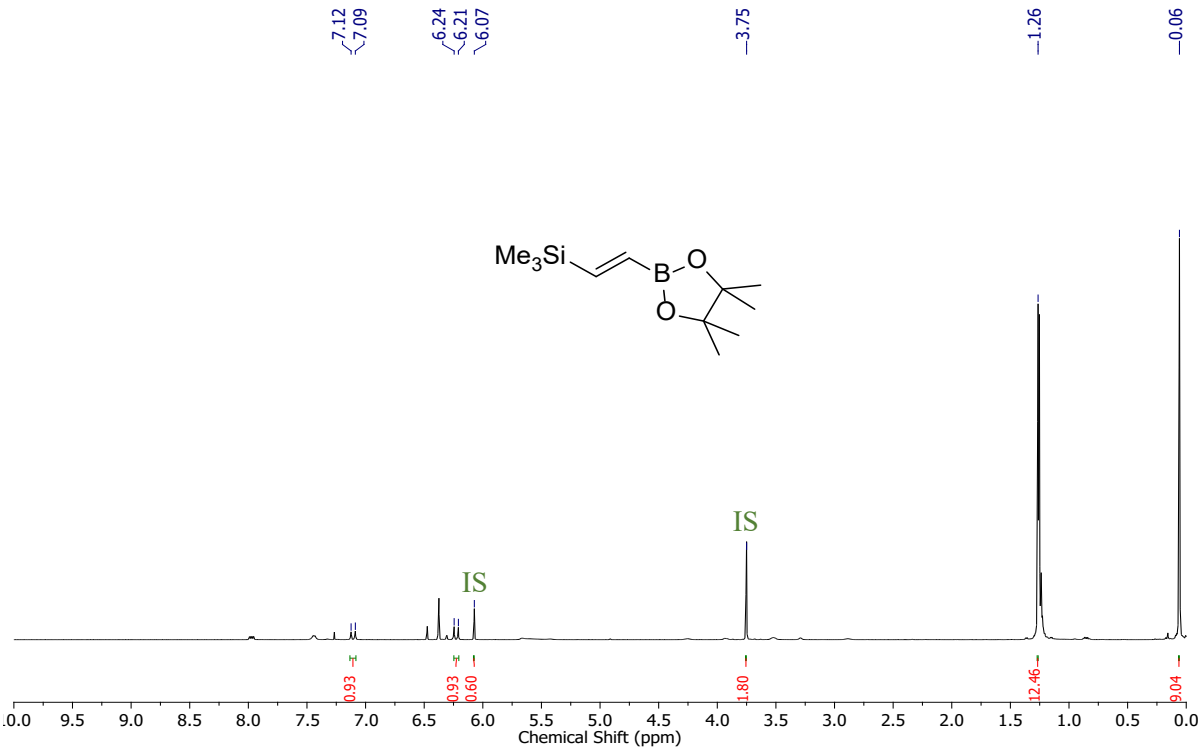


**Figure S141**. $^{1}H$ NMR (400 MHz, $CDCl_3$, 298 K) spectrum of **10l**.

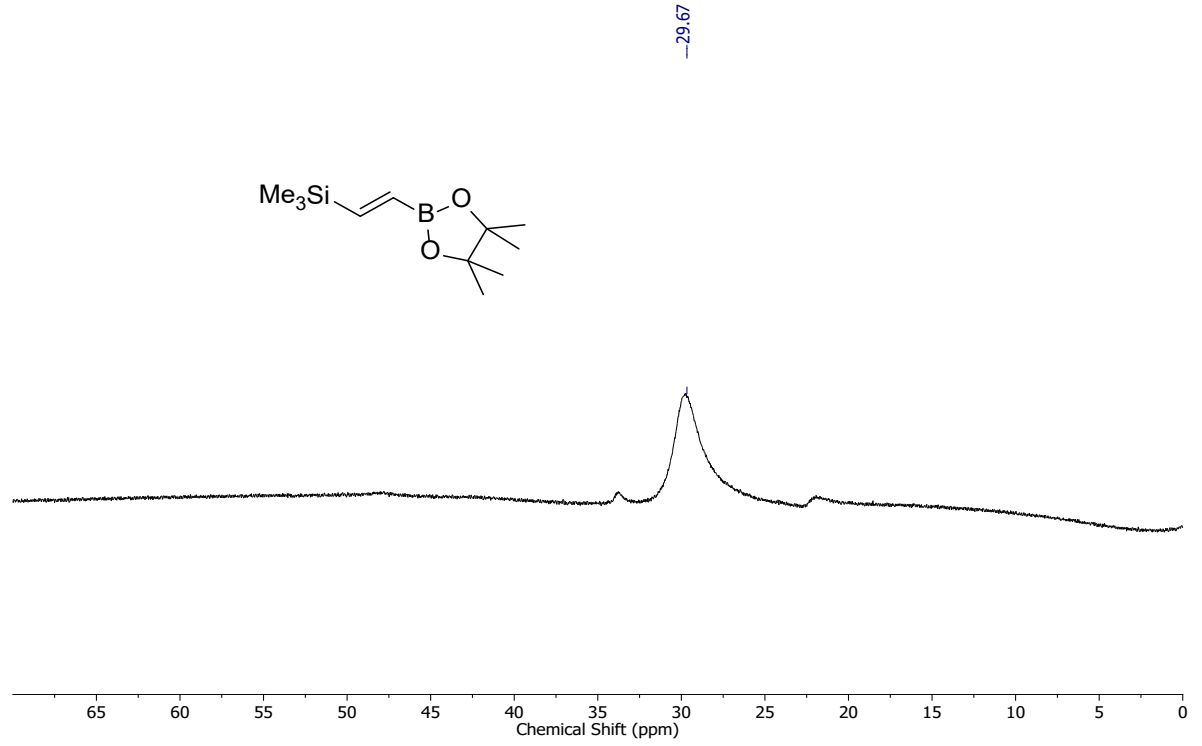


**Figure S142**. $^{11}B\{^{1}H\}$ NMR (128.4 MHz, $CDCl_3$, 298 K) spectrum of **10l**.

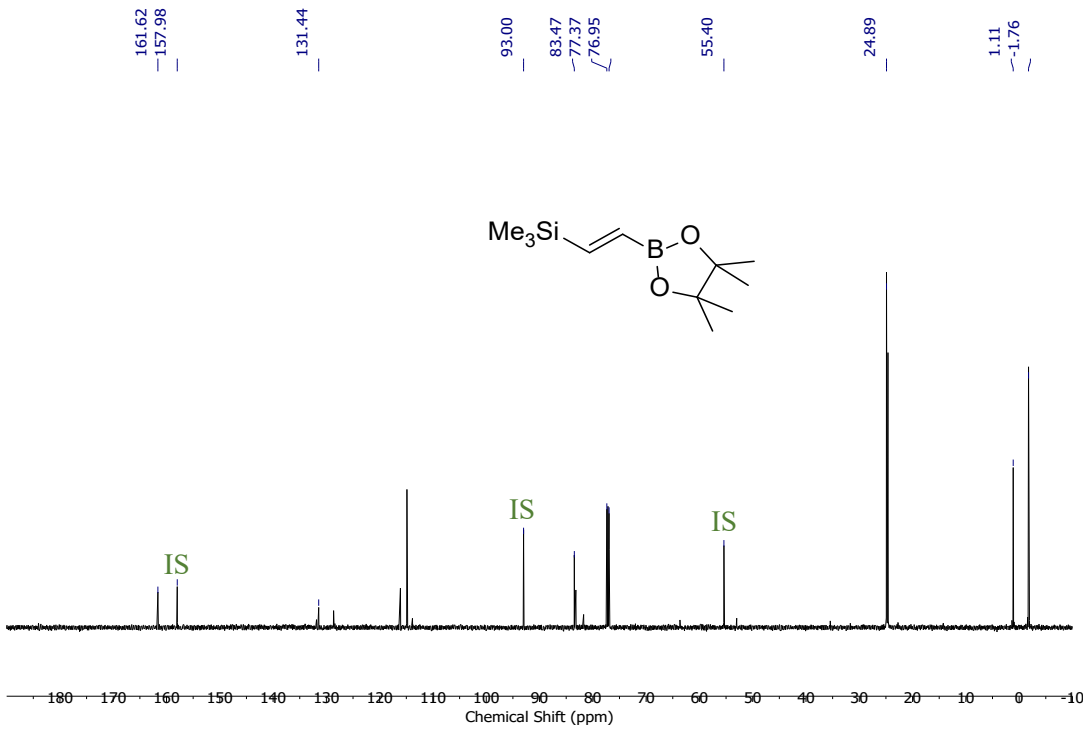


**Figure S143**. $^{13}C\{^{1}H\}$ NMR (100 MHz, $CDCl_3$, 298 K) spectrum of **10l**.

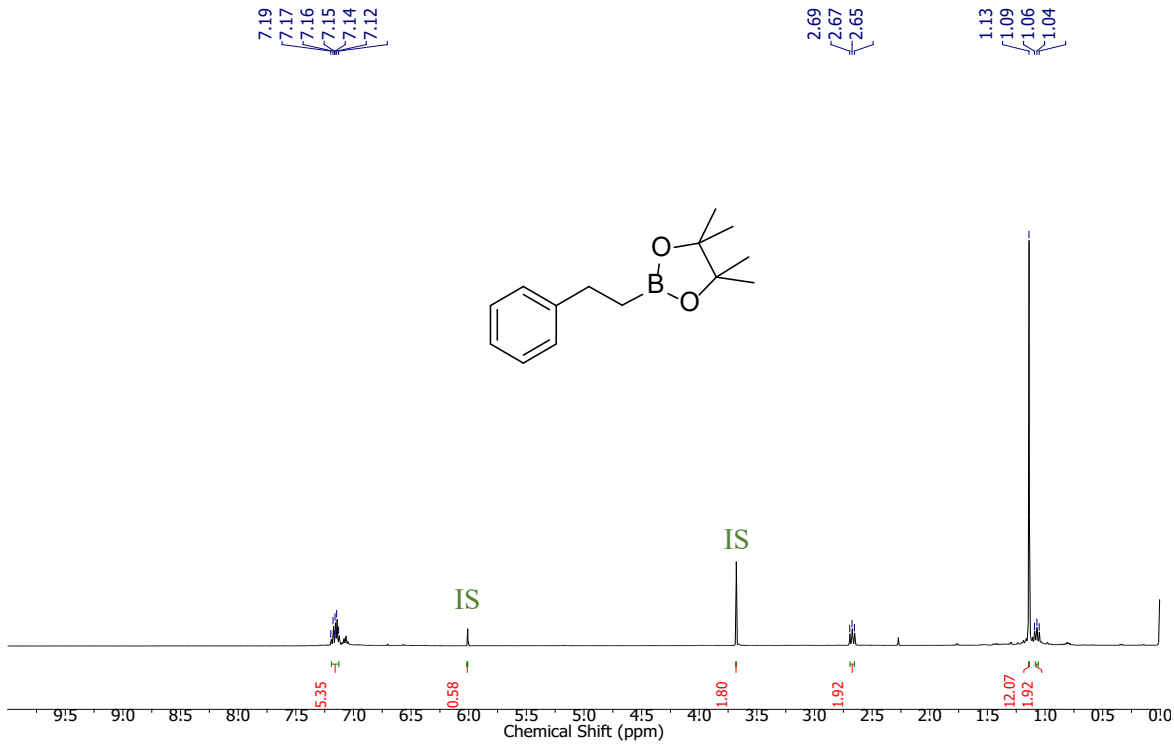


**Figure S144**. $^{1}H$ NMR (400 MHz, $CDCl_3$, 298 K) spectrum of **11a**.

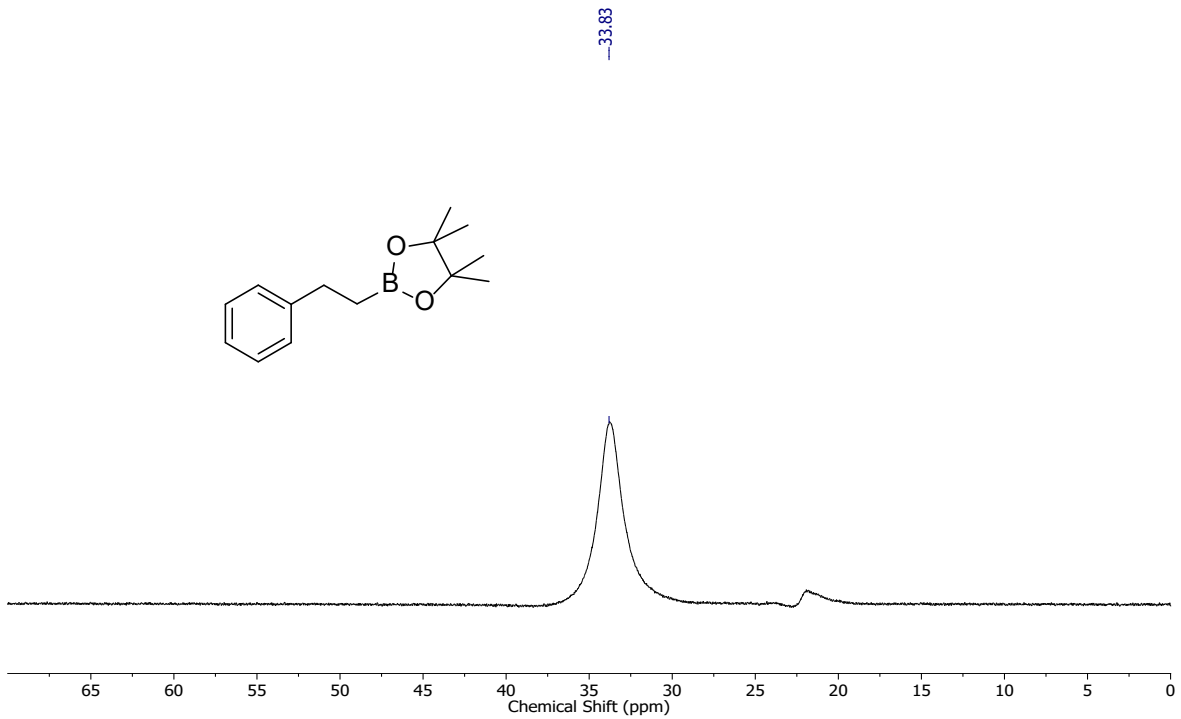


**Figure S145**. $^{11}B\{^{1}H\}$ NMR (128.4 MHz, $CDCl_3$, 298 K) spectrum of **11a**.

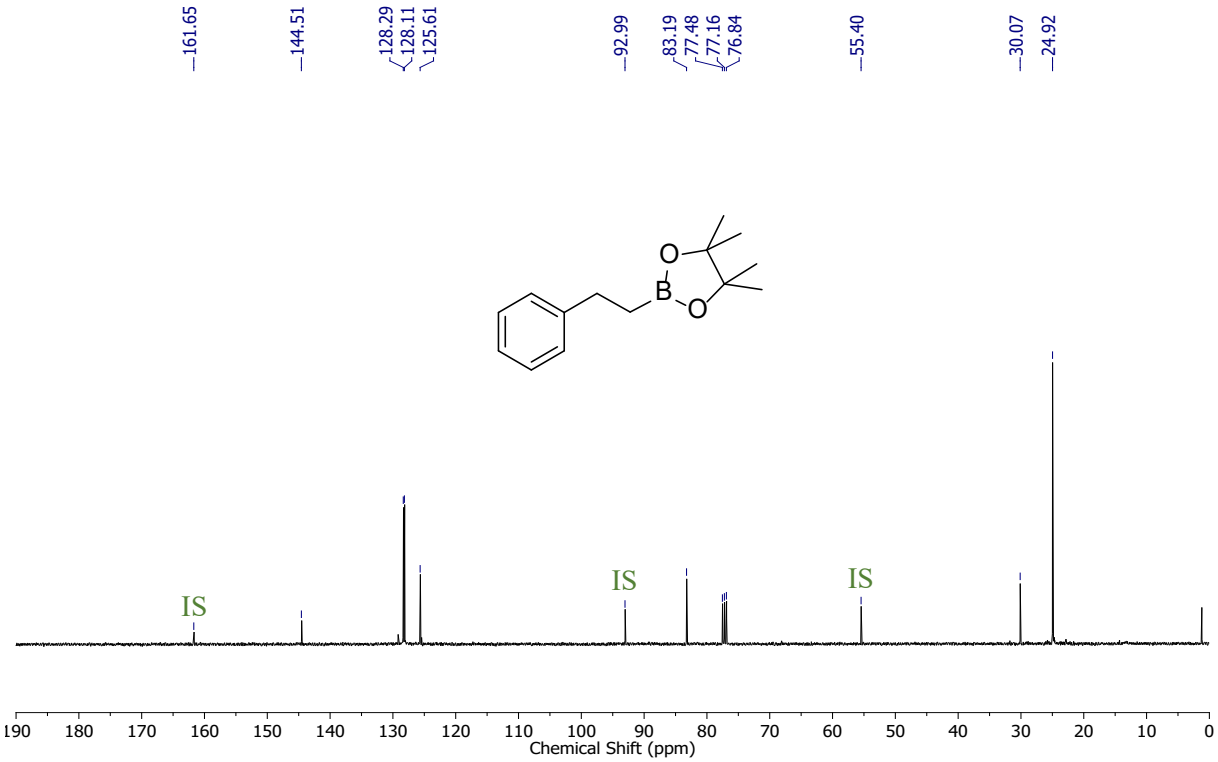


**Figure S146**. $^{13}C\{^{1}H\}$ NMR (100 MHz, $CDCl_3$, 298 K) spectrum of **11a**.

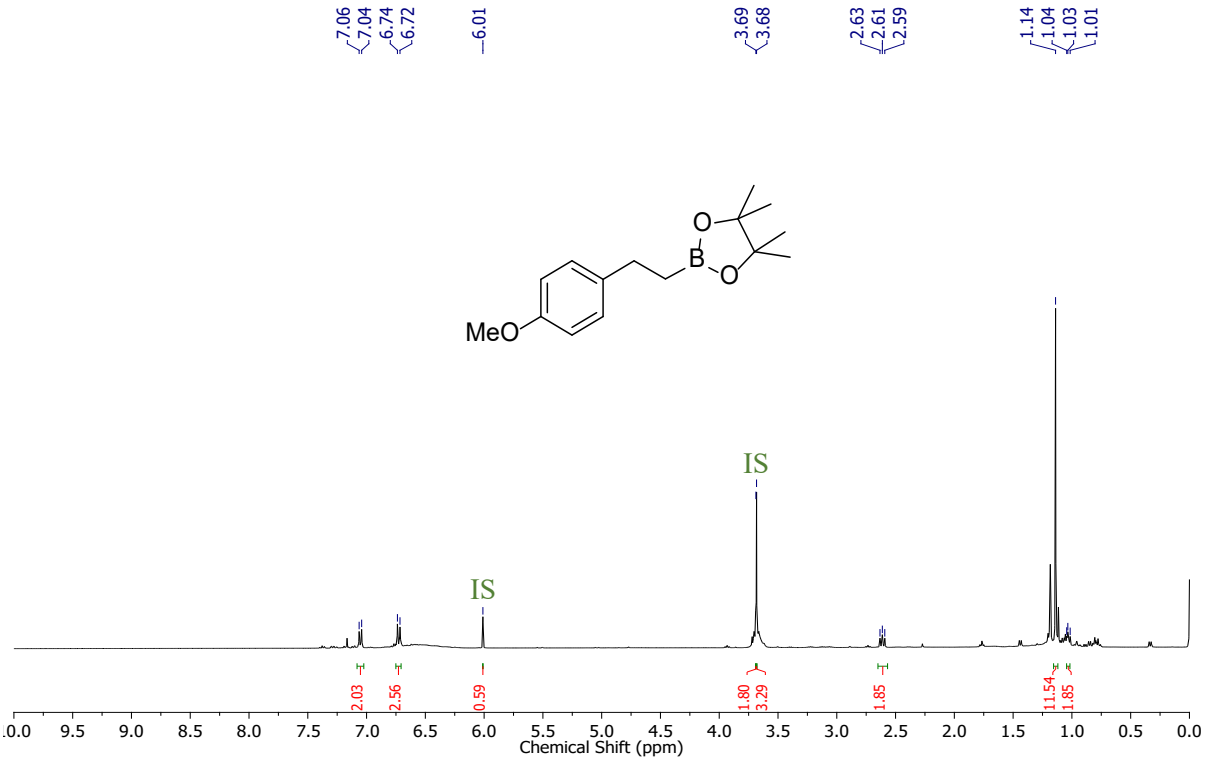


**Figure S147**. $^{1}H$ NMR (400 MHz, $CDCl_3$, 298 K) spectrum of **11b**.

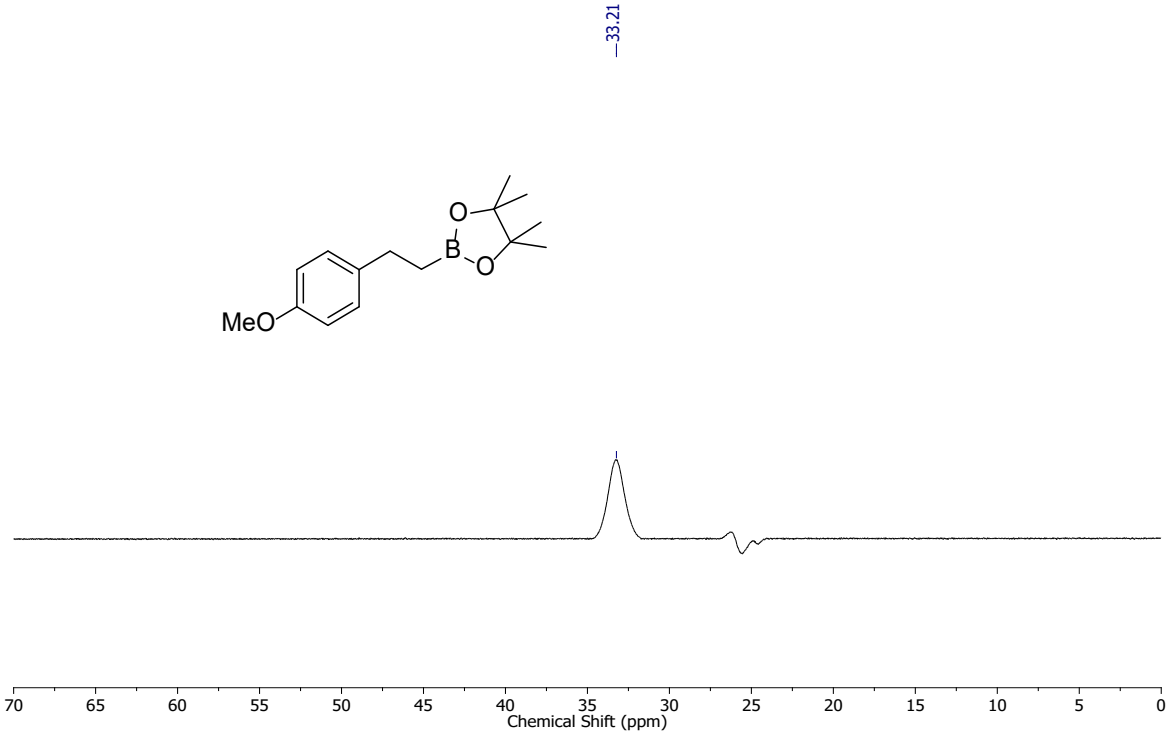


**Figure S148**. $^{11}B\{^{1}H\}$ NMR (128.4 MHz, $CDCl_3$, 298 K) spectrum of **11b**.

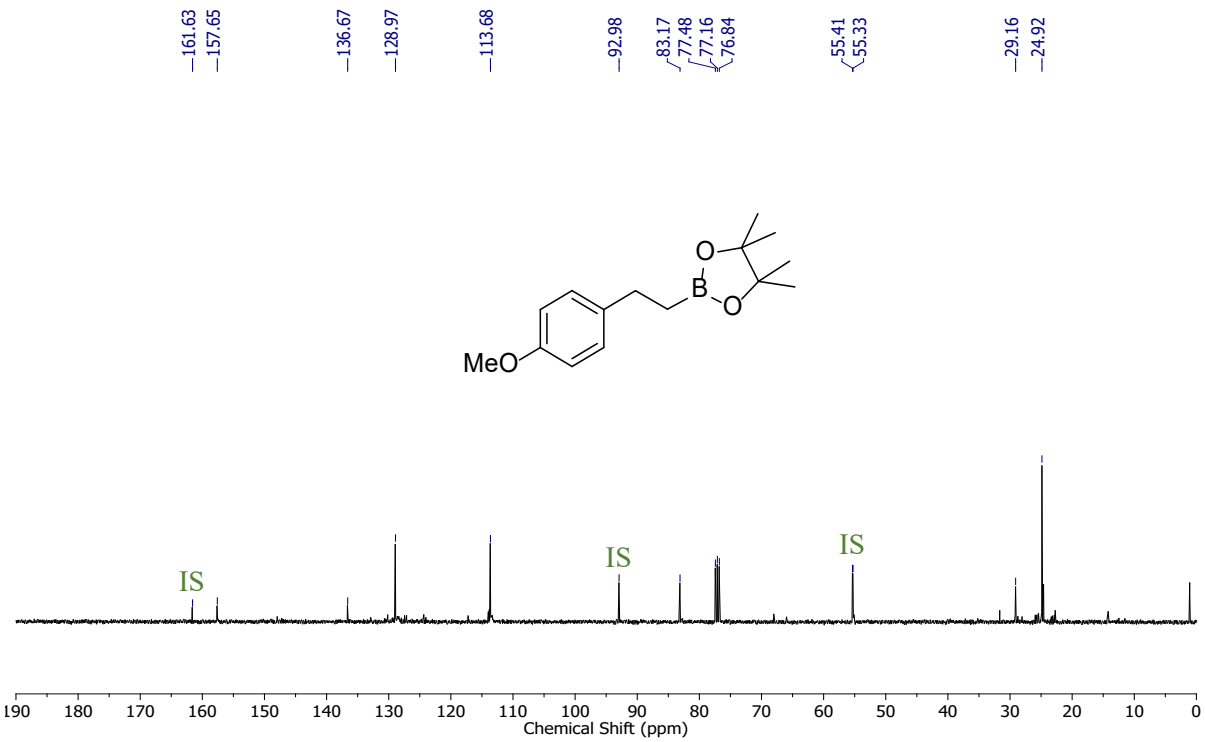


**Figure S149**. $^{13}C\{^{1}H\}$ NMR (100 MHz, $CDCl_3$, 298 K) spectrum of **11b**.

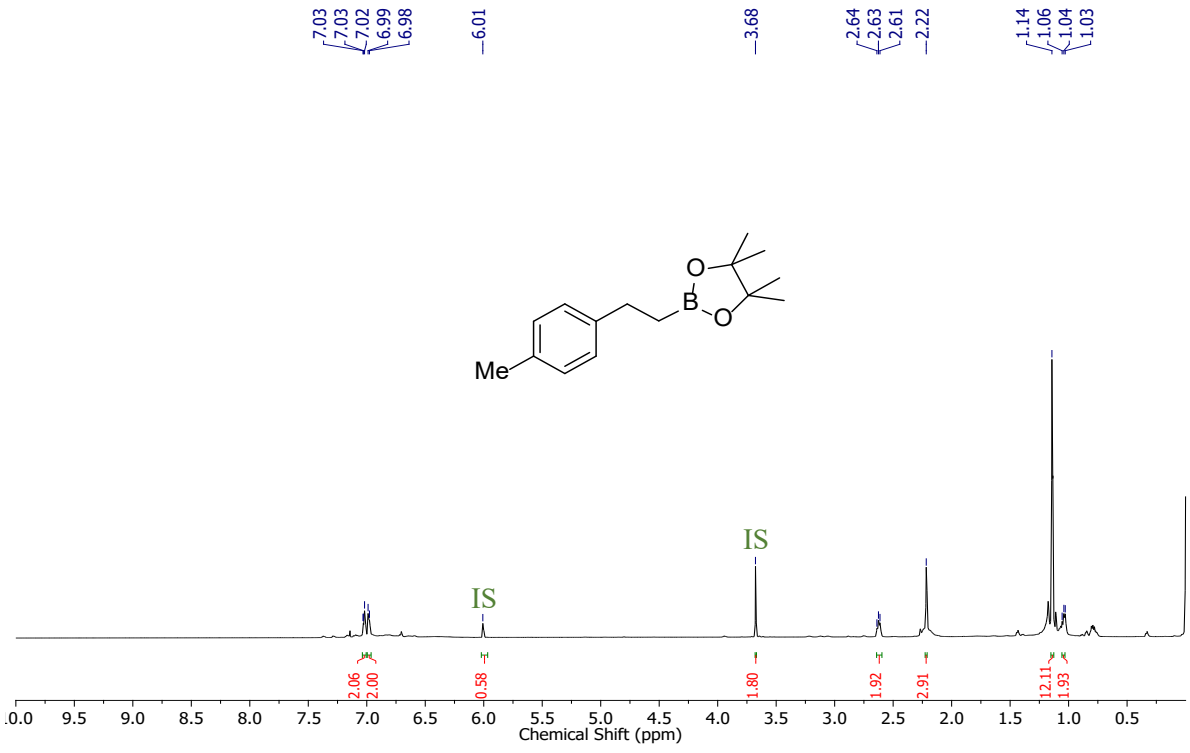


**Figure S150**. $^{1}H$ NMR (400 MHz, $CDCl_3$, 298 K) spectrum of **11c**.

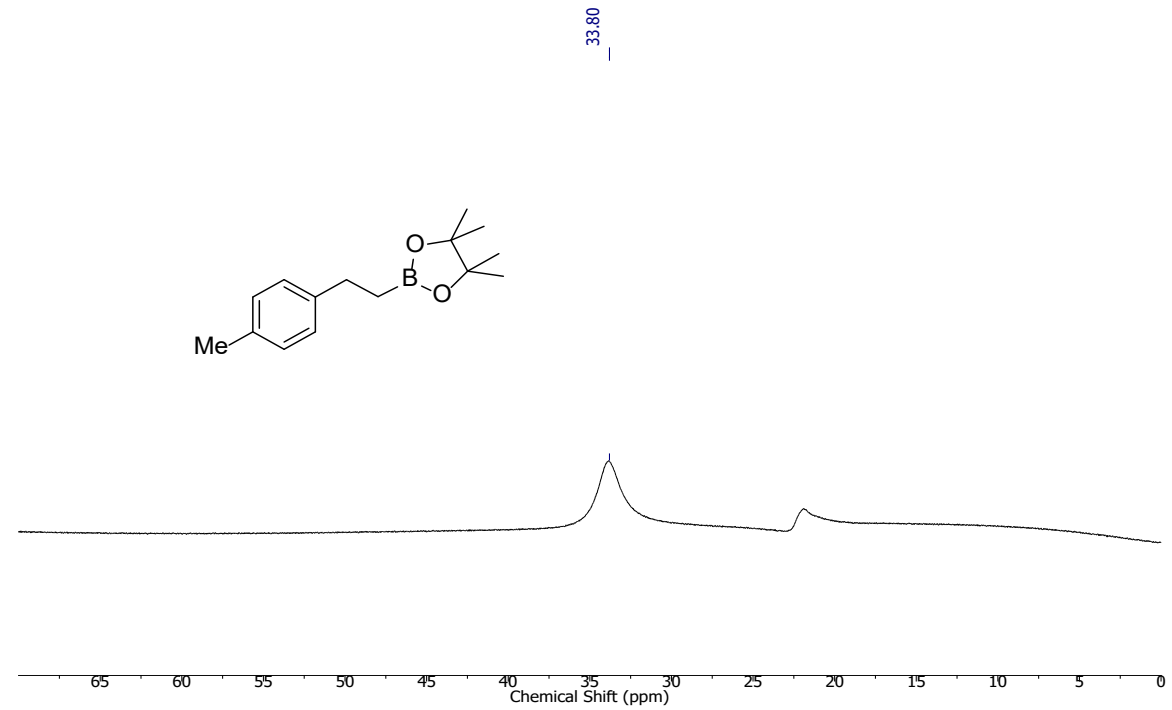


**Figure S151**. $^{11}B\{^{1}H\}$ NMR (128.4 MHz, $CDCl_3$, 298 K) spectrum of **11c**.

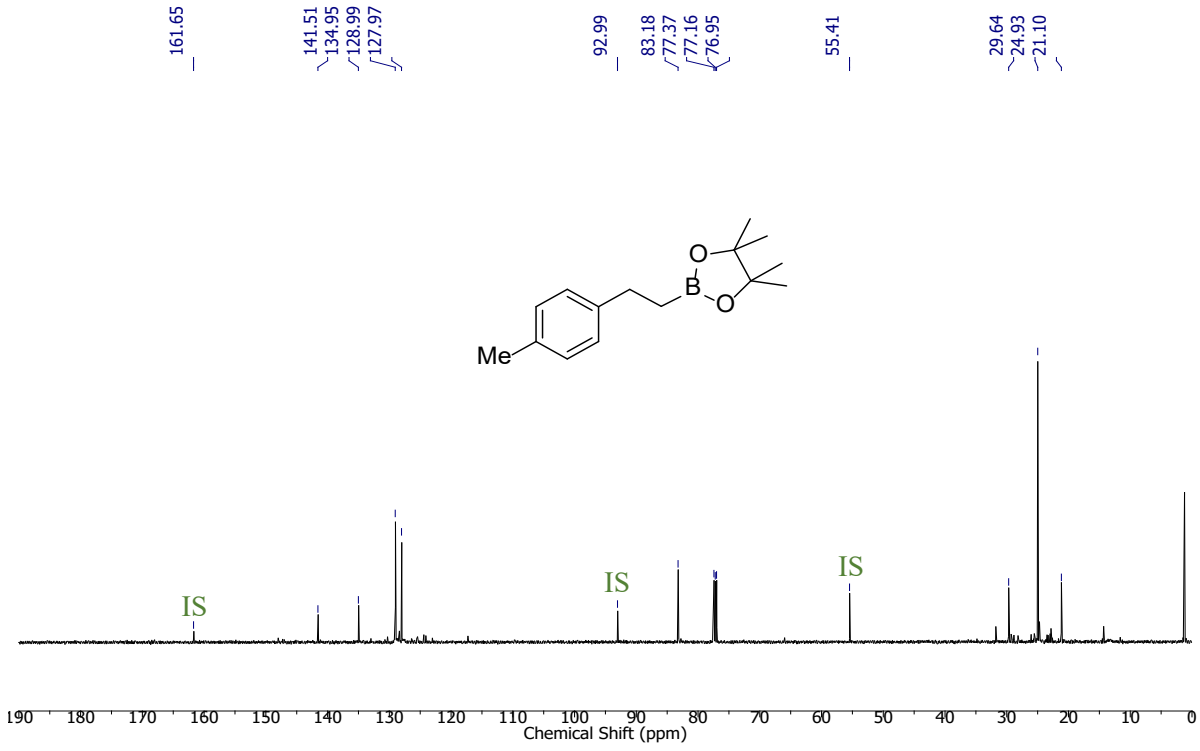


**Figure S152**. $^{13}C\{^{1}H\}$ NMR (100 MHz, $CDCl_3$, 298 K) spectrum of **11c**.

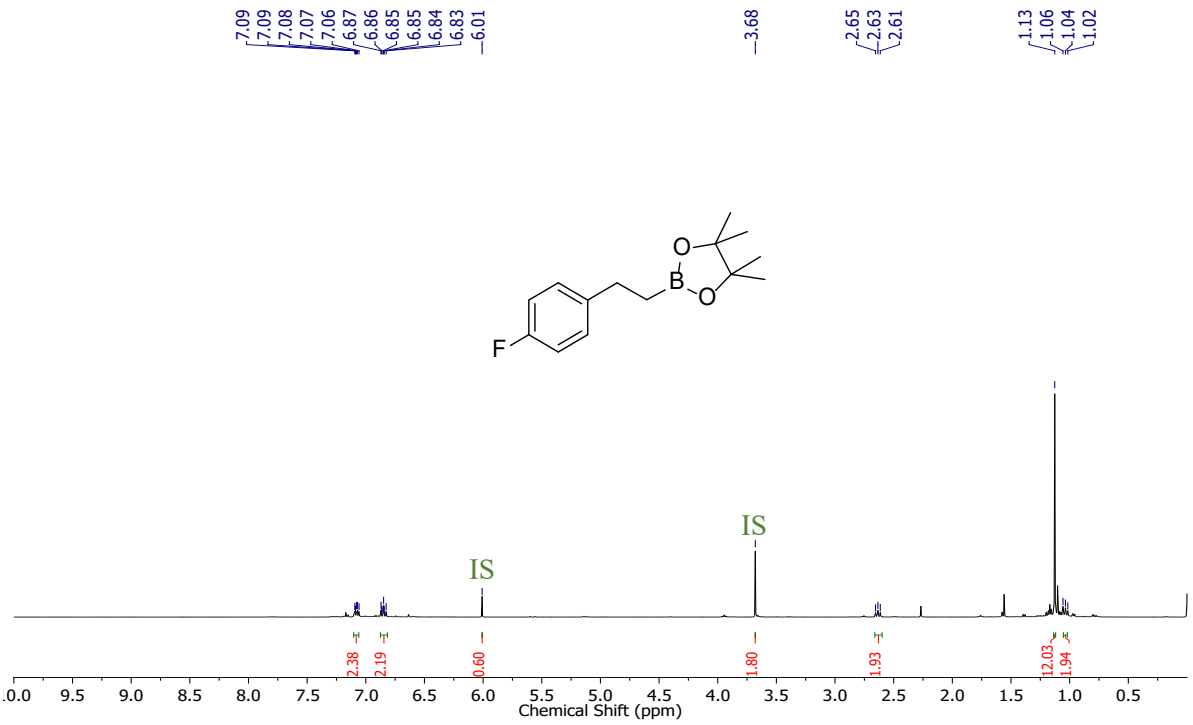


**Figure S153**. $^{1}H$ NMR (400 MHz, $CDCl_3$, 298 K) spectrum of **11d**.

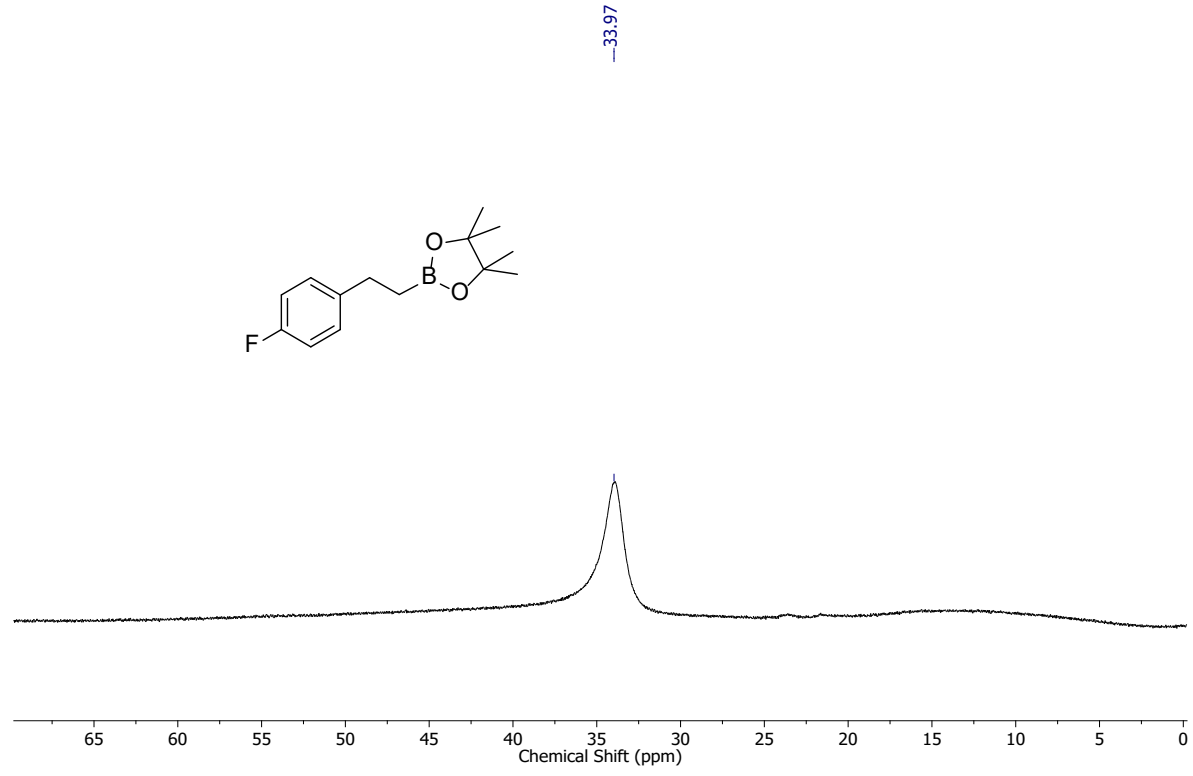


**Figure S154**. $^{11}B\{^{1}H\}$ NMR (128.4 MHz, $CDCl_3$, 298 K) spectrum of **11d**.

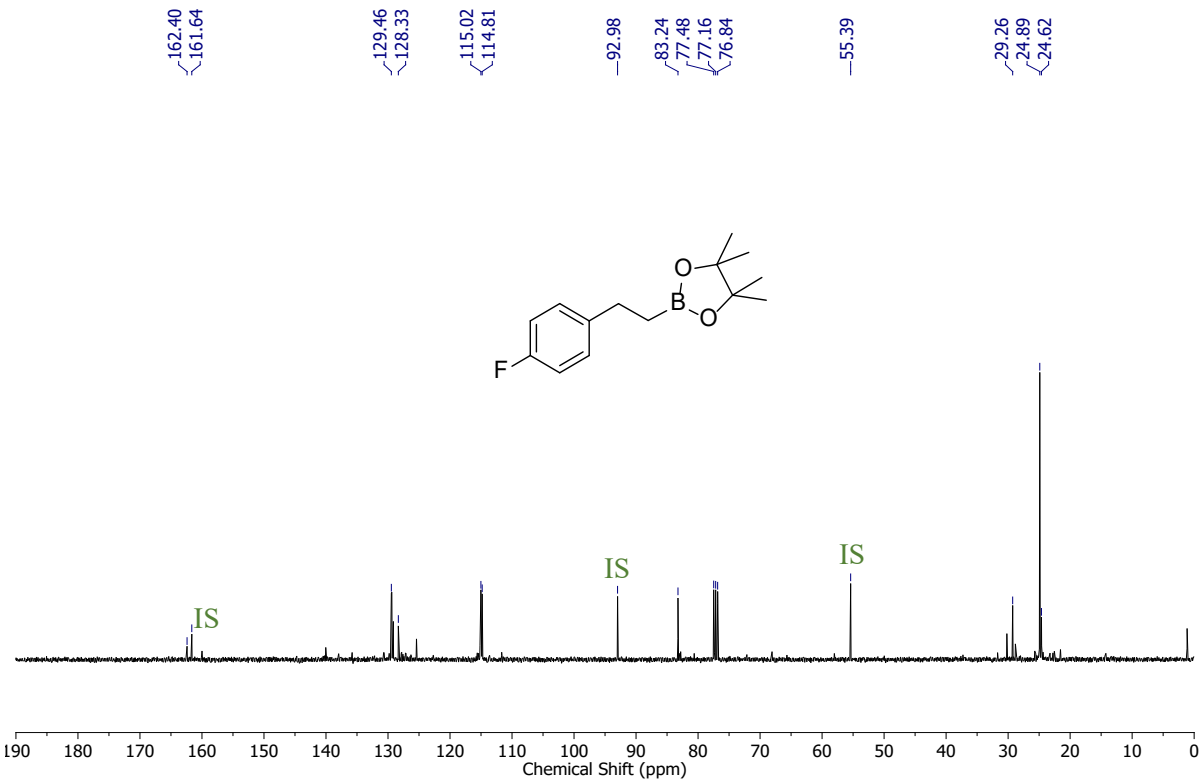


**Figure S155**. $^{13}C\{^{1}H\}$ NMR (100 MHz, $CDCl_3$, 298 K) spectrum of **11d**.

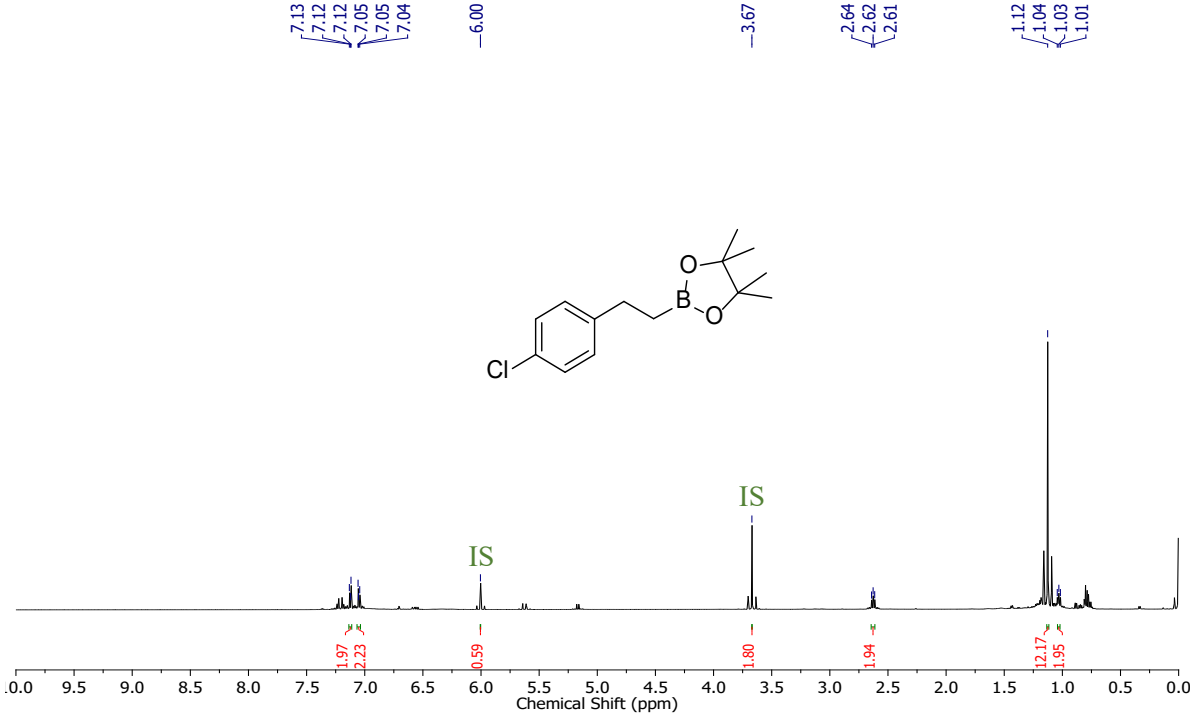


**Figure S156**. $^{1}H$ NMR (400 MHz, $CDCl_3$, 298 K) spectrum of **11e**.

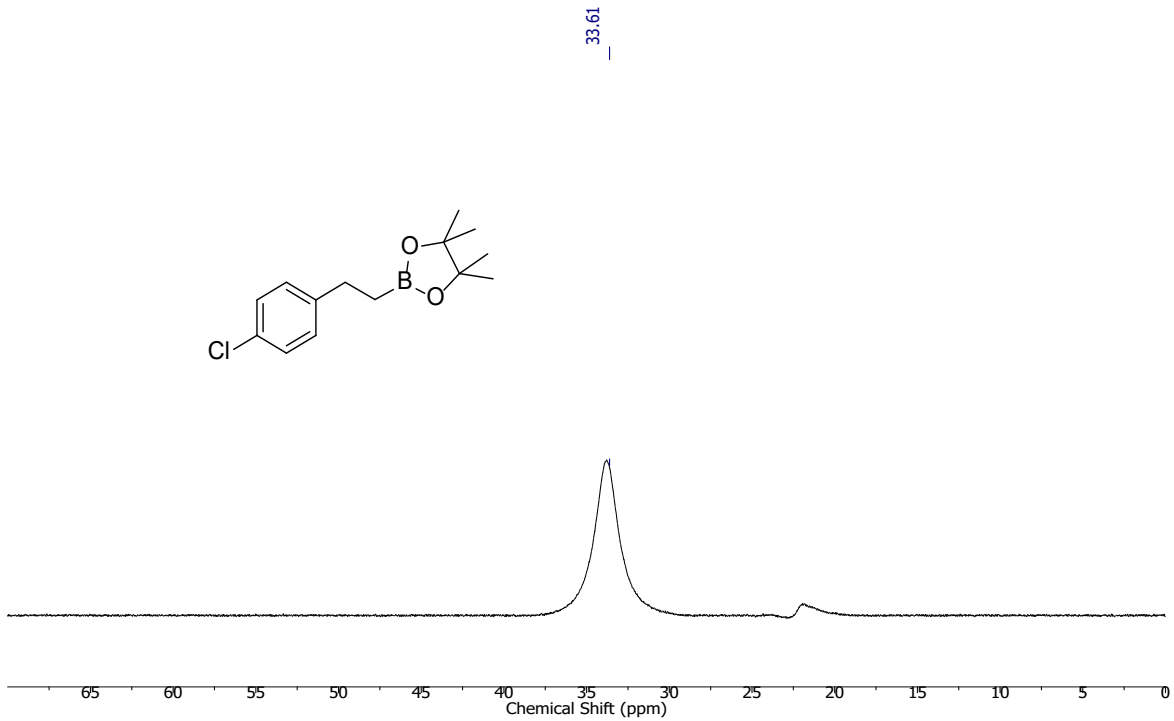


**Figure S157**. $^{11}B\{^{1}H\}$ NMR (128.4 MHz, $CDCl_3$, 298 K) spectrum of **11e**.

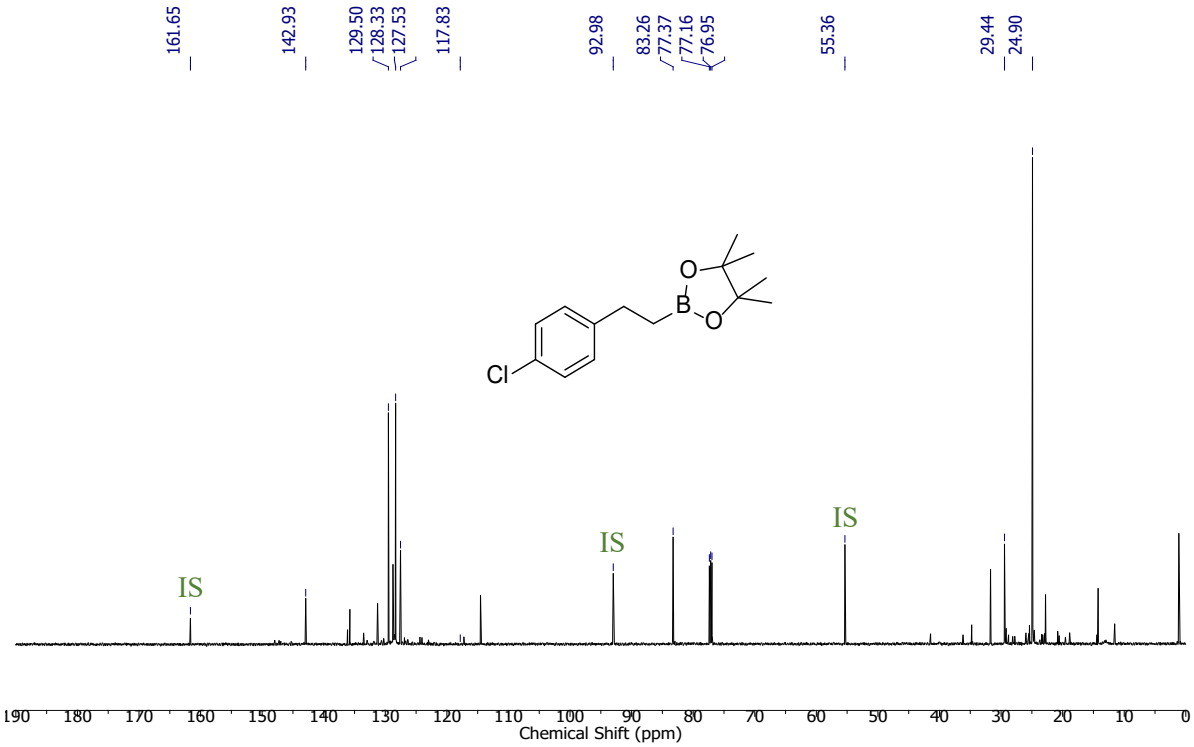


**Figure S158**. $^{13}C\{^{1}H\}$ NMR (100 MHz, $CDCl_3$, 298 K) spectrum of **11e**.

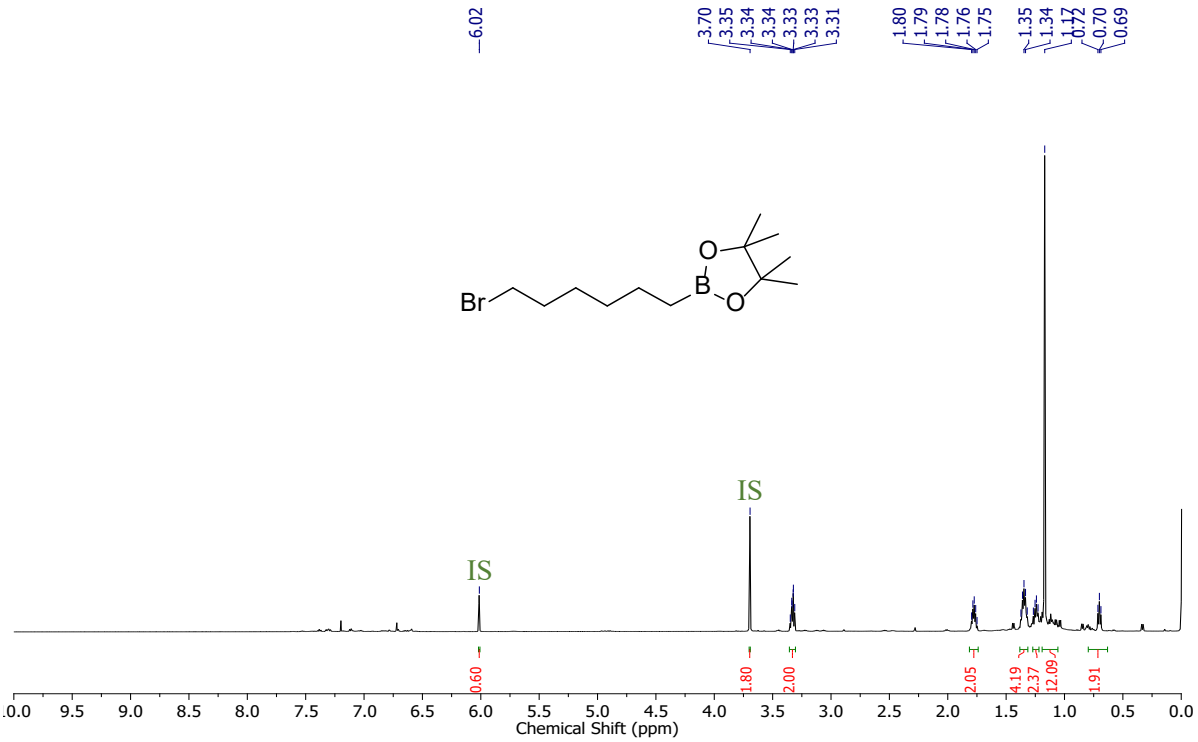


**Figure S159**. $^{1}H$ NMR (400 MHz, $CDCl_3$, 298 K) spectrum of **11f**.

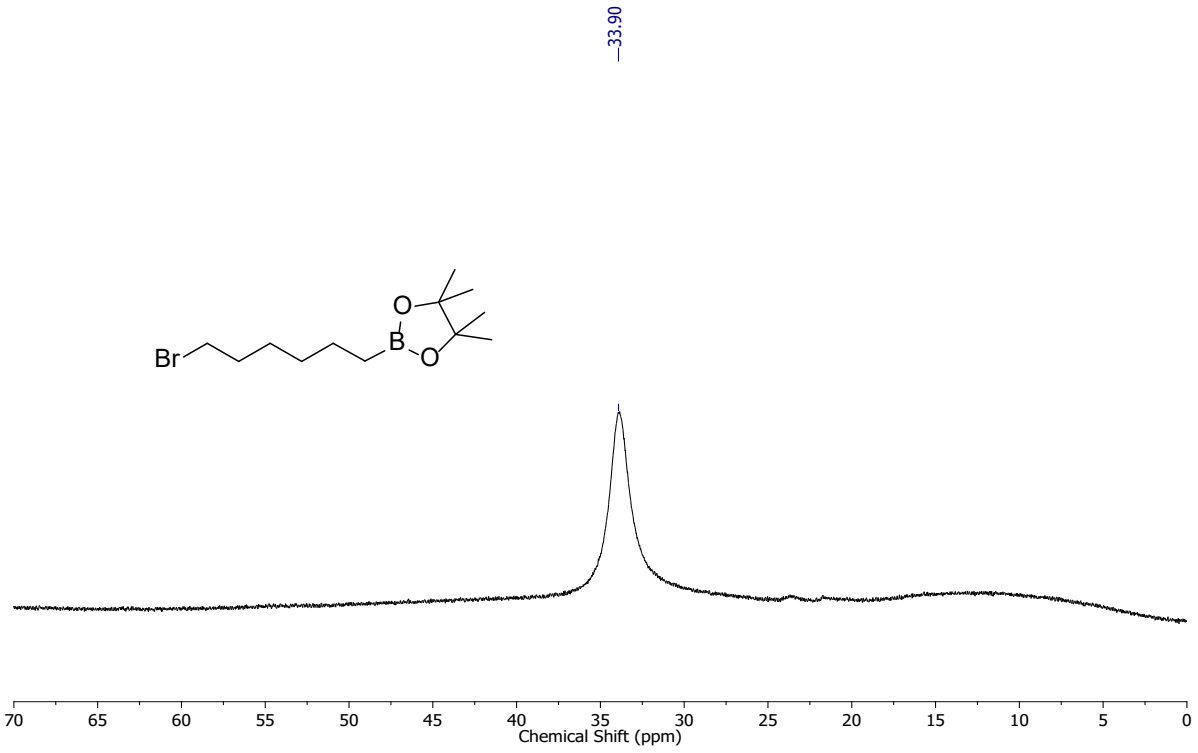


**Figure S160**. $^{11}B\{^{1}H\}$ NMR (128.4 MHz, $CDCl_3$, 298 K) spectrum of **11f**.

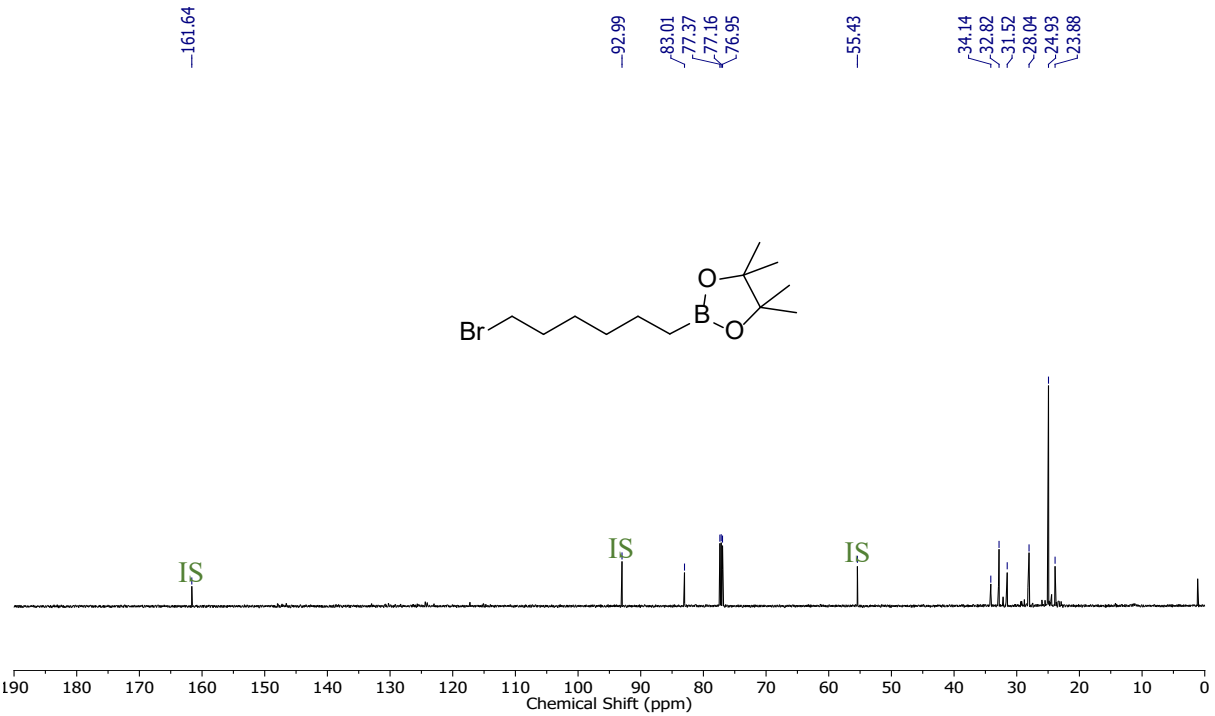


**Figure S161**. $^{13}C\{^{1}H\}$ NMR (100 MHz, $CDCl_3$, 298 K) spectrum of **11f**.

## 9. Stoichiometric reaction between complex 5b and pinacolborane

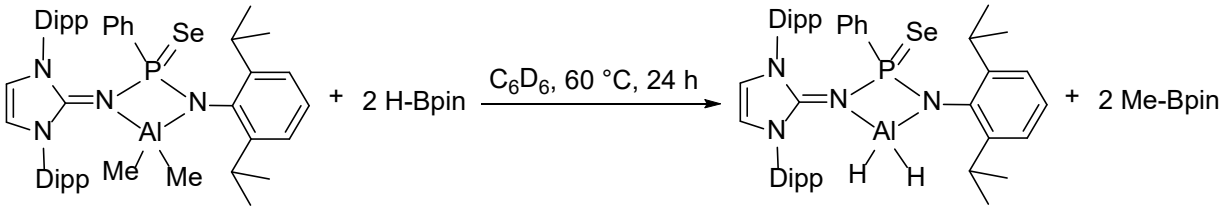


Dipp = 2,6-diisopropylphenyl

**5b**

In an NMR tube, a $C_6D_6$ solution of complex **5b** (20 mg, 0.024 mmol) was treated with two equiv. of pinacolborane (HBpin, 6 mg, 0.048 mmol) and then heated to 60 °C temperature in an oil bath and the reaction was then monitored over time. In $^{11}B$ NMR spectrum initially there was only one signal at $\delta_B$ 28.5 ppm which is accounting for HBpin. Later slowly a new additional peak appears at $\delta_B$ 34.0 ppm with time due to the production of MeBpin.

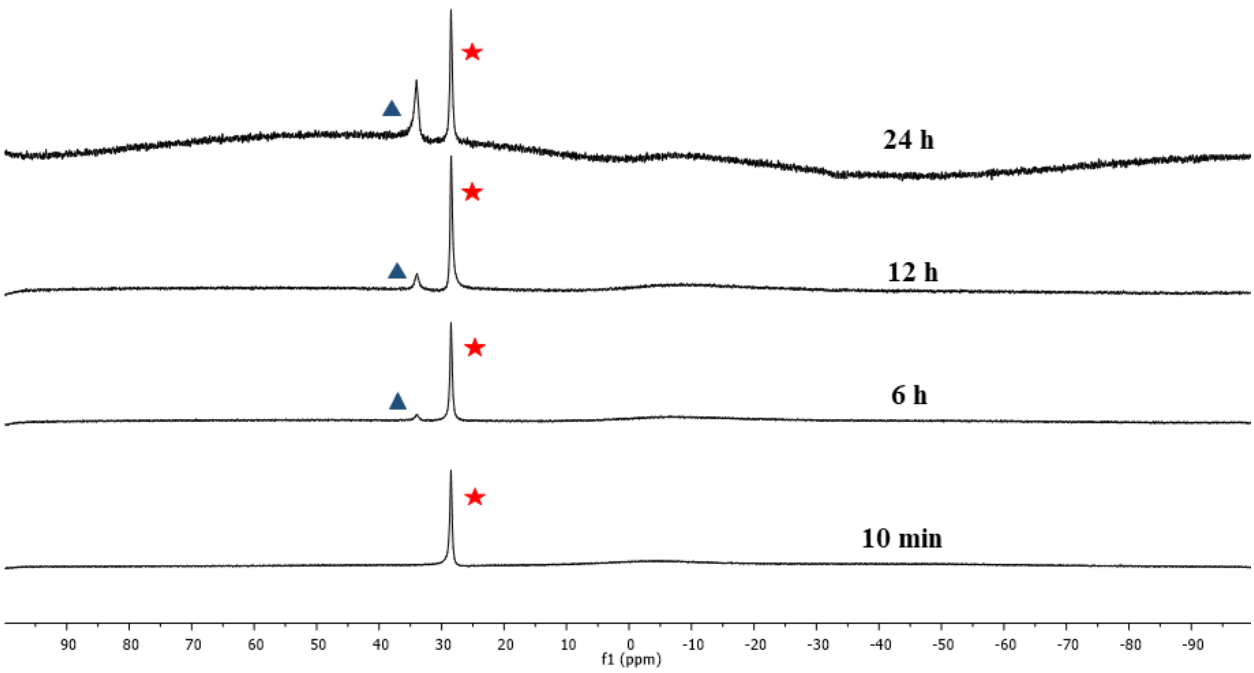


**Figure S162**. In situ observation of methylpinacolborane (MeBpin) formation from stoichiometric reaction of **5b** with pinacolborane (HBpin, 2 equiv.) were correlated by monitoring of the reaction progress using $^{11}B\{^{1}H\}$ NMR (96.3 MHz, $C_6D_6$, 298 K) spectroscopy at different time intervals [★HBpin, ▲MeBpin].

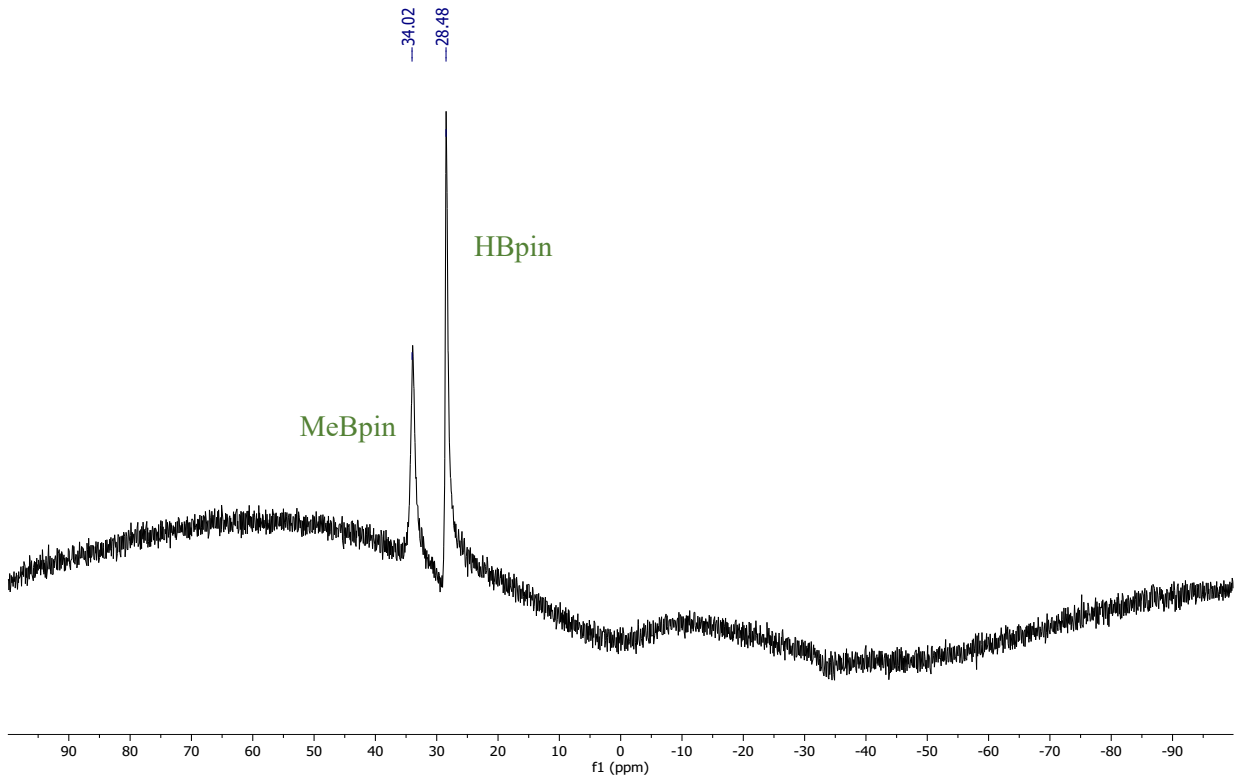


**Figure S163**. $^{11}B\{^{1}H\}$ NMR (96.3 MHz, $C_6D_6$, 298 K) spectrum of stoichiometric reaction between complex **5b** and HBpin (1:2) after 24 h (reaction progress at 60 °C).

**10. Selective hydroboration of carbonyl group over nitrile functionality in presence of one equivalent HBpin:**

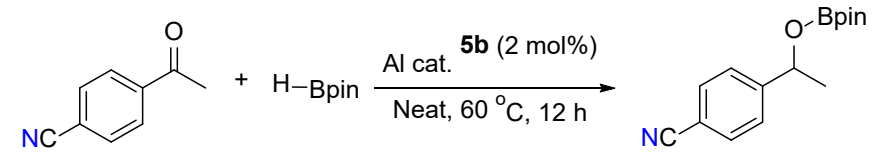


4-acetylbenzonitrile

Inside the glove box, the Al catalyst **5b** (2 mol %) and HBpin (0.5 mmol, 1 equiv) was added to a Schlenk tube followed by the addition of 4-acetylbenzonitrile (0.5 mmol, 1 equiv). The Schlenk tube was taken out from the glove box and the reaction mixture was stirred at 60 °C for 12 hours in neat condition. Finally, volatiles of the mixture were removed under the reduced pressure to obtain the hydroboration product. The progress of the reaction was monitored by $^{1}H$ NMR with the help of 1,3,5-trimethoxy benzene as the internal standard in $CDCl_3$. A quartet resonance at $\delta$ = 5.26-5.29 ppm indicates for the hydroboration of carbonyl group. In $^{11}B\{^{1}H\}$ NMR spectrum, only

one peak was observed at 22.1 ppm, which also confirmed the hydroboration of carbonyl group over nitrile functionality.

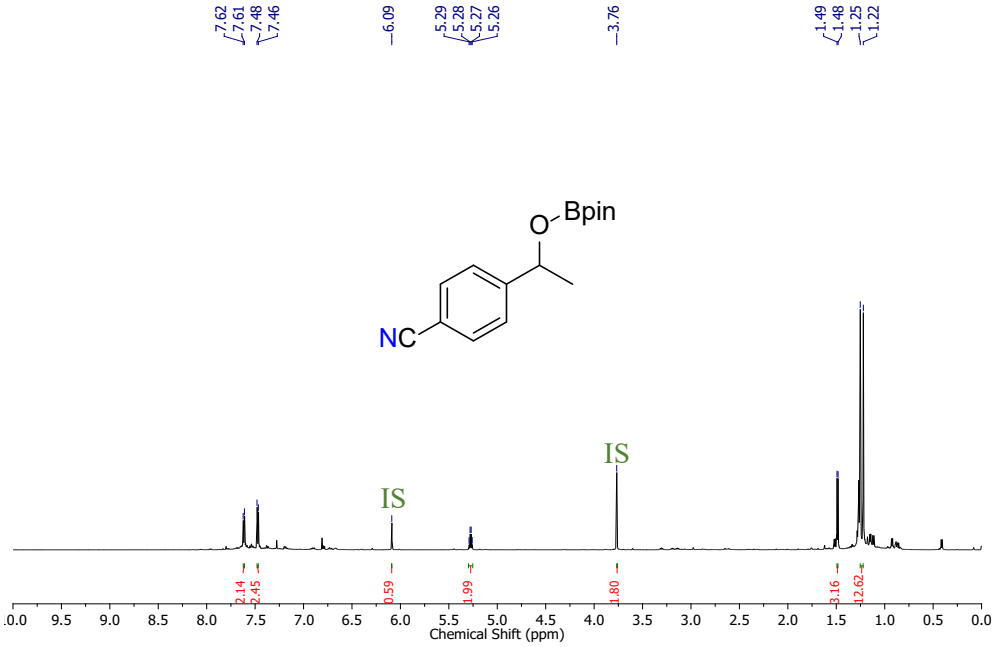


**Figure S164**. $^{1}$H NMR (600 MHz, $C_6D_6$, 298 K) spectrum of the reaction of 4-acetylbenzonitrile with one equiv. HBpin in presence of cat. **5b** (2 mol%) [reaction condition: neat, 60 °C, 12 h].

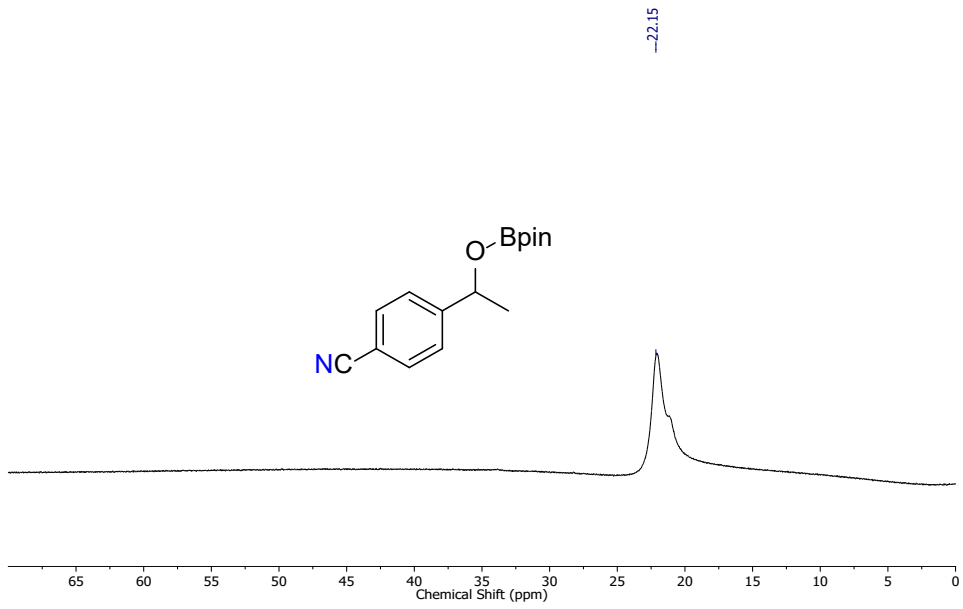

**Figure S165**. $^{11}B\{^{1}H\}$ NMR (193 MHz, $C_6D_6$, 298 K) spectrum of the reaction of 4-acetylbenzonitrile with one equiv. HBpin in presence of cat. **5b** (2 mol%) [reaction condition: neat, 60 °C, 12 h].

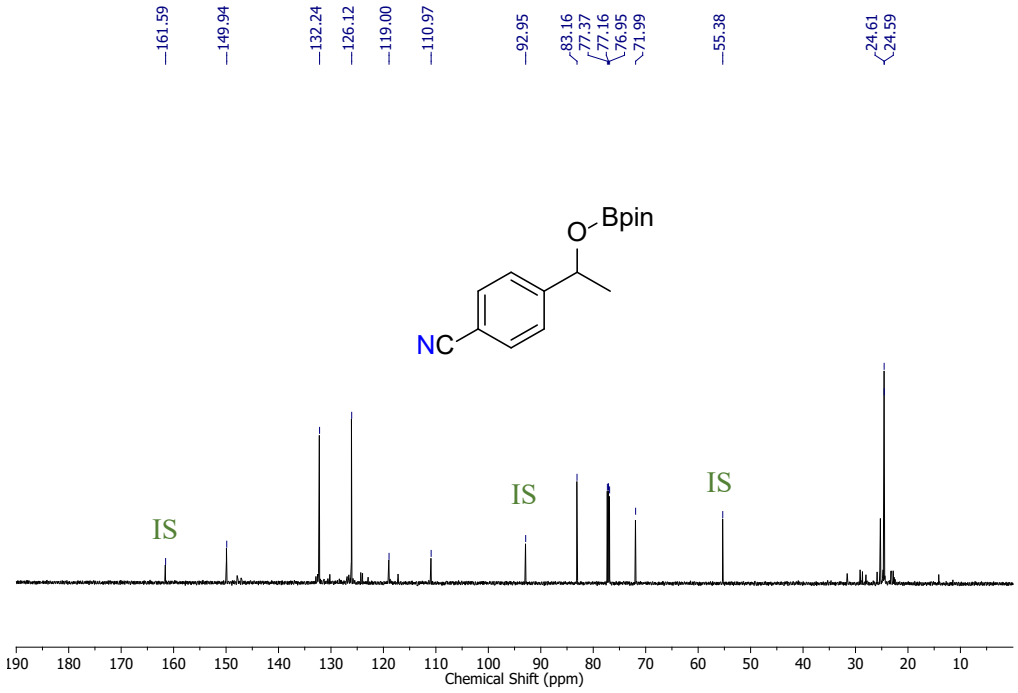


**Figure S166**. $^{13}C\{^{1}H\}$ NMR (150 MHz, $C_6D_6$, 298 K) spectrum of the reaction of 4-acetylbenzonitrile with one equiv. HBpin in presence of cat. **5b** (2 mol%) [reaction condition: neat, 60 °C, 12 h].

## 11. Competitive hydroboration of alkyne and nitrile group in presence of 2 equivalents of HBpin:

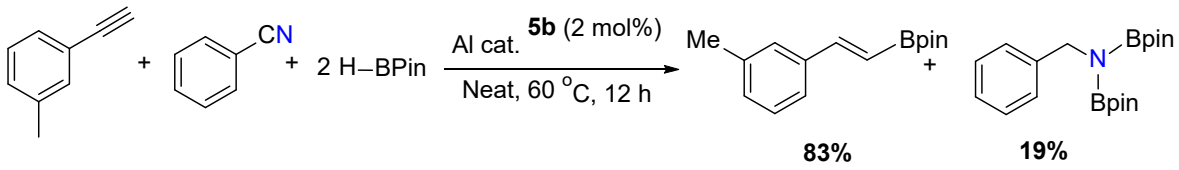


1-ethynyl-3-methylbenzene (0.25 mmol, 1 equiv.), benzonitrile (0.25 mmol, 1 equiv.), pinacolborane (0.5 mmol, 2 equiv.) and Al catalyst **5b** (2 mol %) were charged in a Schlenk tube inside the glove box. The reaction mixture was stirred for 12 hours at 60 °C in neat conditions. Upon completion of the reaction, the progress of the reaction was monitored by $^{1}H$ NMR with the help of 1,3,5-trimethoxy benzene as the internal standard in CDCl3. A sharp singlet resonance at

δ = 4.15 ppm indicates for the formation of hydroboration product from benzonitrile (19% product formation), whereas doublet resonance at δ = 6.07 ppm ($^1J_{HH}$ = 18 Hz) indicates for the formation of hydroboration product from 1-ethynyl-3-methylbenzene (83% product formation).

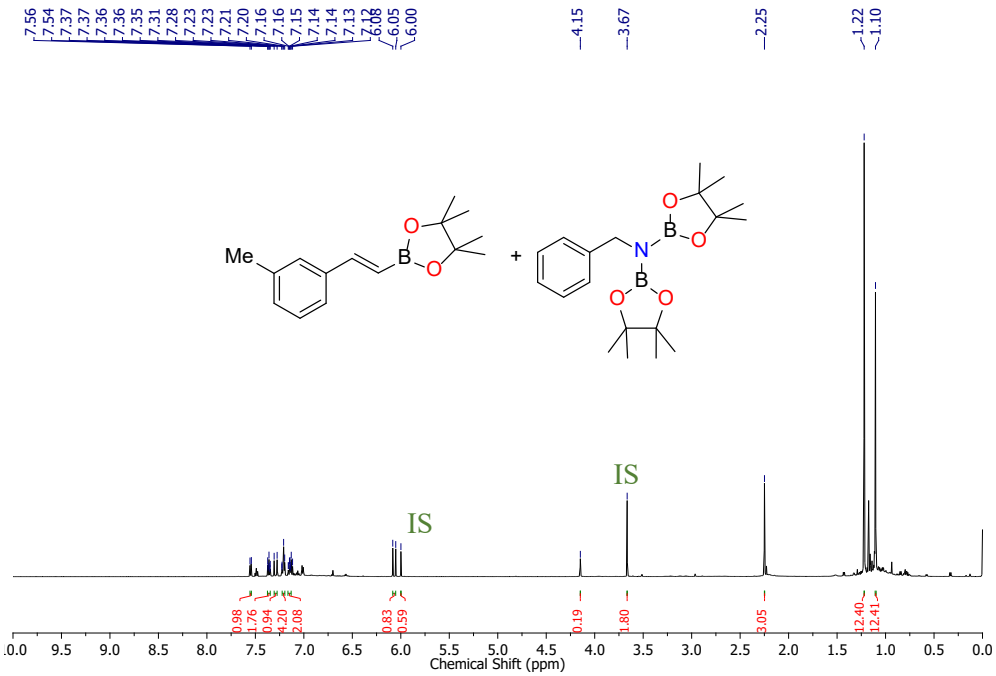


**Figure S167**. $^1$H NMR (600 MHz, $C_6D_6$, 298 K) spectrum of the hydroboration reaction of 1-ethynyl-3-methylbenzene and benzonitrile in presence of cat. **5b** (2 mol%) and 2 equiv. HBpin [reaction condition: neat, 60 °C, 12 h].

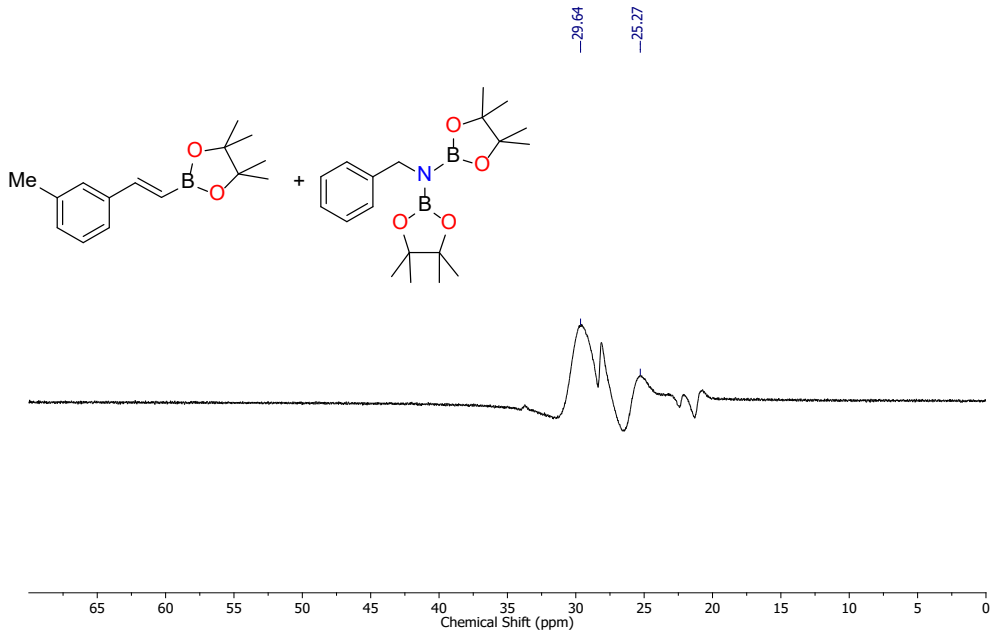


**Figure S168**. $^{11}B\{^{1}H\}$ NMR (193 MHz, $C_6D_6$, 298 K) spectrum of the hydroboration reaction of 1-ethynyl-3-methylbenzene and benzonitrile in presence of cat. **5b** (2 mol%) and 2 equiv. HBpin [reaction condition: neat, 60 °C, 12 h].

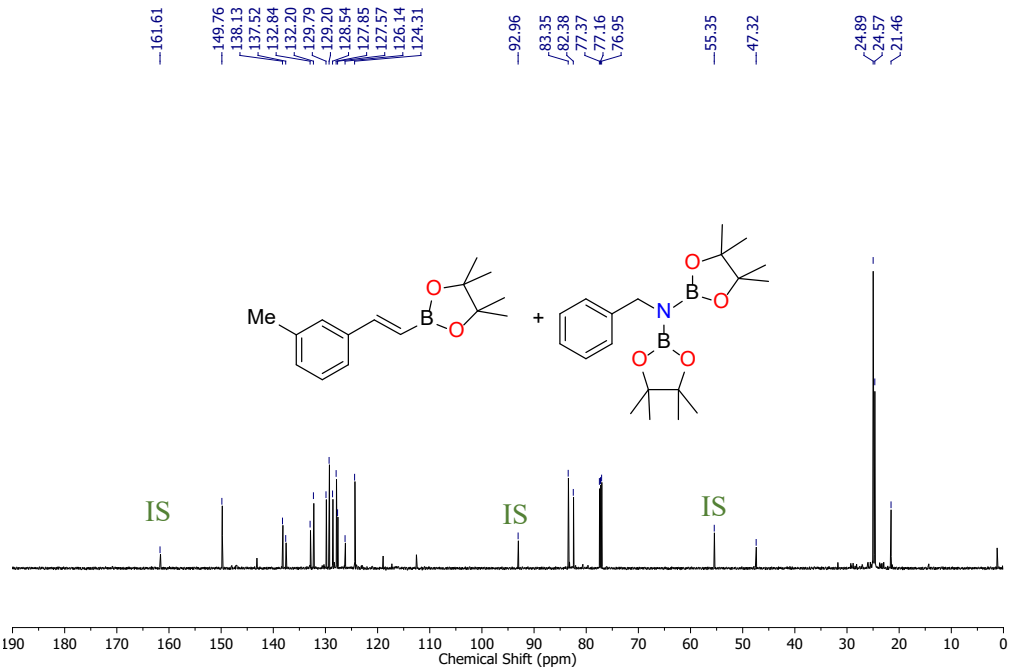

**Figure S169**. $^{13}C\{^{1}H\}$ NMR (150 MHz, $C_6D_6$, 298 K) spectrum of the hydroboration reaction of 1-ethynyl-3-methylbenzene and benzonitrile in presence of cat. **5b** (2 mol%) and 2 equiv. HBpin [reaction condition: neat, 60 °C, 12 h].

**12. Competitive hydroboration of alkyne and alkene group in presence of 1 equivalent of HBpin:**

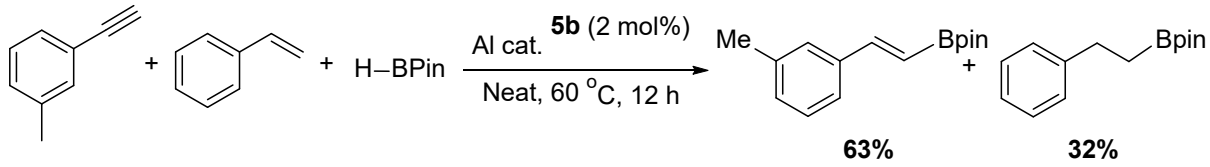


1-ethynyl-3-methylbenzene (0.25 mmol, 1 equiv.), styrene (0.25 mmol, 1 equiv.), pinacolborane (0.25 mmol, 1 equiv.) and Al catalyst **5b** (2 mol %) were charged in a Schlenk tube inside the glove box. The reaction mixture was stirred for 12 hours at 60 °C in neat conditions. Upon completion of the reaction, the progress of the reaction was monitored by $^{1}H$ NMR with the help of 1,3,5-trimethoxy benzene as the internal standard in CDCl3. Doublet resonance at $\delta = 6.07$ ppm ($^{1}J_{HH}$ = 18 Hz) indicates for the formation of hydroboration product from 1-ethynyl-3-methylbenzene (63% product formation), whereas triplet resonance at $\delta = 2.62$ ppm ($^{1}J_{HH}$ = 6 Hz) indicates for the formation of hydroboration product from styrene (32% product formation).

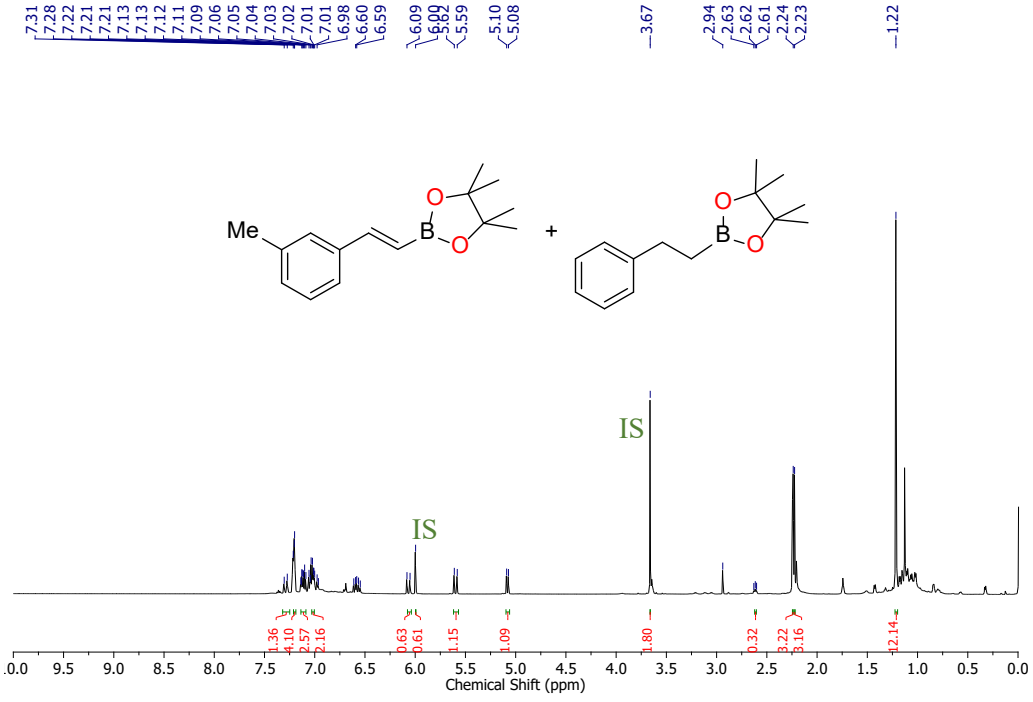

**Figure S170**. $^{1}H$ NMR (600 MHz, $C_6D_6$, 298 K) spectrum of the hydroboration reaction of 1-ethynyl-3-methylbenzene and styrene in presence of cat. **5b** (2 mol%) and 1 equiv. HBpin [reaction condition: neat, 60 °C, 12 h].

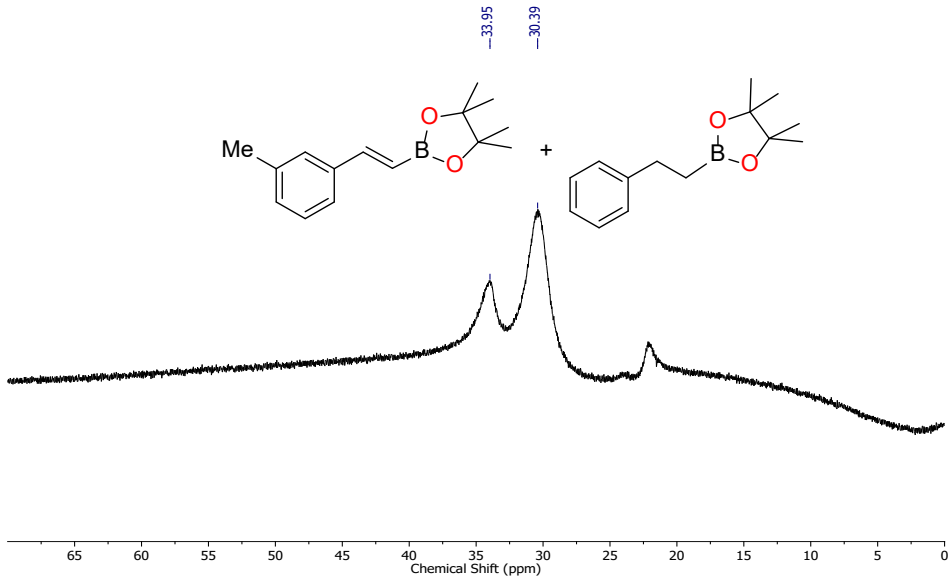


**Figure S171**. $^{11}B\{^{1}H\}$ NMR (193 MHz, $C_6D_6$, 298 K) spectrum of the hydroboration reaction of 1-ethynyl-3-methylbenzene and styrene in presence of cat. **5b** (2 mol%) and 1 equiv. HBpin [reaction condition: neat, 60 °C, 12 h].

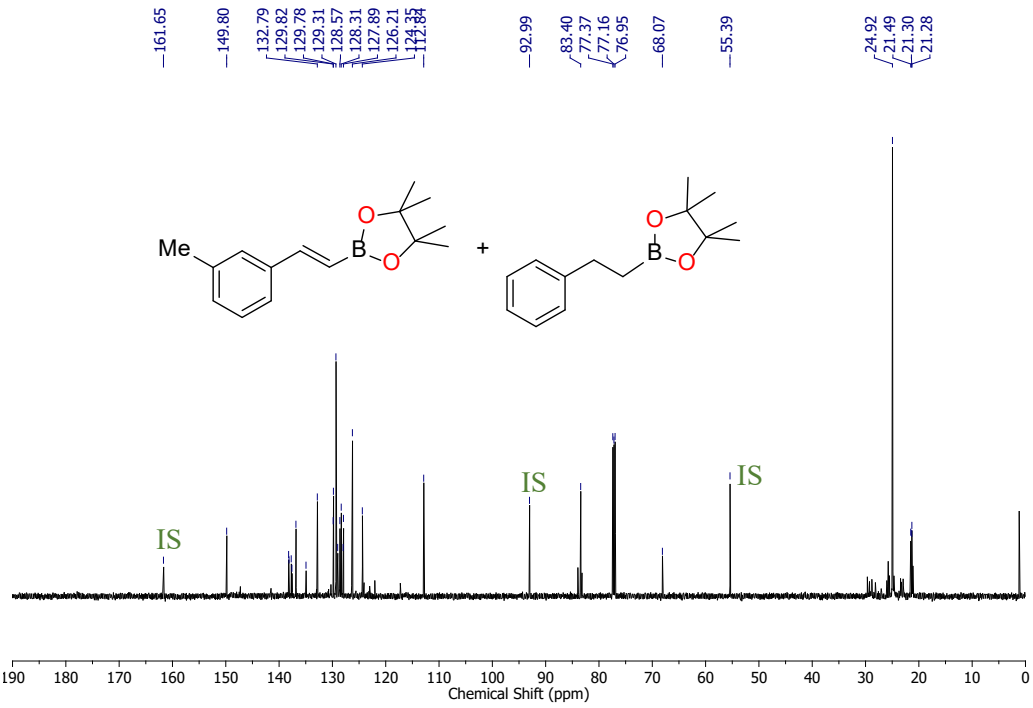


**Figure S172**. $^{13}C\{^{1}H\}$ NMR (150 MHz, $C_6D_6$, 298 K) spectrum of the hydroboration reaction of 1-ethynyl-3-methylbenzene and styrene in presence of cat. **5b** (2 mol%) and 1 equiv. HBpin [reaction condition: neat, 60 °C, 12 h].

## 13. References


(1) G. M. Sheldrick, *Acta Crystallogr*, 2008, **A64**, 112-122.

(2) L. J. Farrugia, *J. Appl. Cryst*., 2012, **45**, 849-854.

(3) S. Saha and M. S. Eisen, *ACS Catal*., 2019, **9**, 5947-5956.

(4) S. H. Doan and T. V. Nguyen, *Green Chem*., 2022, **24**, 7382-7387.

(5) P. Ghosh and A. J. V. Wangelin, *Angew. Chem., Int. Ed*., 2021, **60**, 16035-16043.

(6) T. T. Nguyen, J.-H. Kim, S. Kim, C. Oh, M. Flores, T. L. Groy, M.-H. Baik and R. J. Trovitch, *Chem. Commun*., 2020, **56**, 3959-3962.

(7) A. Harinath, J. Bhattacharjee and T. K. Panda, *Adv. Synth. Catal*., 2019, **361**, 850-857.

(8) N. Sarkar, S. Bera and S. Nembenna, *J. Org. Chem*., 2020, **85**, 4999-5009.

(9) S. Ataie, J. S. Ovensb and R. T. Baker, *Chem. Commun*., 2022, **58**, 8266-8269.

(10) J. Bhattacharjee, A. Harinath, K. Bano and T. K. Panda, *ACS Omega*., 2020, **5**, 1595-1606.

(11) A. Bismuto, S. P. Thomas and M. J. Cowley, *Angew. Chem., Int. Ed*., 2016, **55**, 15356-15359.

(12) S. Li, C. Hu, X. Cui, J. Zhang, L. L. Liu and L. Wu, *Angew. Chem., Int. Ed*., 2021, **60**, 26238-26245.

(13) Q. Zhao, X.-F. Wu, X. Xiao, Z.-Y. Wang, J. Zhao, B.-W. Wang and H. Lei, *Organometallics*, 2022, **41**, 1488-1500.